Engineering Geological and Geotechnical Characterisation of Selected Port Hills Lavas

A thesis

submitted in partial fulfilment of the requirements for the degree

of

Master of Science in Engineering Geology

at the

University of Canterbury

by

Jonathan-Adam Safaa Mukhtar

University of Canterbury

2014

Frontispiece

Redcliffs, Sumner, Christchurch

(Mukhtar J, 2014)

Abstract

This thesis aims to create a specific and robust geotechnical data set for the Lyttelton Volcanic Group, and investigate the effect of emplacement and post-emplacement mechanisms on geotechnical characteristics. The thesis provides an engineering geological model of a representative section of the Lyttelton Volcanic Complex, which, in conjunction with field observations, informed the subdivision of the main lithological groups into geotechnical sub-units.

The sub-units account for the geological variations within the rock types of this study. Eighteen geotechnical sub-units were identified, sampled and characterised: [1]trachytic dykes, [2]trachytic domes, [3]trachytic lava, [4]brecciated basaltic ignimbrite, [5]moderately welded basaltic ignimbrite, [6]highly welded basaltic ignimbrite, [7]red ash, [8]crystal dominated tuff, [9]lithic dominated tuff, [10]rubbly basaltic breccia, [11]unweathered basaltic lava, [12]slightly to moderately weathered basaltic lava, [13]highly to completely weathered basaltic lava, [14]highly vesicular basaltic lava bomb, [15]basaltic dyke, [16]blocky basaltic lava, [17]volcanogenic conglomerate and [18]volcanogenic tuffaceous sandstone. Thirteen units were able geotechnically tested. Sample preparation and geotechnical testing followed ASTM and ISRM guidelines respectively. Geotechnical testing included: uniaxial compressive strength (σ_{ci}), point load strength index ($Is_{(50)}$), porosity (n), density (ρ_d), P and S wave velocities (Vp and Vs), slake durability (Id_2), Young's Modulus (E), Poisson's Ratio (υ), shear modulus (G) and bulk modulus (K). The igneous lithologies included in this study have been characterised using the Detailed Engineering Geological Igneous Descriptive Scheme, developed purposely for the needs of the thesis.

The results of laboratory testing showed many strong trends with geological characteristics and relationships between geotechnical parameters. Parameters such as porosity, density, P-wave velocities, Young's Modulus and point load strength showed very strong correlations with uniaxial compressive strength. Variability in the physical and mechanical properties is attributed to the geological factors, which dictate the material behaviour. These include texture, grain size, composition, welding, lithification, flow banding, percentage and size of phenocrysts/clasts/lithics. Geological factors affecting geotechnical behaviour are a function of emplacement mechanism. Four distinct emplacement mechanisms were identified in this study: lava flows, pyroclastic density currents, intrusions (dykes) and airfall deposits. Typically, lava flows and intrusions have higher strength, durability, density and lower

porosity than pyroclastics and airfall deposits. Importantly, the data illustrates a considerable variability in some geotechnical parameters within the same unit (e.g. 58-193 MPa strength variation in the unweathered basaltic lava). Variability within rocks with similar emplacement mechanisms is attributed to the effects of post-emplacement mechanisms and processes (e.g. weathering, alteration and micro/macro fracturing leading to lower strength).

Evaluation of engineering geological and geotechnical parameters of rock and soil materials are required for engineering purposes, specifically when any form of design is required. This study has highlighted the importance and necessity to identify volcanic lithologies and features correctly as there are consequences for geotechnical behaviour, and that volcanic data from literature data should not be used without the correct degree of ground-truthing and geological context. Location-specific engineering geological data are necessary for the quantitation of variability in engineering geological characterisation for engineering geological models, designs and simulations in the Port Hills Volcanics.

Acknowledgments

Firstly I would sincerely like to thank David Bell, Dr. Samuel Hampton and Dr. Marlène Villeneuve for their support, feedback and guidance as supervisors.

I would also like to offer a massive thank you to the University of Canterbury Geological Sciences Department technical and administrative staff for all their help and kind words throughout this thesis Cathy Higgins, Rob Speirs, Dr. Kerry Swanson, Janet Brehaut, Sacha Baldwin-Cunningham, Matt Cockcroft, Janet Warburton, Pat Roberts, John Southward and Chris Grimshaw.

A special thanks to Dr. Maree Hemmingesn, Dr. Stefan Winkler and Dr. Valerie Zimmer for being excellent mentors and providing me a copious amount of support.

Thank you to Nick Harwood of Coffey International for providing me with the weathered rock cores from the Sumner Area.

Thanks to my classmates and peers for all the laughs and the friendly and encouraging environment from which to work in.

Thanks to my family, Sam, Faten and Anthony Mukhtar for all the love and support over the many years, without which I would not have been able to push as far as I have.

Lastly, but not least, Michelle Bishell for being the greatest inspiration I have ever known, your kind words and encouragement have been my greatest source of strength.

Just Keep Pushing Forward.

-Rocky Balboa

Table of Contents

List of Figures

List of Tables

CHAPTER 1 - Introduction

1.1 Project Background

The Canterbury Earthquake sequence caused extensive rockfall and cliff collapse in the Canterbury region, details of these failures and the rock units involved is limited and require greater analysis to assist in the rebuilding and mitigation for the Canterbury region. As indicated limited geotechnical properties exist for the Lyttelton Volcanic Group, and inadequate applicable data sets are available within literature (i.e. Kiliç and Teyman (2008), Zhang (2005), Goodman (1989), Johnson and De Graff (1988), Lama and Vutukrui (1978) and Kulhawy (1975)). As such this study looks to define the Lyttelton Volcanic Group both geologically and geotechnically, and create a specific and robust geotechnical data set on the Lyttelton Volcanics, which will also indicate the spectrum of rock mechanical properties. In order to create a data set of strength and related parameters for the lithologies present within the Port Hills, a specifically designed engineering geological testing regime is required. The purpose of this study is to analyse the local volcanic features and to determine useful rock mechanical parameters such as uniaxial compressive strength, deformation moduli, slake durability, porosity density and ultrasonic wave velocities. To this end, representative samples have been collected for the purpose of creating testable cores or block samples from locations of interest around the Port Hills and Sumner area situated in south-east Christchurch, New Zealand. A map displaying key locations is presented in Figure 1.1.

This study utilises the following investigations: review of volcanic rock mechanic data sets, description of volcanic materials (geological characteristics, flow type, formation history, emplacement mechanisms), laboratory testing of materials (both rock and soil), relevant petrology and description of defects. By undertaking these investigations accurate engineering geological characterisation can been achieved.

Some of the applications and benefits of this thesis include, but are not limited to, slope stability assessment, rock fall analysis and modelling, machinability and engineering design. An engineering geological dataset on the volcanics lithologies present within the Port Hills would be of a great benefit to the works being undertaken in Christchurch now and in the future.

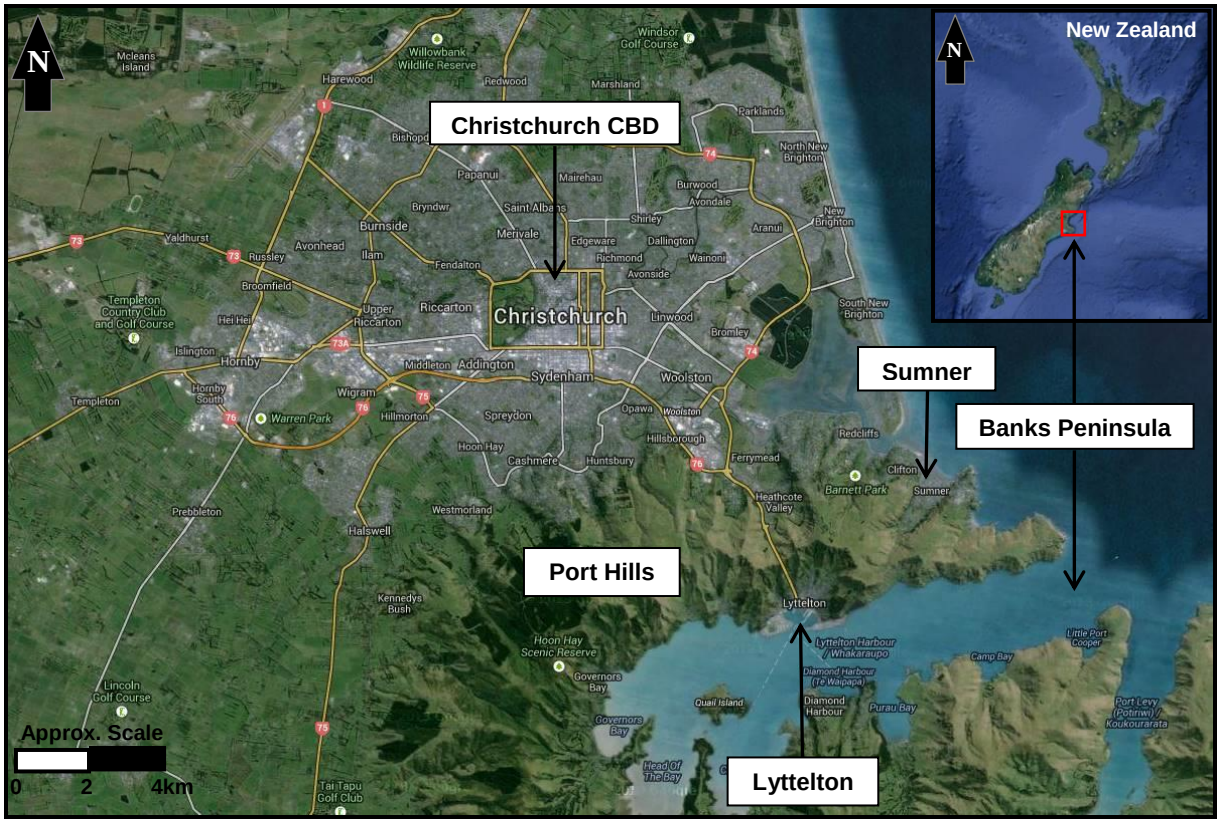

Figure 1.1: Satellite Imagery of Christchurch, New Zealand; showing Christchurch City in the centre and Port Hills and Banks Peninsula in the south and south-east of the image. Inset displays Christchurch's location on the east coast of the South Island of New Zealand. (Base Map Source: Google Maps and TerraMetrics, 2013).

Evaluation of engineering geological parameters of rock and soil materials are required for engineering purposes, specifically when any form of design is required. Area specific engineering geological data allows for the development of more accurate engineering geological models and simulations. Area specific engineering geological data allows for a more accurate representation of mechanical properties of a given lithology.

This study also investigates the relationship between geological emplacement parameters (e.g. flows, dykes, clastic flows, airfall) and geotechnical parameters. The rational for investigating this relationship is that emplacment mechanisms are hypothesised to control geotechnical behaviour. Through investigating this relationship it is possible to show how volcanic features which formed by specific emplacement mechanisms behave mechanically.

1.2 Project Aims and Objectives

The volcanic geology of the Port Hills and Banks Peninsula has been extensively studied, yet there has been no concentrated attempt to study this area from a combined geotechnical and geological perspective. The aim of this thesis is to establish the relationships between

geology, depositional environment, cooling history, lithology and the geotechnical properties of the volcanic strata derived by rock mechanics testing.

The specific objectives of this thesis are to:

- Assess lithologies by petrography, rock core logging, hand specimen and outcrop analysis.
- Develop an engineering geological model of the Lyttelton Volcanic Complex.
- Evaluate rock mechanics characteristics of rock materials through testing and deriving the following: porosity, density, slake-durability, ultrasonic velocities, unconfined compressive strength, point load strength index, Poisson's Ratio and Young's Modulus.
- Create a robust geotechnical data set that can be utilised for engineering purposes both locally and internationally.
- Establish a correlation between the geological and geotechnical characteristics.

1.3 Thesis Methodology

The research methods conducted have included observational field work and limited field mapping of volcanic outcrops and features, development of engineering geology models for the Port Hills, sample collection and preparation of representative volcanic lithologies for rock mechanical testing and detailed geological and engineering geological analysis of selected lithologies.

1.3.1 Data Collection

The data for the thesis has been obtained from field sites located throughout the Port Hills, these field sites are displayed in Figure 1.2 as shown by the red dots A-K. The data collected during this study consists of representative boulder sized samples and hand specimens of various Lyttelton Volcanic Group lithologies. Samples were recovered from outcrops and road cuts. This was done for reasons of ease of access and safety imposed restrictions. The recovered samples were brought back to the university where, they were cored to create testable cylinders of intact rock. Additional to boulder cored samples, deep drilled (>15m below ground level) intact rock cores from Marriner Street, Sumner have also been obtained.

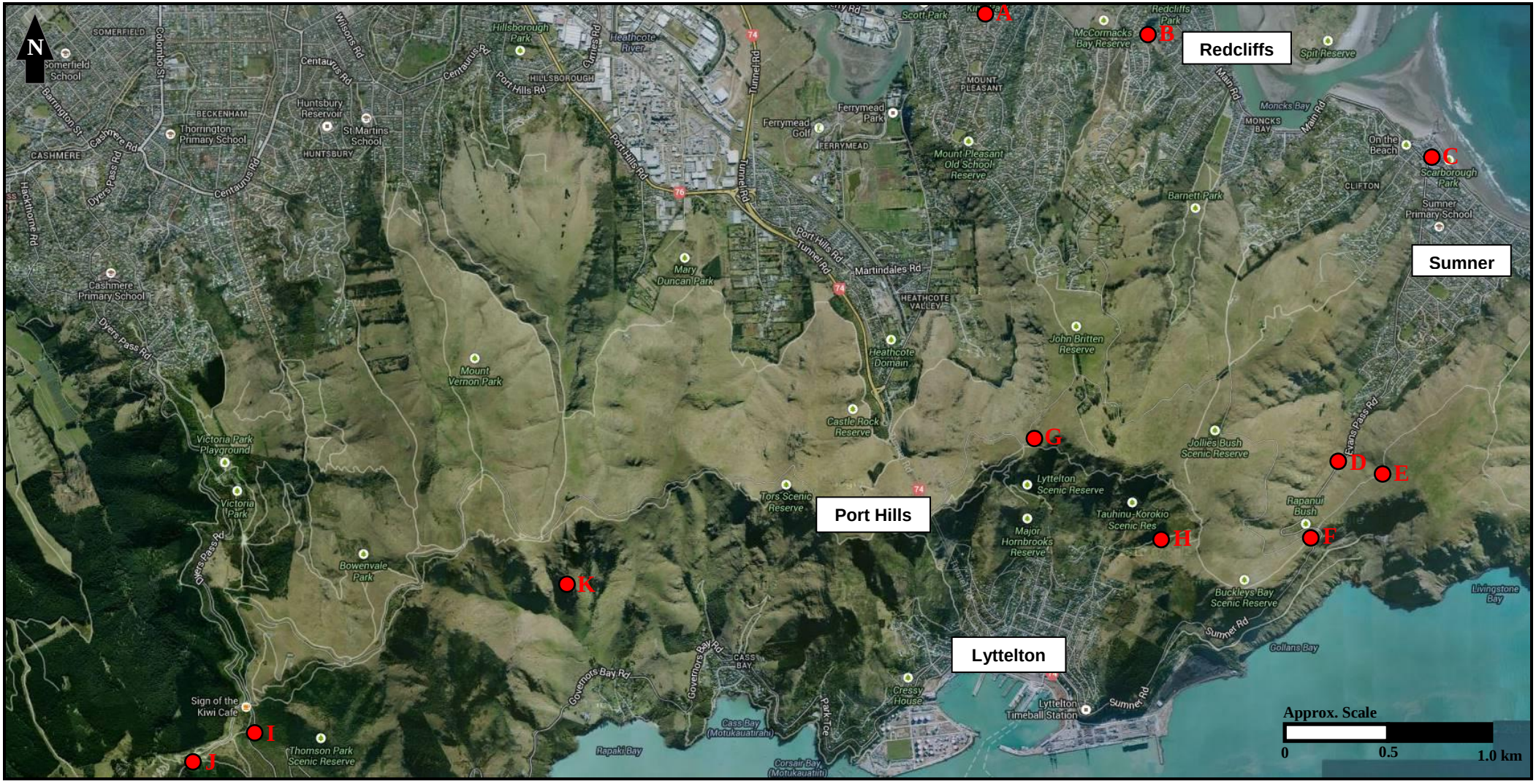

Figure 1.2: Aerial Imagery of the Port Hills displaying study area and field sites: A) Quarry Road, B) Redcliffs School, C) Marriner Street, D) Evans Pass Road, E) Summit Road, F) intersection of Evans Pass, Summit and Sumner Road, G) Mt Cavendish, H) Chalmers Track, I) Dyers Pass Road, J) Worsley Hill (Summit Road) and K) Rapaki . (Base Map Source: Google Maps and TerraMetrics, 2013).

These deep cores were specifically obtained due to their weathered states as locating and recovering highly weathered field samples and successfully coring them with a laboratory drill is very difficult, especially due to the presence of expansive clays (sample swelling in drill barrel). In addition, representative samples of each lithology have been collected for thin section analysis. The targeted volcanic lithologies are covered in detail in Chapter 2. Photographs have been taken at each site visited. Aerial photography/imagery used was sourced from the online Google Maps and Google Earth.

1.3.2 Data Analysis

Data analysis is undertaken by mechanical testing of various cylindrical and cubic block samples of the lithologies targeted by this study. The rock mechanics tests carried out includes: uniaxial compressive strength, determination of deformation moduli, porosity and density, longitudinal and shear wave velocities (P and S waves) and slake durability. The testing procedure was carried out in accordance with Ulusay and Hudson, (2007) the International Society for Rock Mechanics (ISRM) suggested methods for rock characterisation, testing and monitoring. In addition to the rock mechanical characterisation; a representative sample of each lithology was thin sectioned for the purpose of analysing mineralogy and formation history.

1.4 Field Area Description

The field area, the Port Hills, is the northernmost feature of Banks Peninsula (Figure 1.3). The Port Hills form the southern boundary between Christchurch City and the port town of Lyttelton. Banks Peninsula itself covers an approximate area of 1,200km^2. The peninsula is comprised of the Mesozoic greywacke of the Torlesse accretionary wedge and intermediate to silicic Cretaceous and Miocene volcanics (Ring and Hampton, 2012). Banks Peninsula is capped with a layer of loess which is up to 40 metres thick in some places and is connected the South Island by the progressive progradational Canterbury Plains. The connecting Canterbury Plains were formed by repetitive sequences of shore line progradation resulting from fluvio-glacial deposition along rivers and outwash fans followed by post-glacial marine transgression resulting from sea level rise and fall (Steward, 2012).

The Peninsula comprises two main volcanoes, Lyttelton and Akaroa. Both volcanoes have multiple eruptive centres. At least two magma systems are hypothesised to have supplied the volcanoes which ultimately formed the Peninsula (Hampton, 2010).

Topographically, the Port Hills slope gently at approximately 30° towards the north and drop steeply inwards toward the crater in Lyttelton Harbour. The Sugarloaf communications tower marks the highest point in the Port Hills at 493m above sea level. Figure 1.3 displays a digitised map with shaded relief and the actual Port Hills zone boundary.

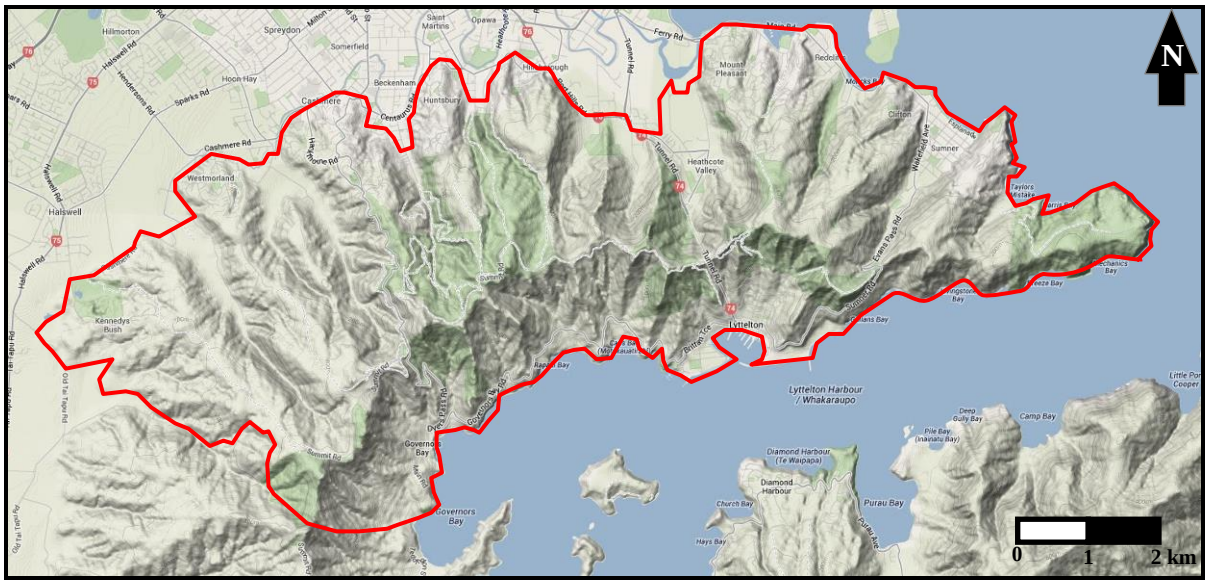

Figure 1.3: Digitised Map of the Port Hills displaying shaded relief to illustrate topography and the Port Hills zone boundary designated by the solid red line. (Base Map Source: Google Maps and TerraMetrics).

1.5 Geological History

The following sections provide an informative overview of the tectonic setting and evolution, formative magmatic processes and of the geological units of the Port Hills and greater Banks Peninsula. The section also discusses the recent seismic episodes which have occurred in Canterbury insofar as these are relevant to the present study and sample limitations.

1.5.1 Tectonic Setting and Evolution

Until the mid-Cretaceous period, the Rangitata 'Orogeny', a compressional regime, kept New Zealand on the eastern margin of Gondwana as a part of a subduction system (Ring and Hampton, 2012; Bradshaw *et al.*, 1981; Bradshaw, 1989). The vast majority of the eastern South Island is comprised of accreted rocks from this subduction zone (Mortimer, 2004) this unit is known as the Torlesse Composite Terrane and forms the basement rock, on which present day Banks Peninsula is situated. Subduction along the east margin of Gondwana ceased at between 110 and 100Ma (Mortimer *et al.*, 2006).

The end of subduction marked a period of extensive rifting and extensional style deformation throughout the South Island in the Late Cretaceous (Hampton, 2010). The change from compressional to extensional tectonics resulted in the development of the Tasman Sea, separating New Zealand from Gondwana, as well as causing local basin subsidence and alkali (silica poor) to tholeiitic (silica rich) volcanism throughout the Canterbury region (Hampton, 2010). Rifting was noted to have ceased by the late Eocene-Oligocene (Sewell *et al.*, 1989).

A tectonic shift to a compressional regime in the early Miocene resulted in an episode of uplift known as the Kaikoura 'Orogeny', causing an increase of sedimentation as well as alkalic to tholeiitic volcanism (Hampton, 2010). In the late Miocene the formation of the Southern Alps took place in the collision zone between two subduction systems. This episode of mountain building occurred contemporaneously with the formation of the Lyttelton Volcanic Complex, the northernmost section of Banks Peninsula and the study area of this thesis (Figure 1.4, Ring and Hampton, 2012).

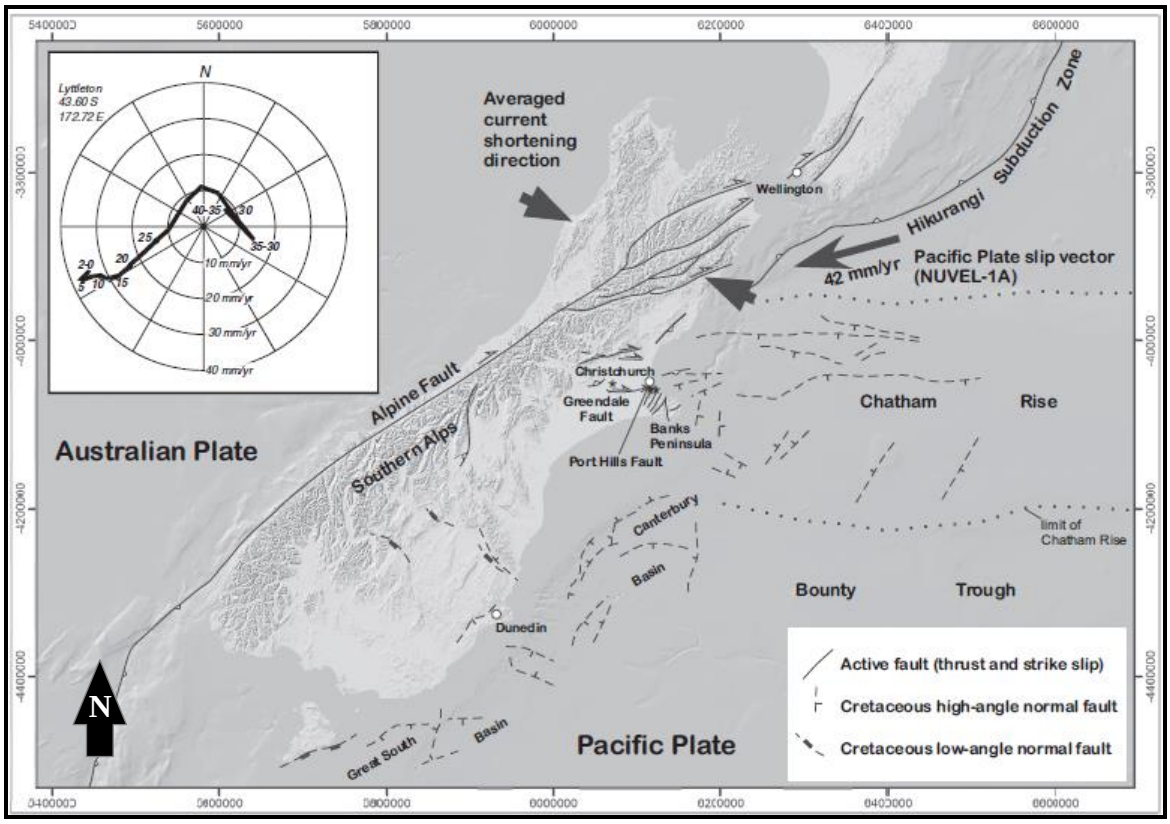

Figure 1.4: Current tectonic setting of the South Island New Zealand displaying the transition from the Hikurangi subduction zone in the north of the South Island to strike-slip faulting the Alpine Fault (Figure from Ring and Hampton, 2012).

The current plate-tectonic regime of the South Island is depicted in Figure 1.4. The most prominent tectonic feature of the South Island is the ~600km long Alpine Fault which runs up the western flank of the Southern Alps. It is the physical on-land expression of the boundary

between the colliding Indo-Australian and Pacific Plates. The convergent oblique motion on this plate boundary is on average 30-40mm/year (DeMets *et al.*, 1994). The Alpine Fault accommodates roughly 70-75% of the total plate motion (Norris and Cooper, 2001). The 25-30% of remaining plate motion is accounted for by a multitude of faults throughout the South Island, including the Hope, Wairau, Ashley, Awatere, Clarence Faults and the recently reactivated Greendale and Port Hills Faults.

Numerous NE-SW striking dextral-oblique strike-slip faults have been identified across Banks Peninsula which, are related to tectonic regimes during Miocene volcanism (Ring and Hampton, 2012). The Port Hills and Gebbies Pass Faults strikes approximately NE-SW across the northern most extent of the study area. Implications of these faults are discussed in section 1.7.

1.5.2 Intra-Plate Magmatism

Magmatism has been occurring in New Zealand since the landmass was separated from Gondwana in the late Cretaceous (84-82Ma) (Gaina *et al.*, 1998). Extensive intra-plate volcanism occurred continuously through the late Cretaceous and Cenozoic (Ring and Hampton, 2012). Volcanism occurred throughout the North, South, Chatham, Auckland, Campbell and Antipodes Islands in New Zealand (Hampton, 2010). Numerous expressions of the volcanic activity are visible on the South Island. The two largest expressions of Miocene intra-plate volcanism in the South Island are the Dunedin and Banks Peninsula volcanic edifices.

Intra-plate volcanism in New Zealand is hypothesised to be a result of a mantle plume, continental rifting or lithospheric detachment (Finn *et al*., 2005; Hoernle *et al*., 2006; Timm *et al.*, 2009). The commencement of volcanic activity in the South Island is believed to largely correspond with the Southern Alps Orogeny. It is uncertain whether or not there is a genetic relationship between both these events (Ring and Hampton, 2012). Volcanism on Banks Peninsula is hypothesised by Ring and Hampton, (2012) to be controlled by a regional horst structure crosscut by NE-SW striking oblique-dextral strike-slip faults, with the intersections of these features becoming concentrated points for volcanic activity to transpire as shown in Figure 1.5.

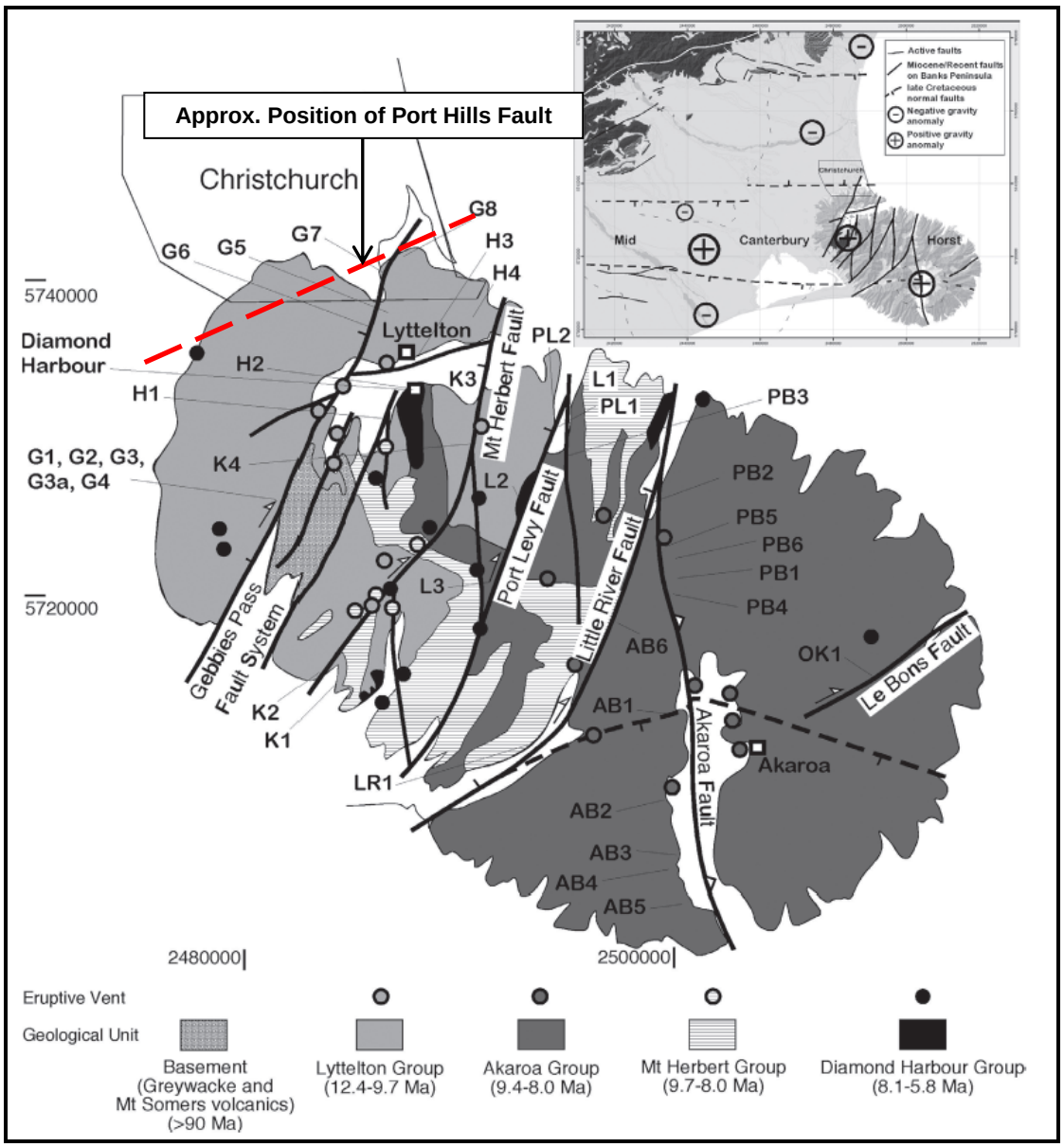

Figure 1.5: Simplified geological map of Banks Peninsula displaying inferred faults, volcanic vents and fault-slip analysis positions. Late Miocene Faults are designated by bold continuous lines and late Cretaceous normal faults by bold dashed lines. Gravitational anomalies delineate the Mid Canterbury Horst, a structure which focused late Miocene volcanism. Approximate position of the Port Hills fault is indicated by the red hashed line (Figure adapted with permission from Ring and Hampton, 2012).

1.5.3 Geological Units of Banks Peninsula

Banks Peninsula is comprised of several volcanic formations, this section draws particular attention to the Lyttetlon Volcanic Group which erupted between 11 and 9.7Ma. The Lyttetlon Volcanic Group forms the Port Hills, which are the primary focus of this thesis. The other geological formations are not the focus of this study, however they have been included in this section to inform the reader. Figure 1.6 from Sewell *et al*., (1992) illustrates the various geological units which comprise Banks Peninsula. Figure 1.7 adapted by Hampton,

(2010) displays the mapped spatial extent of the units listed in Figure 1.6. Prior to undertaking sample collection for material characterisation it was important to have an appreciation of the various geological units assoicated with the field area. This is particularly important in volcanic edifices where lavas or dyke units could have erupted or intruded into a particular volcanic unit. In the case of the Port Hills, the Diamond Harbour Volcanics and Governors Bay Andesite intrude into the Lyttelton Volcanics as seen in Halswell Quarry, Cass and Rapaki Bay as seen in Figure 1.7.

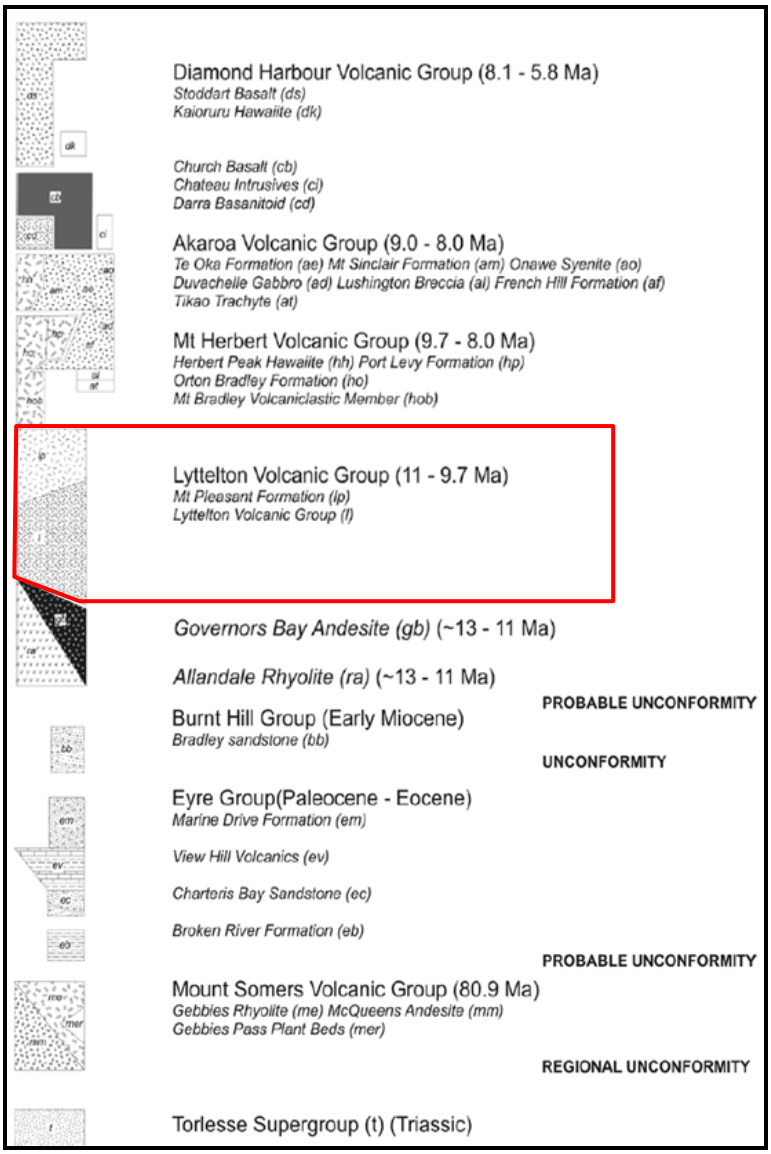

Figure 1.6: Stratigraphic Column of Banks Peninsula Geological Units from Hampton, (2010); adapted from Sewell *et al*., (1992). The Lyttelton Volcanic Group is highlighted with a red box.

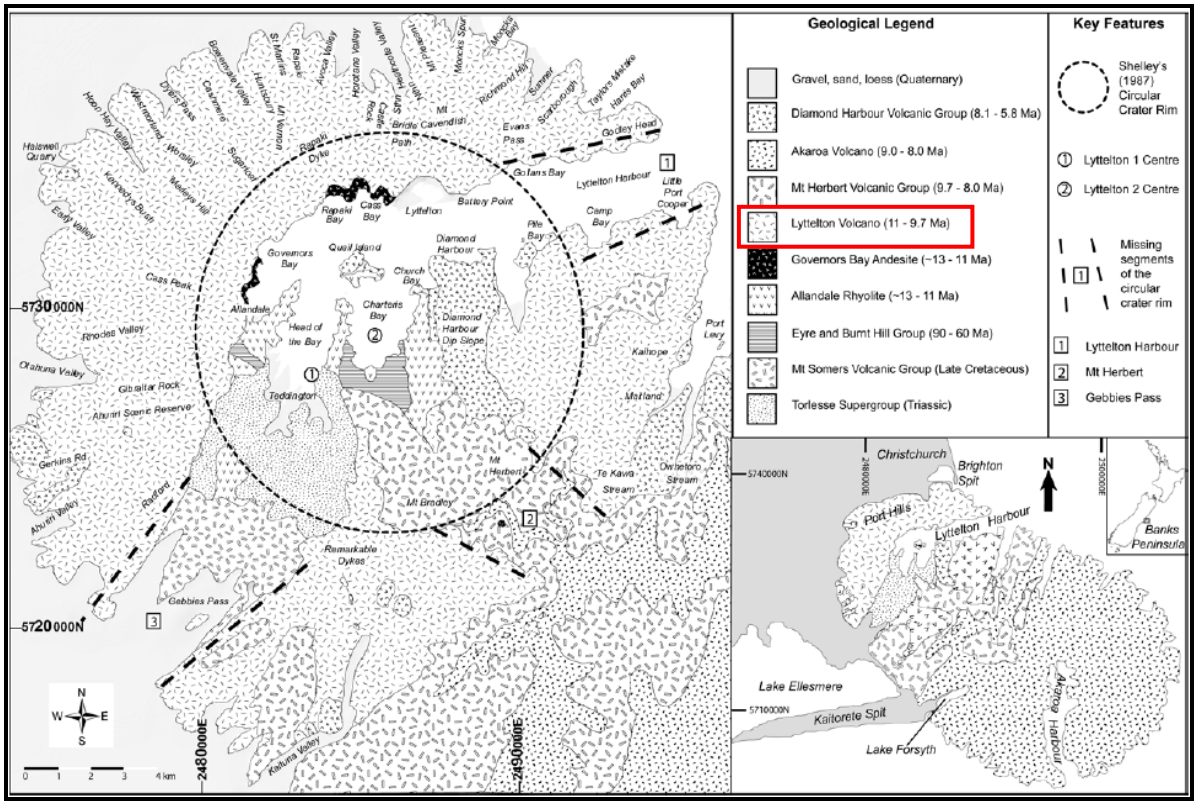

Figure 1.7: Simplified Geological Map of Banks Peninsula and key features of previous Lyttelton Volcano models (Figure adapted on Sewell, (1985) and Shelley, (1987) adapted by Hampton, 2010).

As observed in Figures 1.6 and 1.7, there are nine main geological formations which make up the Banks Peninsula volcanic edifice; Torlesse Supergroup (Triassic), Mt Somers Volcanic Group (Late Cretaceous), Eyre and Burnt Hill Group (90-60Ma), Allandale Rhyolite (~13-11Ma), Governors Bay Andesite (~13-11Ma), Lyttelton Volcanic Group (11-9.7Ma), Mt Herbert Volcanic Group (9.7-8.0Ma), Akaroa Volcanic Group (9.0-8.0Ma) and Diamond Harbour Volcanic Group (8.1-5.8Ma). Detailed breakdowns of these units are presented in Appendix 1.

1.5.4 Lyttelton Volcanic Group

The Lyttelton Volcanic Complex formed in the Late Miocene. The complex is composed of hawaiite lava, subordinate basalt, trachy-andesite (mugearite) lava flows and interbedded clastic sediments (Sewell *et al.*, 1992). The Lyttelton Volcanic complex (Hampton, 2010) comprises five overlapping volcanic cones; Head of the Bay, Governors Bay, Whakaraupo, Mt Evans, Remarkable Cones, with each consisting of stratified lava flows, pyroclastic deposits, radial dykes regimes, interbedded epiclastic deposits and outer flank scoria cones.

The Mt Pleasant Formation is part of the Lyttelton Volcanic Group, and will be referred to in this thesis as Eruptive Package IX following Hampton, (2010). The package was erupted during later stage of Lyttelton volcanism, with lava flows from this eruptive package making up the eastern side of Lyttelton Harbour. This unit of flows is well exposed in the sea cliffs and headlands in the Sumner-Redcliffs area. This unit incorporates a range of lavas from hawaiite to trachyte. Sewell *et al*., (1992) miss-identified a previously unidentified basaltic ignimbrite unit at Redcliffs in Sumner; this unit was previously thought to be a series of basaltic lava flows. The Lyttelton Volcanic Complex spatially extends from the Port Hills in the north to as far as Kaituna Valley in the south-west and Port Levy in the east; a graphical representation is displayed in Figure 1.7.

1.6 Previous Investigations and Hypothesis Review of Lyttelton Volcanic Group

This section reviews the Hampton (2010) model of the Lyttelton Volcanic Complex and the previous theories surrounding the formation and development of the volcanic edifice.

The formation of the Lyttelton Volcanic Complex has been a subject of debate for close to 150 years. Many of the previous studies and investigations focussed largely on geochemistry and seldom on physical volcanology and the structural complexity which is commonly associated with volcanic groups.

The first study and original mapping of the Lyttelton Volcano was undertaken by Haast (1860). Haast identified that Lyttelton Harbour was a part of an extinct volcano, which, was supported by the observation of lava flows dipping out from crater rim. Haast hypothesised that Quail Island was the volcanic centre of activity due to the orientation of dyke swarms. Haast (1878) later altered his model suggesting that the volcanic centre of the volcano was situated south-west of Quail Island near Head of the Bay, as shown in Figure 1.7.

Since the original studies by Haast (1860, 1878), numerous studies have been undertaken continually expanding on understanding the evolution and formation of the Lyttelton Volcano. Shelley (1987) investigated dyke swarm regimes and postulated that there were two eruptive centres; these two locations became known as Lyttelton 1 and Lyttelton 2. Lyttelton 1 was located near Head of the Bay, and Lyttelton 2 in Charteris Bay. These locations are shown in Figure 1.7. Later Neumayr (1999) used topographic features (valleys, ridge lines,

and lava flow trends) to re-assess the location of Lyttelton 1, concluding it was located further north-west of Head of the Bay than stated in Shelley (1987).

Sewell (1985) hypothesised the circular erosional crater rim theory, which was supported by Shelley (1987) who mapped a circular correlation between the peaks surrounding Lyttelton Harbour. These two studies used Lyttelton 1 and 2 to model the formation of the Lyttelton Volcano and the associated Lyttelton Volcanic Group lithologies, with the later addition of the Mt. Pleasant Formation (Eruptive Package IX) which signified a small flank eruption on the north flank of the Lyttelton Volcano. Physical volcanology and petrographic analysis undertaken by Sewell (1985, 1992) resulted in the detailed stratigraphic sequence illustrated in Figure 1.6. Unit ages were determined by K-Ar dating, Sr-Nd isotopes and rare earth element analysis. Determination of unit ages assisted in defining the stratigraphic sequence of events that led to the overall formation of Banks Peninsula.

The Hampton (2010) model is the most recent and detailed study on the Lyttelton Volcanic Complex, and concentrated on investigating growth, structure and the development of the Lyttelton Volcano by analysis of physical volcanology (lavas, flows, deposits and radial dyke orientations) and geomorphology (topography and volcanic cone features). Perhaps the most important part of the Hampton (2010) study was that it suggests that the Lyttelton Volcano was in fact a volcanic complex comprising five overlapping cones (Head of the Bay, Governors Bay, Whakaraupo, Mt Evans and the Remarkable Cone) with at least 15 eruptive stages. Each primary cone constitutes successions of stratified lava flows, pyroclastic deposits, radial dyke regimes, interbedded epiclastic deposits and outer flank (parasitic) scoria cones. The scoria cones and blocky lava flows were used to define the outer zones of larger cone structures and eruptive packages.

Phases of volcanic construction were identified through stratigraphic relationships, lava flow trends and type, dyking regimes and radial erosional features. Each phase of construction regularly terminates with a rubbly basaltic lava breccia, as shown in Figure 1.8. These phases of construction have been termed by Hampton (2010) as eruptive packages. Figure 1.9 illustrates the locations and relationships of the identified cones, eruptive packages and eruptive centres.

The eruptive packages are important as they inform this study of the volcanic structure and components within the field area, and also provide context for observed features. In addition

eruptive package IX reinterprets the Mt Pleasant Formation apart of the Lyttelton Volcanic Group. The basaltic ignimbrite deposits of Redcliffs were previously mapped apart of the Mt Pleasant Formation as interbedded basaltic lava flows. Following the Canterbury Earthquake Sequence Brehaut (2013) and Lo (2013) re-examined these units and identified them as a pyroclastic deposit consisting of variably welded ignimbrites.

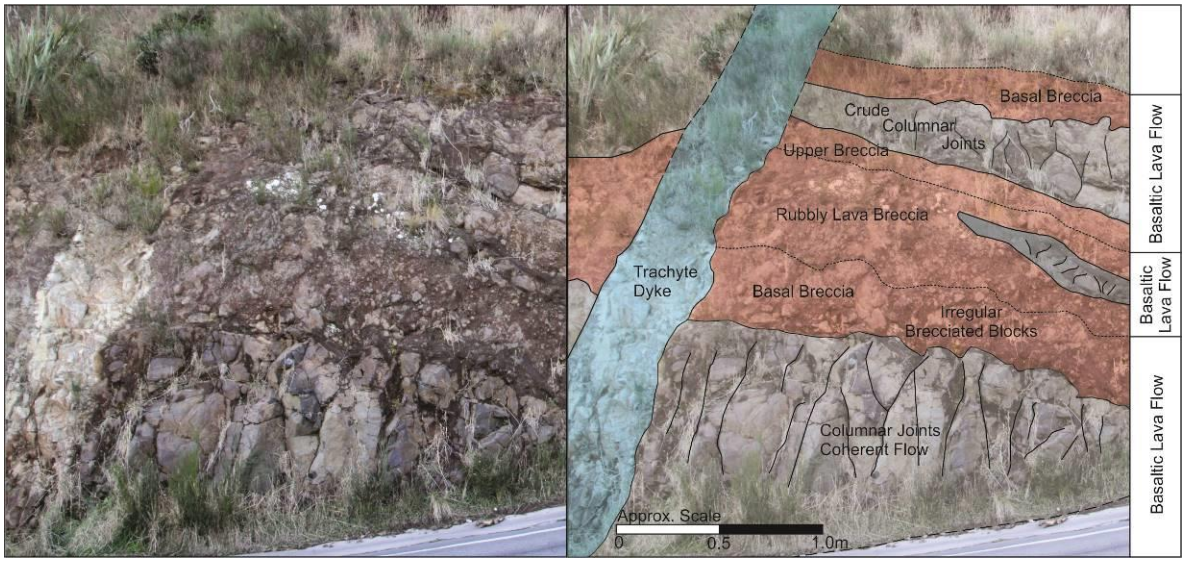

Figure 1.8: Annotated longitudinal section through three basaltic lava flows showing the 'caterpillar track' mechanism which results in the formation of the upper and basal rubbly basaltic breccia.

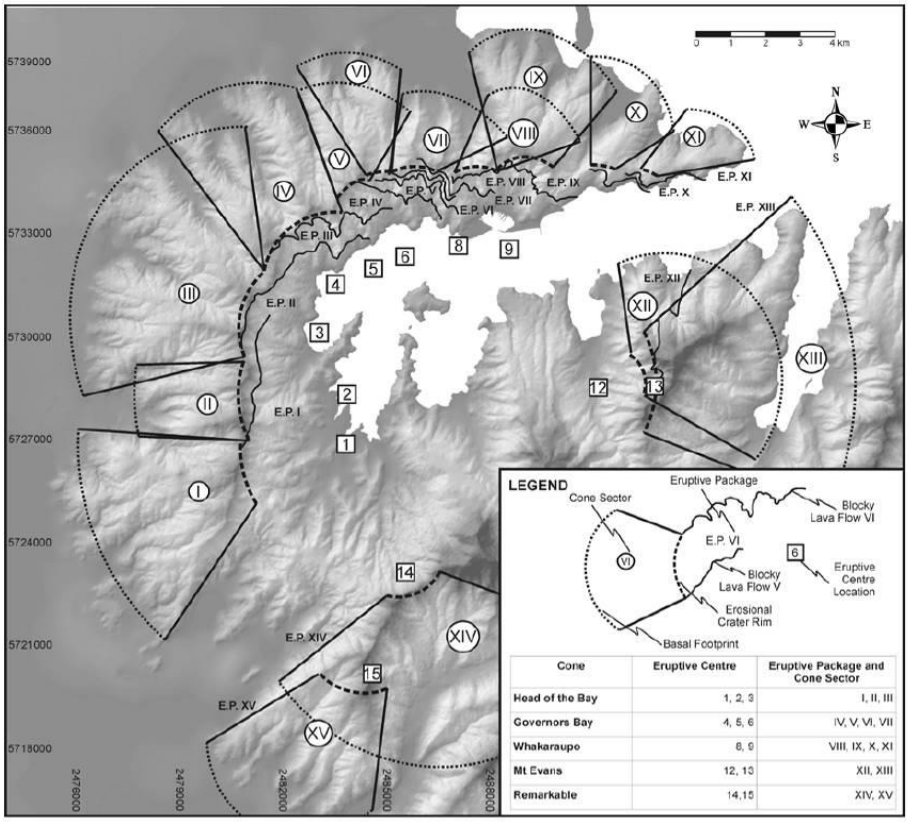

Cone	Eruptive Centre	Eruptive Package and Cone Sector
Head of the Bay	1, 2, 3	I, II, III
Governors Bay	4, 5, 6	IV, V, VI, VII
Whakaraupo	8, 9	VIII, IX, X, XI
Mt Evans	12, 13	XII, XIII
Remarkable	14,15	XIV, XV

Figure 1.9: Location and structural relationships of cones, eruptive centres and eruptive packages associated with the Lyttelton Volcanic Complex. (Figure from Hampton, 2010).

The Hampton (2010) model incorporated two distinct erosional topographic features: radial valleys and cone-controlled valleys. Radial valleys represent radial erosion at the cone summit, whereas cone-controlled valleys occur at the convergence of cones and eruptive packages resulting in forming conduits for runoff. Figure 1.10 illustrates a conceptual model incorporating radial and cone-controlled valleys.

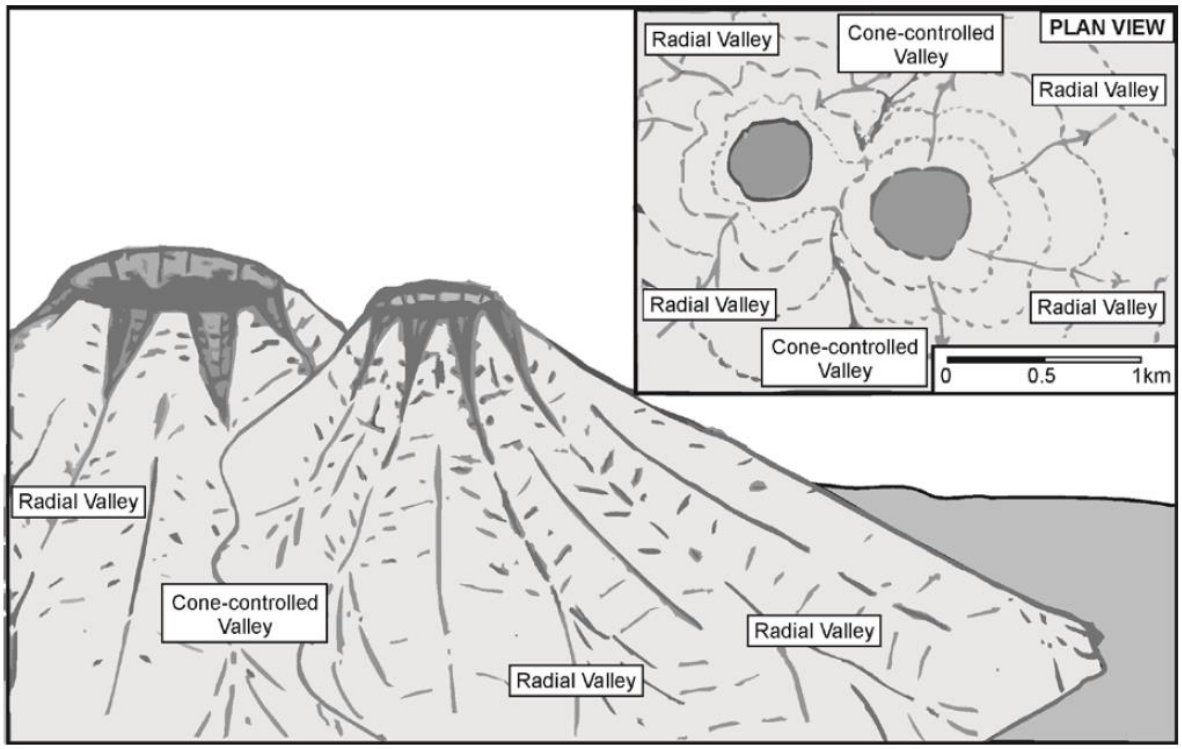

Figure 1.10: Conceptual Model depicting radial and cone-controlled valleys associated with volcanic cones. Radial valleys initiate cone summits where cone-controlled valleys occur between volcanic cones. (Figure from Hampton, 2010).

The information gleaned from Hampton (2010) is important to provide a important understanding of the structures and stratigraphy in the field area necessary before attempting to construct a material testing framework.

1.7 Recent Seismic Episodes

The Canterbury Earthquake sequence and its effects and implications on the various volcanic rock masses in the Port Hills. The Canterbury Region was affected by an M_w 7.1 earthquake, the first in a long sequence of earthquakes and aftershocks on September 4th 2010. The fault rupture occurred on a previously unidentified 'blind' dextral strike-slip fault near the town of Darfield, which is situated approximately 40km inland west of Christchurch (Cubrinovski, 2010). This earthquake became known locally as the Darfield Earthquake, the fault being named the Greendale Fault. The deadliest and most destructive of the ensuing earthquakes and aftershocks was the February 22nd 2011 M_w 6.2 earthquake, which occurred along the Port Hills Fault trending NE-SW across the foot slope of the Port Hills. The earthquake was the result of a rupture along a south dipping oblique thrust fault. The February seismic event came to be known as the Christchurch Earthquake. Figure 1.11 displays the positions of the

earthquakes, aftershocks and fault lines related to the Canterbury earthquake sequence. Prior to the recent seismic episodes the Canterbury Region had an historically low seismicity.

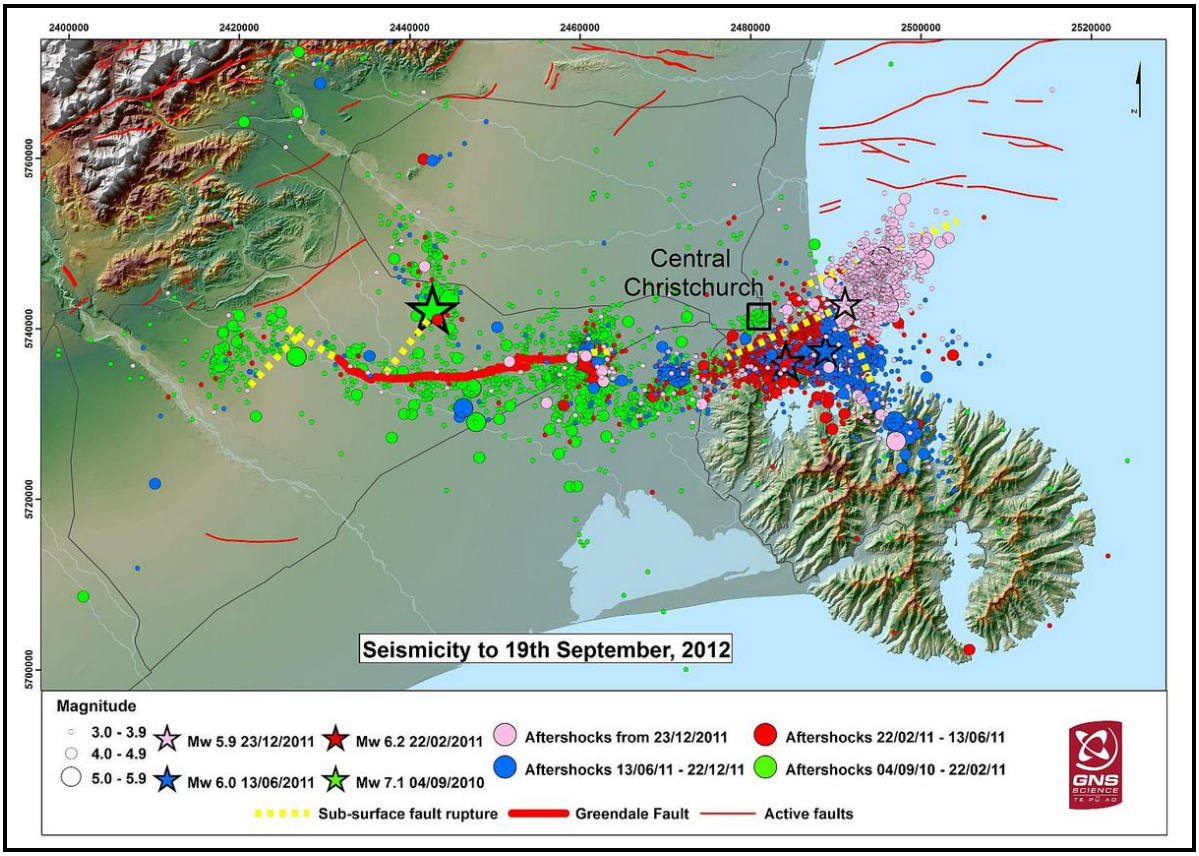

Figure 1.11: Map of the Canterbury Region showing distribution of earthquakes, aftershocks and fault traces until 19th September 2012. The Greendale Fault is seen in the centre left of the image represented as a solid red line and the Port Hills Fault as a dotted yellow line directly south of Central Christchurch (Bradley, 2012, figure from GeoNet, 2012).

Both the Darfield and Christchurch earthquakes occurred at shallow depths within the top 15km of the crust (Browne *et al.*, 2012). The Greendale Fault rupture breached the surface and is approximately 28km in length, although it is postulated to be approximately 40km in extent within the crust (Cubrinovski, 2010). The Port Hills Fault rupture was not observed to have breached the ground surface.

The earthquakes are a direct result of a release of stress energy stored in the Earth's crust under the Canterbury Plains. The release of energy from an earthquake manifests itself in the form of propagating seismic waves. These waves have the potential to negatively impact a rock mass given the intensity and duration of an earthquake, more so with a proximal epicentre, and hence greater shaking potential.

During the February 22nd 2011 Earthquake, very high peak ground acceleration (PGA) values were recorded in the Port Hills within close proximity to the fault rupture. The maximum recorded peak vertical ground acceleration value recorded measured 2.21g in the Heathcote Valley (Bradley and Cubrinovski, 2011). The high vertical and horizontal ground accelerations resulted in releasing hundreds of boulders from the slopes around the Port Hills and Lyttelton, many of which damaged infrastructure, impacted residential buildings and also resulted in casualties. In addition to boulder fall, significant cliff collapse and retreat also occurred in areas such as, Peacocks Gallop, Whitewash Head and Redcliffs.

1.7.1 Implications of Seismic Activity

There are several implications to the Port Hills geology from a rock mass perspective.

The high degree of shaking could have induced the following in the rock mass:

- Increased frequency of micro and macro fracturing.
- Increased aperture and length of discontinuities.
- Increased pathways for water infiltration (permeability), permitting for more extensive chemical and physical weathering and alteration of the rock mass.

Although a significant portion of the damage caused on the Port Hills is related to failures within the loess and loess colluvium due to brittle mechanical movement and/or the effects of water infiltration; either by natural or anthropogenic processes, a large portion of challenging issues still exist in which problems in the rock mass are involved. Consequently, as a result of the earthquakes vast amounts of engineering work has to be undertaken on the Port Hills for people to avoid hazards. Hence, a quantitative data set on the Lyttelton Volcanic Group is of great benefit to projects being undertaken presently and in the future.

1.8 Review of Available Igneous (Volcanic) Rock Mechanical Properties

Available igneous volcanic rock mechanical properties and parameters for this study's field area lithologies (basalt, trachyte, tuff and ash) as presented in section 1.5.4. An extensive search through available literature was undertaken in order to collate mechanical values for these materials (Table 1.1).

Physical rock mechanical properties and derived parameters of interest include, porosity (n, %), dry mass density (ρ_d, kg/m^3), P and S wave velocities (Vp and Vs, ms^{-1}), point load strength index ($Is_{(50)}$, MPa), uniaxial compressive strength (UCS/σ_{ci}, MPa), slake durability index (Id_1 and Id_2, %), Young's modulus (E, GPa), Poissons ratio (v, unitless), shear modulus (G, GPa) and bulk modulus (K, GPa).

It should be noted that although an extensive database search was carried out, no complete datasets including all of the material properties of interest were able to be sourced directly from any one of the mentioned sources and in most cases there is no mention of the material/lithologies state of weathering (i.e. unweathered/fresh or highly weathered) or composition (material description: basalt). As such values for a single material are sourced from multiple sources (Kiliç and Teyman (2008), Zhang (2005), Goodman (1989), Johnson and De Graff (1988), Lama and Vutukrui (1978) and Kulhawy (1975). Values presented in Table 1.1 are utilised in Chapter 6 for comparative purposes.

Table 1.1: Available rock mechanics data from literature for basalt, trachyte tuff/ash and lithic rich tuff (Sources: Kiliç and Teyman (2008), Zhang (2005), Goodman (1989), Johnson and De Graff (1988), Lama and Vutukuri (1978) and Kulhawy (1975).

Rock Mechanics Data for Various Igneous Volcanic Lithologies												
		n (%)	**ρ_d (kg/m^3)**	**Vp (ms^{-1})**	**Vs (ms^{-1})**	**$Is_{(50)}$ (MPa)**	**UCS (MPa)**	**Id_2 (%)**	**E (GPa)**	**υ (unitless)**	**G (GPa)**	**K (GPa)**
Basalt	**M**	3.3	2770	n/a	n/a	4.0	142	n/d	62.6	0.25	n/a	181.4
	R	2.7-10.2	2500-2920	4500-6000	2500-3500	3.0-1.50	64-249	n/d	34.9-100.6	0.08-0.38	3.8-41.5	1.4-756
Trachyte	**M**	6.25	2240	3480	n/d	1.5	70	n/d	7.4	n/d	n/d	n/d
	R	n/d	n/d	n/d	n/d	n/d	n/d	n/d	n/d	n/d	n/d	43.0-165.8
Tuff/Ash	**M**	19.8	n/d	n/d	n/d	n/d	n/d	n/d	n/d	n/d	n/d	n/d
	R	n/d	1600-1920	n/d	n/d	n/d	11.3-35.3	n/d	n/d	n/d	n/d	n/d
Lithic Rich Tuff	**M**	42.5	n/d	n/d	n/d	n/d	3.65	n/d	n/d	n/d	n/d	n/d
	R	n/d	n/d	n/d	n/d	n/d	n/d	n/d	n/d	n/d	n/d	n/d
Note: M=Mean, R=Range, n/d=data un-available												

1.9 Thesis Format

The format of this thesis is as follows:

Chapter 2: Investigation Model and Framework includes a series of field observations regarding all observable Lyttelton Volcanic Group lithologies and structures throughout the field area. The structural and geological information collated from field observations supports the development of a engineering geological block model of the Lyttelton Volcanic Complex.

This chapter illustrates a geotechnical model developed for this thesis from which the observed lithologies are sub-divided into sub-units; these sub-units reflect the materials selected for testing.

Chapter 3: Rock Mechanics Testing Procedure and Descriptive Methodology outlines the methodologies in which the identified Lyttelton Volcanic Group lithologies are sampled and collected from the field, prepared for testing, tested and described. Additionally Chapter 3 illustrates the detailed igneous descriptive scheme devised for describing volcanic materials with a higher degree of accuracy than the NZGS, 2005 scheme.

Chapter 4: Results of Geotechnical Testing and Properties Part 1 – Lava Flow Units includes the results of rock mechanics testing, engineering geological and geological descriptions and thin section analysis of all of the lava flow units included in this study.

Chapter 5: Results of Geotechnical Testing and Properties Part 2 – Assorted Volcanics includes the results of rock mechanics testing, engineering geological and geological descriptions and thin section analysis of the assorted volcanic and volcanogenic units included in this study (includes dykes, airfall deposits, ignimbrites, laharic/volcanogenic deposits etc).

Chapter 6: Discussion and Applications discusses the trends, features and variability observed following analysis of rock mechanical parameters and thin section data and directly links these to emplacement and pre-emplacement mechanisms. Additionally the potential applications of this thesis are discussed.

Chapter 7: Summary Conclusions and Recommendations includes a summary of the findings of the thesis, recommendations for future work and suggestions for further research.

CHAPTER 2 - Investigation Model and Framework

2.1 Introduction

Chapter 2 develops a geological model and framework from which the primary geotechnical investigation can be undertaken. This chapter includes:

- A summary of field observations including locations of observed lithologies, stratigraphic relationships, volcanic features and structures.
- An engineering geological model of the Lyttelton Volcanic Complex which is informed and justified by a series of annotated field photographs, information from previous studies and inference regarding volcanic structures.
- A discussion regarding the need for further geotechnical characterisations of the volcanic units based on observations made from examining hand specimens collected from the field.
- A detailed geotechnical unit classification model. This classification is significant as it illustrates the breakdown within each lithology into individual geotechnical units which ultimately control the strength and thus mechanical behaviour of the material.
- A Chapter synthesis of key points.

2.2 Field Observations

The objectives of the first phase of field work, undertaken between June and August of 2013, was to identify locations of Lyttelton Volcanic Group lithologies in the field, take note of stratigraphic relationships between lava flows, volcanogenic, pyroclastic and airfall deposits, note any geological structures (e.g. faults, shears, lavas, dykes, domes, hydrogeological features) and gain an appreciation of scale and spatial extent of volcanic units. This section lists Lyttelton Volcanic Group lithologies, field observations and respective locations as observed in the field. At each location representative samples were collected and brought back for analysis and testing, the sample collection methodology is presented in Chapter 3.

The following field observations are supported by photographs taken in the field at various scales. Each field observation is used to inform, justify and ground truth the engineering geological model presented in the following section (Section 2.3).

2.2.1 Basaltic Ignimbrites

Main layer of brecciated/non-welded basaltic ignimbrite transitions into an approximately 20m thick layer of variably welded basaltic ignimbrite unit at the base of Redcliffs (Figure 2.1a). The basaltic ignimbrites structure is highly irregular with a high degree of differential welding throughout the mass. Brecciated/non-welded ignimbrite deposit was also observed in Quarry Road, Sumner (Figure 2.1b) the deposit is noted to be at least 3m thick.

Figure 2.1: Field photographs of Basaltic Ignimbrites. A) Redcliffs pyroclastic density current deposit, note thickness of deposit is approximately 40m and main transitional welding zone. B) Brecciated Basaltic Ignimbrite at Quarry Road.

2.2.2 Rubbly Basaltic Breccia

Coherent basaltic lava units are underlain and are capped by rubbly basaltic breccia lava flows (Figure 2.2). Basaltic lava flows are observed throughout the Lyttelton Volcanic Complex and accounts for much of the complex as the most frequent unit. Groundmass is clay rich with mixture of fine to boulder sized basaltic fragments.

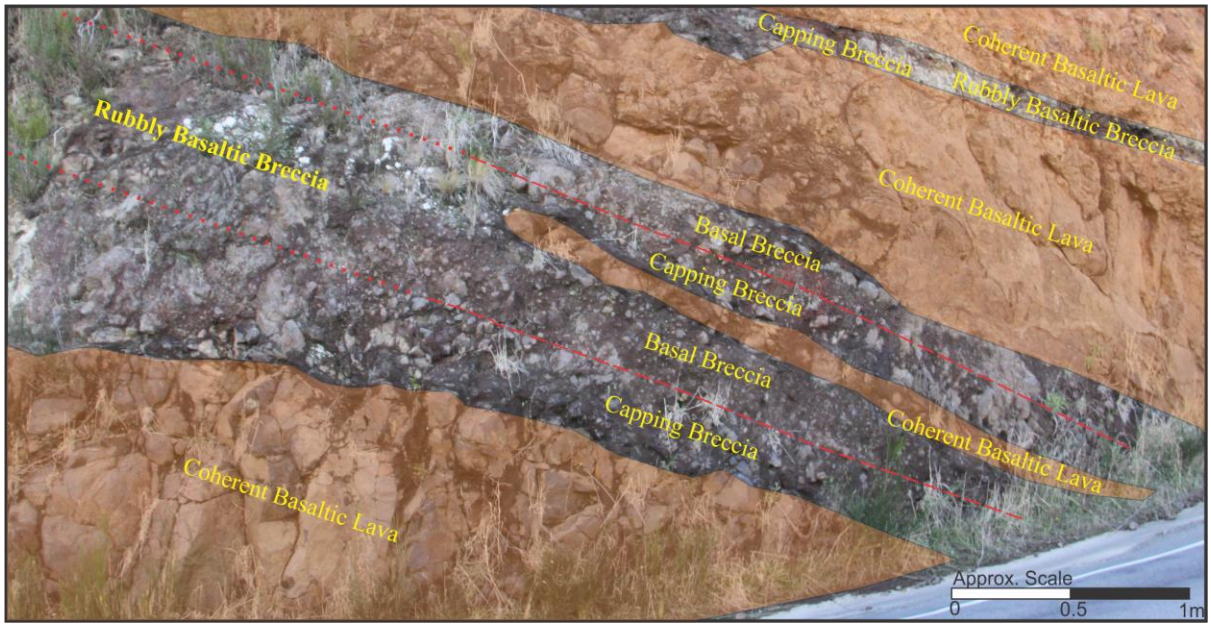

Figure 2.2: Field photographs of Rubbly Basaltic Breccia. Red dashes indicate approximate flow boundaries between capping and basal breccias. Note: alternating relationship with coherent basaltic lava. Each basaltic lava flow consists of two rubbly basaltic breccias and a layer of coherent lava. Site: Dyers Pass Road, Lyttelton side, Port Hills.

2.2.3 Coherent Basaltic Lava

Basaltic units observed to be laterally continuous for hundreds of meters in several locations with thickness vary from between 0.5-25m (Figure 2.3b). Basaltic lava flows varies between massive, columnar and irregularly jointed units (Figure 2.3a/b). Vesicles become more common towards brecciated boundaries. The basaltic lava flows are the most prominent lithological unit in the Port Hills.

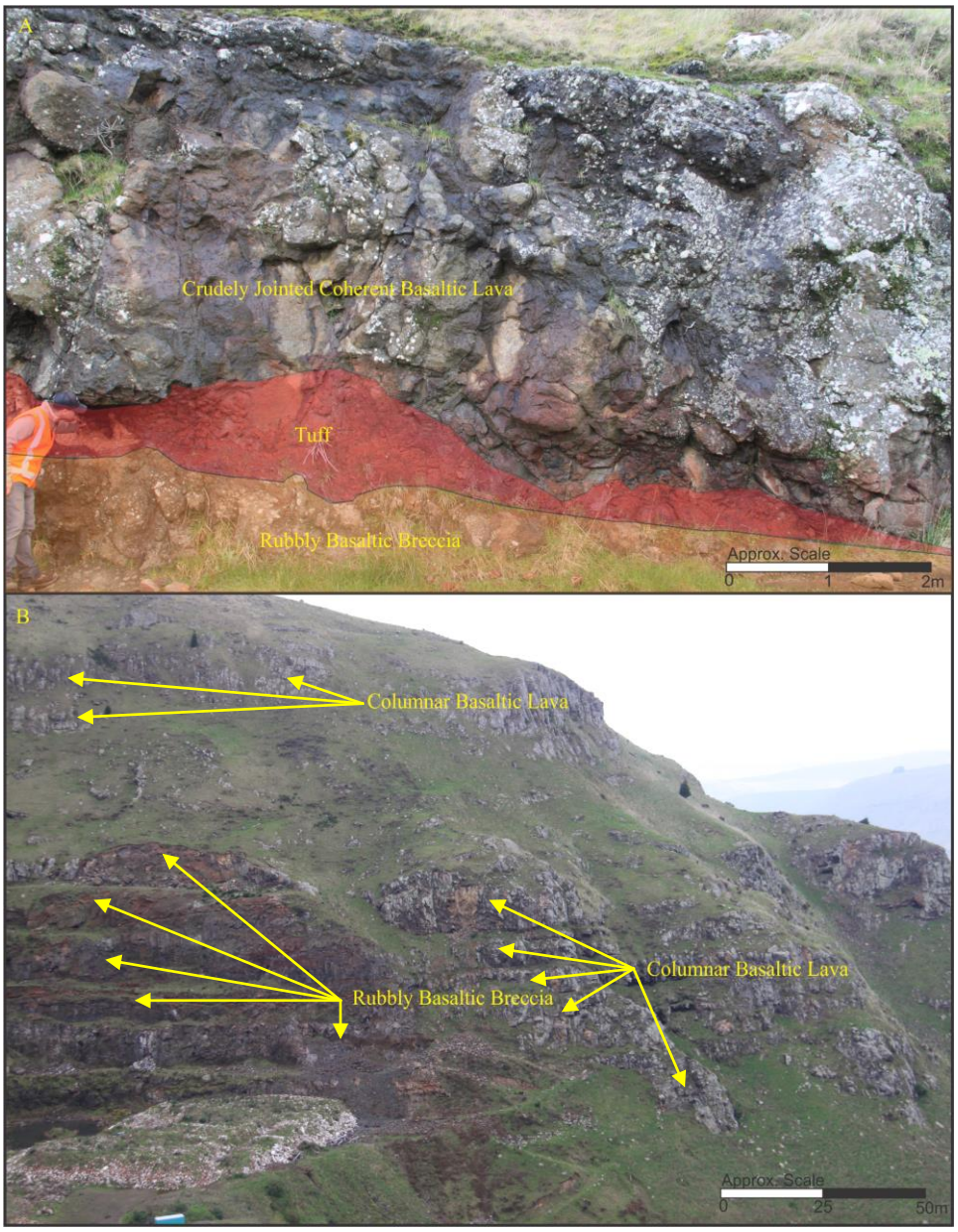

Figure 2.3: Field photographs of Variably Jointed Coherent Basaltic Lava. Note: coherent lava flows can be several hundred meters in flow length and >25m thick. Note back: a singular lava flow consists of two rubbly breccias (cap and basal) and a coherent lava. Sites: A) Evans Pass Road, Port Hills and B) Evans Pass Quarry, Lyttelton.

2.2.4 Blocky Basaltic Lava

Blocky basaltic lava in Chalmers Track is laterally continuous for ≥100m. Basaltic blocks/fragments range in size from a few centimetres to >half a meter. The blocky basaltic lava unit is comprised of a clay rich groundmass and basaltic fragments/blocks which range in size from a few centimetres to a half a meter in diameter (Figure 2.4).

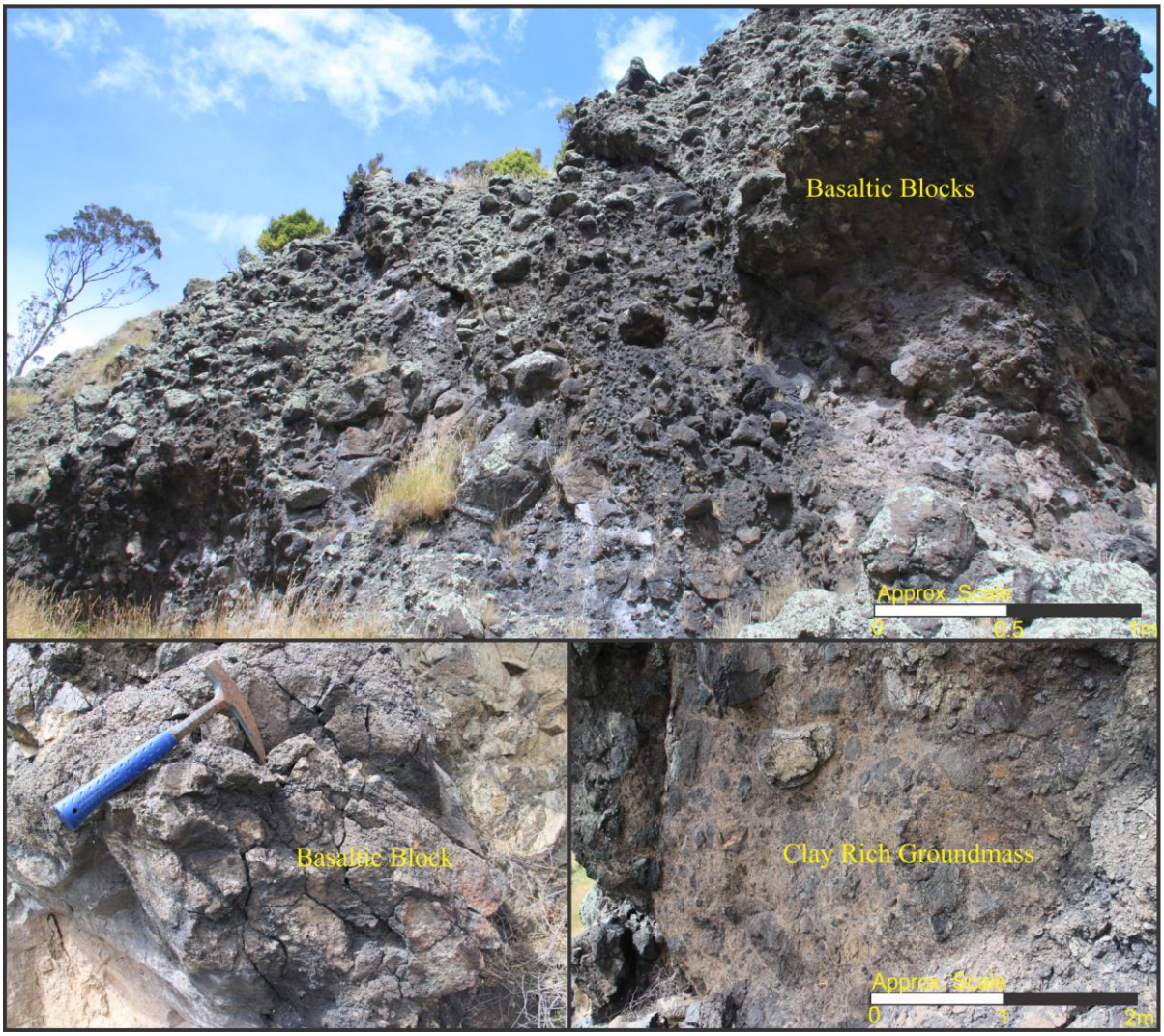

Figure 2.4: Field photograph of Basaltic Blocks. Note: basaltic blocks vary in size from approximately 5cm up to 0.5m. Site: Chalmers Track, Lyttelton.

2.2.5 Basaltic Dyke

Basaltic Dyke observed below Worsley Hill along the Summit Road is brecciated in places and features a tight cubic (approximately right angled) jointing pattern (Figure 2.5). The jointing pattern has resulted in the formation of cubic blocks. The dyke is also highly porphyritic and vesicular near the joints.

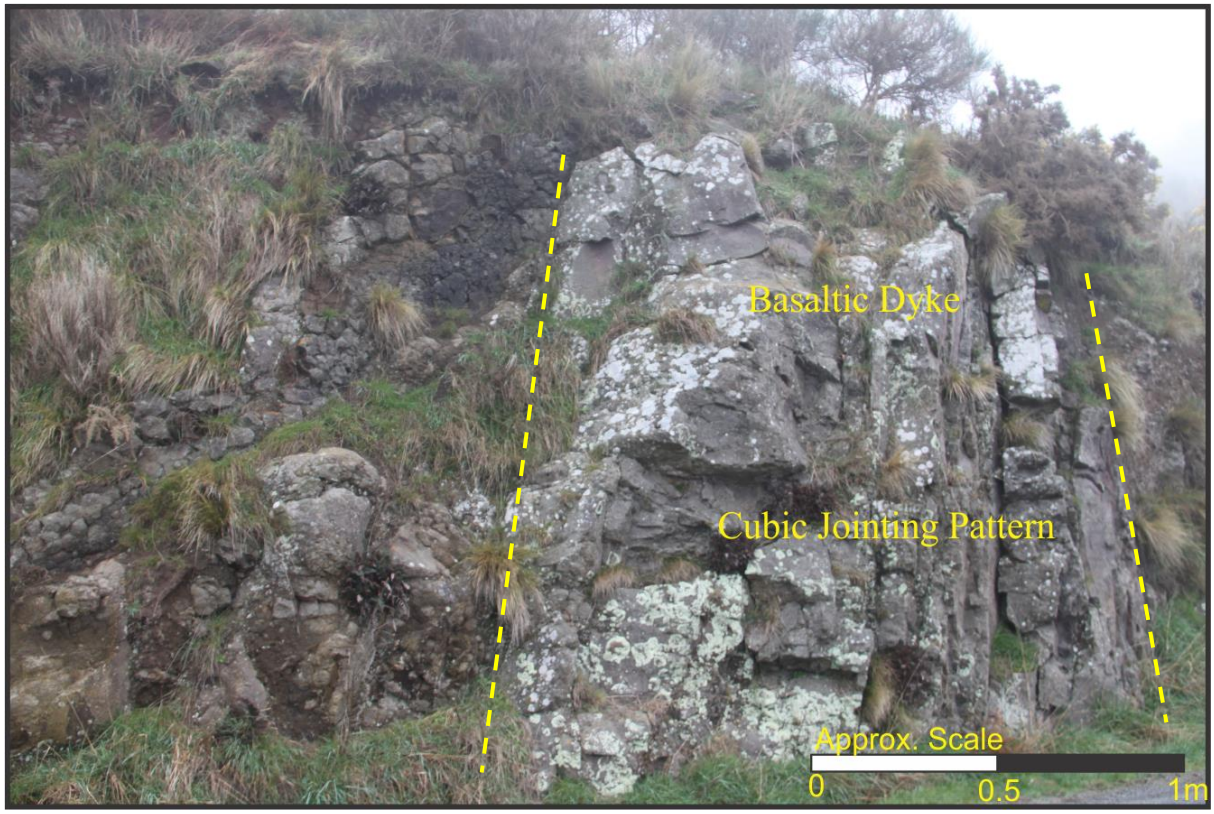

Figure 2.5: Field photograph of Basaltic Dyke. Yellow dashes indicate dyke boundary. Note: closely spaced approximately right angled jointing pattern resulting in block formation and dyke thickness. Site: Worsley Hill Spur, Port Hills.

2.2.6 Vesicular Basaltic Lava Bomb

Most of the observed basaltic lava units are vesicular to some varied degree. However, highly vesicular (≥50%) sections of lava were only observed to occur in 50-150mm thick bands. Several lava bombs were also observed in layers of ash.

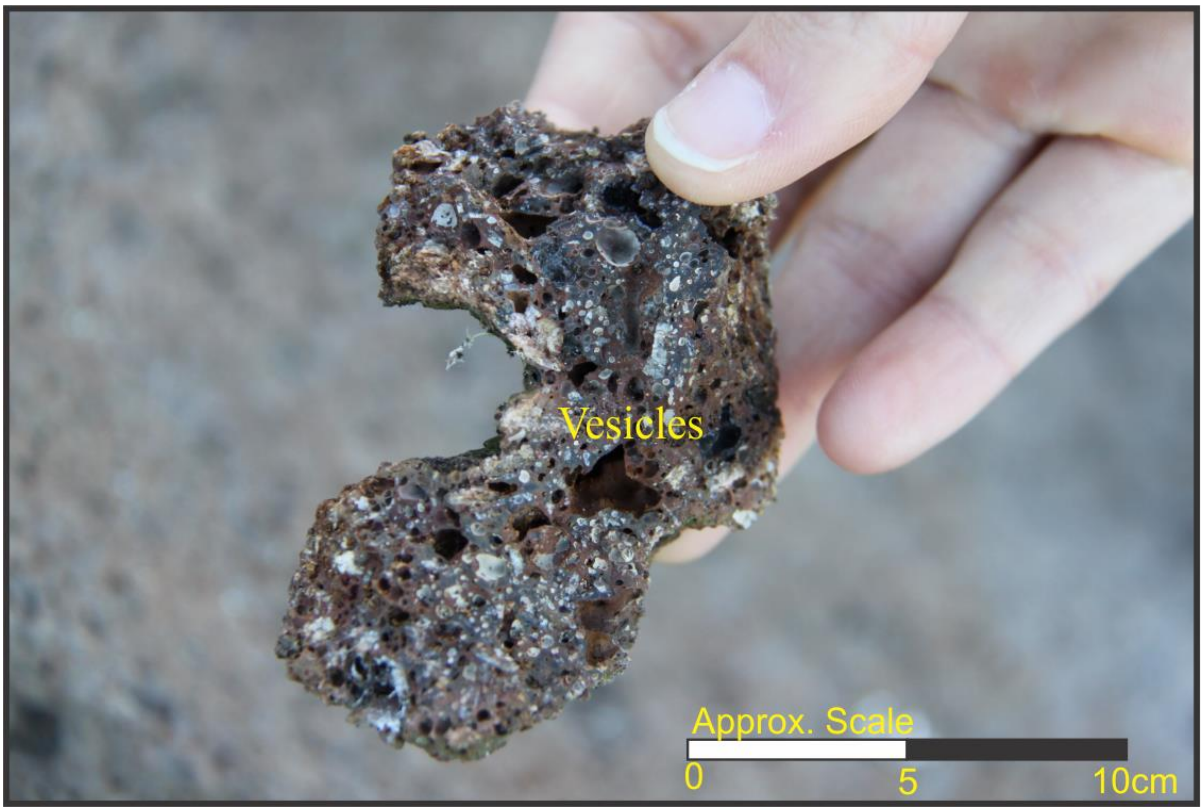

Figure 2.6: Hand specimen of Vesicular Basaltic Lava Bomb. Note: high percentage of vesicles. Site: Summit Road, Port Hills.

2.2.7 Crystal Tuff and Red Ash

Airfall type units observed included tuffs and red ashes (Figures 2.7 and 2.8).Airfall layers frequently occur between or above coherent lava flows (Figures 2.7a and 2.8). Airfall layer thicknesses observed to vary from 0.1m to 5.0m. >5.0m thick deposits may be present, however, are obscured by surface deposits or are at depth. Tuff composition was noted to be highly variable with some tuffs being lithic dominated (Figure 2.8b) and others being phenocryst dominated (Figure 2.7b).

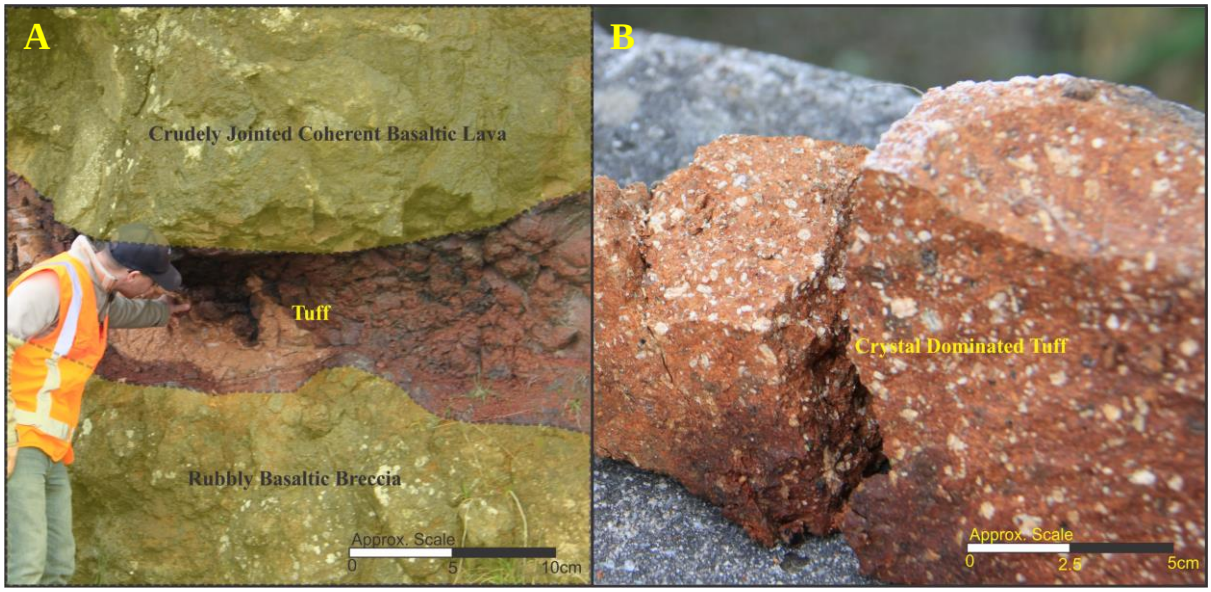

Figure 2.7: Field photographs of Crystal Dominated Tuff. A) airfall derived tuff is situated between a coherent lava and rubbly basal breccia and B) hand specimen of crystal dominated tuff, not the higher percentage of coarse grained phenocrysts. Site: Evans Pass Road.

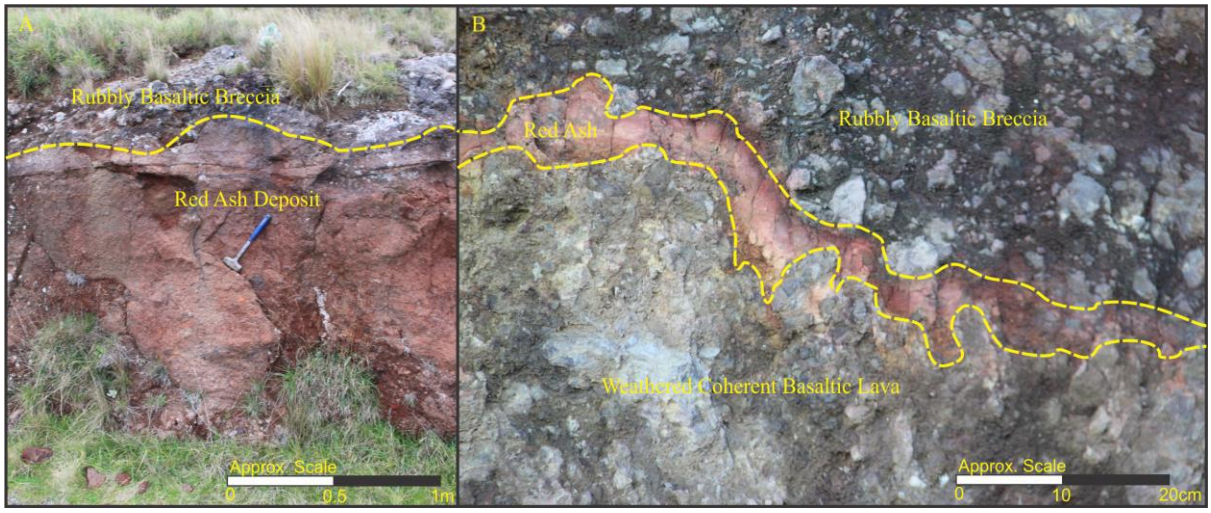

Figure 2.8: Field photographs of Red Ash. Note: ash deposits can vary in size from a few centimetres in thickness to over a meter. A) Rubbly basaltic breccia underlain by a >1m thick lithified red ash deposit. B) Lithified red ash layer between a rubbly basaltic breccia and a weathered coherent basaltic lava flow. Sites: A) Summit Road and B) Dyers Pass Road.

2.2.8 Trachytes (Lava, Dyke and Dome)

Trachytic domes are prominent ridge forming feature, the rock mass is comprised of large columnar blocks (Figure 2.9a).Trachytic dykes intruding through all observable units, indicating late stage intrusion. The dyke features a similar jointing pattern to the basaltic dyke. The tight pattern forms 0.3-0.5m cubic blocks (Figure 2.9b).Trachytic lava observed at top of Mt. Cavendish indicates it as part of a late eruptive sequence (Eruptive Package/Stage IX, as per Hampton, 2010). The trachytic lava features a tight jointing pattern which allows the formation of rectangular blocks (Figure 2.9c/d).

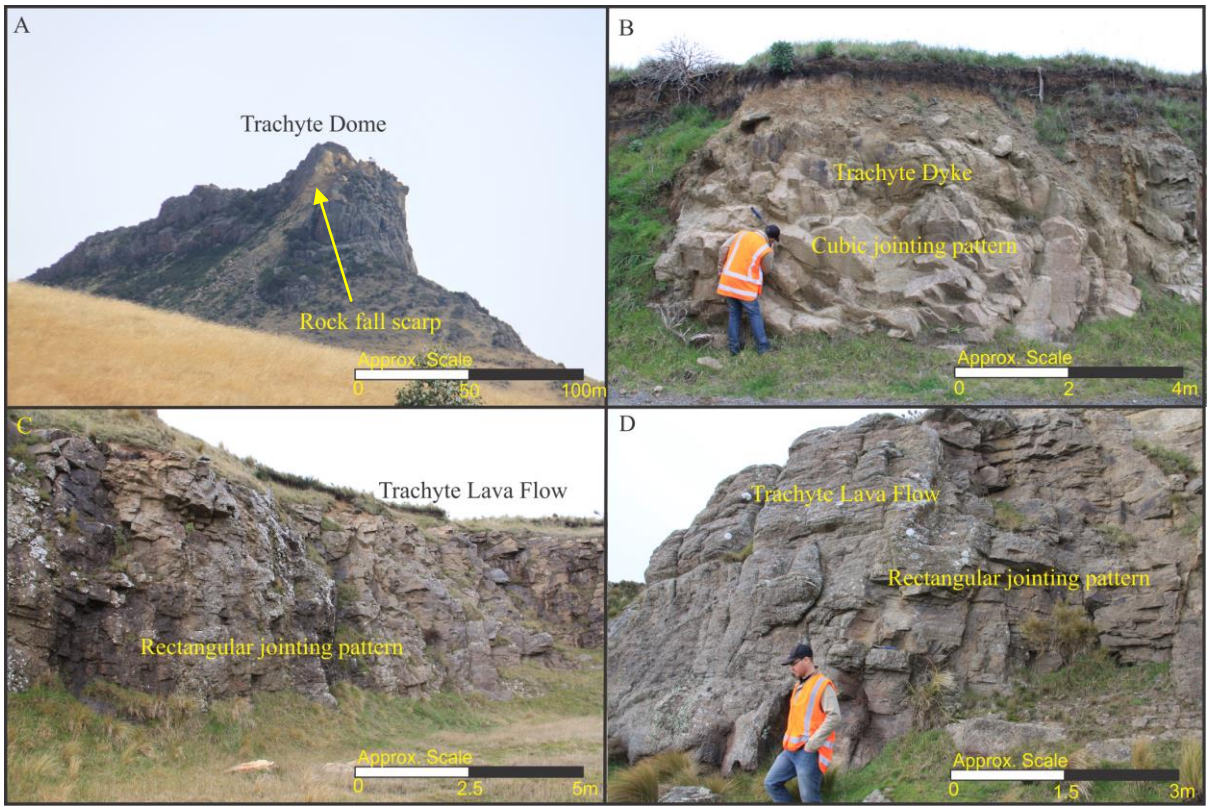

Figure 2.9: Field photographs of Trachytic Units. A) Trachytic Dome, Castle Rock, note rock fall scarp from February 2011 earthquake event. B) Trachytic Dyke, Evans Pass Road, note dyke thickness is >5m and has a cubic jointing pattern similar to the basaltic dyke. C-D) Trachytic lava flow, Mt Cavendish, note rectangular platy jointing pattern, jointing pattern reflects the flow direction.

2.2.9 Faulting/Shear Feature below Worsley Spur

Observed shearing or faulting with approximately 100-150mm of offset next to a basaltic dyke below Worsley Spur along the Summit Road. The basalt is highly brecciated into angular rectangular blocks, no clay gouge was observed. Failure plane is smooth with some evidence of slicken slides.

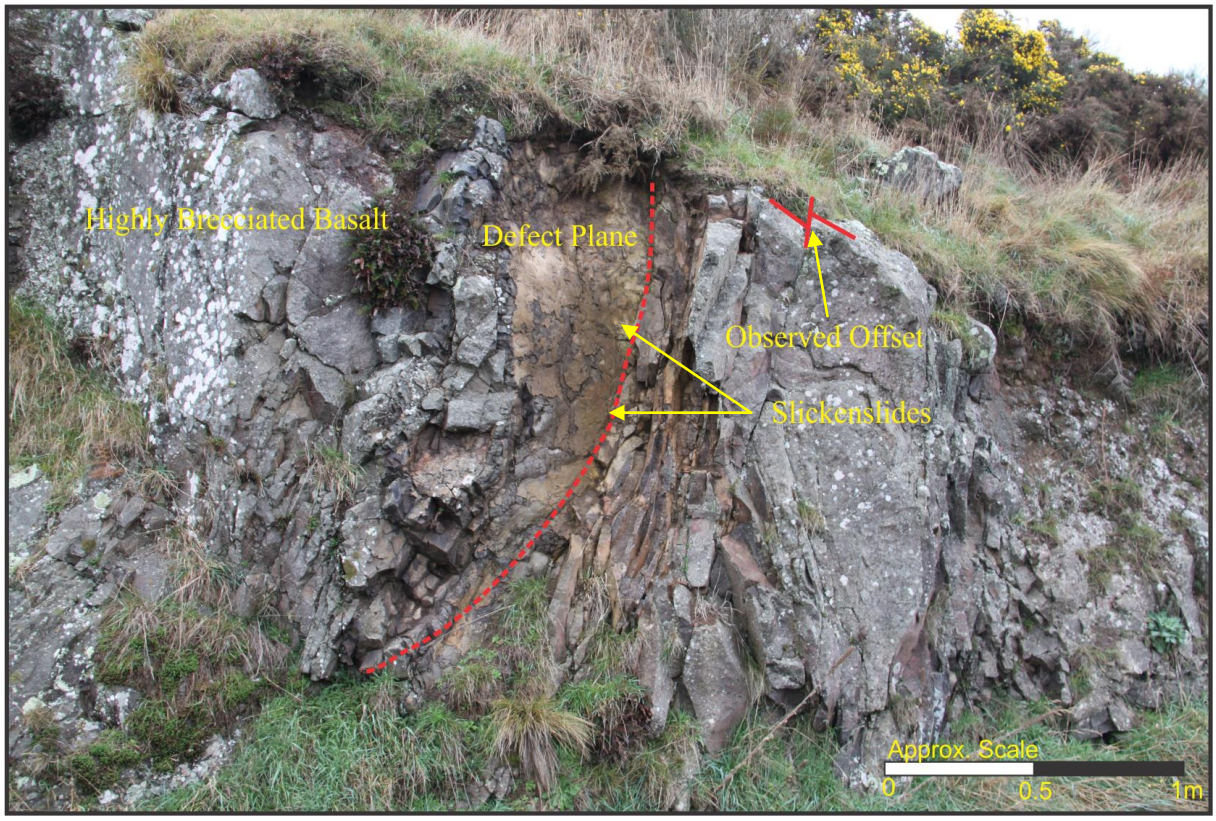

Figure 2.10: Field photograph of observed shear or fault structure. Note: 100-150mm of offset observed. Site: Worsley Spur, Port Hills.

2.2.10 Laharic Deposit (Volcanogenic Conglomerate and Sandstone)

Laharic deposit in Sumner Valley dips at approximately 15°, similar to the most of the other observable flows. Volcanogenic conglomerate is underlain by a volcanogenic tuffaceous sand stone.

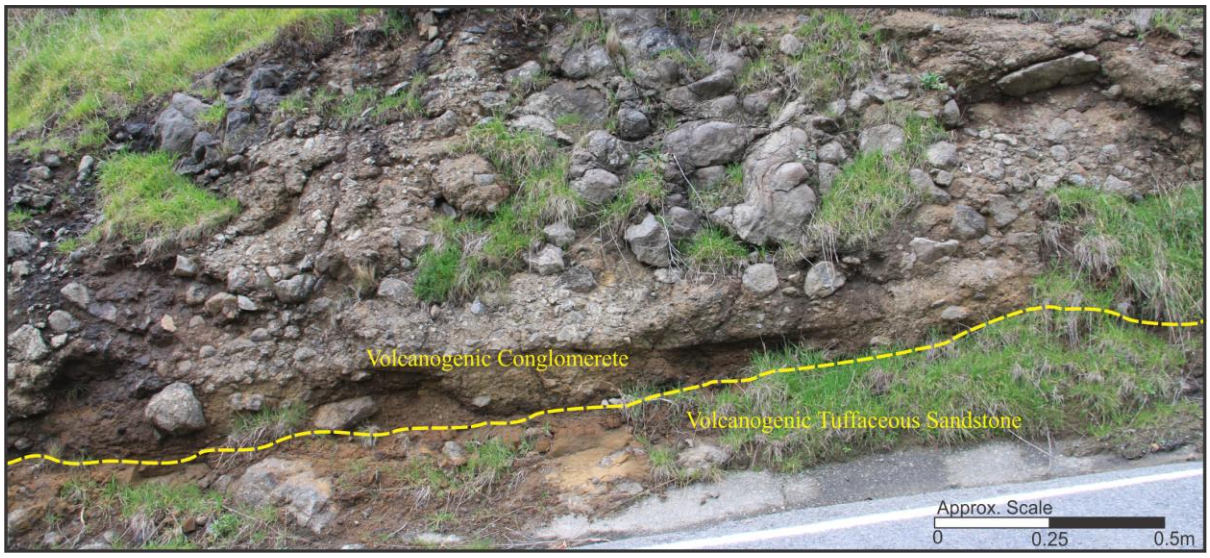

Figure 2.11: Field photograph of laharic deposit in the upper Sumner Valley. Volcanogenic conglomerate is underlain by volcanogenic tuffaceous sandstone. Note: large angular boulders and poor sorting of deposit.

2.3 Engineering Geological Block Model

2.3.1 Engineering Geological Model Overview

The purpose of generating an engineering geological model is to effectively understand, characterise and categorise the nature and properties of a site and its surroundings (Fookes, 1997). An engineering geological model is fundamental for the basis of analysis and design of any engineering project, and consists of four principal components: geological model, structural model, rock mass model and hydrogeological model. The most important aspect of the engineering geological model is the physical geology component; true reflections of ground conditions geological units and the variations within must be understood and accounted for if the model is to be successful and fully utilised. The model must always be objective driven.

A schematic engineering geological model of the Lyttelton Volcanic Complex is presented in Figure 2.12. The model has been ground truthed by field observations presented in the previous section. The model is further informed through three machine borehole cores to a

depth of 35m bgl from Sumner (courtesy of Coffey Geotechnics) and by information gained from previous studies, including Hampton (2010), Shelley (1987) and Sewell (1985).

2.3.2 Applications of Engineering Geology Model

An engineering geological block model was developed to show a representative section of the Lyttelton Volcanic Complex (Figure 2.12), with the main purpose of the model to illustrate the spatial relationship of volcanic lithologies, and to inform the selection of materials for characterisation of intact rock mass characteristics on a large scale. Some key features to observe are the repetitive sequences of coherent basaltic lava flows with cap and base rubbly basaltic lava flow breccia. Also worth noting are the frequency and occurrence of materials such as the laharic/volcanogenic and trachytic deposits, which, although important, do not appear as frequently as basaltic flows based on field observations. It should be noted that rock mass characteristics have been omitted from the block model as they are included in the material characterisation in Chapter 4 and 5. Discontinuities and defects have also been excluded as they are strictly site specific and intact rock properties are the main focus of this study.

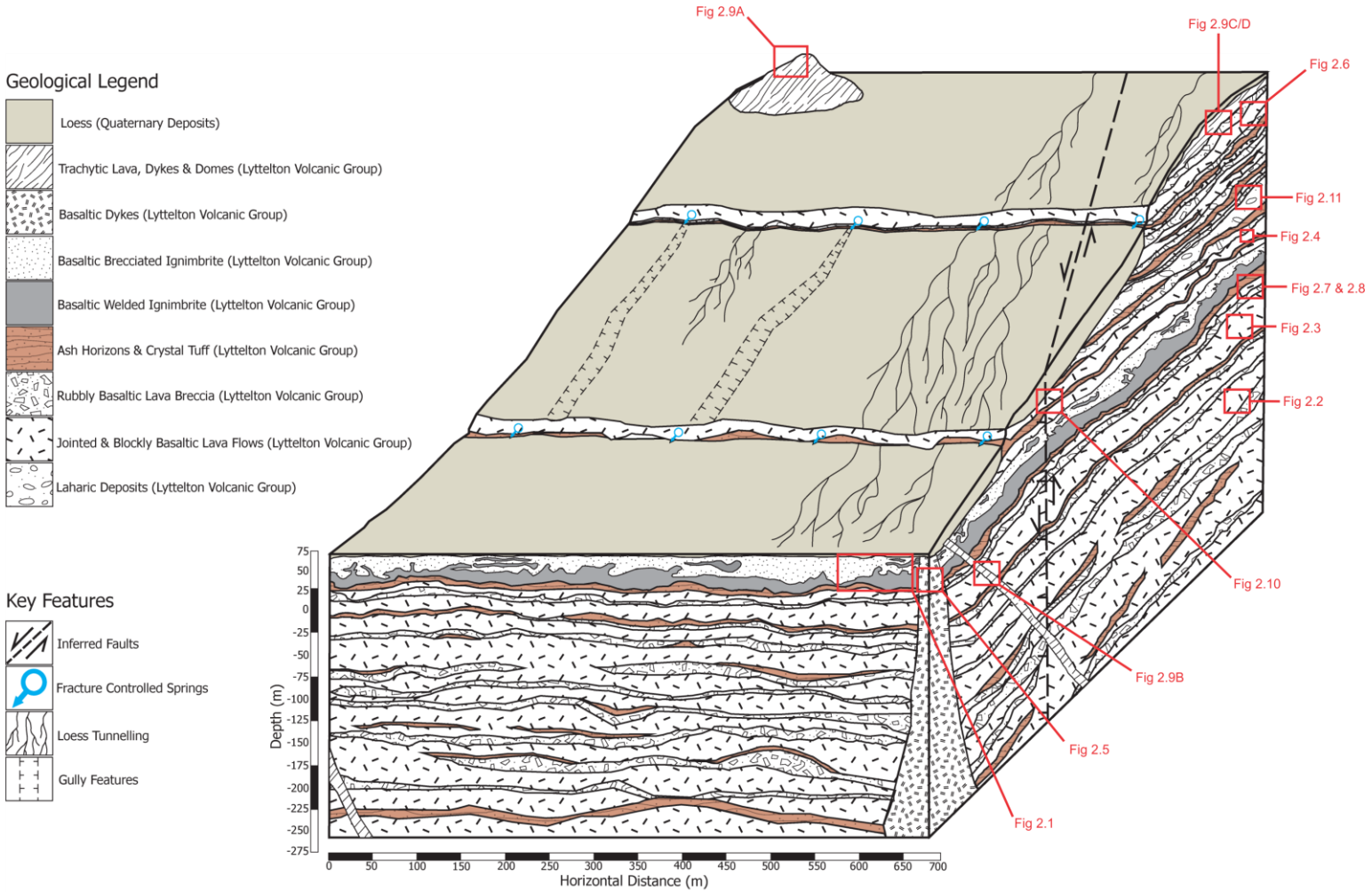

Figure 2.12: Engineering Geology Block Model of the northern flanks of Lyttelton Volcanic Complex. Engineering geological model incorporates three key input parameters; structural, hydrogeological, and geological. Note fault trace is indicative, and do not displace recent surface deposits. Faults are suggested to have occurred contemporaneously with volcanism (Ring and Hampton 2012). Vertical fault displacement is minimal (<0.5m, Hampton 2010) and hence cannot be shown at this scale. Red boxes refer to specific ground truthing figures in Chapter 2.

2.3.3 Key Features of the Lyttelton Volcanic Complex Model

In generating the Lyttelton Volcanic Complex model, it was vital to illustrate the significance of the volcanic structures/features within the field area and to show the importance of the unit relationships (contacts, morphology etc). The detailed objectives of the model are listed below:

- Illustrate importance of spatial and stratigraphic unit relationships e.g. repetitive alternation of coherent basaltic lava flows and rubbly lava flow breccia.
- Display all the expected rock types and lithological units in the Lyttelton Volcanic Group.
- Display hydrogeological features e.g. fracture-controlled springs.
- Display surficial features e.g. loess tunnel gullying.
- Display relevant large scale structural features e.g. faults.
- Display relative unit thicknesses based on field observations where applicable.
- Display correct structural geometry (10-15° dip of lava units away from the eruptive centre) as per the layered volcano model.
- Display variability in layer thicknesses.
- Display respective loess thicknesses (≤1-25m).

Due to the constrained geological information of the interior of the Lyttelton Volcanic Complex, with only road cuts, cliff faces and surface outcrops to inform the model, several inferences were made in order to generate some sections of the model. The inferences that were made are listed below:

- Lateral continuity of the welded and brecciated basaltic ignimbrite units away from the volcanic source and across the slope.
- Units below sea level datum continue to alternate between coherent basaltic jointed/massive/blocky lavas and rubbly cap and base basaltic lava flows with red ash and tuff horizons as per field observations of units exposed in cliffs, road cuts and outcrops around the Port Hills. Reviewed Coffey Geotechnics boreholes from Sumner to a depth of 35m bgl suggest that this is the case.
- Trachytic dome topography.

2.4 Port Hills Geotechnical Unit Classification

During of field reconnaissance and sample collection, a high degree of variation was observed in the visible rock types (e.g. weathering grade, alteration, vesicularity, crystal and lithic/clast percentage and composition). Through observation of the variability within the units in the field, it was evident that detailed classification and description of volcanic units was required. Simply identifying units with broad terms, such as basalt, trachyte and tuff was inadequate to achieve the main goal of this thesis, to "create a robust data set on the lithologies of the Lyttelton Volcanic Group". The variations in lithological composition, method of emplacement and post-emplacement mechanisms had to be taken into account. Therefore a more detailed classification scheme would be needed.

In order to account for the variations within the volcanic units, further classification was necessary and, in doing so, increased the effectiveness, applicability and quality of the data set produced from this study. Further classification is made by dividing each main geological unit into sub-units, representing the natural geological variance and forming the basis and framework for material characterisation and geotechnical testing. For example, Lyttelton Volcanic Group basaltic lavas can be separated into seven sub-units: rubbly basaltic breccia flows, coherent basaltic lava flows (unweathered, slightly-moderately weathered and highly-completely weathered), blocky basaltic lava, basaltic dykes and highly vesicular basaltic lava bombs. It is worth noting that among all of the Lyttelton Volcanic Group units a series of sub-divisions are possible.

Macro-scale photographs presented in Figure 2.13 display two different lithologies: tuff and basaltic ignimbrite. Figure 2.13A and 2.13B display two different tuffs. The two most distinct differences were crystal and lithic/clast percentages. Tuff A has a very high lithic content (>50%) with a low percentage of phenocrysts. Whereas, Tuff B has a very high coarse grained phenocryst percentage. In addition, some tuffs displayed an almost equal percentage of both crystals and lithics. Figure 2.13C and D display a moderately welded basaltic ignimbrite (C) and a highly welded basaltic ignimbrite (D). Ignimbrite welding is noted to be transitional. The ignimbrite sample in C is less welded than sample D with clearly defined clast boundaries. Sample D has no large clasts and the groundmass is highly welded and coherent.

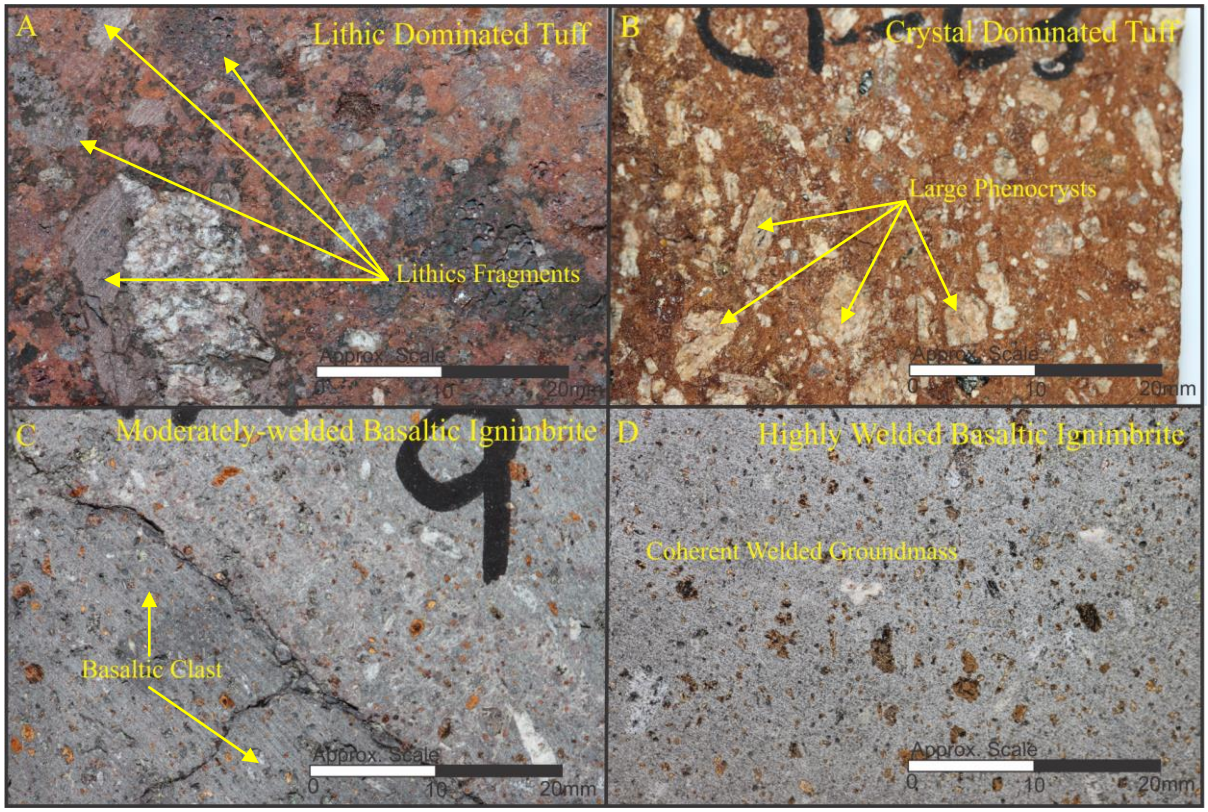

Figure 2.13: Macro-scale photographs of four Lyttelton Volcanic Group units displaying compositional variations. A) Lithic dominated tuff (airfall unit), B) crystal dominated tuff (airfall unit), C) moderately welded basaltic ignimbrite (pyroclastic density current unit) and D) highly welded basaltic ignimbrite. Note: A and B are both tuffs, which when compared to each other are compositionally dissimilar, a similar trend to C and D with regards to degree of welding.

Each identified unit is expected to behave mechanically in a different way in terms of strength, durability, failure mechanism and response to the effects of the interaction with ground/surface water. Figure 2.13 has highlighted some of the differences between two similar units and illustrates the need for further classification of the volcanic units. Thus, the advantage to subdividing units is such that these variations can be accounted for even if the difference is only slight (e.g. compressive strength difference between a highly welded basaltic ignimbrite and a moderately welded basaltic ignimbrite or between a crystal dominated tuff and a dominated lithic tuff).

2.5 Geotechnical Characterisations

All main geological units observed in the field displayed some form of variation (e.g. composition, weathering grade, degree of lithification, welding, jointing pattern). These variations resulted in the need for such a classification model. The Port Hills Geotechnical Unit Classification model, (Table 2.1) was developed to address the need for further classification of the lithologies and the associated variations observed in the field during reconnaissance and sample collection.

The most significant component of Table 2.1 is the unit subdivisions; these sub-units represent the geotechnical units which have been selected for characterisation in this thesis. The unit subdivisions are based on composition, method of emplacement (e.g. intrusion/dyke, lava flow) and, where possible, weathering grade. As previously geological units with varying compositions and properties are expected to have different geotechnical characteristics and behaviours. The geological and engineering geological data gained from the testing of these units represent the primary objective of this thesis. Each unit is individually described in terms of its expected strength, durability and interaction with groundwater.

Material components which appeared to vary considerably were the lithic and crystal content amongst the airfall units (Figure 2.13), frequency of scoriaceous clasts with the red ash and the grade of welding/lithification associated with the basaltic ignimbrite (Figure 2.13). To overcome this, both the airfall tuffs and basaltic ignimbrite units were allocated sub-units to ensure that any mechanical variation was accounted for. The red ash was difficult to separate into scoriaceous and non-scoriaceous due to frequency of the clasts and natural vesicles; as a result the number of testing samples was increased from the standard 5-10 samples to 25 in the attempt to empirically account for the scoria clasts/vesicularity. Weathering grades became another important factor to consider, however, due to time restrictions they could not be thoroughly investigated for each unit. Weathering grades were considered for the basaltic lavas as numerically they make up the majority of the Lyttelton Volcanic Group thus were prioritised above some of the materials which appear less frequently. In total 18 materials are individual considered and tested.

Table 2.1: Lyttelton Volcanic Group Geotechnical Unit Classification displaying the important break down of the main lithological units into sub-units. This break down is important as the subdivided units ultimately will affect the mechanical properties of the material. Unit codes are designated by the bolded letters before the material name. Each unit is then described and commented on regarding the presence of defects and discontinuities, strength and durability and the effects of ground and surface water. Note these observations have been made on the basis of observations in the field and during sample preparation.

Lyttelton Volcanic Group Geotechnical Unit Classification (Pre-Testing)						
Main Unit	**Sub-Unit**	**Secondary Sub-Unit**	**Geotechnical Characteristics**			**Material Source Zone (For Testing)**
			Discontinues and Defects	**Strength and Durability**	**Groundwater and Surface**	
T – Trachyte (Lyttelton Volcanic Group)	**TD** – Trachyte Dykes	N/A	-Cubic pattern joints with fractures	-Expected high strength -Compressible vesicular void spaces	-Groundwater controlled alteration and weathering below ground level	-Evans Pass Road
	Td – Trachyte Domes	N/A	-Not Investigated	-Not Investigated	-Not Investigated	N/A-Safety Imposed Access Restrictions to Castle Rock
	TL – Trachyte Lava	N/A	-Rectangular pattern joints with fractures	-Expected high strength	-Groundwater controlled alteration and weathering below ground level	-Summit Road
IG – Basaltic Ignimbrite (Lyttelton Volcanic Group)	**IGB** – Brecciated/ Un-welded Ignimbrite (End Member)	N/A	-Massive -Defects prevalent at clast/lithic groundmass boundary	-Friable, crumbly -Expected very low - low strength matrix with high strength clasts/lithics -Groundmass controlled	-Erosion and disaggregation observed due to ground/surface water -Expected to disaggregate with addition of water	-Redcliffs -Quarry Road
	IGW – Welded Ignimbrite (End Member)	**IGMW** – Moderately Welded Basaltic Ignimbrite	-Defects prevalent at clast/lithic groundmass boundary	-Expected moderate strength matrix with high strength clasts/lithics	-Erosion and disaggregation observed due to ground/surface water	-Redcliffs
		IGW – Highly Welded Basaltic Ignimbrite	-Columnar jointed -Cooling joints	-Expected High strength	-Groundwater controlled alteration and weathering below ground level	-Redcliffs
A – Air Fall Volcanics (Lyttelton Volcanic Group)	**RA** – Red Ash	N/A	-Lithified -Massive -Fractures	-Low slaking and disaggregation potential due to lithification/welding -Expected medium strength (welded) -Compressible scoriaceous clasts -Compressible vesicular void spaces	-Erosion and disaggregation observed due to ground/surface water -Expected to disaggregate slowly with addition of water due to welding	-Godley Head Road
	CT – Crystal Tuff	**CTC** – Crystal Dominated Tuff	-Massive -Fractures	-Friable, crumbles under pressure -Prone to slaking and disaggregation -Expected low strength -Groundmass controlled -Compressible vesicular void spaces	-Erosion and disaggregation observed due to ground/surface water -Expected to disaggregate when saturated.	-Redcliffs -Evans Pass Road
		CTL – Lithic Dominated Tuff	-Massive -Fractures	-Friable, crumbles under pressure -Prone to slaking and disaggregation -Expected low strength -Groundmass controlled -Compressible vesicular void spaces	-Erosion and disaggregation observed due to ground/surface water -Expected to disaggregate when saturated.	-Evans Pass Road
B – Basaltic Lavas (Lyttelton Volcanic Group)	**RCB**– Rubbly Lava Flow Breccia (Cap and Basal)	N/A	-Massive, rubbly -Fractures	-Expected moderate - high strength -Groundmass controlled -Brecciated	-Groundwater controlled alteration and weathering below ground level	-Marriner Street, Sumner
	BL – Coherent Basaltic Lava	**BLUW** – Unweathered coherent Basaltic Lava	-Columnar jointed -Fractures	-Expected very high strength -Minor compressible scoriaceous clasts -Compressible vesicular void spaces	-Groundwater controlled alteration and weathering below ground level	-Evans Pass Road
		BLSM – Slightly – moderately weathered coherent Basaltic Lava	-Columnar jointed -Fractures	-Expected moderate – strength -Compressible vesicular void spaces	-Groundwater controlled alteration and weathering below ground level	-Marriner Street, Sumner
		BLHC – Highly – completely weathered coherent Basaltic Lava	-Massive -Clay/altered material infill of joints and fractures	-Expected very low strength -Slaking potential due to clay mineral alteration	-Groundwater controlled alteration and weathering below ground level	-Marriner Street, Sumner
		BLV – Highly Vesicular Basaltic Lava Bomb	-Fractures -Highly vesicular	-Expected low-medium strength	-Groundwater controlled alteration and weathering below ground level -High porosity due to vesicular texture	-Godley Head Road
	Table 2.1 is continued over the page					

	BD – Basaltic Dykes	N/A	-Cubic pattern joints with fractures	-Expected high strength	-Groundwater controlled alteration and weathering below ground level	-Marley Hill / Worsley Spur
	BBL – Blocky Basaltic Lava	N/A	-Blocky -Defects prevalent at clast/lithic groundmass boundary	-Expected moderate – high strength -Groundmass controlled	-Groundwater controlled alteration and weathering below ground level	-Chalmers Track, Lyttelton
L – Laharic Deposits (Lyttelton Volcanic Group)	**VC** – Volcanogenic Conglomerate	N/A	-Defects prevalent at clast/lithic matrix boundary	-Expected very weak – weak strength -Friable -Matrix controlled	-Groundwater controlled alteration and weathering below ground level	-Sumner Pass Road
	VTS – Volcanogenic Tuffaceous Sandstone	N/A	-Massive	-Expected very weak strength -Expected low durability, disaggregation due -Friable	-Expected to disaggregate with addition of water	-Sumner Pass Road

2.6 Synthesis

This chapter has combined a series of field observations to inform the development of the engineering geological block model of the Lyttelton Volcanic Complex, and introduces the Port Hills/Lyttelton Volcanic Group Geotechnical Unit Classification.

Field observations were used in conjunction with information gained from previous research to inform and ground-truth the engineering geological block model. The main purpose of the engineering geological block model is to display a representative section of the Port Hills, clearly illustrating the spatial relationship of all the volcanic lithologies present within the field area and to inform the selection of materials for testing.

The variability of the volcanic lithologies observed both during field reconnaissance, sample collection and in sample preparation highlighted the need for further refinement to the classification of volcanic units. To address this need, the Lyttelton Volcanic Group Geotechnical Unit Classification was developed and detailed. Unit classification model demonstrates the breakdown of the volcanic units into sub-units. The geotechnical characterisation model allowed a structured approach in determining a final list of materials that would be characterised in this study. Furthermore, the model forms the foundation and framework for the following three chapters.

Additionally, both the engineering geological block model and geotechnical classification model can be utilised as a framework for future projects involving the Lyttelton Volcanic Complex or adapted for other igneous complexes.

Chapter 3 outlines the methodology for which samples were collected, prepared and geotechnically tested. Chapters 4 and 5 present the results of the rock mechanics testing and thin section analysis and form the mainstay of the dataset this thesis presents.

CHAPTER 3 - Rock Mechanics Testing Procedure and Descriptive Methodology

3.1 Introduction

This chapter outlines methodologies used to undertake sample recovery and collection, sample preparation for testing, thin section/hand specimen analysis, and rock mechanics testing. Rock mechanics testing philosophy follows '*The complete ISRM suggested methods for rock characterisation, testing and monitoring: 1974-2006*' as outlined by the International Society for Rock Mechanics (Ulusay and Hudson, 2007) with the only deviation from the ISRM methodology being the rock core sample length to diameter ratio following the ASTM, (2004). This chapter examines the New Zealand Geotechnical Society (NZGS) (Burns *et al.*, 2005) rock mass classification scheme and its usage within this study. In light of this examination, a detailed engineering geological description for igneous rocks has been proposed for the purpose of detailing and describing igneous materials included in this study.

3.2 Sample Collection

Sample collection took place between July and September 2013. Prior to sample collection, Lyttelton Volcanic Group lithologies were classified into sub-groups (Chapter 2, Table 2.1). Samples were collected firstly on the basis that recovery could be undertaken safely without undue risk (given origin, seismic activity and access issues) and secondly by the size of the sample (Figure 3.1a/b). Samples needed to be intact, reasonably devoid of any large defects with an ideal size of approximately 300mm × 200mm × 200mm to achieve a good number of drilling positions. Large samples were collected for in laboratory coring, with smaller hand specimens for thin section analysis and descriptive purposes. Sample orientation and position of in-situ samples was recorded and preserved wherever possible (Refer to Figure 3.1c). In-situ samples where possible were chiselled out along joints in order to avoid damage to the sample during recovery (Figure 3.1d).

Sample Collection Procedure

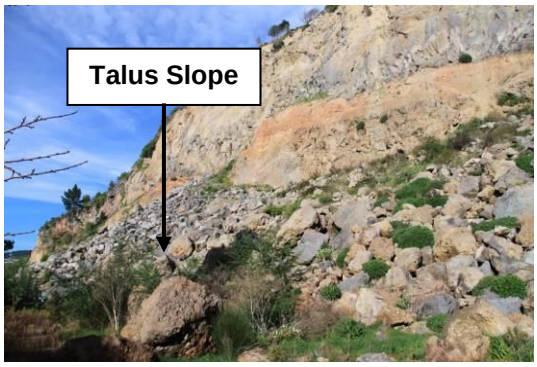

Figure 3.1a: Source zones were first scoped for safety, in this instance at Redcliffs, and samples were only recovered from the base of the talus apron.

Figure 3.1b: Samples were only recovered at the base of outcrops in order to avoid slips, trips or falls.

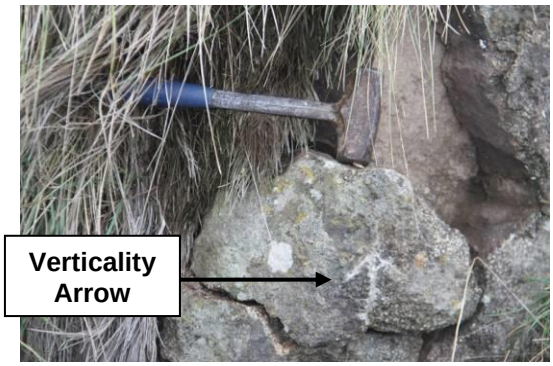

Figure 3.1c: Arrow carved into in-situ samples to preserve vertically for drilling purposes. Preservation of verticality was maintained wherever possible.

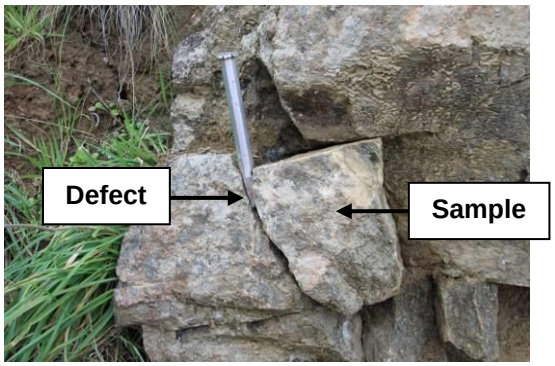

Figure 3.1d: In-situ samples were chiselled out along joint planes in order to avoid potential damage to the sample.

Figure 3.1: Sample Collection Procedure illustrated with annotated images. A and B) Safety check of source zone for hazards, C) preservation of stratigraphic verticality for drilling purposes whenever possible, D) in-situ samples were recovered by chiselling open defect planes to lever the samples out intact and without any unnecessary damage instead of hammering them loose with a rock hammer/mallet.

3.3 Igneous Rock Descriptive Method (NZGS, 2005)

3.3.1 Basis of Description

The NZ Geotechnical Society 2005 soil and rock descriptive method, covers both soil and rock descriptions and ultimately forms the standard for all engineering geological description in New Zealand (Burns *et al.*, 2005). The purpose of this guideline is to allow for the identification and communication of soil and rock properties that are of engineering significance. An example of this scheme is illustrated in Table 3.1.

Table 3.1: Engineering geological description of a columnar jointed Lyttelton Volcanic Group Basalt using the NZGS Guideline 2005 (Burns *et al.*, 2005). The table displays all the required engineering geological components present in the NZGS rock classification scheme.

NZGS 2005 Guideline Components	
Component	**Example**
Visual Characteristics	
Weathering Grade	Slightly weathered (SW)
Colour	Dark grey
Fabric	Massive
Bedding	Not observed
Rock Name	BASALT
Qualifying Paragraph	
Strength	Very strong
Discontinuities • Orientation • Spacing • Persistence • Roughness • Wall Strength • Aperture • Infill • Seepage • Number of Sets • Block Size and Shape	Closely spaced joints, smooth, narrow, no infill, blocks are medium sized, columnar.
Geological Information	[LYTTELTON VOLCANIC GROUP]
Full Description	
Slightly weathered, dark grey, massive, BASALT; very strong, closely spaced joints, smooth, narrow, no-infill, medium columnar blocks [LYTTELTON VOLCANIC GROUP].	

3.3.2 Method Limitations

At the outset of this study, the NZGS classification scheme was used for describing volcanic rock cores, hand specimens and features. It quickly became apparent that many key volcanic attributes for the volcanic units in this thesis could not be accounted for or adequately described using the NZGS classification scheme. The use of the NZGS descriptive method did not account for unit variability or details required to achieve the outcomes of this study.

Key volcanic characteristics that are not included in the NZGS scheme are (but are not limited to) textures, vesicularity, groundmass to crystal/clast ratio, mineralogy, composition and volcanic context. The guideline also does not provide an example of a fully classified volcanic rock using this system. Thus, any volcanic rock or volcanic feature described with the NZGS scheme would be, from a volcanological perspective, very rudimentary. From an

engineer's perspective, the concern mainly lies with weathering grade, strength and defects in a rock mass as the key features. However, the method of emplacement, resulting textural and alteration properties and other volcanic components may play a vital part in the mechanical behaviour of a volcanic rock (which this thesis investigates). If the scheme, however, were to be expanded to enable description of volcanic features and characteristics it could enable engineers to develop more representative ground models and arrive, therefore, at better outcomes.

It should be noted that the NZGS guideline is geared towards engineering application, therefore attention is paid to the degree of weathering and presence of discontinuities within the rock mass, which will influence to an extent the mechanical behaviour and failure type of the material. Hence the NZGS scheme was not designed for the purposes this thesis requires.

As the NZGS guideline does not satisfy the needs of the study it was necessary to devise a scheme which covered both engineering geological and volcanic aspects in sufficient detail. Before a scheme could be developed it was fundamental to understand what the essential volcanic aspects which the NZGS classification scheme did not address.

3.3.3 Review of Key Volcanic Features

A review of volcanic features and properties was conducted during sample collection and preparation, resulting in the collation of terms presented in Table 3.2. The characteristics listed in Table 3.2 combined with a descriptive engineering geological framework such as the NZGS would allow for a volcanic material to be fully characterised with sufficient geological information such as the type of feature, composition, mineralogy, textures and macro and micro scale structure.

Table 3.2 shows the important volcanic properties for the volcanic deposits and formations that were observed on the Port Hills. The formations and deposits are broken down into individual features with corresponding key characteristics. Key volcanic properties and descriptors in Table 3.2 noted in italics are considered important this study. This is because these volcanic characteristics are most likely determined by emplacement and post emplacement mechanisms which may influence geotechnical behaviour. For example, lithic groundmass boundaries may act as likely propagation defect surfaces during strength testing and high percentages of phenocrysts in a sample may influence strength characteristics

which, when combined with a trachytic texture (phenocrysts are aligned in the direction of flow) parallel to compression may act to decrease the strength of a sample.

Table 3.2: Volcanic Units of the Port Hills showing key properties which require attention during characterisation. Properties in italics indicate key properties to be utilised in the detailed engineering geological igneous rock descriptive scheme featured in Table 3.3 which are not part of the NZGS classification scheme.

Volcanic Units of Port Hills		
Volcanic Deposit / Formation	**Volcanic Feature**	**Key Volcanic Properties / Descriptors**
Intrusives (Lyttelton Volcanic Group)	Dykes	*Crystal alignment*, jointing, thickness, *alteration*
	Domes	*Crystal alignment*, jointing, *alteration*
Basaltic Ignimbrite (Lyttelton Volcanic Group)	Brecciated/ Un-welded Ignimbrite (End Member)	*Crystal alignment*, jointing, *clasts*, *groundmass*, *crystal content*, *welding*, *vesicularity*, thickness
	Welded Ignimbrite (End Member)	Crystal alignment, jointing, *clasts*, *groundmass*, *crystal content*, *welding*, thickness
Air Fall (Lyttelton Volcanic Group)	Red Ash / Paleosols	*Crystal alignment*, jointing, *clasts*, *groundmass/matrix*, *crystal content*, induration, thickness
	Crystal/Lithic Tuffs	*Crystal alignment*, jointing, *clasts*, *groundmass/matrix*, *crystal content*, induration, thickness
Lavas (Lyttelton Volcanic Group)	Rubbly Cap/Base Breccia	Thickness, *clast size*, angularity, *vesicularity*, *alteration*, induration, *welding*, thickness
	Coherent Jointed Lava	*Crystal alignment*, thickness, jointing, *groundmass*, *crystal content*, *vesicularity*, *alteration*, induration, thickness, cooling margins, columnar jointing, joint spacing
	Blocky Lava Flow	*Groundmass clast interaction*, *ratio of ground mass to clasts*, alteration, welding, thickness, angularity
Lahar / Debris Flow (Lyttelton Volcanic Group)	Tuffaceous Sandstone	*Groundmass/matrix*, thickness, angularity of individual grains
	Conglomerate	*Groundmass/matrix*, *clasts*, *groundmass and clast boundary interaction*, *ratio of groundmass to clasts*, thickness, *alteration*

3.3.4 Detailed Engineering Geological Igneous Descriptive Scheme

The Detailed Engineering Geological Igneous Rock Descriptive Scheme is presented in Table 3.3. This scheme has been developed utilising key volcanic descriptors outlined in Table 3.2 and the important engineering geological descriptors from the NZGS 2005 (Burns *et al.*, 2005) scheme in Table 3.1. Developing the detailed engineering geological igneous rock descriptive scheme was necessary to achieve the objectives of this study. This descriptive method has been used to describe all the materials covered in this study, the results of which are given in Chapters 4 and 5. The

Table 3.3: Detailed Engineering Geological Igneous Rock Descriptive Scheme with a trachytic dyke for an example. The scheme covers both important volcanic and engineering geological parameters recorded in the field by analysing features and hand specimens and can be supplemented by additional testing data.

Detailed Engineering Geological Igneous Rock Descriptive Scheme	
Component	**Example**
Geological Context (Unit Feature, Emplacement Mechanism, Formation, Group)	[DYKE, LYTTELTON VOLCANIC GROUP]
Location	Corner of Evans Pass, Sumner Pass and Summit Road
Date Sampled, Identification Number	14/08/2014, TD-1-1
Colour	Bluish grey to green
Weathering and Alteration	Slightly weathered (SW), iron oxide staining
Structure and Texture (Outcrop, Hand Specimen)	Porphyritic, trachytic, flow banding
Groundmass Grain Size	Fine grained groundmass
Crystal Grain Size	Fine to coarse grained phenocrysts
Fragment/Clast/Lithic Grain Size	N/A
Component Analysis (Hand Specimen)	
% Groundmass/Matrix	57%
% Crystals	40%
% Fragments, Clasts and Lithics	0%
% Vesicles	3%
Mineralogy (Hand Specimen and Thin Section)	Alkali feldspar 15%, Clinopyroxene 10%, Iddingsite 5%, Augite, 5%, Opaques 3%, Orthopyroxene 2%
Rock Name	TRACHYTE
Discontinuities	
Orientation and Joint Sets	Near right angled joints, three sets
Spacing	moderately widely spaced
Aperture	narrow aperture
Additional	no infill
Intact Strength	
In field	Moderately Strong – Strong
Testing (UCS/PLS/Schmidt Hammer)	UCS: 40-60 MPa
Full Expanded Description	
[DYKE, LYTTELTON VOLCANIC GROUP], Evans Pass, TD-1-1, bluish grey to green, slightly weathered, iron oxide staining, porphyritic, trachytic, flow banding, fine grained groundmass, fine to coarse grained phenocrysts. Groundmass 57%, crystals 40% (alkali feldspar 15%, clinopyroxene 10%, iddingsite 5%, augite, 5%, opaques 3%, orthopyroxene 2%), vesicles 3%, TRACHYTE. Near right angled joints, three joint sets, moderately widely spaced, narrow aperture, no infill, moderately strong-strong (40-60 MPa).	
Summary Description	
Bluish grey to green, slightly weathered, iron oxide staining, porphyritic, trachytic, flow banding, fine grained groundmass, fine to coarse grained phenocrysts. Groundmass 57%, crystals 40%, vesicles 3%, TRACHYTE. Near right angled joints, three joint sets, no infill, moderately widely spaced, narrow aperture, moderately strong-strong (40-60 MPa).	

In the utilisation of this scheme one works by first examining: 1) the type of feature which is directly related to method of emplacement (e.g. lava flow, dyke, sill, pyroclastic deposit,

airfall, volcanogenic deposit etc.), the relevant geological formation (e.g. Lyttelton Volcanic Group), location, and date. 2) Visual characteristics: colour, weathering and obvious alterations (e.g. clay or hematite/iron oxide alteration), structures and textural characteristics (e.g. aphyric, porphyritic, trachytic etc.), grain sizes of groundmass, crystals and lithics/clast/fragment are also recorded. 3) A quantitative account of all components including groundmass, crystals, clasts and lithics and vesicles (expressed in percentages). 4) Components identification; either in hand specimen or in thin section (for the purpose of thoroughness this study's materials have been described using both hand specimen and thin section). 5) Rock name, 6) Presence of defects and discontinuities are recorded. 7) Rock strength, recorded from either laboratory testing (UCS, $I_{s(50)}$/schmidt hammer correlation) only qualitatively from blows with geological hammer. 8) Fully expanded description, 9) an additional shorter summary description. An example of this methodology is provided in Table 3.3.

The greatest strength of this scheme is that it can successfully describe an igneous rock in both a volcanic and geotechnical manner. This method is considerably more detailed than the NZGS descriptive method. It should be noted for continuity that the Detailed Engineering Geological Igneous Rock Descriptive Scheme follows the same descriptions of rock mass weathering, rock strength and discontinues terminology as used in the NZGS, (2005) scheme.

The framework for this method is set out clear and in an ordered manner as to make it as user friendly and efficient as possible. Following the Canterbury earthquake sequence, there are many professionals working in the region with a variety of skill levels and backgrounds, therefore it is essential to have a easily followed descriptive method. It should also be noted that this Detailed Engineering Geological Igneous Descriptive Scheme is not Christchurch specific and can be utilised for any igneous rock/unit irrespective of geographical location.

3.4 Thin Section Analysis

As indicated in the previous section, thin sections were undertaken to establish details of the crystal content, weathering, alteration, crystal interactions with groundmass, micro-fracturing etc. An attempt to try and account for variability observed within volcanic unit (i.e. ignimbrite, tuffs). After samples were collected from the field and catalogued, representative hand samples of all the lithologies were thin sectioned to 30µm for thin section analysis. The thin section analysis was carried out for the purpose of investigating mineralogy and

composition, volcanic textures, alteration, degree of crystal alignment, welding and clast/lithic matrix boundary interactions. The thin section analysis additionally informs the mineralogy section in Table 3.3. Results of thin section analysis are presented in Chapters 4 and 5.

3.5 Sample Preparation

After samples were recovered from the field, the larger boulder-sized samples were drilled to produce cores suitable for rock mechanics testing (Figure 3.2). Before commencing drilling, each sample was photographed, dimensions recorded (Figure 3.2a/b) and examined thoroughly for any obvious discontinuities or defects (Figure 3.2d/e) both pre and post drilling. Each recovered sample was then cored in the laboratory with a 50mm diameter diamond tipped drill bit (Figure 3.2c). Between four and ten cores were obtained per lithology. Cores were cut to approximately 100mm length with a diamond tipped saw (Figure 3.2f), in keeping with the recommended 2-2.5:1 length to diameter ratio in accordance with the ASTM (2004) guideline. Recovering as many cores as possible for analysis was a priority. As such, the ISRM 2.5-3:1 length to diameter ratio was not followed.

After cutting the core to the specified length, the sample is ground as parallel as possible, with intact corners where possible. Samples which were unable to be cored due to the nature of the material were cut into cubic blocks; this was commonly the case when dealing with friable samples such as the ignimbrites, ashes and tuffs. The sample preparation process is illustrated in Figure 3.2. Cores, provided by Coffey Geotechnics, are approximately 60mm diameter cores and as such were cut to approximately 120mm length. Cores provided by Coffey include: slightly-moderately weathered basaltic lava (BLSM), highly-completely weathered basaltic lava (BLHC), and rubbly basaltic lava breccia (RCB). These samples were recovered from depths ≥15.0m bgl.

a

Figure 3.2a: Samples photographed and dimensions recorded.

b

Figure 3.2b: Samples photographed and dimensions recorded.

c

Figure 3.2c: Sample coring with a 50mm diameter bit.

d

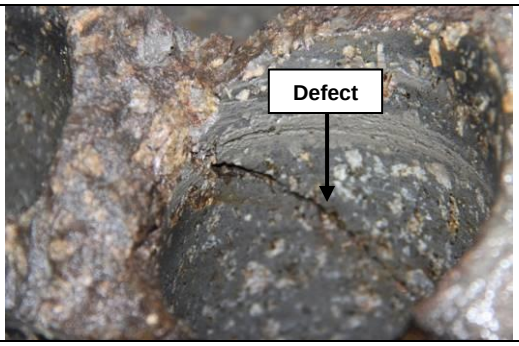

Figure 3.2d: Defect and discontinuity analysis pre-drilling.

e

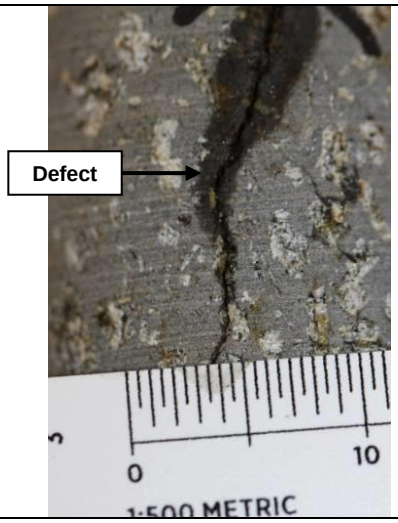

Figure 3.2e: Defect and discontinuity analysis post-drilling.

f

Figure 3.2f: Core cutting, grinding and labelling.

Figure 3.2: Sample Preparation Process. Samples in the figure are Trachytic Lava (a), Trachytic Dyke (b, d) and Basaltic Dyke (e–f). Image 3.2d and 3.2e displays a fracture in the rock which was only observed after drilling.

3.6 Testing Philosophy

Rock mechanics testing is utilised to determine the strength and durability of each lithology. Tests conducted include: porosity and density determination, P and S wave velocities, point load strength index, uniaxial compressive strength testing with strain gauge augmentation, and slake durability (Table 3.4). Deformation moduli have been derived for both static and

dynamic conditions wherever possible. The rock mechanics testing philosophy for this study follows the ISRM suggested methods for rock characterisation (Ulusay and Hudson, 2007), with the only exception being a 2:1 length to diameter ratio for cored specimens (ASTM, 2004). For brevity, please refer to Ulusay and Hudson, (2007) for the full rock mechanics testing methodology.

Geotechnical testing investigates the various types of intact volcanic rock, including both the geological and geotechnical properties. Therefore, no specific geotechnical testing has been carried out on defects and discontinuities (e.g. joint roughness coefficient (JRC) and joint compressive strength (JCS). However, defects and discontinuities are descriptively characterised by the Detailed Engineering Geological Igneous Rock Descriptive Scheme on a site specific basis with results included in the material characterisation sections in Chapters 4 and 5.

For consistency, all samples are strength and ultrasonically tested in a dry state, as each core or cube has been saturated and oven dried in determining porosity and density parameters. Samples which have been oven dried tend to have higher recorded strength values than those which have been saturated (Ulusay and Hudson, 2007). Dry state testing has been carried out in this study in order to graph correlations and determine relationships between geotechnical characteristics such as UCS and dry mass density, P and S wave velocity and UCS, UCS and point load strength index in the same (dry) state. Graphing these relationships aids in illustrating the effect that one characteristic/parameter can have on the other, and also provides a quantitative comparative tool to analyse different emplacement/post-emplacement mechanisms.

Some materials included in this study have not been tested due to various complications during sample preparation and/or rock mechanics testing (Table 3.5). The red ash (RA), crystal dominated tuff (CTC), lithic dominated tuff (CTL), brecciated basaltic ignimbrite (IGB) and moderately welded basaltic ignimbrite (IGMW) all encountered complications during the laboratory coring process. Coring failures mainly occurred due to breakages at lithic/clast groundmass boundaries where the rock is weakest and due to clay expansion in the drill barrel. Clay expansion occurred with the red ash (RA) and with both tuff units (CTC and CTL).

Table 3.4: Rock Mechanics testing methods utilised in testing the Lyttelton Volcanic Group lithologies. Relevant testing guidelines are presented with the relevant page number in the ISRM 'blue book' (Ulusay and Hudson, 2007). Sample preparation has followed ASTM, (2004) guidelines.

Rock Mechanics Tests and Derived Parameters		
Physical Tests		
Name of Test	**Description of Test**	**ISRM Page**
P and S Wave Velocity	Determines the velocity of propagation of elastic waves (Vp and Vs) through a cylindrical intact rock core or block specimen using a pulse generator. Non-destructive and carried out on the specimen prior to the uniaxial compressive strength test. Also used to determine dynamic deformation moduli.	116-118
Slake Durability	Measures the resistance of a rock specimen to weakening and disintegration when subjected to two cycles of drying and wetting (Id_1 and Id_2).	96-98
Porosity and Density Determination	Determines the porosity (n%), dry density (ρ_d) and related properties of rock samples. Due to the varying behaviour of materials encountered two separate methods were used. The first is the 'double weight method' which is used for intact samples which have a regular geometry (Saturation and Calliper Technique). The second the 'triple weight method' is for samples of an irregular geometry (Saturation and Buoyancy Techniques).	87-88
Point Load Strength Index	Intended as an index test for strength classification of rock specimens. The test measures the Point Load Strength Index ($I_{s(50)}$). The point load strength index test can be carried out on either cylindrical core or irregular lump samples. This test is useful for rock materials where cores could not be made due to the friable or low strength nature of the matrix and, as such, would not be suitable for UCS testing.	125-132
Uniaxial Compressive Strength	Measured uniaxial compressive strength (σ_{ci}) of a cylindrical intact rock core specimen of a regular geometry (loading rate of 0.1-0.5MPa/s used). Most commonly used for strength classification and characterisation for intact rock. UCS has been correlated using the Broch and Franklin (1972) $Is_{(50)}\times 24$ where UCS could not be directly tested.	153-154
Deformation Moduli		
Poisson's Ratio **Young's Modulus** **Shear Modulus** **Bulk Modulus** **(Static and Dynamic)**	Poisson's ratio (υ) defines the ratio between transverse contraction strain to longitudinal extension strain in the direction of the stretching force. Young's Modulus (E) is a measure of the stiffness of an elastic material. Static moduli are determined using strain gauges augmented onto intact specimens during uniaxial compressive strength testing. Dynamic moduli are derived P and S wave velocities which are determined by wave arrival times (non-destructive test). Additionally, shear (G) and bulk (K) moduli are calculated using Poisson's Ratio and Young Modulus. Shear modulus (G) and Bulk Modulus (K) are defined by the following equations: $G = E/(2(1+\upsilon))$, $K = E/(3(1-2\upsilon))$ (Goodman, 1989).	154-156

Table 3.5: Testing regimes and number of tests performed on each Lyttelton Volcanic Group units. * designates that diamond saw cut blocks have been used for testing purposes as the material behaviour did not lend itself to creating cylindrical cores, this is either due to weathering, ash/clay content or brecciation. Boxes designated with no data (n/d) indicate that a test has not been carried out either due to testing issues or that the test was not required for that material (as discussed in Section 3.6).

Tests Undertaken and Number of Samples Tested									
		Tests							
		Porosity	**Density**	**P and S Wave Velocities**	**Point Load Strength Index**	**Uniaxial Compressive Strength**	**Strain Gauge Augmentation**	**Slake Durability**	**Thin Sections**
Individual Sub-Units	Trachytic Dyke (**TD**)	6	6	6	9	6	6	n/d	1
	Trachytic Lava (**TL**)	9	9	9	9	9	9	n/d	1
	Brecciated Basaltic Ignimbrite (**IGB**)	6	6	n/d	13*	n/d	n/d	1 set (10 samples)	1
	Moderately Welded Basaltic Ignimbrite (**IGMW**)	11*	11*	n/d	11*	n/d	n/d	n/d	2
	Highly Welded Basaltic Ignimbrite (**IGW**)	6*	6*	6*	6*	n/d	n/d	n/d	1
	Red Ash (**RD**)	25*	25*	n/d	10*	n/d	n/d	1 set (10 samples)	1
	Crystal Tuff (**CTC**)	5*	5*	n/d	5*	n/d	n/d	1 set (10 samples)	2
	Lithic Tuff (**CTL**)	12*	12*	n/d	12*	n/d	n/d	1 set (10 samples)	2
	Rubbly Basaltic Lava Breccia (**RCB**)	10	10	n/d	15	10	n/d	n/d	1
	Unweathered Basaltic Lava (**BLUW**)	10	10	10	13	9	9	1 set (10 samples)	1
	Slightly-Moderately Weathered Basaltic Lava (**BLSM**)	7	7	7	30	7	9	n/d	1

	Highly-Completely Weathered Basaltic Lava (**BLHC**)	5	5	n/d	10	5	n/d	n/d	1
	Highly Vesicular Basaltic Lava Bomb (**BLV**)	n/d	n/d	n/d	n/d	n/d	n/d	n/d	1
	Basaltic Dykes (**BD**)	4	4	4	9	4	4	n/d	1
	Blocky Basaltic Lava Clasts (**BBLC**)	n/d	n/d	n/d	n/d	n/d	n/d	n/d	1
	Blocky Basaltic Lava Matrix (**BBLM**)	n/d	n/d	n/d	n/d	n/d	n/d	n/d	1
	Volcanogenic Deposit Tuffaceous Sandstone (**VTS**)	n/d	n/d	n/d	n/d	n/d	n/d	n/d	1
	Volcanogenic Conglomerate (**VC**)	n/d	n/d	n/d	n/d	n/d	n/d	n/d	1
	Total Number of Samples Tested	**116**	**116**	**42**	**152**	**50 cores**	**37**	**5 sets (50 balls)**	**21**

3.7 Synthesis

This chapter presents sample collection methodology, a review of the NZGS descriptive method and its limitations for the applicability in this study, a review and discussion of key volcanic features and attributes, a Detailed Engineering Geological Igneous Rock Descriptive Scheme devised for this thesis, the sample preparation procedure, purpose of thin section analysis and the rock mechanics testing philosophy utilised.

Collection of samples involved first identifying locations of outcrops and road cuts where samples could be recovered from safely (Figure 3.1). Samples were recovered based on size and were recovered intact and in-situ by chiselling open defects were possible.

The NZGS descriptive method for soil and rock was used in the initial stages of this study (Table 3.1). It quickly became apparent that the scheme was limited in the sense that it could not describe in detail an igneous rock or feature. In light of this, a review of key volcanic features was undertaken, (Table 3.2), and utilised in the development and implementation a Detailed Engineering Geological Igneous Rock Classification Scheme (Table 3.3). A scheme which successfully describes igneous rocks in both a igneous (geological) and geotechnical manner. This scheme is used to describe and characterise all of the, as presented in Chapters 4 and 5.

Preparation of field samples for testing involved coring boulder-sized samples with a diamond tipped drill in order to produce testable cylinders of rock core (Figure 3.2). Cores were cut to size and ground parallel. Lithologies which could not be cored were cut into blocks for testing purposes. During sample preparation representative samples of each lithology were thin sectioned for analysis. The findings of the thin section analysis are used in conjunction with hand specimens to describe the igneous materials included in this study (Table 3.3). This study follows the rock mechanics testing philosophy as outlined by the ISRM, (Ulusay and Hudson, 2007) with sample length to diameter ratio (2:1) following the ASTM (2004) method as being the only exception. Tests conducted include porosity and density determination, P and S wave velocities, point load strength index, uniaxial compressive strength testing with strain gauge augmentation (where possible) and slake durability (Tables 3.4 and 3.5). The results of this study and presented in Chapters 4 and 5.

CHAPTER 4 - Results of Geotechnical Testing and Properties Part 1-Lava Flows

4.1 Introduction

Chapters 4 and 5 present the results of this study. The results of this study have been divided into two chapters. Chapter 4 presents key findings on the properties of lava flows recognised in this study as, the key and most prominent unit type of the Lyttelton Volcanic Group. Chapter 5 covers the 'assorted' volcanic units which include: intrusives (dykes), airfall, pyroclastic and volcanogenic units. Results are presented for geotechnical sub-units individually. Findings are compartmentalised into the following aspects: unit descriptions, thin section analysis and rock mechanics data.

Sub-unit descriptions follow attributes outlined in the *Detailed Engineering Geological Igneous Rock Descriptive Scheme*, supported by supplementary annotated field and laboratory photographs. *Thin section* results include detailed descriptions and analysis of representative thin sections supplemented by high resolution micrographs. *Thin section* analysis investigated textures, mineralogy, crystal alignment, alteration, micro-fracturing and crystal/clast groundmass boundaries. Results of *thin section* analysis are used to supplement the engineering geological and igneous rock descriptions. *Rock mechanics testing* conducted has been summarised in Tables 3.4 and 3.5. Key results are presented in tabulated, graphical and figure format. Units with no associated data sets, have not been tested either due to difficulties in sourcing a sufficient volume of similar material or due to rock mechanics testing difficulties. All relevant datasets are included in Appendix 2, with selected key datasets and analyses presented in Chapters 4 and 5.Please note that discontinuity and defect descriptions included in both Chapters 4 and 5 are strictly site specific. This is important as defect characteristics vary within the outcrop and from one outcrop to another. As such discontinuity descriptions are derived from field sites only. Field site locations are included in the descriptive scheme presented for each unit. For number of samples tested see Table 3.5.

Units included in Chapter 4 include: unweathered basaltic lava (BLUW), slightly-moderately weathered basaltic lava (BLSM), highly-completely weathered basaltic lava (BLHC), rubbly

basaltic breccia (RCB), vesicular basaltic lava (BLV), blocky basaltic lava (BBL) and trachytic lava (TL).

4.2 Unweathered Basaltic Lava (BLUW)

Detailed descriptions are presented with relevant supporting annotated figures (Table 4.1 and Figure 4.1), followed by key datasets and results of rock mechanics testing (Tables 4.2, 4.3 and Figure 4.2).

Detailed Engineering Geological Igneous Rock Description

Table 4.1: Detailed Engineering Geological Igneous Rock Description for unweathered basaltic lava (BLUW).

Detailed Engineering Geological Igneous Rock Descriptive Scheme	
Component	**Description**
Geological Context (Unit Feature, Emplacement Mechanism, Formation, Group)	[LAVA FLOW, LYTTELTON VOLCANIC GROUP]
Location	Corner of Evans Pass, Sumner Pass and Summit Road
Date Sampled, Identification Number	14/08/2013, BLUW
Colour	Grey to black
Weathering and Alteration	Unweathered, localised iron staining to fractures (Figure 4.1c)
Structure and Texture (Outcrop, Hand Specimen)	Porphyritic
Groundmass Grain Size	Fine grained groundmass (Figure 4.1a)
Crystal Grain Size	Medium grained phenocrysts (Figure 4.1b)
Fragment/Clast/Lithic Grain Size	N/A
Component Analysis (Hand Specimen) *% Groundmass/Matrix* *% Crystals* *% Fragments, Clasts and Lithics* *% Vesicles*	 55% 43% 0% 2%
Mineralogy (Hand Specimen and Thin Section)	Plagioclase feldspar 25%, iddingsite 12%, alkali feldspar 3%, opaques 2%, clinopyroxene 2%, orthopyroxene 1% (Figures 4.1e/f)
Rock Name	BASALT
Discontinuities *Orientation and Joint Sets* *Spacing* *Aperture* *Additional*	 Two joint sets Widely spaced Narrow aperture Columnar, no infill, minor seepage
Intact Strength *In field* *Testing (UCS/PLS/Schmidt Hammer)*	 Strong –very strong 58-193 MPa
Full Expanded Description	
[LAVA FLOW, LYTTELTON VOLCANIC GROUP], Evans Pass, BLUW, grey to black, unweathered, iron oxide staining, porphyritic, fine grained groundmass, medium grained phenocrysts. Groundmass 55%, crystals 43% (Plagioclase feldspar 25%, iddingsite 12%, alkali feldspar 3%, opaques 2%, clinopyroxene 2%, orthopyroxene 1%), vesicles 2%, BASALT. Two joint sets, widely spaced, narrow aperture, columnar, no infill, minor seepage, strong-very strong (UCS 58-193 MPa).	
Summary Description	
Grey to black, unweathered, iron oxide staining, porphyritic, fine grained groundmass, medium grained phenocrysts. Groundmass 55%, crystals 43%, vesicles 2%, BASALT. Two joint sets, widely spaced, narrow aperture, columnar, no infill, minor seepage, strong-very strong (UCS 58-193 MPa).	

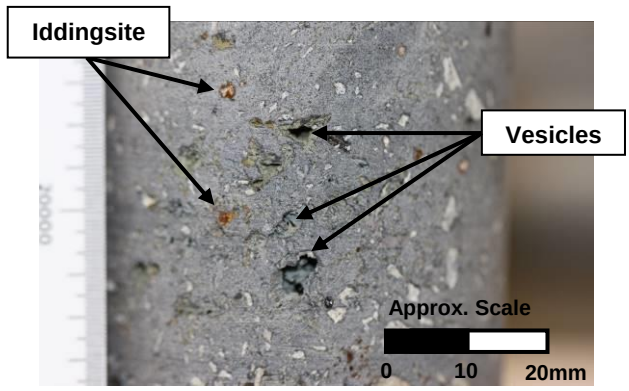

Figure 4.1a) Photograph of BLUW core. Note cluster of vesicles and the altered olivines (iddingsite).

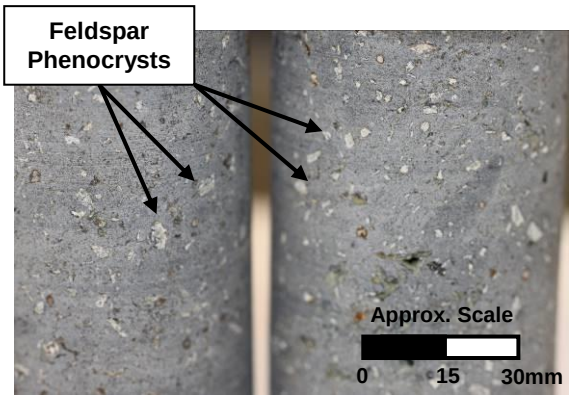

Figure 4.1b) Photograph of BLUW cores. Note the relatively high percentage of phenocrysts.

Figure 4.1c) Photograph of boulder of BLUW used for coring samples. Note weathering is only visible on the outside of the boulder.

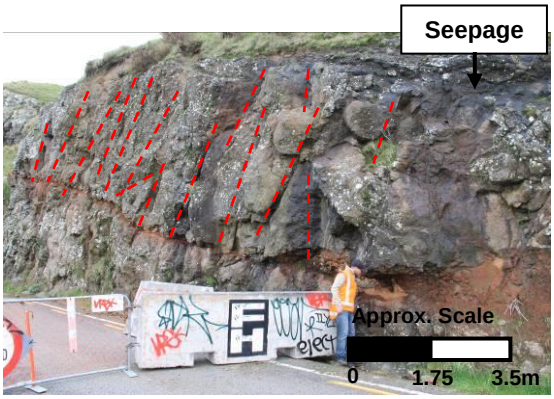

Figure 4.1d) Field photograph of outcrop/road cut of BLUW. Note crudely formed columns shown by red dashed lines. Also note areas of seepage.

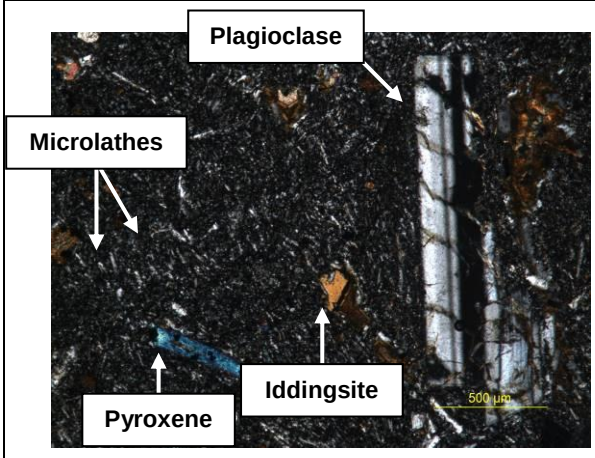

Figure 4.1e) Porphyritic texture and fine grained groundmass formed from microlathes. Note olivine has altered to iddingsite. Section is in cross polarised light (CPL).

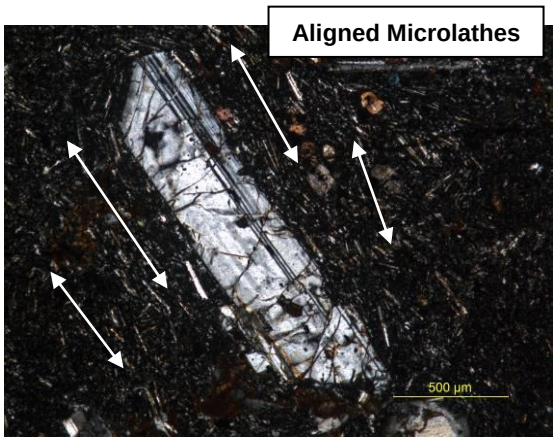

Figure 4.1f) Large damaged feldspar phenocryst surrounded by microlathes. Note slight alignment/orientation of crystals. Section is in cross polarised light (CPL).

Figure 4.1: Annotated images at hand specimen, outcrop and microscopic scales of BLUW.

Rock Mechanics Data

The unweathered basaltic lava produced very low porosity values with a mean of 2.3% (Table 4.2). PLS and UCS testing yielded respectively means of 6.6 and 123MPa indicating the basalt as being strong to very strong (NZGS, 2005 terminology as outlined in Burns *et al.*, 2005); however based on the relatively 'unweathered' state of the basalt a higher mean strength was expected. Static and dynamic deformation moduli produced reasonably consistent results with only approximately 1 order of magnitude of variation (Table 4.3). A variety of different failures during UCS testing were observed. Failure types ranged from vertical fractures and 60° shearing (Figure 4.2b/d) to conical type failures (Figure 4.2a/c). Slake durability testing (Figure 4.2e) showed that only 0.4% of the basalt was lost during two cycles. Point load strength testing (Figure 4.2f) was consistent with only one sample being influenced by an iron stained fracture.

Table 4.2: Key physical rock mechanics data for BLUW.

Key Data for Unweathered Basaltic Lava (BLUW) - Physical Rock Mechanics Tests										
	Porosity n (%)	Dry Mass Density ρ_d (kg/m^3)	Bulk Volume V (m^3)	P and S Wave Velocities		Point Load Strength Index $Is_{(50)}$ (MPa)	Correlated UCS using $Is_{(50)}\times24$ (MPa)	UCS σ_{ci} (MPa)	Slake Durability First Cycle Id_1 (%)	Slake Durability Second Cycle Id_2 (%)
				Vp (m/s)	Vs (m/s)					
Range	0.8-5.6	2680-2890	1.9×10^{-4}-2.3×10^{-4}	4291-5185	2680-2975	5.64-8.26	135.4-198.4	58.2-192.8	99.8*	99.6*
Mean	2.3	2820	2.09×10^{-4}	4740	2806	6.65	159.5	123.1	-	-
Median	2.2	2830	2.10×10^{-4}	4735	2807	6.61	158.6	109.5	-	-
Standard Deviation	1.4	61.1	1.06×10^{-5}	251.5	87.6	0.57	13.58	42.2	-	-
***Note: Slake durability first/second cycle have no range, mean, median or standard deviation as only one test was conducted.										

Table 4.3: Key deformation moduli test data for BLUW.

Key Data for Unweathered Basaltic Lava (BLUW) - Deformation Moduli						
	Static Young's Modulus Estat (GPa)	Static Poisson's Ratio υstat (unitless)	Dynamic Young's Modulus Edyn (GPa)	Dynamic Poisson's Ratio υdyn (unitless)	Static Shear Modulus Gstat (GPa)	Static Bulk Modulus Kstat (GPa)
Range	40.2-69.2	0.1-0.4	45.8-64.0	0.17-0.28	14.87-24.88	19.03-86.50
Mean	51.5	0.23	54.8	0.23	20.0	36.0
Median	51.6	0.22	56.0	0.22	18.5	28.0
Standard Deviation	10.9	0.08	5.0	0.03	4.0	21.8

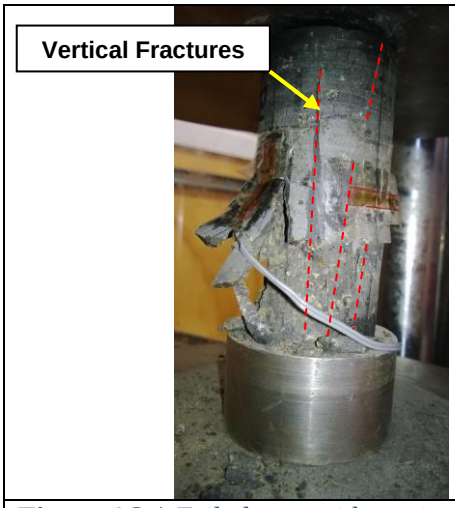

Figure 4.2a) Failed core with vertical fractures and upper cone formation (BLUW-1-5).

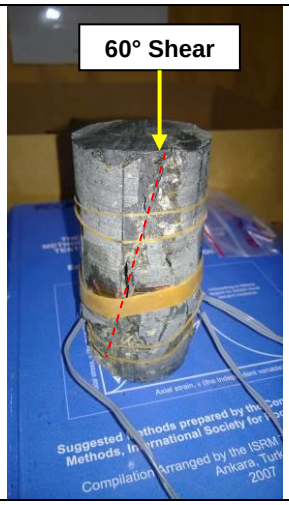

Figure 4.2b) Failed core with vertical fractures and 60° shearing type failure (BLUW-1-9).

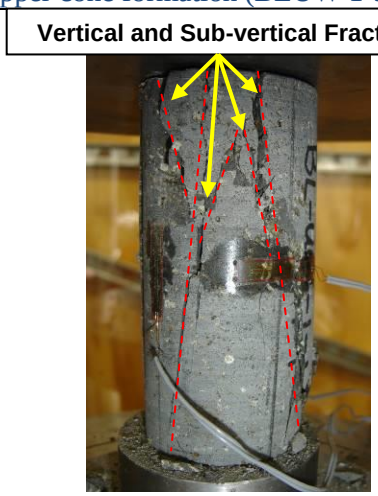

Figure 4.2c) Failed core with vertical and sub-vertical fractures (BLUW-1-1).

Figure 4.2d) Failed core with lower cone formation/conical type failure (BLUW-1-2).

Figure 4.2e) Second cycle slake durability >99% material remaining.

Figure 4.2f) Failed point load samples.

Figure 4.2: Annotated images of unweathered basaltic lava testing: A-D) UCS testing, E) slake durability and F) point load strength index testing.

4.3 Slightly to Moderately Weathered Basaltic Lava (BLSM)

Detailed rock descriptions are presented with relevant supporting annotated figures (Table 4.4 and Figure 4.3), followed by key datasets and results of rock mechanics testing (Table 4.5, Table 4.6 and Figure 4.4).

Detailed Engineering Geological Igneous Rock Description

Table 4.4: Detailed Engineering Geological Igneous Rock Description for slightly-moderately weathered basaltic lava (BLSM).

Detailed Engineering Geological Igneous Rock Descriptive Scheme	
Component	**Description**
Geological Context (Unit Feature, Emplacement Mechanism, Formation, Group)	[LAVA FLOW, LYTTELTON VOLCANIC GROUP]
Location	Marriner Street, Sumner
Date Sampled, Identification Number	12/03/2013, BLSM
Colour	Reddish grey to light purple
Weathering and Alteration	Slightly to moderately weathered, frequent iron staining and minor clay alteration (Figures 4.3a/d)
Structure and Texture (Outcrop, Hand Specimen)	Porphyritic
Groundmass Grain Size	Fine grained groundmass (Figures 4.3b/c)
Crystal Grain Size	Fine to coarse grained phenocrysts (Figure 4.3c)
Fragment/Clast/Lithic Grain Size	N/A
Component Analysis (Hand Specimen) *% Groundmass/Matrix* *% Crystals* *% Fragments, Clasts and Lithics* *% Vesicles*	 45% 53% 0% 2%
Mineralogy (Hand Specimen and Thin Section)	Plagioclase feldspar 25%, iddingsite 15%, clinopyroxene 6%, alkali feldspar 5%, olivine 5%, opaques 3%, orthopyroxene 1% (Figures 4.3e-h)
Rock Name	BASALT
Discontinuities *Orientation and Joint Sets* *Spacing* *Aperture* *Additional*	 N/A Closely spaced Stepped, narrow aperture Clay infill (Figure 4.3a)
Intact Strength *In field* *Testing(UCS/PLS/Schmidt Hammer)*	 Moderately strong-strong 27-83 MPa
Full Expanded Description	
[LAVA FLOW, LYTTELTON VOLCANIC GROUP], Marriner Street, Sumner, BLSM, reddish grey to light purple, slightly-moderately weathered, frequent iron staining and minor clay alteration, porphyritic, fine grained groundmass, fine to coarse grained phenocrysts. Groundmass 45%, crystals 53% (Plagioclase feldspar 20%, iddingsite 15%, clinopyroxene 6%, alkali feldspar 5%, olivine 5%, opaques 3%, orthopyroxene 1%), vesicles 2%, BASALT. Closely spaced joints, stepped, narrow, aperture, clay infill, moderately strong-strong (UCS 27-83 MPa).	
Summary Description	
Reddish grey to light purple, slightly-moderately weathered, frequent iron staining and minor clay alteration, porphyritic, fine grained groundmass, fine to coarse grained phenocrysts. Groundmass 45%, crystals 53%, vesicles 2%, BASALT. Closely spaced joints, stepped, narrow, aperture, clay infill, moderately strong-strong (UCS 27-83 MPa).	

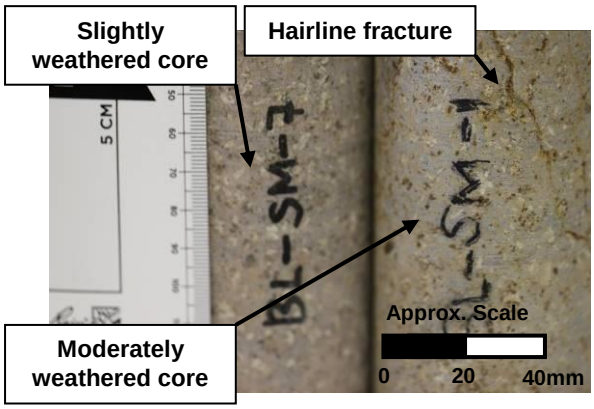

Figure 4.3a) Two BLSM cores, note variability in weathering grades and clay infilling fractures.

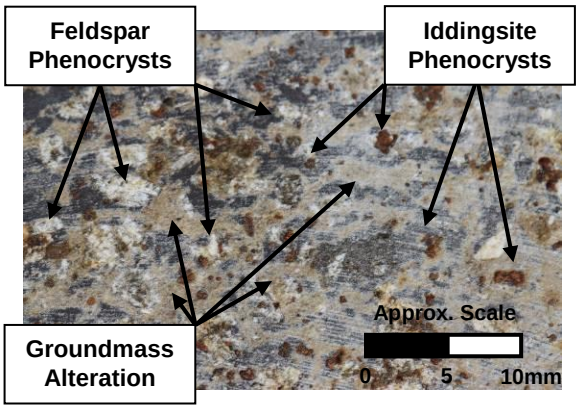

Figure 4.3b) Photograph of BLSM section. Note the relatively high percentage of phenocrysts.

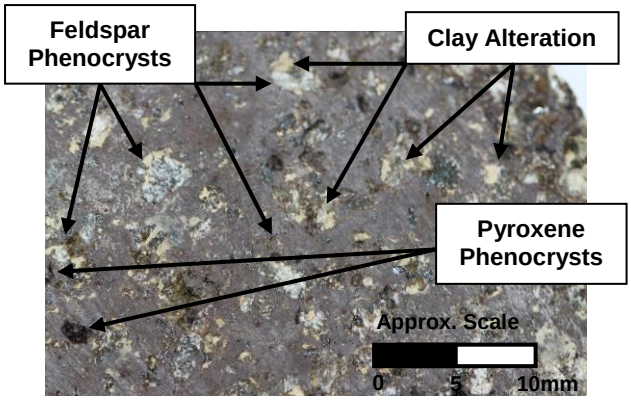

Figure 4.3c) Photograph of BLSM section. Note importantly the alteration/weathering of feldspar to clays.

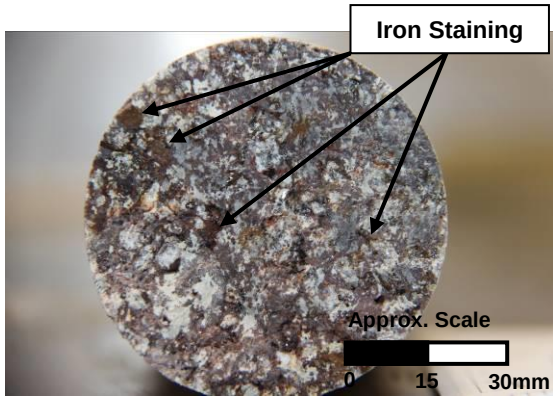

Figure 4.3d) Photograph of BLSM section. Note iron/hematite staining.

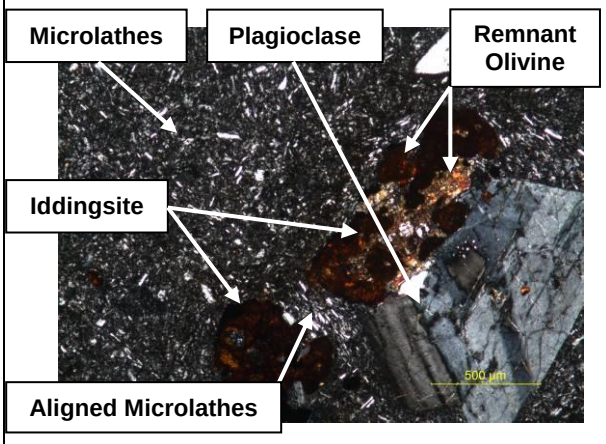

Figure 4.3e) Porphyritic texture and fine grained groundmass formed from microlathes. Note olivine has altered to iddingsite. Section is in cross polarised light (CPL).

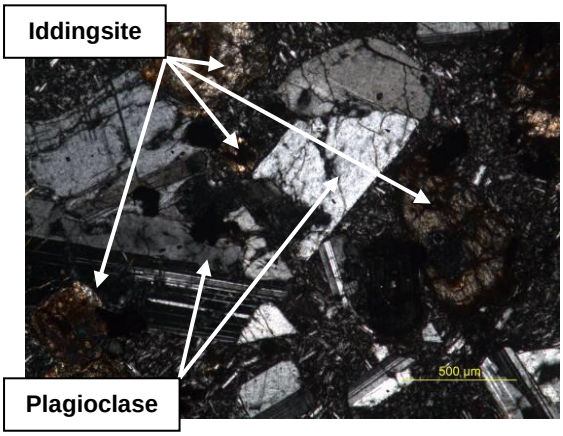

Figure 4.3f) Large damaged feldspar phenocryst. Note slight alignment/orientation of crystals. Section is in cross polarised light (CPL).

Figure 4.3 is continued over the page.

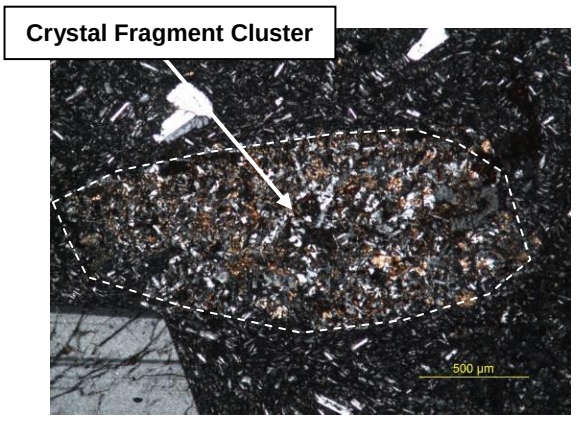

Figure 4.3g) Large cluster of angular phenocryst fragments. Section is in cross polarised light (CPL).

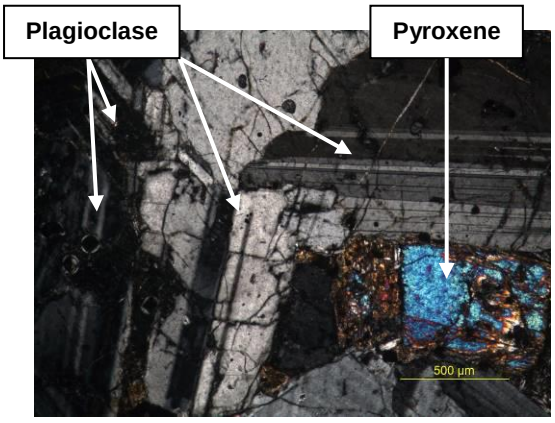

Figure 4.3h) Coarse grained phenocrysts. Section is in cross polarised light (CPL).

Figure 4.3: Annotated images at hand specimen, outcrop and microscopic scales of BLSM.

Rock Mechanics Data

The slightly-moderately weathered basaltic lava produced low porosity values with a mean of 8.3% (Table 4.5), PLS and UCS testing yielded respectively means of 2.24 and 50MPa indicating the basalt as being moderately strong to strong; this was expected due to weathering and alteration present within the rock mass. Static and dynamic deformation moduli produced reasonably consistent results with only approximately 1 order of magnitude of variation however; the Poissons Ratio displayed a slightly higher variation (Table 4.6). UCS testing failure types included mainly 60° shearing with cone formation with some vertical fracturing (Figure 4.4).

Table 4.5: Key physical rock mechanics data for BLSM.

Key Data for Slightly to Moderately Weathered Basaltic Lava (BLSM) - Physical Rock Mechanics Tests										
	Porosity n (%)	Dry Mass Density ρ_d (kg/m^3)	Bulk Volume V (m^3)	P and S Wave Velocities		Point Load Strength Index $Is_{(50)}$ (MPa)	Correlated UCS using $Is_{(50)}$×24 (MPa)	UCS σ_{ci} (MPa)	Slake Durability First Cycle Id_1 (%)	Slake Durability Second Cycle Id_2 (%)
				Vp (m/s)	Vs (m/s)					
Range	4.6-14.2	2230-2470	3.6×10^{-4} - 3.8×10^{-4}	4330-2626	2475-1467	1.12-3.44	26.98-82.64	29.4-80.0	-	-
Mean	8.3	2360	3.65×10^{-4}	3610	2094	2.24	53.8	50.0	-	-
Median	7.3	2380	3.67×10^{-4}	3840	2121	2.26	54.3	49.0	-	-
Standard Deviation	2.9	74.1	6.25×10^{-6}	523.2	340.3	0.59	14.3	15.7	-	-
***Note: Slake durability first/second cycle have no range, mean, median or standard deviation as only one test was conducted.										

Table 4.6: Key Deformation moduli test data BLSM.

Key Data for for Slightly to Moderately Weathered Basaltic Lava (BLSM) - Deformation Moduli						
	Static Young's Modulus Estat (GPa)	Static Poisson's Ratio υstat (unitless)	Dynamic Young's Modulus Edyn (GPa)	Dynamic Poisson's Ratio υdyn (unitless)	Static Shear Modulus Gstat (GPa)	Static Bulk Modulus Kstat (GPa)
Range	12.2-28.4	0.10-0.46	12.5-36.8	0.20-0.28	5.04-12.14	7.01-67.25
Mean	20.2	0.21	26.4	0.25	8.46	19.13
Median	20.5	0.17	27.3	0.26	8.95	9.63
Standard Deviation	4.9	0.12	8.03	0.03	2.35	19.98

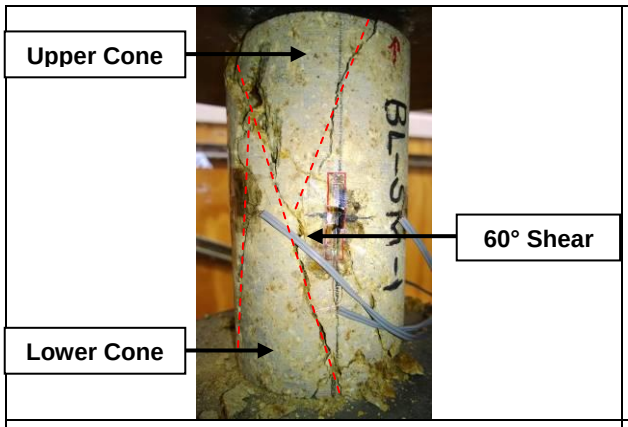

Figure 4.4a) Failed core with 60° shear, upper and lower cone formation (BLSM-1).

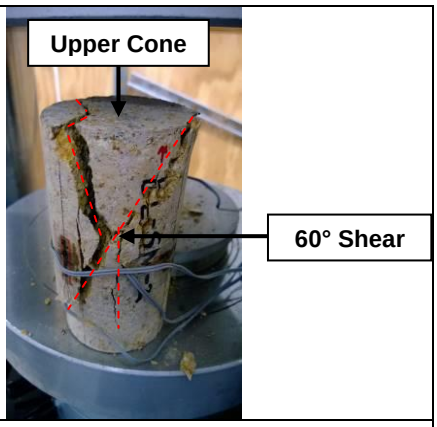

Figure 4.4b) Failed core with 60° shearing type failure and upper cone formation (BLSM-2).

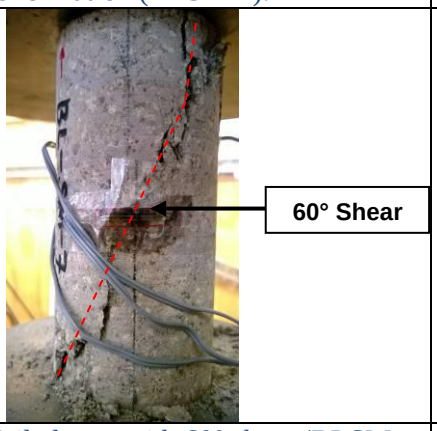

Figure 4.4c) Failed core with 60° shear (BLSM-7).

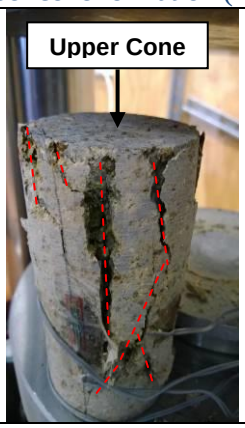

Figure 4.4d) Failed core with vertical fractures and upper cone formation (BLSM-4).

Figure 4.4: Annotated representative microscopic images of slightly to moderately weathered basaltic lava (BLSM).

4.4 Highly to Completely Weathered Basaltic Lava (BLHC)

Detailed rock descriptions are presented with relevant supporting annotated figures (Table 4.7 and Figures 4.5), followed by key datasets and results of rock mechanics testing (Table 4.8 and Figure 4.6). No deformation moduli data was able to be derived for this unit.

Detailed Engineering Geological Igneous Rock Description

Table 4.7: Detailed Engineering Geological Igneous Rock Description for highly-completely weathered basaltic lava (BLHC).

Detailed Engineering Geological Igneous Rock Descriptive Scheme	
Component	**Description**
Geological Context (Unit Feature, Emplacement Mechanism, Formation, Group)	[LAVA FLOW, LYTTELTON VOLCANIC GROUP]
Location	Marriner Street, Sumner
Date Sampled, Identification Number	12/03/2013, BLHC
Colour	Creamy orange
Weathering and Alteration	Highly to completely weathered, extensive clay alteration (Figures 4.5a/b)
Structure and Texture (Outcrop, Hand Specimen)	Porphyritic
Groundmass Grain Size	Fine grained groundmass (Figure 4.5d)
Crystal Grain Size	Fine to coarse grained phenocrysts (Figure 4.5c)
Fragment/Clast/Lithic Grain Size	N/A
Component Analysis (Hand Specimen) *% Groundmass/Matrix* *% Crystals* *% Fragments, Clasts and Lithics* *% Vesicles*	 45% 55% 0% 0%
Mineralogy (Hand Specimen and Thin Section)	Plagioclase feldspar 20%, opaques 10%, clinopyroxene 8%, olivine 5%, augite 5%, iddingsite 3%, alkali feldspar 2%, orthopyroxene 2% (Figures 4.5e-h)
Rock Name	BASALT
Discontinuities *Orientation and Joint Sets* *Spacing* *Aperture* *Additional*	 N/A Closely spaced rough, narrow aperture Clay infill
Intact Strength *In field* *Testing (UCS/PLS/Schmidt Hammer)*	 Very weak-weak 2.0-5.6MPa
Full Expanded Description	
[LAVA FLOW, LYTTELTON VOLCANIC GROUP], Marriner Street, Sumner, BLHC creamy orange, highly-completely weathered, extensive clay alteration, porphyritic, fine grained groundmass, fine to coarse grained phenocrysts. Groundmass 45%, crystals 55% (Plagioclase feldspar 20%, opaques 10%, clinopyroxene 8%, olivine 5%, augite 5%, iddingsite 3%, alkali feldspar 2%, orthopyroxene 2%), BASALT. Closely spaced joints, rough, narrow aperture, clay infill, very weak-weak (UCS 2.0-5.6 MPa).	
Summary Description	
Creamy orange, highly-completely weathered, extensive clay alteration, porphyritic, fine grained groundmass, fine to coarse grained phenocrysts. Groundmass 45%, crystals 55%, BASALT. Closely spaced joints, rough, narrow aperture, clay infill, very weak-weak (UCS 2.0-5.6 MPa).	

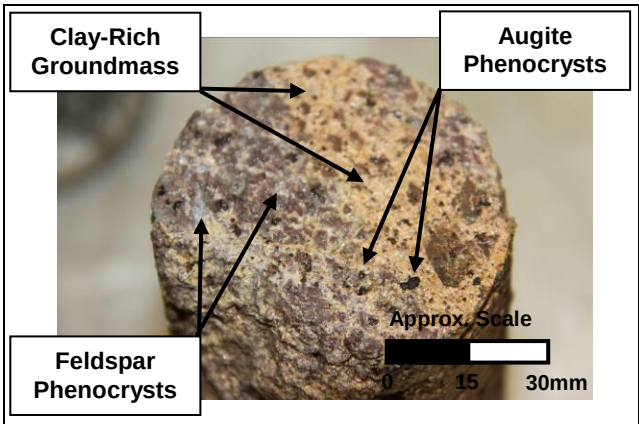

Figure 4.5a) Photograph of cut section of BLHC core. Note variability in composition.

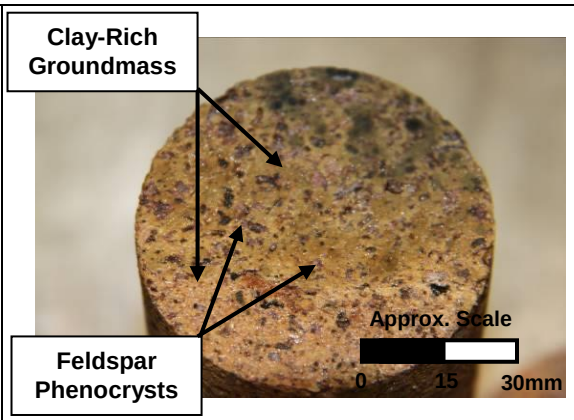

Figure 4.5b) Photograph of cut section of BLHC core. Note the relatively high percentage of phenocrysts.

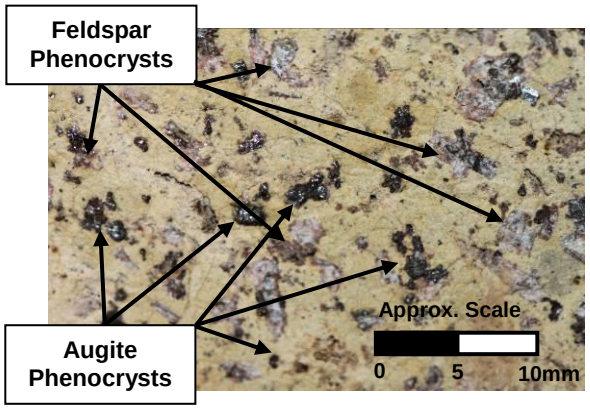

Figure 4.5c) Macro-photograph of BLHC section. Note the groundmass has almost completely weathered to clay.

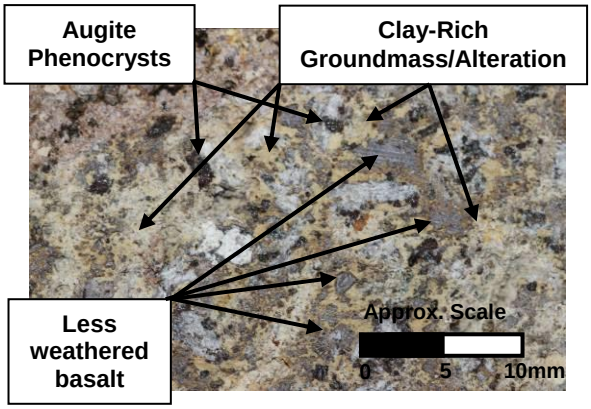

Figure 4.5d) Macro-photograph of BLHC section. Note areas of less weathered basalt.

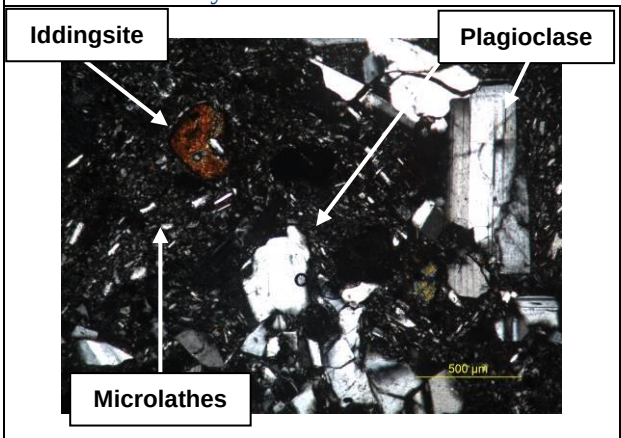

Figure 4.5e) Porphyritic texture and fine grained groundmass formed from microlathes. Section is in cross polarised light (CPL).

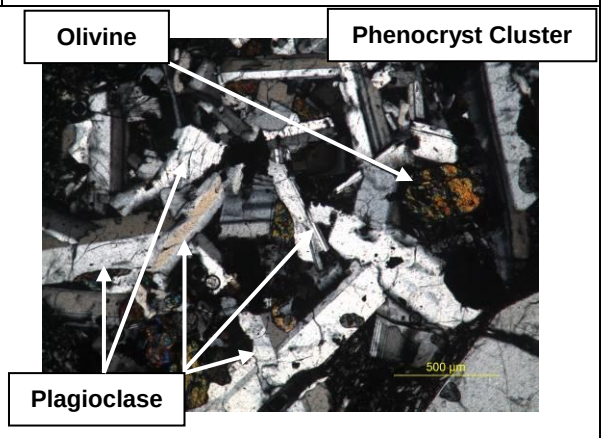

Figure 4.5f) Large damaged phenocrysts. Note. Section is in cross polarised light (CPL).

Figure 4.5 is continued over the page.

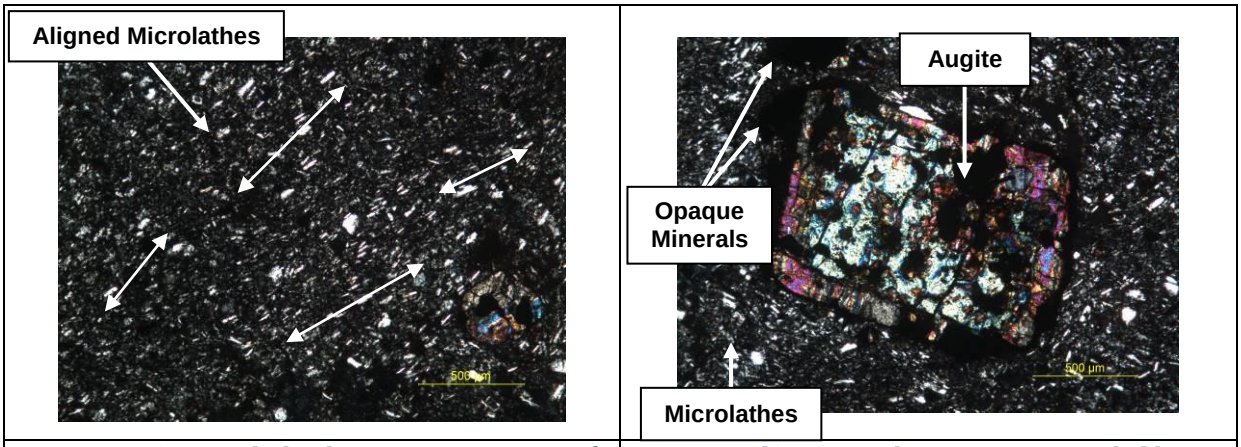

Figure 4.5g) Note slight alignment/orientation of crystals. Section in cross polarised light (CPL).

Figure 4.5h) Augite phenocryst surrounded by microlathes. Section in cross polarised light (CPL).

Figure 4.5: Annotated images at hand specimen, outcrop and microscopic scales of BLHC.

Rock Mechanics Data

The highly to completely weathered basaltic lava produced high porosity values with a mean of 36% (Table 4.8), PLS and UCS testing yielded respectively averages of 0.27 and 3.5MPa indicating the basalt as being very weak to weak; this was expected as the vast majority of the groundmass and feldspars have altered to clay. Figure 4.6 shows that sample failures during UCS testing consisted mainly of 60° shearing with lower cone formation (Figure 4.6a, c and d) and vertical fracturing (Figure 4.6b).

Table 4.8: Key physical rock mechanics data for BLHC.

Key Data for Highly to Completely Weathered Basaltic Lava (BLHC) - Physical Rock Mechanics Tests										
	Porosity n (%)	Dry Mass Density ρ_d (kg/m^3)	Bulk Volume V (m^3)	P and S Wave Velocities		Point Load Strength Index $Is_{(50)}$ (MPa)	Correlated UCS using $Is_{(50)}$×24 (MPa)	UCS σ_{ci} (MPa)	Slake Durability First Cycle Id_1 (%)	Slake Durability Second Cycle Id_2 (%)
				Vp (m/s)	Vs (m/s)					
Range	32.0-39.3	1630-1830	1.1×10^{-4} - 1.5×10^{-4}	-	-	0.18-0.38	4.2-9.1	2.0-5.6	-	-
Mean	35.9	1740	1.2×10^{-4}	-	-	0.27	6.50	3.46	-	-
Median	36.7	1720	1.1×10^{-4}	-	-	0.27	6.46	3.34	-	-
Standard Deviation	2.7	70.0	1.65×10^{-5}	-	-	0.04	0.93	1.19	-	-
*Note: Slake durability first/second cycle have no range, mean, median or standard deviation as only one test was conducted.										

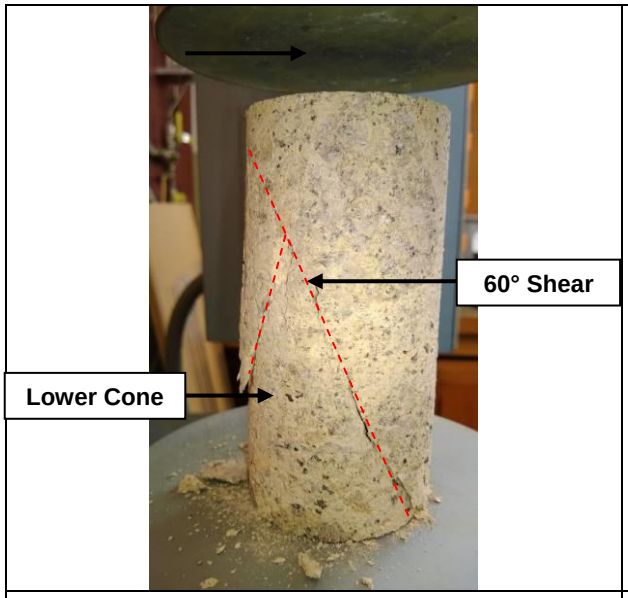

Figure 4.6a) Failed core with 60° shear and lower cone (conical) type failure (BLHC-2).

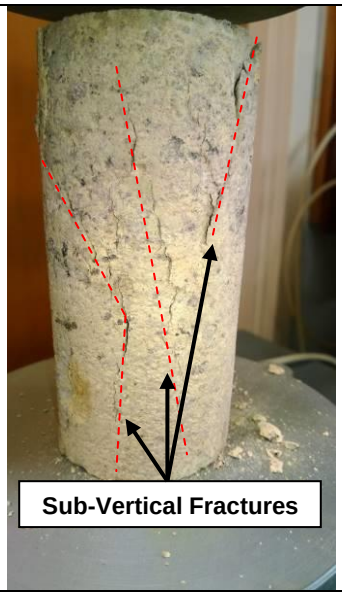

Figure 4.6b) Failed core with sub vertical fractures (BLHC-3).

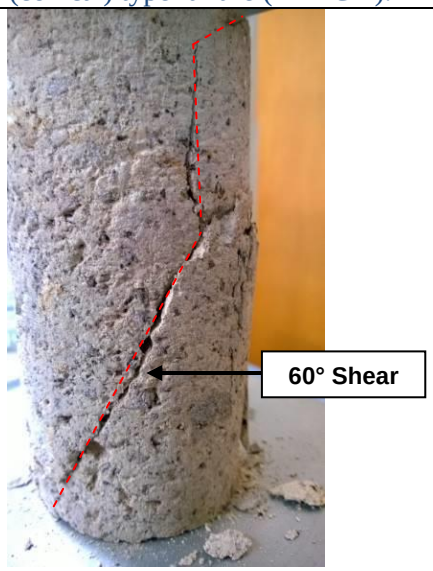

Figure 4.6c) Failed core with 60° shear and lower cone formation (BLHC-4).

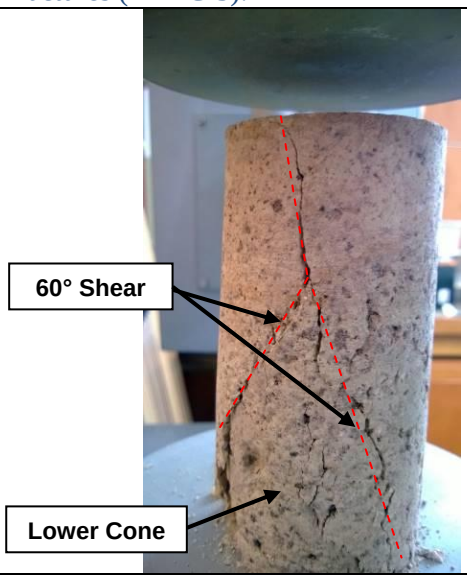

Figure 4.6d) Failed core with two 60° shears and lower cone (conical) formation (BLHC-5).

Figure 4.6: Annotated representative microscopic images of highly to completely weathered basaltic lava (BLHC).

4.5 Rubbly Basaltic Breccia (RCB)

Detailed rock descriptions are presented with relevant supporting annotated figures (Table 4.9 and Figure 4.7), followed by key datasets and results of rock mechanics testing (Table 4.10 and Figure 4.8).

Detailed Engineering Geological Igneous Rock Description

Table 4.9: Detailed Engineering Geological Igneous Rock Description for rubbly basaltic breccia (RCB).

Detailed Engineering Geological Igneous Rock Descriptive Scheme	
Component	**Description**
Geological Context (Unit Feature, Emplacement Mechanism, Formation, Group)	[RUBBLY BRECCIA, LYTTELTON VOLCANIC GROUP]
Location	Marriner Street, Sumner
Date Sampled, Identification Number	12/03/2013, RCB
Colour	Orange grey
Weathering and Alteration	Moderately to highly weathered, extensive clay alteration (Figure 4.7a)
Structure and Texture (Outcrop, Hand Specimen)	Brecciated, porphyritic (Figure 4.7b)
Groundmass Grain Size	Fine grained groundmass (Figure 4.7c)
Crystal Grain Size	Fine to medium grained phenocrysts
Fragment/Clast/Lithic Grain Size	Fine to coarse grained fragments (Figure 4.7d)
Component Analysis (Hand Specimen) *% Groundmass/Matrix* *% Crystals* *% Fragments, Clasts and Lithics* *% Vesicles*	 25% 25% 50% 0%
Mineralogy (Hand Specimen and Thin Section)	Plagioclase feldspar 10%, olivine 5%, clinopyroxene 5%, opaques 3%, iddingsite 2% (Figure 4.7e-h)
Rock Name	BASALT
Discontinuities *Orientation and Joint Sets* *Spacing* *Aperture* *Additional*	 N/A Very closely spaced Rough, moderately narrow aperture Clay infill
Intact Strength *In field* *Testing (UCS/PLS/Schmidt Hammer)*	 Very weak-weak 2-16 MPa
Full Expanded Description	
[RUBBLY BRECCIA, LYTTELTON VOLCANIC GROUP], Marriner Street, Sumner, RCB, orange grey, moderately-highly weathered, extensive clay alteration, brecciated, porphyritic, fine grained groundmass, fine to medium grained phenocrysts, fine to coarse fragments. Groundmass 25%, crystals 25% (Plagioclase feldspar 10%, olivine 5%, clinopyroxene 5%, opaques 3%, iddingsite 2%), fragments 50%, BASALT. Very closely spaced joints, rough, moderately narrow aperture, clay infill, very weak-weak (UCS 2-16 MPa).	
Summary Description	
Orange grey, moderately-highly weathered, extensive clay alteration, brecciated, porphyritic, fine grained groundmass, fine to medium grained phenocrysts, fine to coarse fragments. Groundmass 25%, crystals 25%, fragments 50%, BASALT. Very closely spaced joints, rough, moderately narrow aperture, clay infill, very weak-weak (UCS 2-16 MPa).	

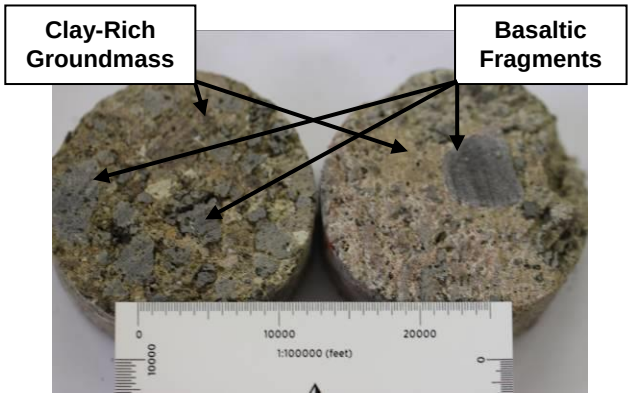

Figure 4.7a) Photograph of two cut sections of RCB core. Note variability in percentage of basaltic fragments.

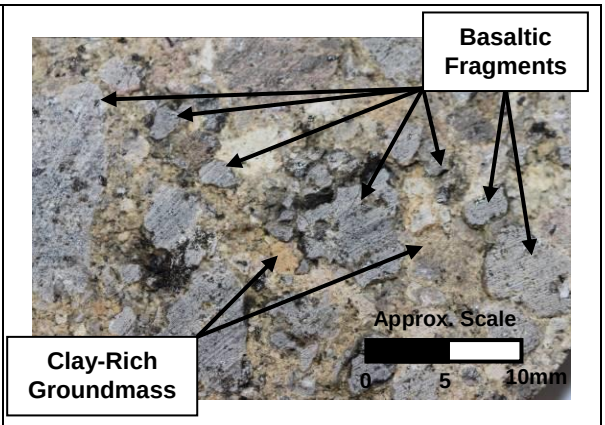

Figure 4.7b) Macro photograph of a cut section of RCB. Note variability in composition and percentage.

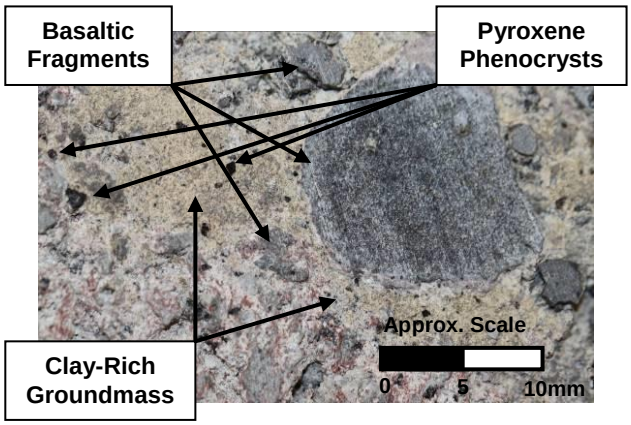

Figure 4.7c) Macro photograph of a cut section of RCB. Note variability in composition and percentage.

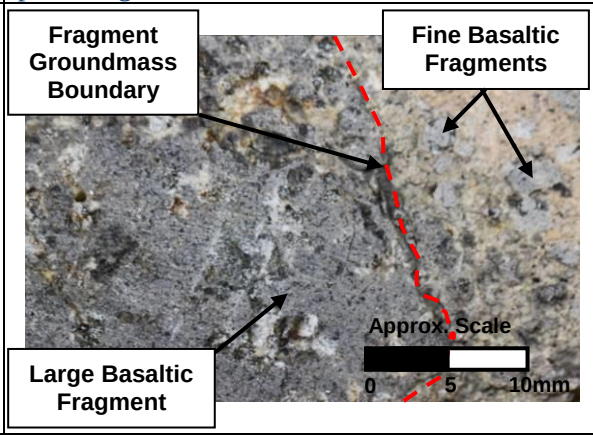

Figure 4.7d) Macro photograph of a cut section of RCB. Note fragment groundmass boundary.

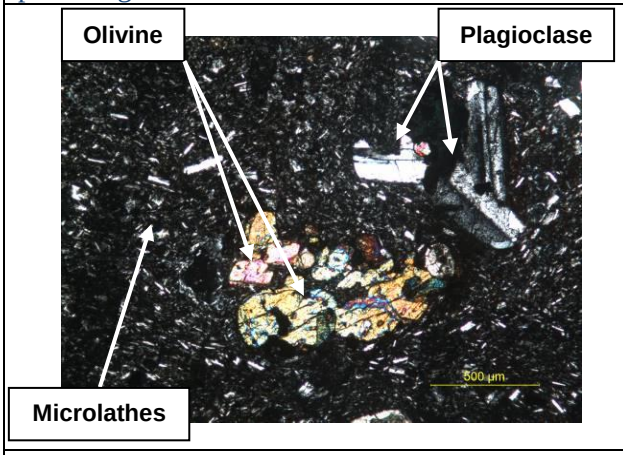

Figure 4.7e) Porphyritic texture and fine to medium grained groundmass formed from microlathes. Section is in cross polarised light (CPL).

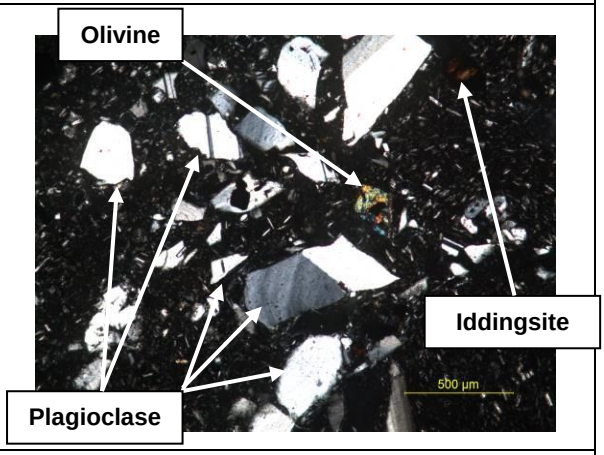

Figure 4.7f) Large damaged and fragmented phenocrysts. Note. Section is in cross polarised light (CPL).

Figure 4.7 is continued over the page.

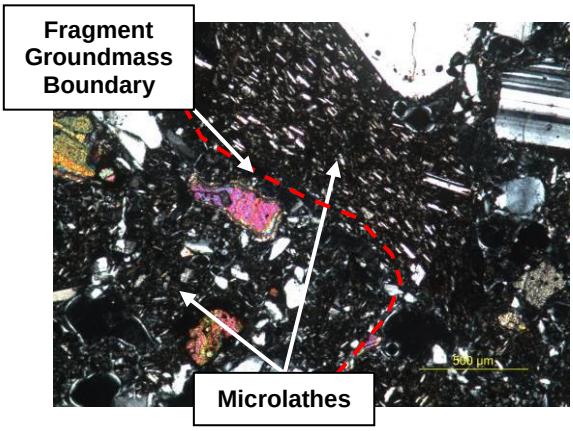

Figure 4.7g) Fragment groundmass boundary. Note difference in weathering and alignment of microlathes. Section is in cross polarised light (CPL).

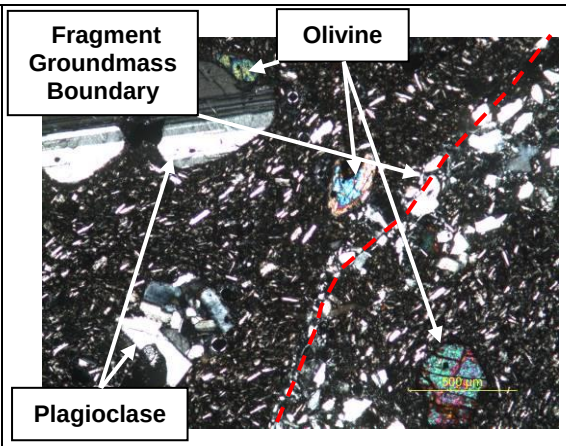

Figure 4.7h) Fragment groundmass boundary. Note difference in weathering and alignment of microlathes. Section is in cross polarised light (CPL).

Figure 4.7: Annotated images at hand specimen, outcrop and microscopic scales of RCB.

Rock Mechanics Data

The rubbly basaltic breccia produced high porosity values with a mean of 32% (Table 4.10), PLS and UCS testing yielded respectively means of 0.2 and 4.8MPa indicating the breccia as being very weak to weak. Figure 4.8 shows that sample failures during UCS testing consisted mainly of 60° shearing (Figure 4.8a/d) and expansion (barrelling) (Figure 4.8c) type failures. Failures in several cases initiated along fragment groundmass boundaries (Figure 4.8b).

Table 4.10: Key physical rock mechanics data for RCB.

Key Data for Rubbly Basaltic Lava Breccia (RCB) - Physical Rock Mechanics Tests										
	Porosity n (%)	Dry Mass Density ρ_d (kg/m^3)	Bulk Volume V (m^3)	P and S Wave Velocities		Point Load Strength Index $Is_{(50)}$ (MPa)	Correlated UCS using $Is_{(50)}\times24$ (MPa)	UCS σ_{ci} (MPa)	Slake Durability First Cycle Id_1 (%)	Slake Durability Second Cycle Id_2 (%)
				Vp (m/s)	Vs (m/s)					
Range	25.1-37.0	1640-1980	4.0×10^{-5} - 1.3×10^{-4}	-	-	0.05-0.44	1.22-10.65	1.8-15.8	-	-
Mean	31.8	1790	7.2×10^{-5}	-	-	0.20	4.84	5.35	-	-
Median	31.7	1780	6.9×10^{-5}	-	-	0.20	4.83	3.84	-	-
Standard Deviation	3.2	86.4	2.6×10^{-5}	-	-	0.09	2.06	3.98	-	-

*Note: Slake durability first/second cycle have no range, mean, median or standard deviation as only one test was conducted.

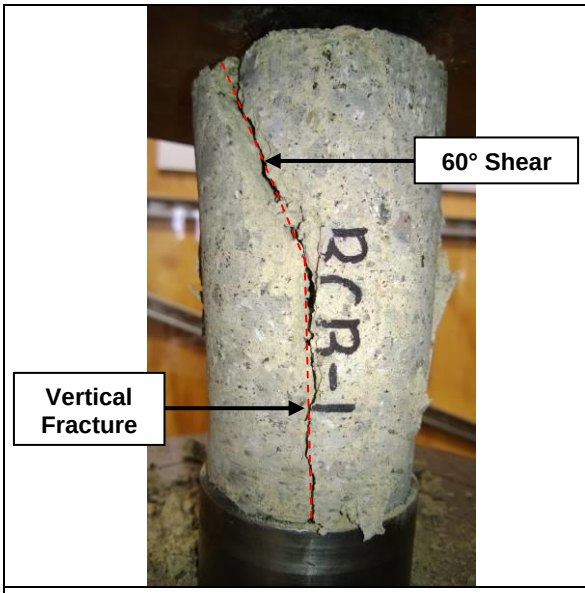

Figure 4.8a) Failed core with 60° shear transitioning into a vertical fracture (RCB-1).

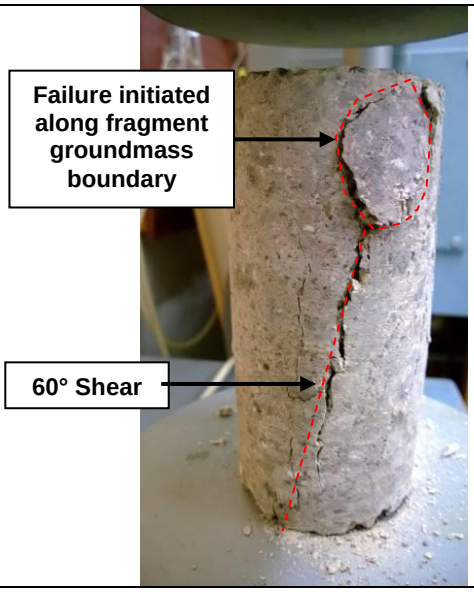

Figure 4.8b) Failed core with 60° shear initiating along a fragment and groundmass boundary (RCB-3).

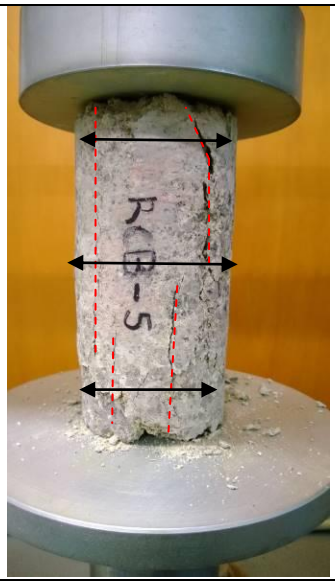

Figure 4.8c) Failed core with vertical fractures and barrelling (horizontal expansion) type failure (RCB-5).

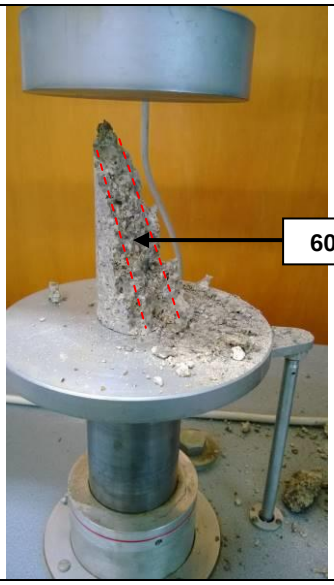

Figure 4.8d) Failed core with two 60° shear (RCB-6).

Figure 4.8: Annotated representative microscopic images of rubbly basaltic breccia (RCB).

4.6 Highly Vesicular Basaltic Lava Bomb (BLV)

Detailed rock descriptions are presented with relevant supporting annotated figures (Table 4.11 and Figure 4.9). No rock mechanics testing was carried for this unit as in-sufficient similar intact material was un-able to be recovered.

Detailed Engineering Geological Igneous Rock Description

Table 4.11: Detailed Engineering Geological Igneous Rock Description for highly vesicular basaltic lava bomb (BLV).

Detailed Engineering Geological Igneous Rock Descriptive Scheme	
Component	**Description**
Geological Context (Unit Feature, Emplacement Mechanism, Formation, Group)	[LAVA BOMB, LYTTELTON VOLCANIC GROUP]
Location	Summit Road
Date Sampled, Identification Number	14/08/2013, BLV
Colour	Grey to black
Weathering and Alteration	Unweathered to slightly weathered (Figures 4.9a/b)
Structure and Texture (Outcrop, Hand Specimen)	Highly vesicular, porphyritic (Figure 4.9c)
Groundmass Grain Size	Fine grained groundmass (Figure 4.9c)
Crystal Grain Size	Medium grained phenocrysts
Fragment/Clast/Lithic Grain Size	N/A
Component Analysis (Hand Specimen) *% Groundmass/Matrix* *% Crystals* *% Fragments, Clasts and Lithics* *% Vesicles*	 50% 10% 0% 40% (Figures 4.9g/h)
Mineralogy (Hand Specimen and Thin Section)	Iddingsite 4%, plagioclase feldspar 4%, clinopyroxene 2% (Figures 4.9e/f)
Rock Name	BASALT
Discontinuities *Orientation and Joint Sets* *Spacing* *Aperture* *Additional*	 N/A (Figure 4.9d) N/A N/A N/A
Intact Strength *In field* *Testing*	 Very weak N/A
Full Expanded Description	
[LAVA BOMB, LYTTELTON VOLCANIC GROUP], Summit Road, BLV, grey to black, unweathered-slightly weathered, highly vesicular, porphyritic, fine grained groundmass, medium grained phenocrysts Groundmass 50%, crystals 10% (Iddingsite 4%, plagioclase 4%, clinopyroxene 2%), vesicles 40%, BASALT. No visible defects. Very weak.	
Summary Description	
Grey to black, unweathered-slightly weathered, highly vesicular, porphyritic, fine grained groundmass, medium grained phenocrysts Groundmass 50%, crystals 10%, vesicles 40%, BASALT. No visible defects. Very weak.	

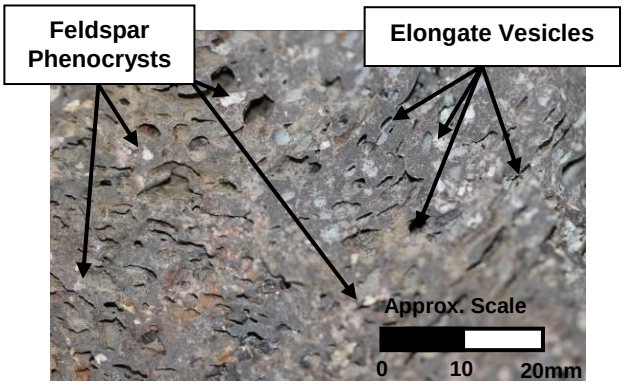

Figure 4.9a) Photograph of BLV hand sample. Note: percentage of vesicles.

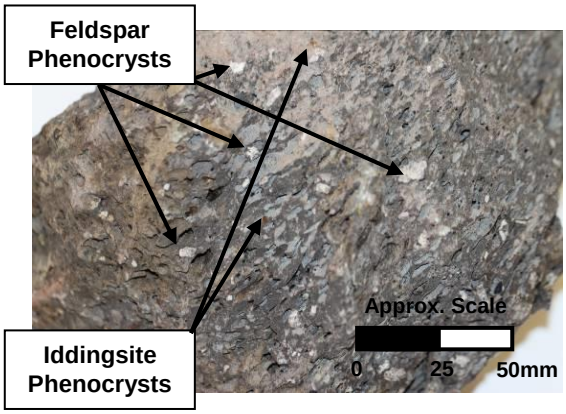

Figure 4.9b) Photograph of BLV hand samples. Note: percentage of vesicles.

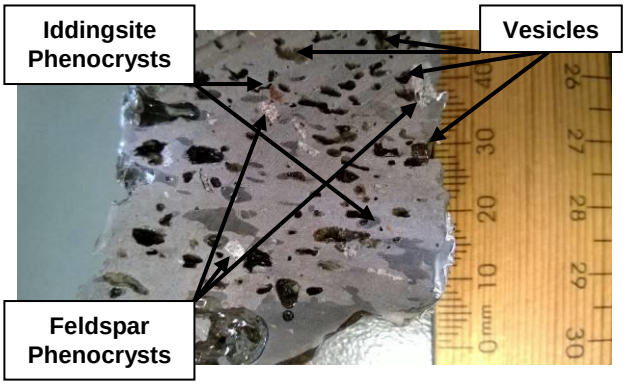

Figure 4.9c) Photograph of BLV cut section. Note the medium grained phenocrysts.

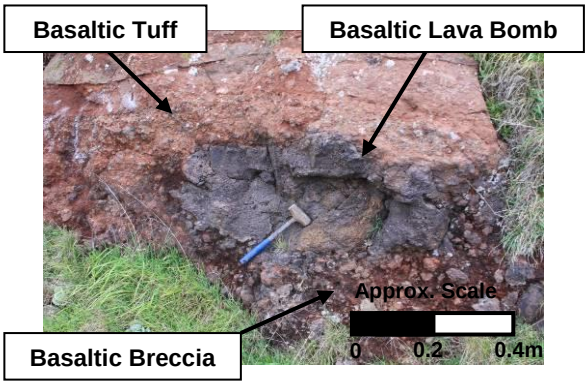

Figure 4.9d) Field photograph of highly vesicular basaltic lava bomb (BLV) between a tuff and breccia unit.

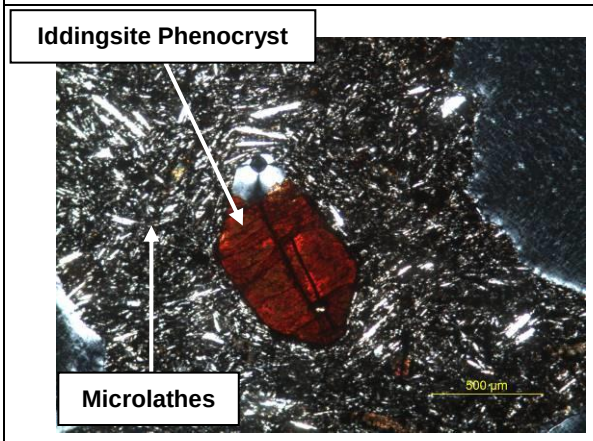

Figure 4.9e) Porphyritic texture and fine to medium grained groundmass formed from microlathes. Section is in cross polarised light (CPL).

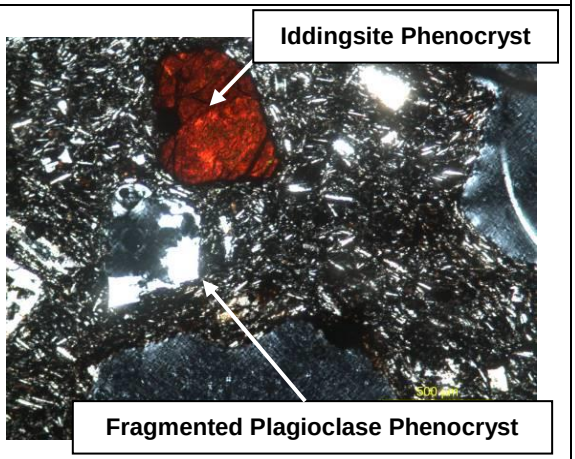

Figure 4.9f) Large fragmented plagioclase and iddingsite phenocrysts. Note. Section is in cross polarised light (CPL).

Figure 4.9 is continued over the page

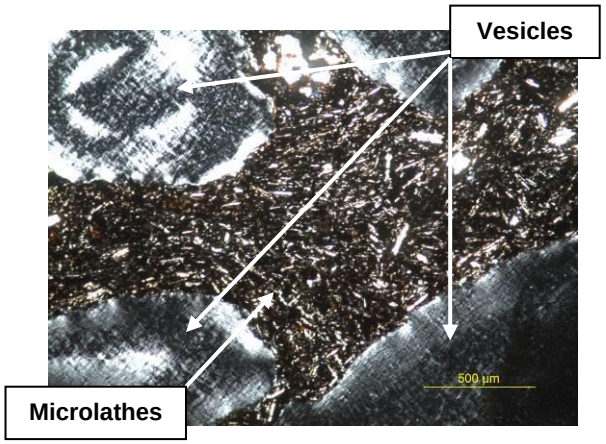

Figure 4.9g) Microlathes formed groundmass surrounded by vesicles. Section is in cross polarised light (CPL).

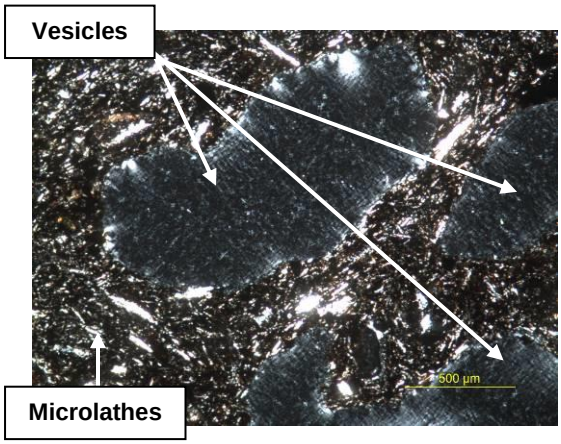

Figure 4.9h) Microlathes formed groundmass surrounded by vesicles. Section is in cross polarised light (CPL).

Figure 4.9: Annotated images at hand specimen, outcrop and microscopic scales of BLV.

4.7 Blocky Basaltic Lava (BBL)

Detailed rock descriptions are presented with relevant supporting annotated figures (Table 4.12 and Figure 4.10). No rock mechanics testing was carried for this unit as in-sufficient similar intact material was un-able to be recovered. Note, BBL is compositionally highly variable, as such component percentages are only representative of material collected.

Detailed Engineering Geological Igneous Rock Description

Table 4.12: Detailed Engineering Geological Igneous Rock Description for blocky basaltic lava (BBL).

Detailed Engineering Geological Igneous Rock Descriptive Scheme	
Component	**Description**
Geological Context (Unit Feature, Emplacement Mechanism, Formation, Group)	[BLOCKY LAVA FLOW, LYTTELTON VOLCANIC GROUP]
Location	Chalmers Track, Lyttelton
Date Sampled, Identification Number	12/03/2013, BBL
Colour	Reddish Black
Weathering and Alteration	Slightly-moderately weathered, frequent iron staining and clay alteration (Figures 4.10a/b)
Structure and Texture (Outcrop, Hand Specimen)	Brecciated, porphyritic, glassy, vesicular
Groundmass Grain Size	Fine grained groundmass (Figure 4.10a)
Crystal Grain Size	Fine to coarse grained phenocrysts (Figure 4.10c)
Fragment/Clast/Lithic Grain Size	Fine to boulder grained fragments (Figures 4.10d-f)
Component Analysis (Hand Specimen) *% Groundmass/Matrix* *% Crystals* *% Fragments, Clasts and Lithics* *% Vesicles*	 20% 20% 55% 5%
Mineralogy (Hand Specimen and Thin Section)	Plagioclase feldspar 10%, olivine 4%, clinopyroxene 2%, augite 2%, iddingsite 1%, opaques 1% (Figures 4.10g-j)
Rock Name	BASALT
Discontinuities *Orientation and Joint Sets* *Spacing* *Aperture* *Additional*	 Irregular joints (Figures 4.10d/e) Very closely spaced Planar, tight aperture Clay infill
Intact Strength *In field* *Testing (UCS/PLS/Schmidt Hammer)*	 Very weak-weak N/A
Full Expanded Description	
[BLOCKY LAVA FLOW, LYTTELTON VOLCANIC GROUP], Chalmers Track, Lyttetlon, BBL, Reddish Black, slightly-moderately weathered, frequent iron stating and clay alteration, brecciated, porphyritic, fine grained groundmass, fine to coarse grained phenocrysts, fine to boulder fragments. Groundmass 20%, crystals 20% (Plagioclase feldspar 10%, olivine 4%, clinopyroxene 2%, augite 2%, iddingsite 1%, opaques 1%), fragments 55%, vesicles 5%, BASALT. Irregular joints, very closely spaced, planar, tight, clay infill, very weak-weak.	
Summary Description	
Reddish Black, slightly-moderately weathered, frequent iron stating and clay alteration, brecciated, porphyritic, fine grained groundmass, fine to coarse grained phenocrysts, fine to boulder fragments. Groundmass 20%, crystals 20%, fragments 55%, vesicles 5%, BASALT. Irregular joints, very closely spaced, planar, tight, clay infill, very weak-weak.	

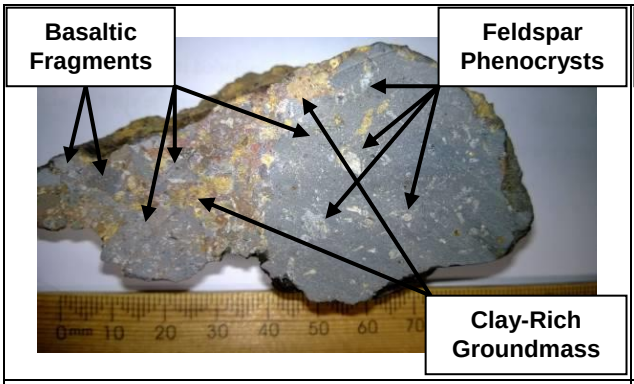

Figure 4.10a) Photograph of BBL cut section. Note size of fragments and variability in groundmass.

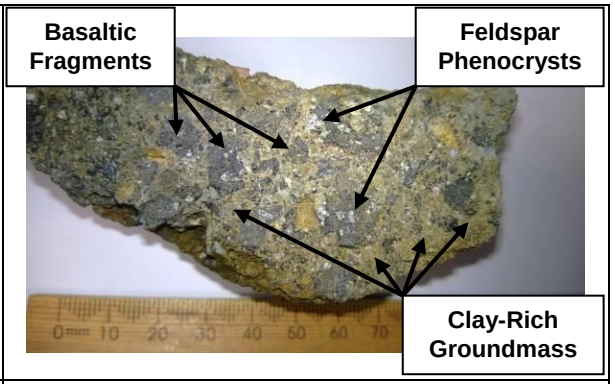

Figure 4.10b) Photograph of BBL cut section. Note brecciated basaltic fragments and further and weathering in the groundmass.

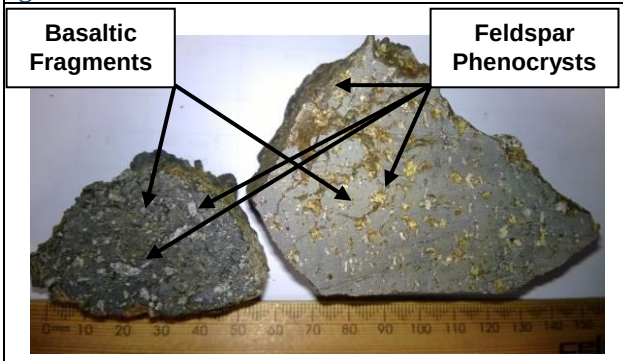

Figure 4.10c) Photograph of two BBL cut sections. Note variability in weathering between fragments.

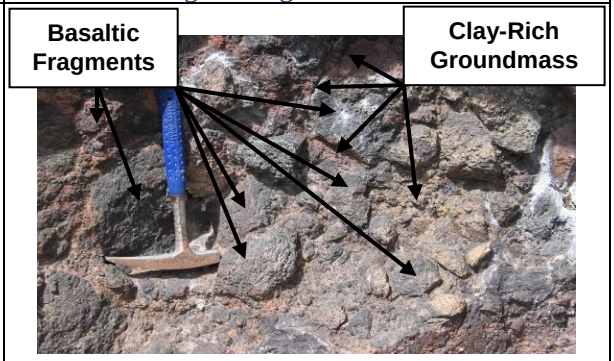

Figure 4.10d) Photograph of BBL outcrop. Note size variability in size of basaltic fragments.

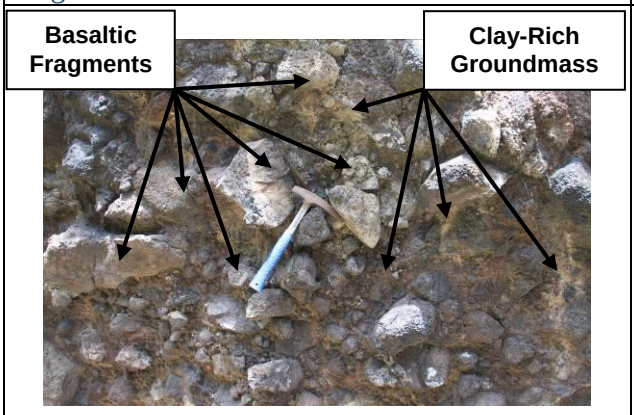

Figure 4.10e) Photograph of BBL outcrop. Note size variability in size of basaltic fragments.

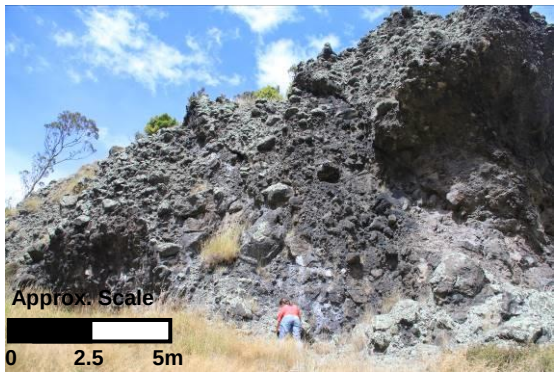

Figure 4.10f) Field photograph of BBL outcrop. Note some basaltic fragment are boulder sized (>200mm).

Figure 4.10 is continued over the page

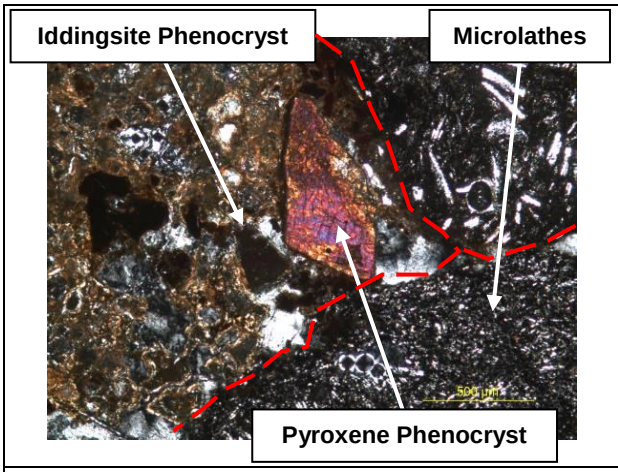

Figure 4.10g) Porphyritic texture and fine to medium grained groundmass formed from microlathes. Also note fragment groundmass boundary. Section is in cross polarised light (CPL).

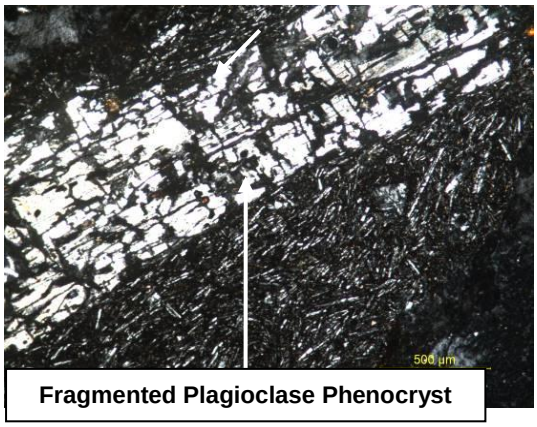

Figure 4.10h) Large fragmented plagioclase phenocryst surrounded by microlathes. Section is in cross polarised light (CPL).

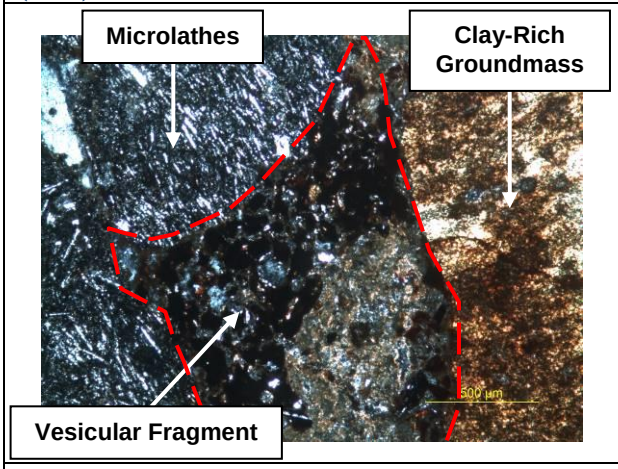

Figure 4.10i) Fragment groundmass boundary. Note difference in composition and weathering. Section is in cross polarised light (CPL).

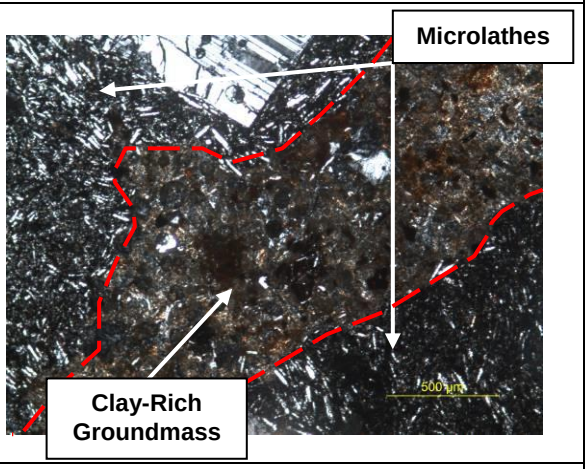

Figure 4.10j) Fragment groundmass boundary. Note difference in composition and weathering. Section is in cross polarised light (CPL).

Figure 4.10: Annotated images at hand specimen, outcrop and microscopic scales of BBL.

Rock Mechanics Data

As previously stated, no rock mechanics testing has been carried due to the compositional complexity of this unit. It should be noted that observed defects for BBL are prevalent at fragment groundmass boundaries; therefore it is the strength of the clay-rich groundmass which should ultimately control the failure of the unit. The groundmass may have similar strength values to that of BLHC or RCB (Section 4.4 and 4.5). Complexities observed between the groundmass and fragments limit these comparisons and will be required to be studied in greater detail.

4.8 Trachytic Lava (TL)

Detailed rock descriptions are presented with relevant supporting annotated figures (Table 4.13 and Figure 4.11), followed by key datasets and results of rock mechanics testing (Table 4.14, Table 4.15 and Figure 4.12).

Detailed Engineering Geological Igneous Rock Description

Table 4.13: Detailed Engineering Geological Igneous Rock Description for trachytic lava (TL)

Detailed Engineering Geological Igneous Rock Descriptive Scheme	
Component	**Description**
Geological Context (Unit Feature, Emplacement Mechanism, Formation, Group)	[LAVA FLOW, LYTTELTON VOLCANIC GROUP]
Location	Mt Cavendish, Port Hills
Date Sampled, Identification Number	14/08/2013, TL
Colour	Creamy blue grey
Weathering and Alteration	Slightly weathered, iron staining limited to flow bands (Figures 4.11a/b)
Structure and Texture (Outcrop, Hand Specimen)	Porphyritic, trachytic, flow banded
Groundmass Grain Size	Fine grained groundmass (Figures 4.11a/e)
Crystal Grain Size	Fine to medium grained phenocrysts (Figure 4.11a)
Fragment/Clast/Lithic Grain Size	N/A
Component Analysis (Hand Specimen) *% Groundmass/Matrix* *% Crystals* *% Fragments, Clasts and Lithics* *% Vesicles*	 60% 38% 0% 2%
Mineralogy (Hand Specimen and Thin Section)	Alkali feldspar 30%, plagioclase feldspar 5%, opaques 2%, iddingsite 1% (Figures 4.11e-h)
Rock Name	TRACHYTE
Discontinuities *Orientation and Joint Sets* *Spacing* *Aperture* *Additional*	 Three right angled joint sets (Figures 4.11c/d) Closely spaced Planar, tight aperture Platy jointing, no infill, minor seepage
Intact Strength *In field* *Testing (UCS/PLS/Schmidt Hammer)*	 Moderately strong-strong 44-73 MPa
Full Expanded Description	
[LAVA FLOW, LYTTELTON VOLCANIC GROUP], Mt Cavendish, Port Hills, TL, creamy blue grey, slightly-weathered, iron oxide staining limited to flow bands, porphyritic, trachytic, flow bands, fine grained groundmass, fine-medium grained phenocrysts. Groundmass 60%, crystals 38% (alkali feldspar 30%, plagioclase feldspar 5%, opaques 2%, iddingsite 1%), vesicles 2%, TRACHYTE. Three right angled joint sets, closely spaced, planar, tight aperture, platey jointing, no infill, minor seepage, moderately strong-strong (UCS 44-73 MPa).	
Summary Description	
Creamy blue grey, slightly-weathered, iron oxide staining limited to flow bands, porphyritic, trachytic, flow bands, fine grained groundmass, fine-medium grained phenocrysts. Groundmass 60%, crystals 38, vesicles 2%, TRACHYTE. Three right angled joint sets, closely spaced, planar, tight aperture, platey jointing, no infill, minor seepage, moderately strong-strong (UCS 44-73 MPa).	

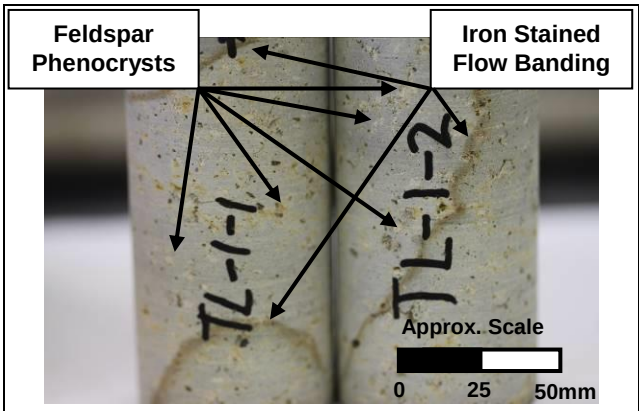

Figure 4.11a) Photograph of TL core. Note iron stained flow banding and white/cream coloured phenocrysts.

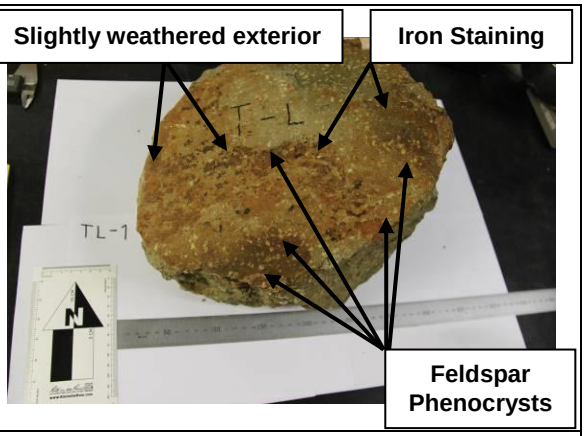

Figure 4.11b) Photograph of TL boulder. Note slightly weathered exterior and coarse grained feldspar phenocrysts.

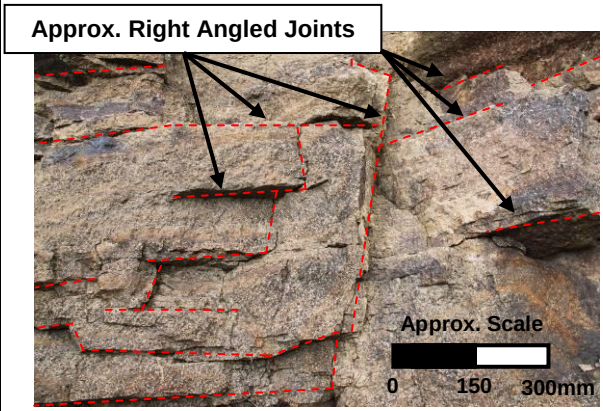

Figure 4.11c) Field photograph of TL outcrop. Note tabular blocks formed by orientation of right angled intersecting joints.

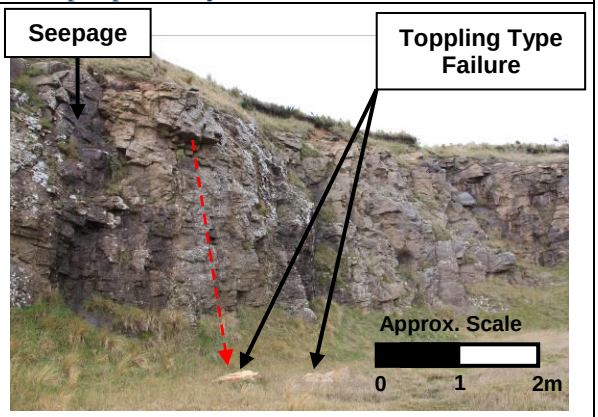

Figure 4.11d) Field photograph of outcrop of TL. Note seepage and tabular blocks. Also note tabular released blocks.

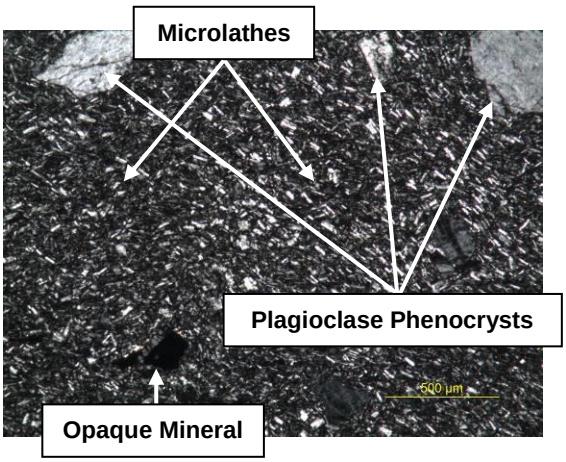

Figure 4.11e) Porphyritic texture and fine grained groundmass formed from microlathes. Note olivine has altered to iddingsite. Section is in cross polarised light (CPL).

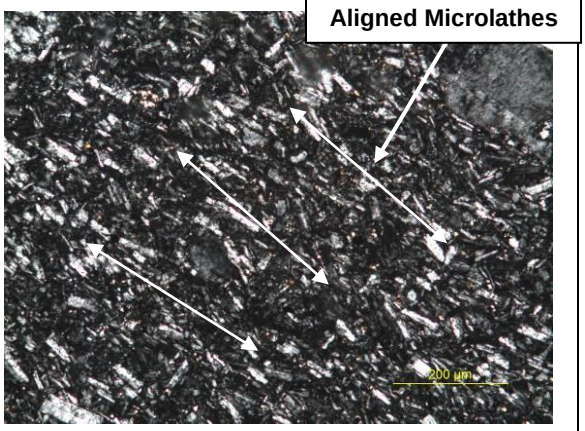

Figure 4.11f) Large damaged feldspar phenocryst surrounded by microlathes. Note strong alignment/orientation of crystals. Section is in cross polarised light (CPL).

Figure 4.11 is continued over the page

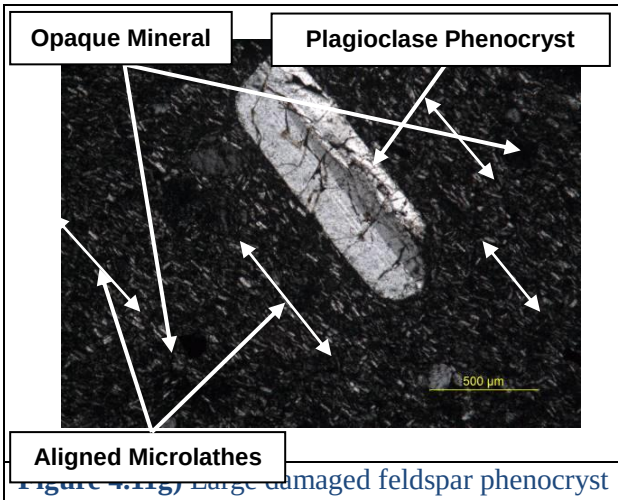

Figure 4.11g) Large damaged feldspar phenocryst surrounded by microlathes. Note strong alignment/orientation of crystals. Section is in cross polarised light (CPL).

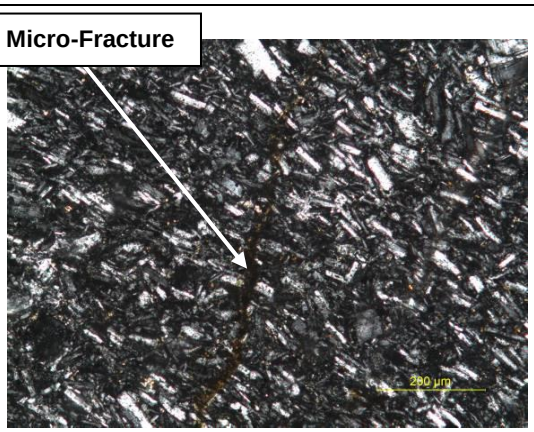

Figure 4.11h) Micro-fracture in groundmass, note alteration within the fracture. Section is in cross polarised light (CPL).

Figure 4.11: Annotated images at hand specimen, outcrop and microscopic scales of TL.

Rock Mechanics Data

Trachytic lava (TL) produced low porosity values with a mean of 4.2% (Table 4.14), PLS and UCS testing yielded respectively means of 2.03 and 56.9MPa indicating the trachyte as being moderately strong to strong. Static and dynamic deformation moduli produced reasonably consistent results with only approximately 1 order of magnitude of variation however, the range of the static bulk modulus was effected by a very high value of 261 (Table 4.15). Failures during UCS testing consisted mainly of vertical fracturing along flow banding (Figure 4.12)

Table 4.14: Key physical rock mechanics data for TL.

Key Data for Trachytic Lava (TL) - Physical Rock Mechanics Tests										
	Porosity n (%)	Dry Mass Density ρ_d (kg/m^3)	Bulk Volume V (m^3)	P and S Wave Velocities		Point Load Strength Index $Is_{(50)}$ (MPa)	Correlated UCS using $Is_{(50)}\times24$ (MPa)	UCS σ_{ci} (MPa)	Slake Durability First Cycle Id_1 (%)	Slake Durability Second Cycle Id_2 (%)
				Vp (m/s)	Vs (m/s)					
Range	3.4-5.4	2380-2430	1.9×10^{-4}-2.1×10^{-4}	3524-4014	2106-2476	1.23-2.62	29.5-62.9	44.2-73.3	-	-
Mean	4.2	2410	2.01×10^{-4}	3688	2270	2.03	48.75	56.9	-	-
Median	3.9	2410	2.03×10^{-4}	3693	2190	2.12	50.91	57.0	-	-
Standard Deviation	0.7	18.5	5.98×10^{-6}	149.4	143.1	0.45	10.78	8.72	-	-

*Note: Slake durability first/second cycle have no range, mean, median or standard deviation as only one test was conducted.

Table 4.15: Key deformation moduli test data for TL.

Key Data for Trachytic Lava (TL) - Deformation Moduli						
	Static Young's Modulus Estat (GPa)	Static Poisson's Ratio υstat (unitless)	Dynamic Young's Modulus Edyn (GPa)	Dynamic Poisson's Ratio υdyn (unitless)	Static Shear Modulus Gstat (GPa)	Static Bulk Modulus Kstat (GPa)
Range	13.4-24.8	0.12-0.49	26.0-35.5	0.13-0.27	5.36-11.07	8.93-261.67
Mean	19.0	0.23	29.6	0.19	7.88	41.84
Median	18.5	0.18	28.0	0.19	7.84	10.58
Standard Deviation	3.8	0.11	3.2	0.04	2.06	83.09

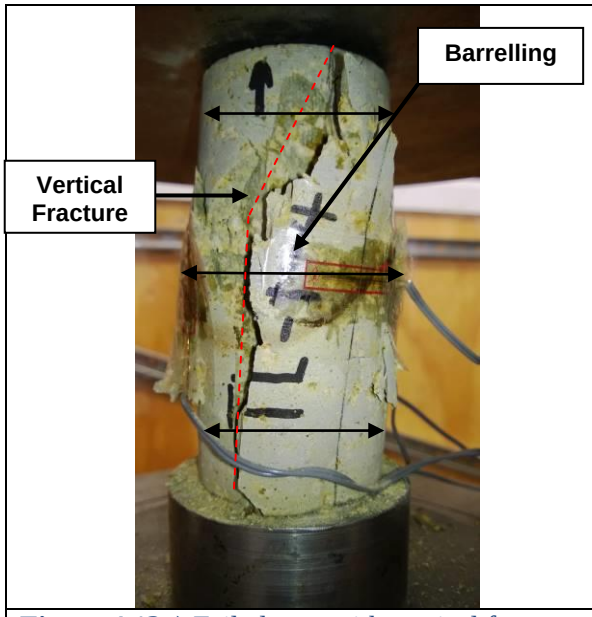

Figure 4.12a) Failed core with vertical fractures and barrelling (horizontal expansion) type failure (TL-1-4).

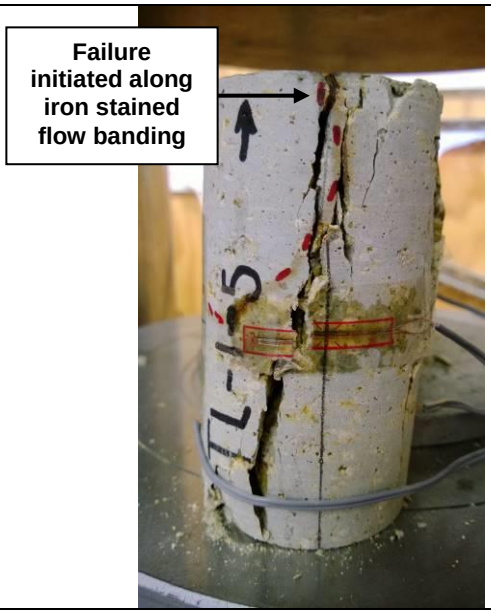

Figure 4.12b) Failed core with vertical fractures prevalent along iron stained flow banding flow banding (TL-1-5).

Figure 4.12c) Failed core with vertical fractures and barrelling (horizontal expansion) type failures (TL-1-1).

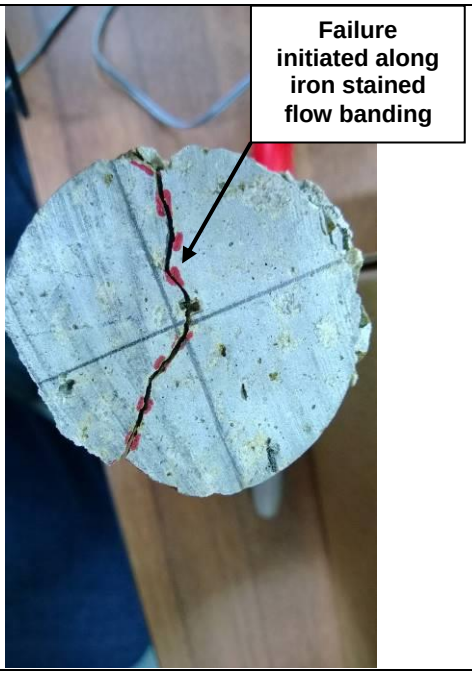

Figure 4.12d) Failed core with vertical fractures prevalent along iron stained flow banding flow banding (TL-1-5).

Figure 4.12: Annotated images of trachytic lava (TL) testing.

4.9 Synthesis

This chapter has presented the engineering geological igneous rock descriptions and key rock mechanics data supported by a series of annotated figures and tables (where relevant) for lava flow units included in this study. A full summary table of all key rock mechanical parameters in this study is presented in the Chapter 5 synthesis. Following on from Chapter 4, Chapter 5 presents the remaining units of this study 'assorted volcanics', these units include ignimbrites, tuffs, ashes, dykes and laharic deposits. The results of Chapters 4 and 5 are discussed in detail in Chapter 6 'Discussion and Applications'.

CHAPTER 5 - Results of Geotechnical Testing and Properties Part 2 - Assorted Volcanics

5.1 Introduction

Chapter 5 presents data sets on 'accessory volcanics' of the Lyttelton Volcanic Group and follows the sub-unit classification scheme as set out in Table 2.1. Data included in this chapter includes unit descriptions, thin section analysis, rock mechanics data and a series of annotated figures and data tables where relevant; for a detailed description see Section 4.1.

Units included in Chapter 5 include: basaltic dyke (BD), trachytic dyke (TD), brecciated basaltic ignimbrite (IGB), moderately welded basaltic ignimbrite (IGMW), highly welded basaltic ignimbrite (IGW), crystal dominated tuff (CTC), lithic dominated tuff (CTL), red ash (RD), volcanogenic conglomerate (VC) and volcanogenic tuffaceous sandstone (VTS).

5.2 Basaltic Dyke (BD)

Detailed rock descriptions are presented with relevant supporting annotated figures (Table 5.1 and Figure 5.1), followed by key datasets and results of rock mechanics testing (Table 5.2, Table 5.3 and Figure 5.2).

Detailed Engineering Geological Igneous Rock Description

Table 5.1: Detailed Engineering Geological Igneous Rock Description for Basaltic Dyke (BD).

Detailed Engineering Geological Igneous Rock Descriptive Scheme	
Component	**Description**
Geological Context (Unit Feature, Emplacement Mechanism, Formation, Group)	[DYKE, LYTTELTON VOLCANIC GROUP]
Location	Worsley Spur, Port Hills
Date Sampled, Identification Number	14/08/2013, BD
Colour	Grey to black
Weathering and Alteration	Slightly weathered, localised iron staining to fractures and flow bands (Figures 5.1a/b)
Structure and Texture (Outcrop, Hand Specimen)	Porphyritic, trachytic (Figure 5.1e)
Groundmass Grain Size	Fine grained groundmass
Crystal Grain Size	Medium-coarse grained phenocrysts (Figure 5.1c)
Fragment/Clast/Lithic Grain Size	N/A
Component Analysis (Hand Specimen) *% Groundmass/Matrix* *% Crystals* *% Fragments, Clasts and Lithics* *% Vesicles*	 57% 40% 0% 3%
Mineralogy (Hand Specimen and Thin Section)	Plagioclase feldspar 20%, iddingsite 12%, opaques 5%, alkali feldspar 2%, clinopyroxene 1% (Figures 5.1f-h)
Rock Name	BASALT
Discontinuities *Orientation and Joint Sets* *Spacing* *Aperture* *Additional*	 Two joint sets (Figure 5.1d) Closely spaced Smooth, narrow aperture No infill, minor seepage
Intact Strength *In field* *Testing (UCS/PLS/Schmidt Hammer)*	 Strong 61-71 MPa
Full Expanded Description	
[DYKE, LYTTELTON VOLCANIC GROUP], Worsley Spur, Port Hills, BD, grey to black, Slightly weathered, localised iron staining to flow banding and fractures, porphyritic, fine grained groundmass, medium-coarse grained phenocrysts. Groundmass 57%, crystals 40% (Plagioclase feldspar 20%, iddingsite 12%, opaques 5%, alkali feldspar 2%, clinopyroxene 1%), vesicles 3%, BASALT. Two joint sets, closely spaced, smooth, narrow aperture, no infill, minor seepage, strong (UCS 61-71 MPa).	
Summary Description	
Grey to black, Slightly weathered, localised iron staining to flow banding and fractures, porphyritic, fine grained groundmass, medium-coarse grained phenocrysts. Groundmass 57%, crystals 40%, vesicles 3%, BASALT. Two joint sets, closely spaced, smooth, narrow aperture, no infill, minor seepage, strong (UCS 61-71 MPa).	

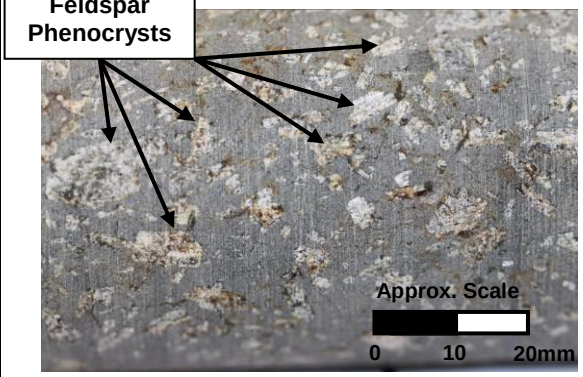

Figure 5.1a) Photograph of side of BD core. Note high percentage of medium and coarse phenocrysts.

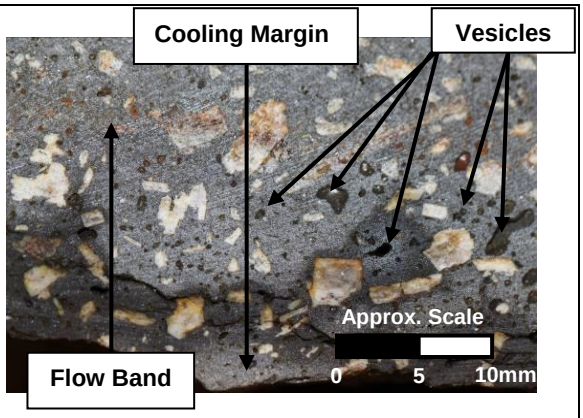

Figure 5.1b) Photograph of cut section of BD. Note increasing number of vesicles towards cooling margin. Also note flow band.

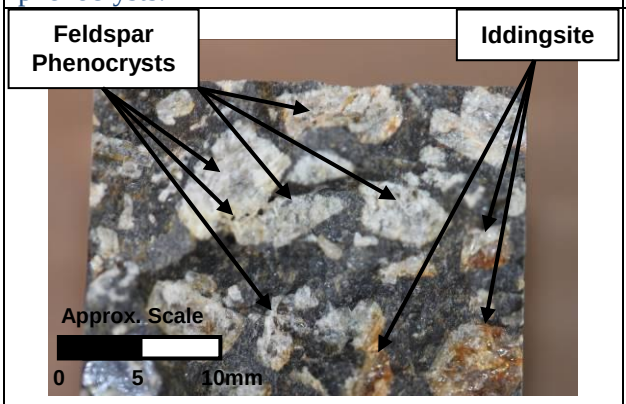

Figure 5.1c) Photograph of failed BD point load sample, not size and percentage of coarse medium-coarse grained phenocrysts.

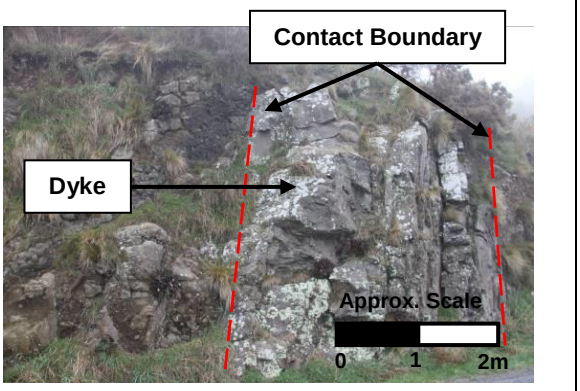

Figure 5.1d) Field photograph of outcrop/road cut of BD. Note crudely formed cubic blocks

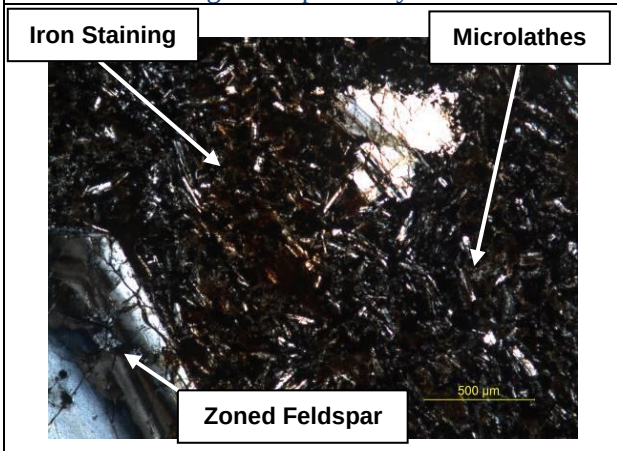

Figure 5.1e) Porphyritic texture and fine to medium grained groundmass formed from microlathes. Note the patch of iron/hematite staining in the centre of them image. Also note micro-fractures in the phenocrysts. Section is in cross polarised light (CPL).

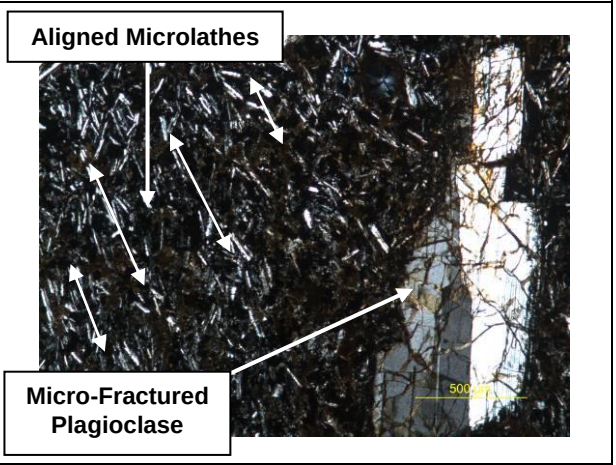

Figure 5.1f) Large fractured feldspar phenocryst surrounded by microlathes. Note alignment/orientation of crystals. Section is in cross polarised light (CPL).

Figure 5.1 is continued over the page

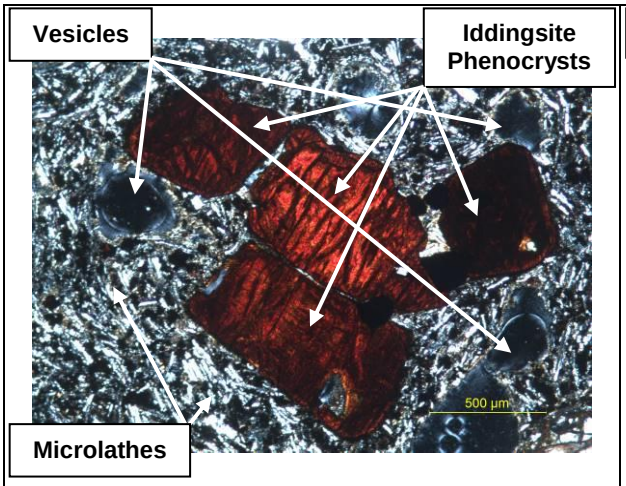

Figure 5.1g) Iddingsite phenocrysts surrounded by microlathes. Section is in cross polarised light (CPL).

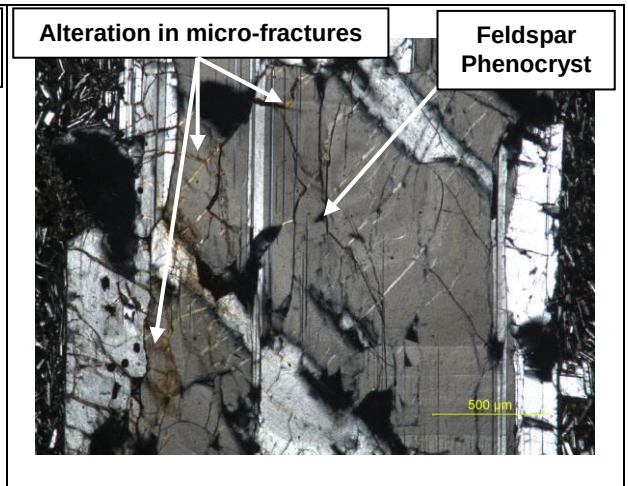

Figure 5.1h) Micro-fractured plagioclase in groundmass, note alteration within the fracture. Section is in cross polarised light (CPL).

Figure 5.1: Annotated images at hand specimen, outcrop and microscopic scales of BD.

Rock Mechanics Data

The basaltic dyke (BD) produced low porosity values with a mean of 3.0% (Table 5.2), PLS and UCS testing yielded respectively means of 3.07 and 66.8 MPa indicating the basalt as being strong. Static and dynamic deformation moduli produced reasonably consistent results with only approximately 1 order of magnitude of variation (Table 5.3). Types of sample failures during UCS testing mainly consisted of upper cone formation and vertical fracturing (Figure 5.2).

Table 5.2: Key physical rock mechanics data for BD.

Key Data for Basaltic Dyke (BD) - Physical Rock Mechanics Tests										
	Porosity n (%)	Dry Mass Density ρ_d (kg/m^3)	Bulk Volume V (m^3)	P and S Wave Velocities		Point Load Strength Index $Is_{(50)}$ (MPa)	Correlated UCS using $Is_{(50)}$×24 (MPa)	UCS σ_{ci} (MPa)	Slake Durability First Cycle Id_1 (%)	Slake Durability Second Cycle Id_2 (%)
				Vp (m/s)	Vs (m/s)					
Range	2.2-3.9	2750-2780	2.0×10^{-4}-2.2×10^{-4}	4458-4774	2575-2727	1.48-3.97	35.55-95.31	61.6-71.1	-	-
Mean	3.0	2760	2.01×10^{-4}	4665	2648	3.07	73.8	66.8	-	-
Median	2.9	2770	2.03×10^{-4}	4714	2645	3.44	82.6	67.4	-	-
Standard Deviation	0.62	11.2	6.0×10^{-6}	125.3	56.0	0.76	18.4	3.4	-	-

*Note: Slake durability first/second cycle have no range, mean, median or standard deviation as only one test was conducted.

Table 5.3: Key deformation moduli test data for BD.

Key Data for Basaltic Dyke (BD) - Deformation Moduli						
	Static Young's Modulus Estat (GPa)	Static Poisson's Ratio υstat (unitless)	Dynamic Young's Modulus Edyn (GPa)	Dynamic Poisson's Ratio υdyn (unitless)	Static Shear Modulus Gstat (GPa)	Static Bulk Modulus Kstat (GPa)
Range	21.1-43.8	0.12-0.23	46.7-51.3	0.24-0.29	8.3-18.4	12.2-21.3
Mean	31.8	0.20	48.9	0.26	13.3	18.1

Median	31.2	0.21	48.8	0.26	13.2	18.3
Standard Deviation	8.4	0.05	1.8	0.02	3.6	4.5

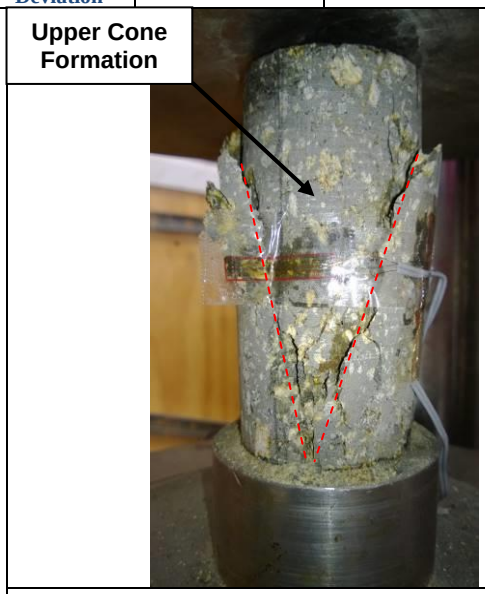

Figure 5.2a) Failed core with upper cone formation (conical type failure) (BD-1-1).

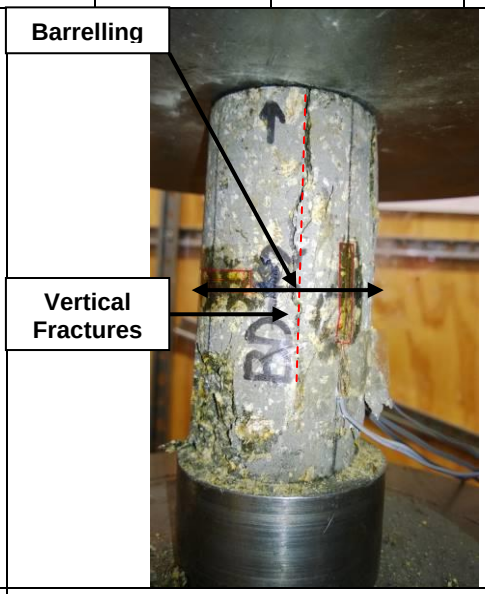

Figure 5.2b) Failed core with vertical fractures and barrelling (horizontal expansion) (BD-1-2).

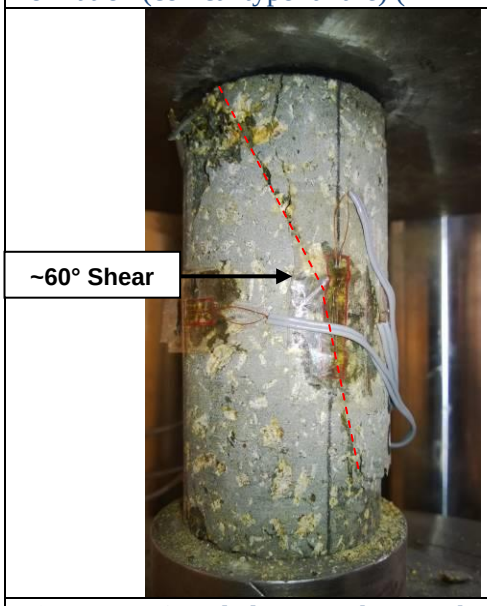

Figure 5.2C) Failed core with ~60° shear (BD-1-3).

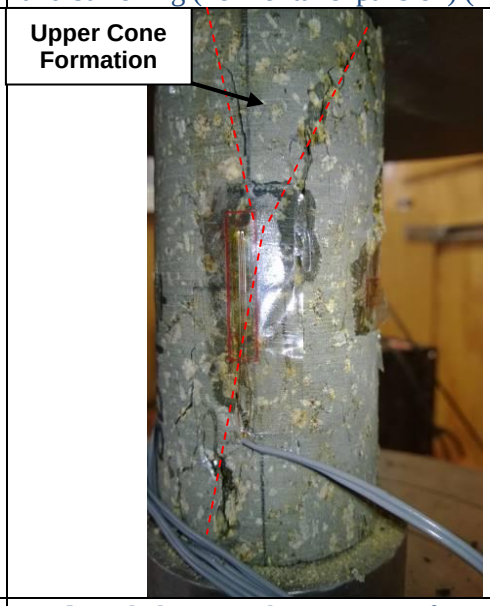

5.2d) Failed core with upper cone formation (conical type failure) and a ~60° shear (BD-1-4).

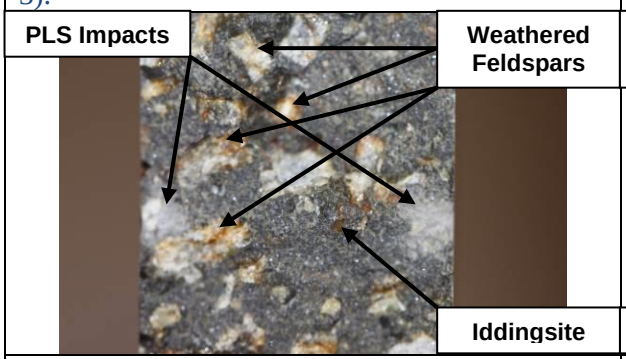

Figure 5.2e) Failed point load sample, note impact marks from PLS test, relatively unweathered groundmass and altered/weathered

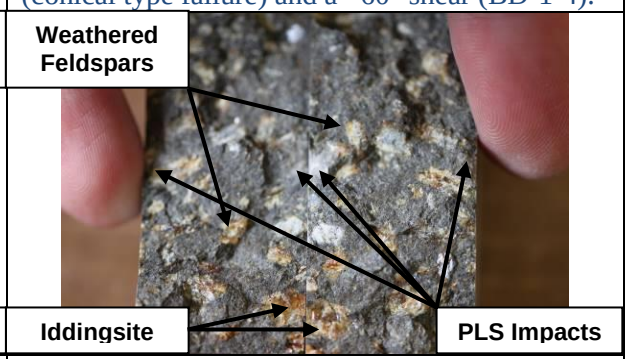

Figure 5.2F) Failed point load sample, note impact marks from PLS test, relatively unweathered groundmass and altered/weathered

phenocrysts.	phenocrysts.

Figure 5.2: Annotated images of basaltic dyke (BD) testing.

5.3 Trachytic Dyke (TD)

Detailed rock descriptions are presented with relevant supporting annotated figures (Table 5.4 and Figure 5.3), followed by key datasets and results of rock mechanics testing (Table 5.5, Table 5.6 and Figure 5.4).

Detailed Engineering Geological Igneous Rock Description

Table 5.4: Detailed Engineering Geological Igneous Rock Description for Trachytic Dyke (TD).

Detailed Engineering Geological Igneous Rock Descriptive Scheme	
Component	**Description**
Geological Context (Unit Feature, Emplacement Mechanism, Formation, Group)	[DYKE, LYTTELTON VOLCANIC GROUP]
Location	Corner of Evans Pass, Sumner Pass and Summit Road
Date Sampled, Identification Number	14/08/2013, TD
Colour	Bluish grey to green
Weathering and Alteration	Slightly weathered, frequent iron oxide staining (Figures 5.3b, g, h)
Structure and Texture (Outcrop, Hand Specimen)	Porphyritic, trachytic, flow banding (Figure 5.3a)
Groundmass Grain Size	Fine grained groundmass
Crystal Grain Size	Fine to coarse grained phenocrysts (Figure 5.3c)
Fragment/Clast/Lithic Grain Size	N/A
Component Analysis (Hand Specimen) *% Groundmass/Matrix* *% Crystals* *% Fragments, Clasts and Lithics* *% Vesicles*	 57% 40% 0% 3%
Mineralogy (Hand Specimen and Thin Section)	Alkali feldspar 15%, Clinopyroxene 10%, Iddingsite 5%, Augite, 5%, Opaques 3%, Orthopyroxene 2% (Figures 5.3e/f)
Rock Name	TRACHYTE
Discontinuities *Orientation and Joint Sets* *Spacing* *Aperture* *Additional*	 Near right angled joints, three sets (Figure 5.3d) moderately widely spaced narrow aperture no infill
Intact Strength *In field* *Testing (UCS/PLS/Schmidt Hammer)*	 Moderately Strong - Strong 40-60 MPa
Full Expanded Description	
[DYKE, LYTTELTON VOLCANIC GROUP], Evans Pass, TD, bluish grey to green, slightly weathered, iron oxide staining, porphyritic, trachytic, flow banding, fine grained groundmass, fine to coarse grained phenocrysts. Groundmass 57%, crystals 40% (alkali feldspar 15%, clinopyroxene 10%, iddingsite 5%, augite, 5%, opaques 3%, orthopyroxene 2%), vesicles 3%, TRACHYTE. Near right angled joints, three joint sets, moderately widely spaced, narrow aperture, no infill, moderately strong-strong (UCS 40-60 MPa).	
Summary Description	
Bluish grey to green, slightly weathered, iron oxide staining, porphyritic, trachytic, flow banding, fine grained groundmass, fine to coarse grained phenocrysts. Groundmass 57%, crystals 40%, vesicles 3%, TRACHYTE. Near right angled joints, three joint sets, no infill, moderately widely spaced, narrow aperture, moderately strong-strong (UCS 40-60 MPa).	

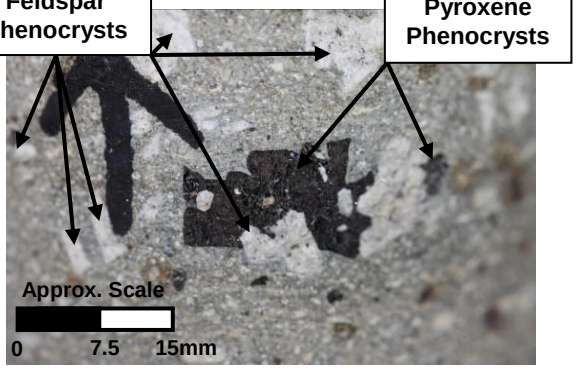

Figure 5.3a) Photograph of side of TD core. Note high percentage of medium and coarse phenocrysts.

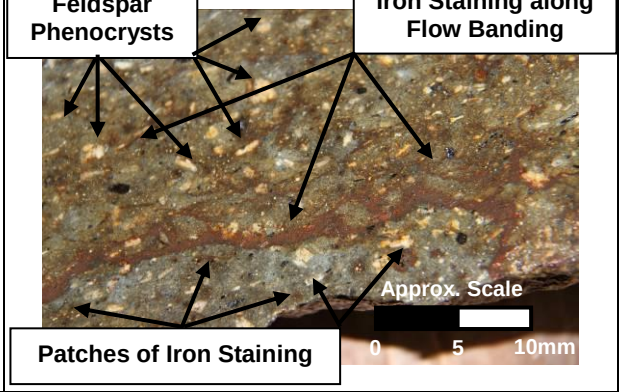

Figure 5.3b) Photograph of cut section of TD. Note section is wet and that iron staining is mainly controlled by flow banding but also appears in patches.

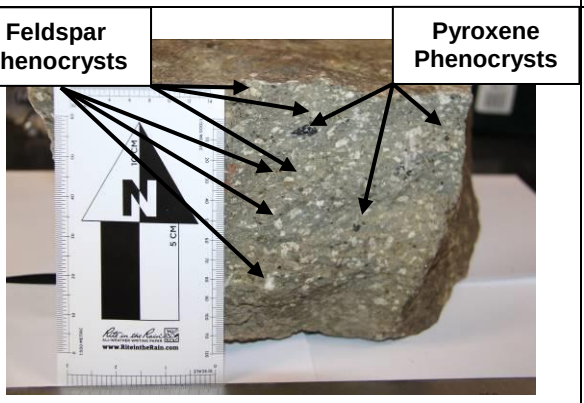

Figure 5.3c) Photograph of boulder of TD used for coring samples. Note percentage of phenocrysts.

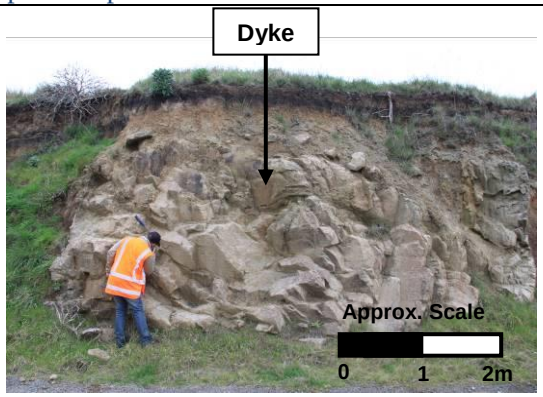

Figure 5.3d) Field photograph of outcrop/road cut of TD. Note well-formed angular cubic blocks.

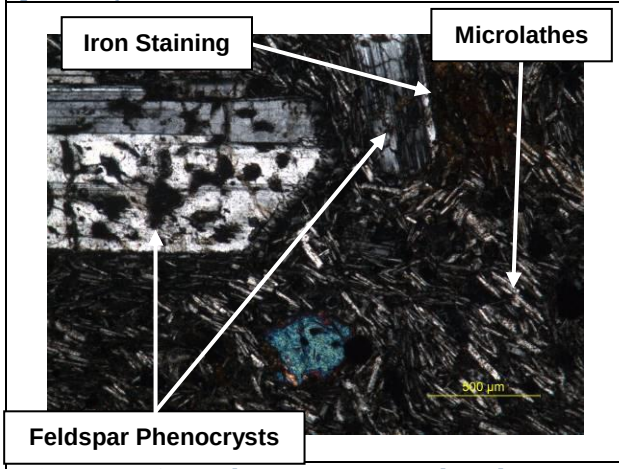

Figure 5.3e) Porphyritic texture and medium grained groundmass formed from microlathes. Note the patch of iron/hematite staining in the right corner of them image. Also note micro-fractures in the phenocrysts. Section is in cross polarised light (CPL).

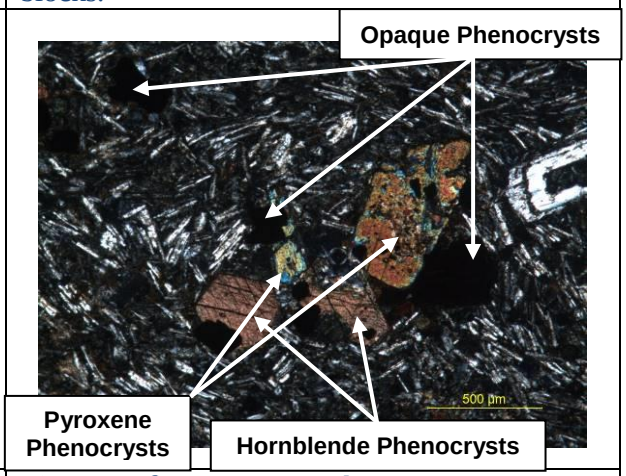

Figure 5.3f) Coarse grained pyroxene, opaque and hornblende phenocrysts surrounded by microlathes. Note alignment/orientation of microlathes. Section is in cross polarised light (CPL).

Figure 5.3 is continued over the page

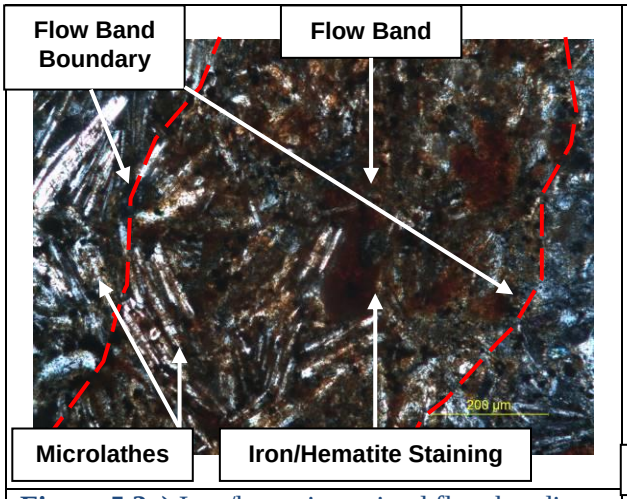

Figure 5.3g) Iron/hematite stained flow banding. Note un-altered microlathes to the left and right of the banding boundary. Section is in cross polarised light (CPL).

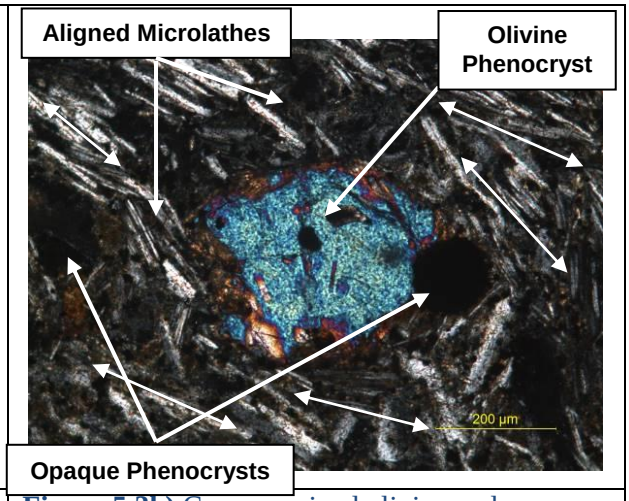

Figure 5.3h) Coarse grained olivine and opaque phenocrysts surrounded by microlathes. Note alignment/orientation of microlathes. Section is in cross polarised light (CPL).

Figure 5.3: Annotated images at hand specimen, outcrop and microscopic scales of TD.

Rock Mechanics Data

The trachytic dyke produced low porosity values with a mean of 6.0% (Table 5.5), PLS and UCS testing yielded respectively means of 2.82 and 54.0 MPa indicating the trachyte as being moderately strong to strong. Static and dynamic deformation moduli produced reasonably consistent results with only approximately 1 order of magnitude of variation (Table 5.6). All TD cores during UCS testing displayed upper cone formation (conical) (Figure 5.4).

Table 5.5: Key physical rock mechanics data for TD.

Key Data for Trachytic Dyke (TD) - Physical Rock Mechanics Tests										
	Porosity n (%)	Dry Mass Density ρ_d (kg/m^3)	Bulk Volume V (m^3)	P and S Wave Velocities		Point Load Strength Index $Is_{(50)}$ (MPa)	Correlated UCS using $Is_{(50)}$×24 (MPa)	UCS σ_{ci} (MPa)	Slake Durability First Cycle Id_1 (%)	Slake Durability Second Cycle Id_2 (%)
				Vp (m/s)	Vs (m/s)					
Range	3.9-10.6	2290-2350	2.0×10^{-4}-2.3×10^{-4}	3121-3474	1888-1986	1.93-4.91	46.4-118.0	42.4-61.0	-	-
Mean	6.0	2330	2.13×10^{-4}	3249	1948	2.82	67.6	54.0	-	-
Median	5.4	2350	2.10×10^{-4}	3215	1969	2.76	66.2	55.1	-	-
Standard Deviation	2.2	27.2	8.61×10^{-6}	118.7	41.5	0.40	9.7	6.6	-	-

*Note: Slake durability first/second cycle have no range, mean, median or standard deviation as only one test was conducted.

Table 5.6: Key deformation moduli test data for TD.

Key Data for Trachytic Dyke (TD) - Deformation Moduli						
	Static Young's Modulus Estat (GPa)	Static Poisson's Ratio υstat (unitless)	Dynamic Young's Modulus Edyn (GPa)	Dynamic Poisson's Ratio υdyn (unitless)	Static Shear Modulus Gstat (GPa)	Static Bulk Modulus Kstat (GPa)
Range	10.3-20.1	0.13-0.28	19.7-22.2	0.18-0.26	4.6-8.0	4.6-13.4
Mean	16.0	0.21	21.6	0.22	6.6	9.6
Median	16.5	0.21	21.7	0.22	6.8	9.3
Standard Deviation	3.0	0.05	1.1	0.02	1.1	2.7

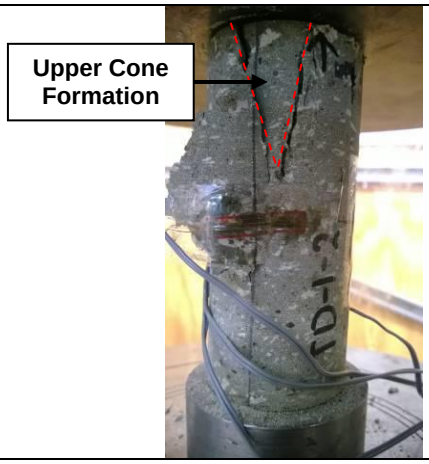

Figure 5.4a) Failed core with upper cone formation (conical type failure) (TD-1-2).

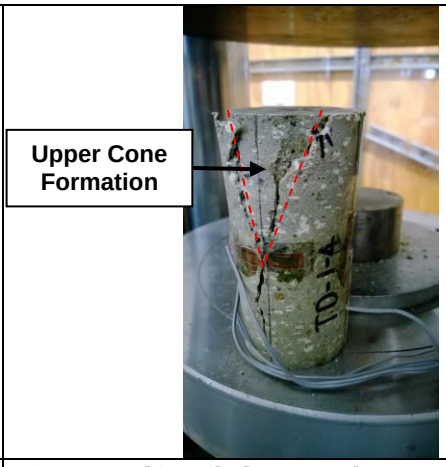

Figure 5.4b) Failed core with upper cone formation (conical type failure) (TD-1-4).

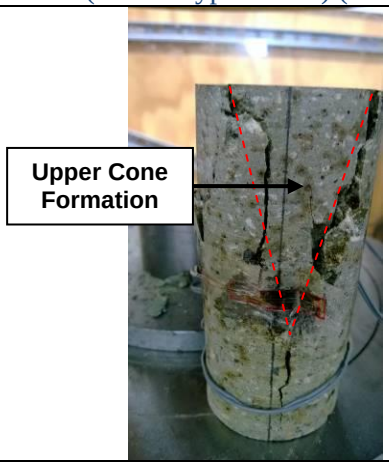

Figure 5.4c) Failed core with upper cone formation (conical type failure) (TD-2-1).

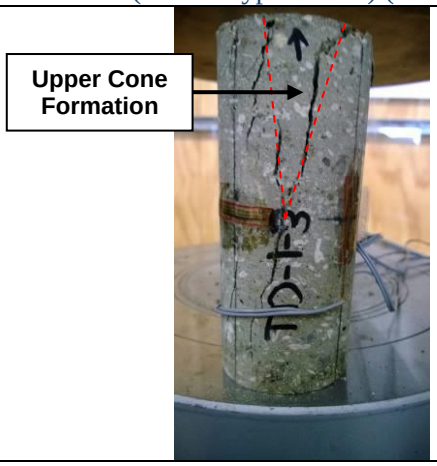

Figure 5.4d) Failed core with upper cone formation (conical type failure) (TD-1-3).

Figure 5.4: Annotated images of trachytic dyke (TD) testing.

5.4 Brecciated Basaltic Ignimbrite (IGB)

Detailed rock descriptions are presented with relevant supporting annotated figures (Figure 5.5 and 5.8), followed by key datasets and results of rock mechanics testing (Table 5.5 and Figure 5.9).

Detailed Engineering Geological Igneous Rock Descriptions

Table 5.7: Detailed Engineering Geological Igneous Rock Description for Brecciated Basaltic Ignimbrite (IGB).

Detailed Engineering Geological Igneous Rock Descriptive Scheme	
Component	**Description**
Geological Context (Unit Feature, Emplacement Mechanism, Formation, Group)	[PYROCLASTIC DENSITY CURRENT, LYTTELTON VOLCANIC GROUP]
Location	Redcliffs, Sumner
Date Sampled, Identification Number	14/08/2013, IGB
Colour	Light grey
Weathering and Alteration	Slightly weathered, minor iron staining
Structure and Texture (Outcrop, Hand Specimen)	Brecciated, porphyritic
Groundmass Grain Size	Fine grained groundmass (Figure 5.5)
Crystal Grain Size	Fine grained phenocrysts (Figure 5.5a)
Fragment/Clast/Lithic Grain Size	Fine to boulder sized fragments (Figures 5.5a-c)
Component Analysis (Hand Specimen) *% Groundmass/Matrix* *% Crystals* *% Fragments, Clasts and Lithics* *% Vesicles*	 35% 15% 50% 0%
Mineralogy (Hand Specimen and Thin Section)	Iddingsite 8%, plagioclase feldspar 3%, olivine 2%, opaques 2% (Figures 5.5e/f)
Rock Name	BRECCIATED BASALTIC IGNIMBRITE
Discontinuities *Orientation and Joint Sets* *Spacing* *Aperture* *Additional*	 N/A N/A N/A Micro-fractures with defects prevalent at fragment groundmass boundaries (Figure 5.5b)
Intact Strength *In field* *Testing(UCS/PLS/Schmidt Hammer)*	 Extremely weak PLS: 0.04-0.34 MPa
Full Expanded Description	
[PYROCLASTIC DENSITY CURRENT, LYTTELTON VOLCANIC GROUP], Redcliffs, Sumner, IGB, light grey, slightly weathered, minor iron oxide staining, brecciated, porphyritic, fine grained groundmass, fine grained phenocrysts, fine to boulder sized fragments. Groundmass 35%, crystals 15% (iddingsite 8%, plagioclase 3%, olivine 2%, opaques 2%), fragments 50%, BRECCIATD BASALTIC IGNIMBRITE. Micro-fractures with defects prevalent at fragment groundmass boundaries. Extremely weak (Point Load Strength Index 0.04-0.34 MPa).	
Summary Description	
Grey, slightly weathered, minor iron oxide staining, brecciated, porphyritic, fine grained groundmass, fine grained phenocrysts, fine to boulder sized fragments. Groundmass 35%, crystals 15%, fragments 50%, BRECCIATED BASALTIC IGNIMBRITE. Micro-fractures with defects prevalent at fragment groundmass boundaries. Extremely weak (Point Load Strength Index 0.04-0.34 MPa).	

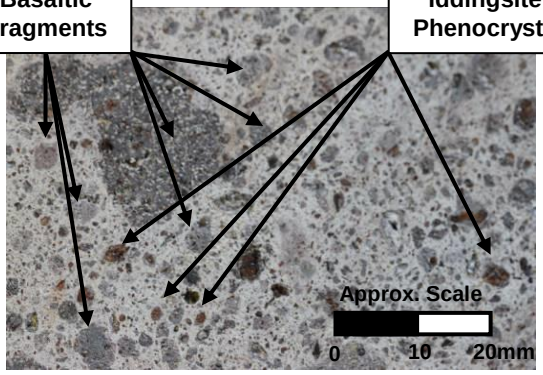

Figure 5.5a) Photograph of cut section of IGB. Note high percentage of fine to medium grained fragments surrounded by fine grained ash groundmass.

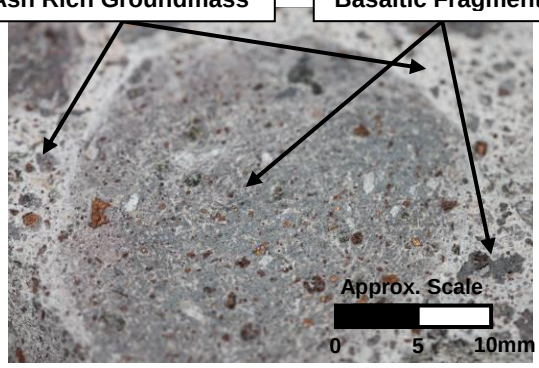

Figure 5.5b) Photograph of cut section of IGB. Note coarse grained basaltic fragment surrounded by fine grained ash groundmass.

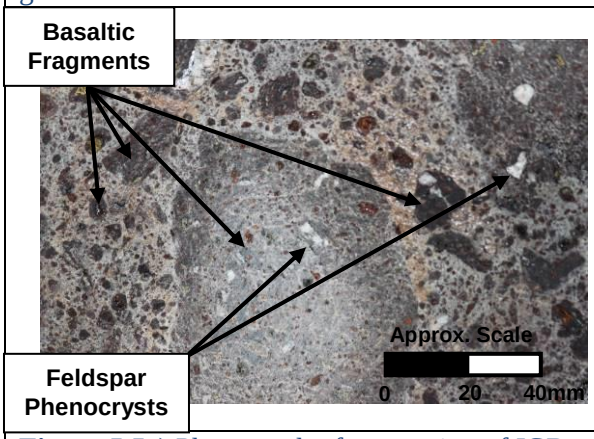

Figure 5.5c) Photograph of cut section of IGB. Note high percentage of fine to coarse grained fragments surrounded by fine grained ash groundmass. Also note section is partially wet.

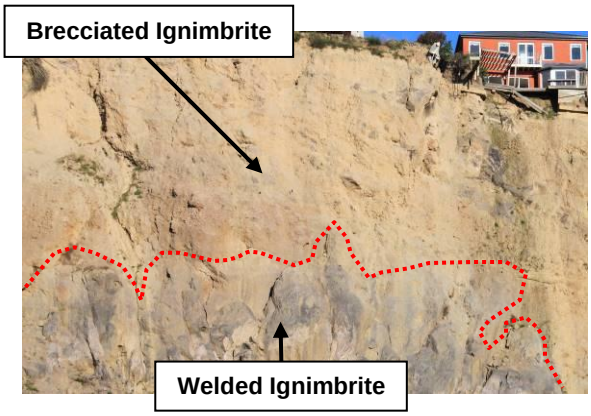

Figure 5.5d) Field photograph of IGB in Redcliffs. Note the brecciated ignimbrite transitions into welded ignimbrite (red dotted line).

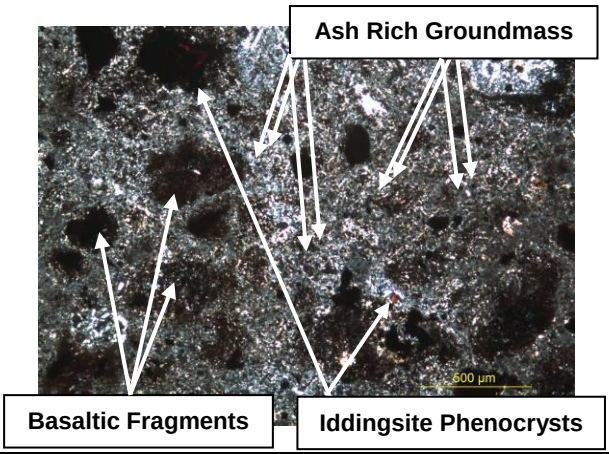

Figure 5.5e) Porphyritic texture and fine grained ash groundmass. Section is in cross polarised light (CPL).

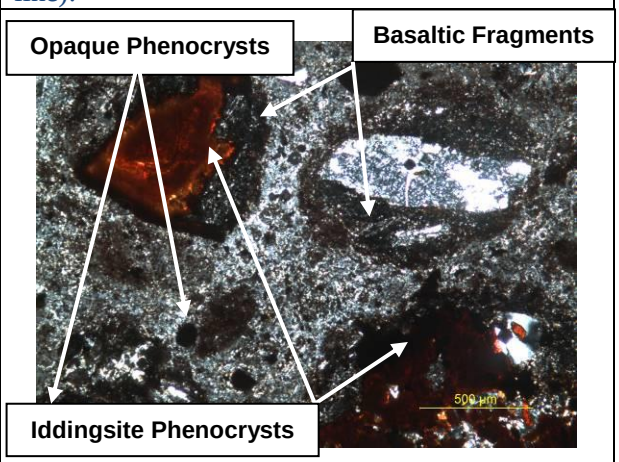

Figure 5.5f) Porphyritic texture and fine grained ash groundmass. Note coarse grained phenocrysts. Section is in cross polarised light (CPL).

Figure 5.5: Annotated images at hand specimen, outcrop and microscopic scales of IGB.

Rock Mechanics Data

The brecciated basaltic ignimbrite produced high porosity values with a mean of 40.9% (Table 5.8), PLS and correlated UCS testing yielded respectively means of 0.14 and 3.4 MPa indicating the ignimbrite as being extremely weak to very weak (NZGS 2005 terminology). Slake durability tested that a lot of material lost occurred fragment groundmass boundaries (Figure 5.6) which, was indicated by the remaining material at the end of the second cycle (Id_2).

Table 5.8: Key physical rock mechanics data for IGB.

Key Data for Brecciated Basaltic Ignimbrite (IGB) - Physical Rock Mechanics Tests										
	Porosity n (%)	Dry Mass Density ρ_d (kg/m^3)	Bulk Volume V (m^3)	P and S Wave Velocities		Point Load Strength Index $Is_{(50)}$ (MPa)	Correlated UCS using $Is_{(50)}\times24$ (MPa)	UCS σ_{ci} (MPa)	Slake Durability First Cycle Id_1 (%)	Slake Durability Second Cycle Id_2 (%)
				Vp (m/s)	Vs (m/s)					
Range	25.9-47.6	1490-2020	4.7×10^{-5} - 8.1×10^{-5}	-	-	0.04-0.34	0.9-8.3	-	93.7	83.7
Mean	40.9	1660	6.3×10^{-5}	-	-	0.14	3.4	-	-	-
Median	46.6	1520	6.2×10^{-5}	-	-	0.1	2.2	-	-	-
Standard Deviation	8.8	219.4	1.1×10^{-5}	-	-	0.08	2.0	-	-	-
***Note: Slake durability first/second cycle have no range, mean, median or standard deviation as only one test was conducted.										

Figure 5.6a) Pre-Test slake durability balls (IGB).

Figure 5.6b) Slake durability end of first cycle (IGB).

Figure 5.6c) Slake durability end of second cycle (IGB).

Figure 5.6d) IGB material left at end of slake durability test.

Figure 5.6: Annotated images of brecciated basaltic ignimbrite (IGB) testing.

5.5 Moderately Welded Basaltic Ignimbrite (IGMW)

Detailed rock descriptions are presented with relevant supporting annotated figures (Table 5.9 and Figure 5.7), followed by key datasets and results of rock mechanics testing (Table 5.10 and Figure 5.8).

Detailed Engineering Geological Igneous Rock Description

Table 5.9: Detailed Engineering Geological Igneous Rock Description for Moderately Welded Basaltic Ignimbrite (IGMW).

Detailed Engineering Geological Igneous Rock Descriptive Scheme	
Component	**Description**
Geological Context (Unit Feature, Emplacement Mechanism, Formation, Group)	[PYROCLASTIC DENSITY CURRENT, LYTTELTON VOLCANIC GROUP]
Location	Redcliffs, Sumner
Date Sampled, Identification Number	14/08/2013, IGMW
Colour	Grey to purple grey
Weathering and Alteration	Slightly weathered, minor iron staining and clay alteration
Structure and Texture (Outcrop, Hand Specimen)	Moderately welded, brecciated, porphyritic (Figure 5.7a)
Groundmass Grain Size	Fine-medium grained groundmass
Crystal Grain Size	Fine-medium grained phenocrysts
Fragment/Clast/Lithic Grain Size	Fine to coarse sized fragments (Figure 5.7b)
Component Analysis (Hand Specimen) *% Groundmass/Matrix* *% Crystals* *% Fragments, Clasts and Lithics* *% Vesicles*	 60% (Figure 5.7a) 20% 20% 0%
Mineralogy (Hand Specimen and Thin Section)	Iddingsite 10%, plagioclase feldspar 5%, clinopyroxene 4%, opaques 1% (Figure 5.7c-f)
Rock Name	MODERATELY WELDED BASALTIC IGNIMBRITE
Discontinuities *Orientation and Joint Sets* *Spacing* *Aperture* *Additional*	 N/A N/A N/A Micro-fractures with defects prevalent at fragment groundmass boundaries (Figure 5.7b)
Intact Strength *In field* *Testing(UCS/PLS/Schmidt Hammer)*	 Moderately strong PLS: 0.3-2.6 MPa
Full Expanded Description	
[PYROCLASTIC DENSITY CURRENT, LYTTELTON VOLCANIC GROUP], Redcliffs, Sumner, IGMW, grey to purple grey, slightly weathered, minor iron oxide staining and clay alteration, moderately welded, brecciated, porphyritic, fine-medium grained groundmass, fine-medium grained phenocrysts, fine-medium sized fragments. Groundmass 60%, crystals 20% (Iddingsite 10%, plagioclase feldspar 5%, clinopyroxene 4%, opaques 1%), MODERATELY WELDED BASALTIC IGNIMBRITE. Micro-fractures with defects prevalent at fragment groundmass boundaries. Extremely weak (Point Load Strength Index 0.3-2.6 MPa).	
Summary Description	
Grey to purple grey, slightly weathered, minor iron oxide staining and clay alteration, moderately welded, brecciated, porphyritic, fine-medium grained groundmass, fine-medium grained phenocrysts, fine-medium sized fragments. Groundmass 60%, crystals 20%, fragments 20%, MODERATELY WELDED BASALTIC IGNIMBRITE. Micro-fractures with defects prevalent at fragment groundmass boundaries. Extremely weak (Point Load Strength Index 0.3-2.6 MPa).	

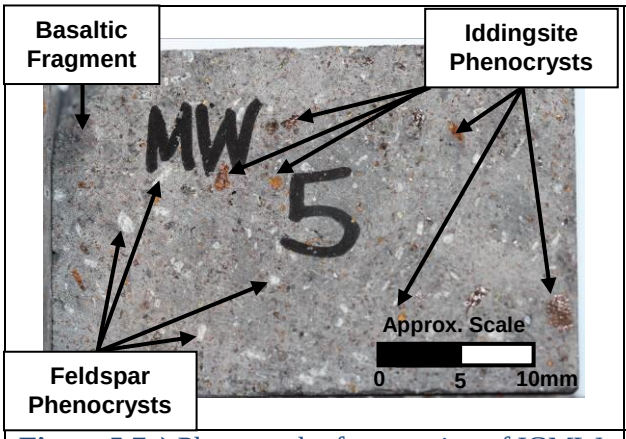

Figure 5.7a) Photograph of cut section of IGMW. Note higher percentage of well-formed phenocrysts and lower percentage of fragments than IGB Figure 5.7.

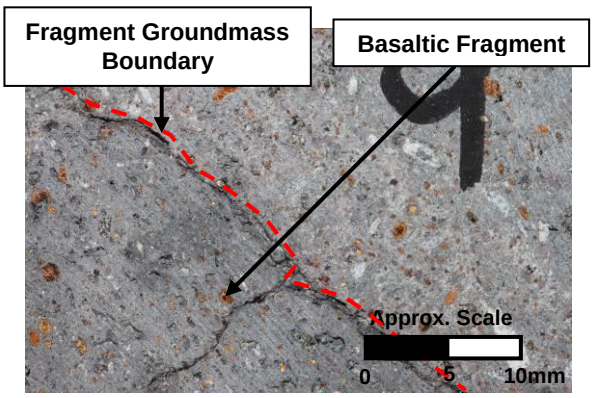

Figure 5.7b) Photograph of cut section of IGMW. Note welded groundmass and basaltic fragment boundary. Defects are prevalent at these boundaries.

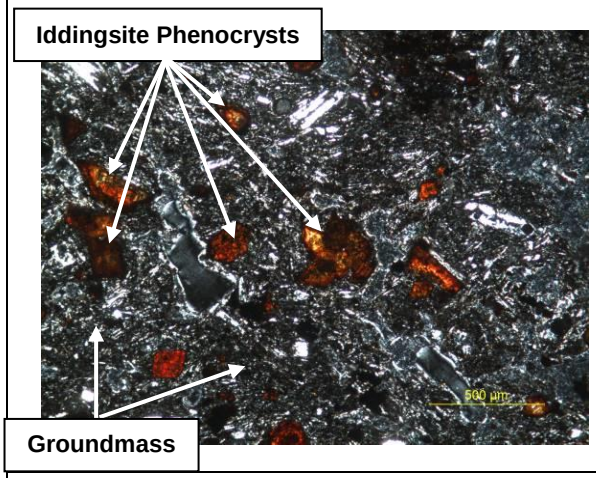

Figure 5.7c) Porphyritic texture and fine grained groundmass formed from microlathes. Section is in cross polarised light (CPL).

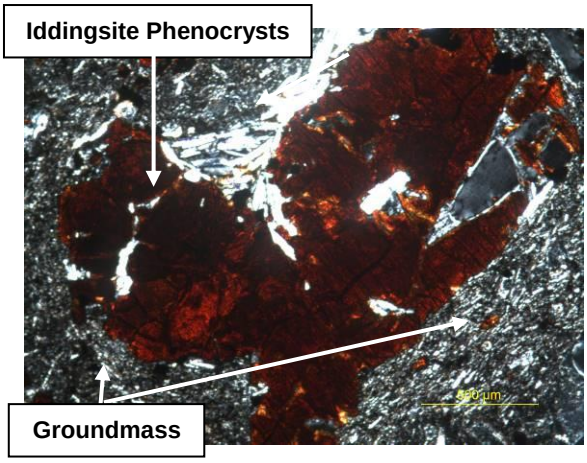

Figure 5.7d) Coarse grained iddingsite phenocryst surrounded by microlathes. Section is in cross polarised light (CPL).

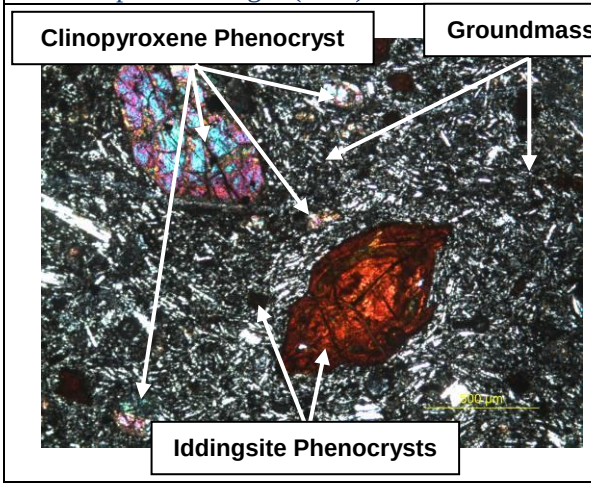

Figure 5.7e Clinopyroxene and iddingsite phenocrysts surrounded by microlathes. Section is in cross polarised light (CPL).

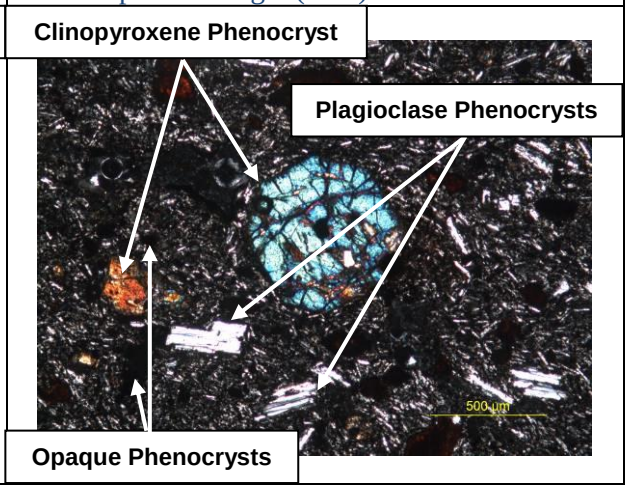

Figure 5.7f) Coarse and fine grained clinopyroxene phenocrysts. Section is in cross polarised light (CPL).

Figure 5.7: Annotated images at hand specimen, outcrop and microscopic scales of IGMW.

Rock Mechanics Data

The moderately welded basaltic ignimbrite produced high porosity values with a mean of 25.5% (Table 5.10), PLS and correlated UCS testing yielded respectively means of 1.1 and 25.7 MPa indicating the ignimbrite as being moderately strong. Point load strength testing showed that the basaltic fragment groundmass boundaries act as planes of weakness (Figure 5.8).

Table 5.10: Key physical rock mechanics data for IGMW.

Key Data for Moderately Welded Basaltic Ignimbrite (IGMW) - Physical Rock Mechanics Tests										
	Porosity n (%)	Dry Mass Density ρ_d (kg/m^3)	Bulk Volume V (m^3)	P and S Wave Velocities		Point Load Strength Index $Is_{(50)}$ (MPa)	Correlated UCS using $Is_{(50)}\times24$ (MPa)	UCS σ_{ci} (MPa)	Slake Durability First Cycle Id_1 (%)	Slake Durability Second Cycle Id_2 (%)
				Vp (m/s)	Vs (m/s)					
Range	18.2-29.8	1940-2190	2.4×10^{-5} - 7.6×10^{-5}	-	-	0.3-2.6	7.5-63.6	-	-	-
Mean	25.5	2030	4.8×10^{-5}	-	-	1.1	25.7	-	-	-
Median	26.1	2010	5.2×10^{-5}	-	-	0.9	21.6	-	-	-
Standard Deviation	3.9	89.0	1.6×10^{-5}	-	-	0.6	14.0	-	-	-
***Note: Slake durability first/second cycle have no range, mean, median or standard deviation as only one test was conducted.										

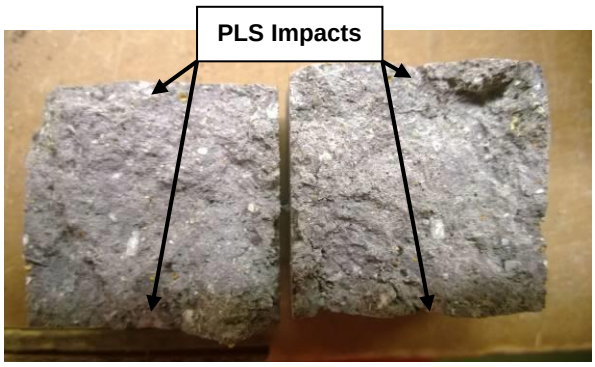

Figure 5.8a) Failed point load strength (PLS) block.

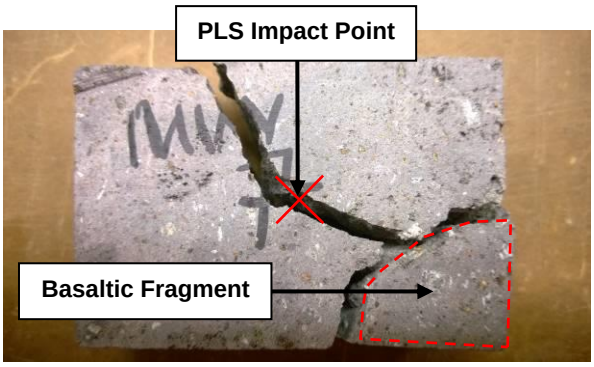

Figure 5.8b) Failed point load strength (PLS) block. Note that defect developed around fragment boundary.

Figure 5.8: Annotated images of moderately welded basaltic ignimbrite (IGMW) testing.

5.6 Highly Welded Basaltic Ignimbrite (IGW)

Detailed rock descriptions are presented with relevant supporting annotated figures (Table 5.11 and Figure 5.9), followed by key datasets and results of rock mechanics testing (Table 5.12, Table 5.13 and Figure 5.10).

Detailed Engineering Geological Igneous Rock Description

Table 5.11: Detailed Engineering Geological Igneous Rock Description for Highly Welded Basaltic Ignimbrite (IGW).

Detailed Engineering Geological Igneous Rock Descriptive Scheme	
Component	**Description**
Geological Context (Unit Feature, Emplacement Mechanism, Formation, Group)	[PYROCLASTIC DENSITY CURRENT, LYTTELTON VOLCANIC GROUP]
Location	Redcliffs, Sumner
Date Sampled, Identification Number	14/08/2013, IGW
Colour	Light grey
Weathering and Alteration	Slightly weathered, minor iron staining
Structure and Texture (Outcrop, Hand Specimen)	Highly welded, porphyritic (Figure 5.9a)
Groundmass Grain Size	Fine grained groundmass (Figure 5.9a)
Crystal Grain Size	Fine-medium grained phenocrysts
Fragment/Clast/Lithic Grain Size	Fine sized fragments (Figure 5.9b)
Component Analysis (Hand Specimen)	
% Groundmass/Matrix	68% (Figure 5.9e-h)
% Crystals	30%
% Fragments, Clasts and Lithics	2%
% Vesicles	0%
Mineralogy (Hand Specimen and Thin Section)	Iddingsite 15%, plagioclase feldspar 5%, olivine 5%, clinopyroxene 4%, opaques 1%
Rock Name	HIGHLY WELDED BASALTIC IGNIMBRITE
Discontinuities	
Orientation and Joint Sets	Two joint sets (Figure 5.9c/d)
Spacing	Widely spaced
Aperture	Smooth, tight aperture
Additional	Columnar, no infill, minor amounts of seepage
Intact Strength	
In field	Very strong
Testing (UCS/PLS/Schmidt Hammer)	PLS: 6-8 MPa
Full Expanded Description	
[PYROCLASTIC DENSITY CURRENT, LYTTELTON VOLCANIC GROUP], Redcliffs, Sumner, IGW, light grey, slightly weathered, minor iron oxide staining, highly welded, porphyritic, fine grained groundmass, fine-medium grained phenocrysts, fine sized fragments. Groundmass 68%, crystals 30% (Iddingsite 15%, plagioclase feldspar 5%, olivine 5%, clinopyroxene 4%, opaques 1%), fragments 2%, HIGHLY WELDED BASALTIC IGNIMBRITE. Two joint sets, widely spaced, smooth, tight aperture, no infill, minor amounts of seepage. Very strong (Point Load Strength Index 6-8 MPa).	
Summary Description	
Light grey, slightly weathered, minor iron oxide staining, highly welded, porphyritic, fine grained groundmass, fine-medium grained phenocrysts, fine sized fragments. Groundmass 68%, crystals 30%, fragments 2%, HIGHLY WELDED BASALTIC IGNIMBRITE. Two joint sets, widely spaced, smooth, tight aperture, columnar, no infill, minor amounts of seepage. Very strong (Point Load Strength Index 6-8 MPa).	

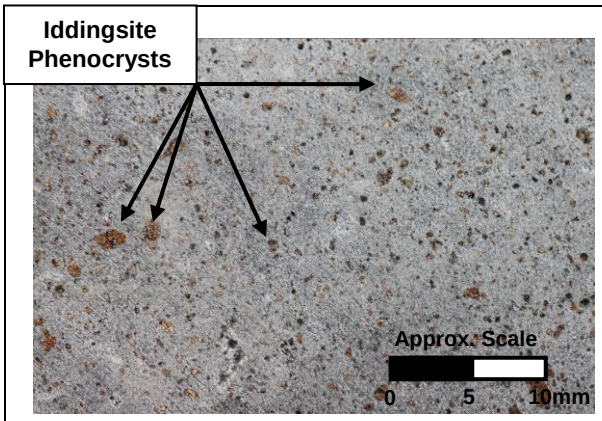

Figure 5.9a) Macro photograph of cut section of IGW. Note fine and medium grained phenocrysts and fine grained welded groundmass.

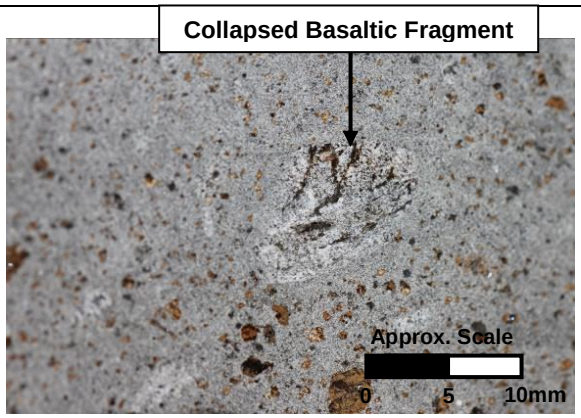

Figure 5.9b) Macro photograph of cut section of IGW. Note collapsed basaltic fragment.

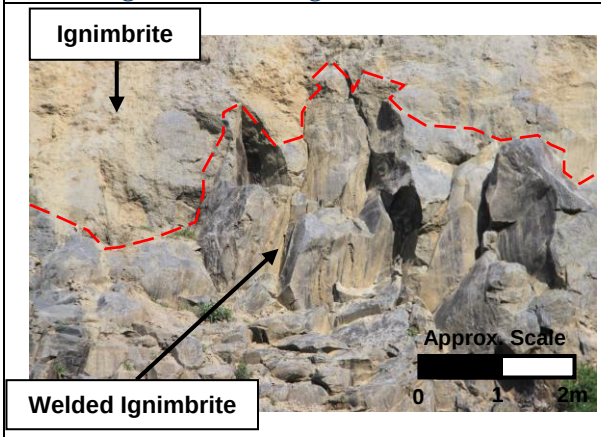

Figure 5.9c) Field photograph of IGW in Redcliffs. Note that brecciated/low welded grade ignimbrite transitions into columnar jointed IGW.

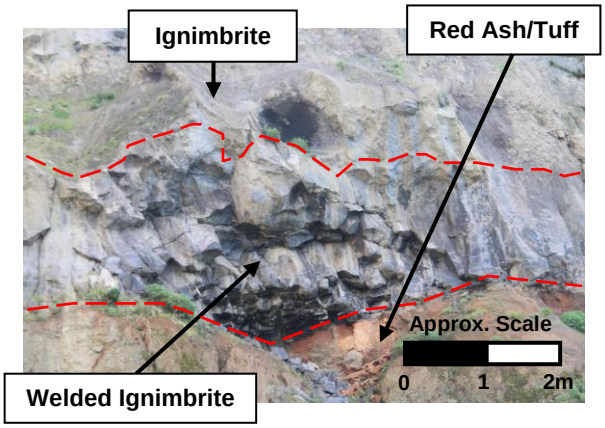

Figure 5.9d) Field photograph of IGW in Redcliffs. Note that brecciated/low welded grade ignimbrite transitions into columnar jointed IGW.

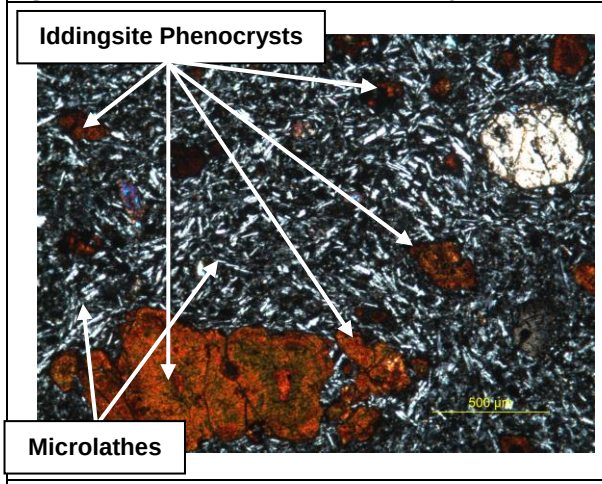

Figure 5.9e) Porphyritic texture and fine grained groundmass formed from microlathes. Note variation in iddingsite phenocryst grain sizes. Section is in cross polarised light (CPL).

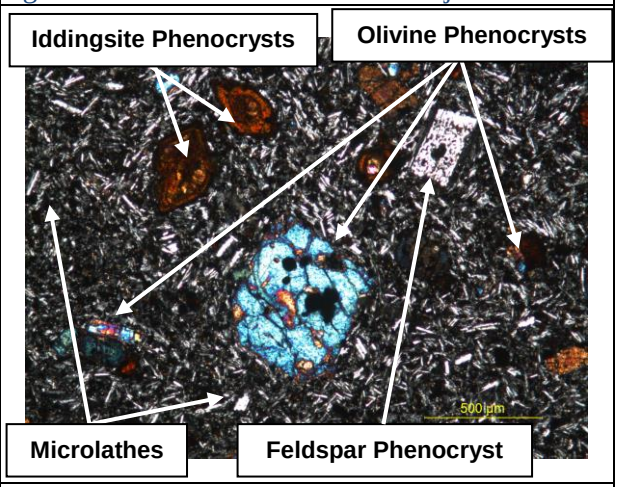

Figure 5.9f) Coarse grained olivine phenocryst surrounded by microlathes. Section is in cross polarised light (CPL).

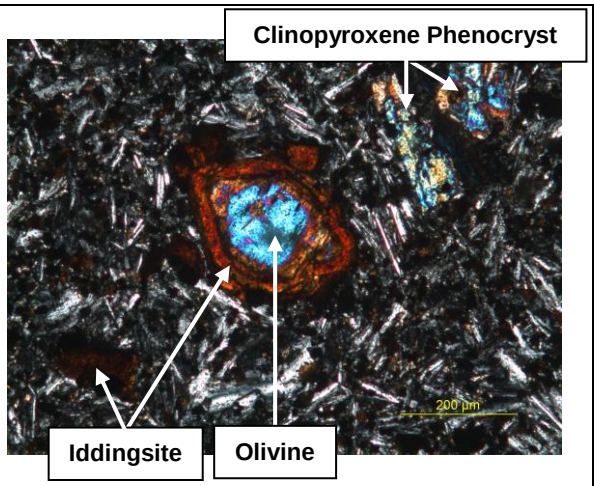

Figure 5.9g) Olivine phenocryst rimmed by iddingsite. Section is in cross polarised light (CPL).

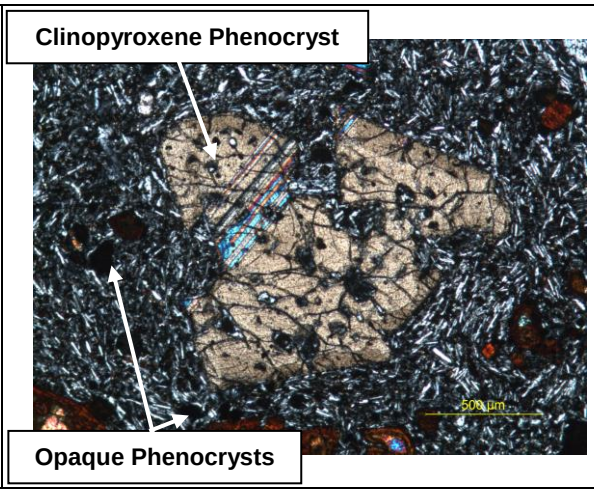

Figure 5.9h) Coarse grained clinopyroxene phenocryst surrounded by microlathes. Section is in cross polarised light (CPL).

Figure 5.9: Annotated images at hand specimen, outcrop and microscopic scales of IGW.

Rock Mechanics Data

The highly welded basaltic ignimbrite produced very low porosity values with a mean of 4.6% (Table 5.12), PLS and correlated UCS testing yielded respectively means of 6.9 and 165.3 MPa indicating the welded ignimbrite as being very strong. Deformation moduli for IGW were derived under dynamic conditions using Vp and Vs wave velocities as no static data was available (Table 5.13).

Table 5.12: Key physical rock mechanics data for IGW.

Key Data for Highly Welded Basaltic Ignimbrite (IGW) - Physical Rock Mechanics Tests										
	Porosity n (%)	Dry Mass Density ρ_d (kg/m^3)	Bulk Volume V (m^3)	P and S Wave Velocities		Point Load Strength Index $Is_{(50)}$ (MPa)	Correlated UCS using $Is_{(50)}\times24$ (MPa)	UCS σ_{ci} (MPa)	Slake Durability First Cycle Id_1 (%)	Slake Durability Second Cycle Id_2 (%)
				Vp (m/s)	Vs (m/s)					
Range	4.2-5.1	2730-2760	5.8×10^{-5} - 8.4×10^{-5}	4217-4364	2252-2450	5.9-7.9	141.2-189.0	-	-	-
Mean	4.6	2750	6.9×10^{-5}	4307	2388	6.9	165.3	-	-	-
Median	4.6	2750	6.5×10^{-5}	4320	2340	6.9	165.7	-	-	-
Standard Deviation	0.3	14.7	9.3×10^{-6}	48.0	71.0	0.3	7.5	-	-	-

*Note: Slake durability first/second cycle have no range, mean, median or standard deviation as only one test was conducted.

Table 5.13: Key deformation moduli test data for IGW.

Key Data for Highly Welded Basaltic Ignimbrite (IGW) - Deformation Moduli						
	Static Young's Modulus Estat (GPa)	Static Poisson's Ratio υstat (unitless)	Dynamic Young's Modulus Edyn (GPa)	Dynamic Poisson's Ratio υdyn (unitless)	Dynamic Shear Modulus Gdyn (GPa)	Dynamic Bulk Modulus Kdyn (GPa)
Range	-	-	36.2-41.7	0.26-0.30	13.9-16.6*	28.4-31.1*
Mean	-	-	40.0	0.28	15.7*	30.0*
Median	-	-	40.4	0.28	15.9*	30.4*
Standard Deviation	-	-	1.9	0.02	0.9*	0.9*

*Note: Shear modulus and bulk modulus are derived under dynamic conditions as no static data was available.

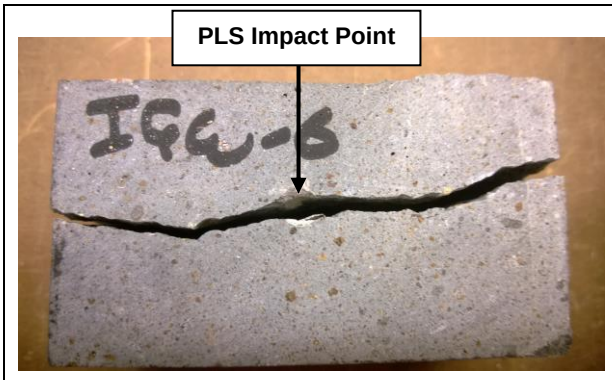

Figure 5.10a) Failed point load strength (PLS) block (IGW-6).

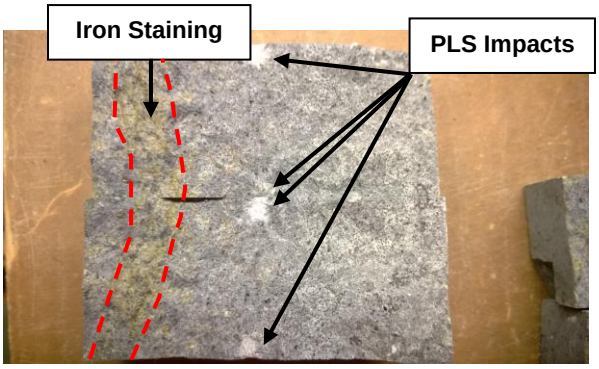

Figure 5.10b) Failed point load strength (PLS) block (IGW-6. Note staining on right hand side.

Figure 5.10: Annotated images of highly welded basaltic ignimbrite (IGW) testing.

5.7 Crystal Dominated Tuff (CTC)

Detailed rock descriptions are presented with relevant supporting annotated figures (Table 5.14 and Figure 5.11), followed by key datasets and results of rock mechanics testing (Table 5.9 and Figure 5.12).

Detailed Engineering Geological Igneous Rock Description

Table 5.14: Detailed Engineering Geological Igneous Rock Description for Crystal Dominated Tuff (CTC).

Detailed Engineering Geological Igneous Rock Descriptive Scheme	
Component	**Description**
Geological Context (Unit Feature, Emplacement Mechanism, Formation, Group)	[AIRFALL TUFF, LYTTELTON VOLCANIC GROUP]
Location	Redcliffs, Sumner
Date Sampled, Identification Number	14/08/2013, CTC
Colour	Orange brown
Weathering and Alteration	Slightly weathered, minor iron staining
Structure and Texture (Outcrop, Hand Specimen)	Porphyritic, microcrystalline
Groundmass Grain Size	Fine-medium grained groundmass (Figure 5.11a)
Crystal Grain Size	Fine-coarse grained phenocrysts (Figure 5.11a/c)
Fragment/Clast/Lithic Grain Size	Fine sized fragments (Figure 5.11b)
Component Analysis (Hand Specimen) *% Groundmass/Matrix* *% Crystals* *% Fragments, Clasts and Lithics* *% Vesicles*	 45% 50% 5% 0%
Mineralogy (Hand Specimen and Thin Section)	Plagioclase feldspar 25%, quartz 10%, olivine 5%, orthopyroxene 5%, clinopyroxene 3%, 2 opaques 2% (Figure 5.11e-h)
Rock Name	CRYSTAL TUFF
Discontinuities *Orientation and Joint Sets* *Spacing* *Aperture* *Additional*	 N/A (Figure 5.11d) N/A N/A Micro-fractures with defects prevalent at phenocryst and fragment groundmass boundaries
Intact Strength *In field* *Testing (UCS/PLS/Schmidt Hammer)*	 Weak-extremely weak PLS: 0.05-0.18 MPa
Full Expanded Description	
[AIRFALL TUFF, LYTTELTON VOLCANIC GROUP], Redcliffs, Sumner, CTC, orange brown, slightly weathered, minor iron oxide staining, porphyritic, microcrystalline, fine-medium grained groundmass, fine-medium grained phenocrysts, fine-medium sized fragments. Groundmass 45%, crystals 50% (Plagioclase feldspar 25%, quartz 10%, olivine 5%, orthopyroxene 5%, clinopyroxene 3%, 2 opaques 2%), fragments 5%, CRYSTAL TUFF. Micro-fractures with defects prevalent at phenocryst and fragment groundmass boundaries. Weak-extremely weak (Point Load Strength Index 0.05-0.18 MPa).	
Summary Description	
Orange brown, slightly weathered, minor iron oxide staining, porphyritic, microcrystalline, fine-medium grained groundmass, fine-medium grained phenocrysts, fine-medium sized fragments. Groundmass 45%, crystals 50%, fragments 5%, CRYSTAL TUFF. Micro-fractures with defects prevalent at phenocryst and fragment groundmass boundaries. Weak-extremely weak (Point Load Strength Index 0.05-0.18 MPa).	

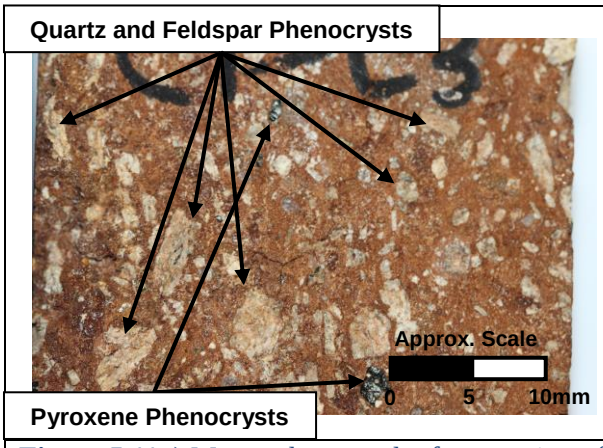

Figure 5.11a) Macro photograph of cut section of CTC. Note percentage of fine and coarse grained phenocrysts and fine to medium grained groundmass.

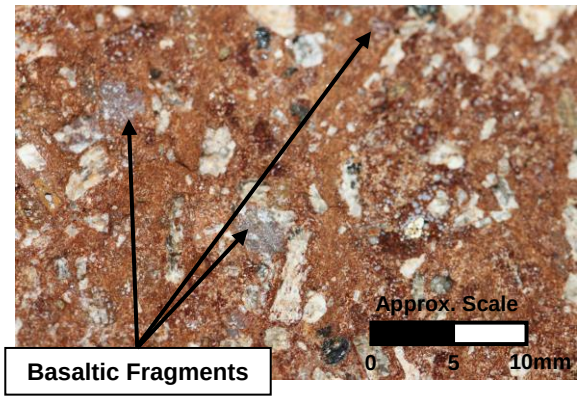

Figure 5.11b) Macro photograph of cut section of CTC. Note fine to medium grained basaltic fragments.

Figure 5.11c) Photograph of CTC PLS testing blocks. Crystal content was observed to vary between samples but generally was accounted for ~50% of the tuff. The left tuff (CT-C3) has a higher crystal percentage than the right tuff (CT-C1).

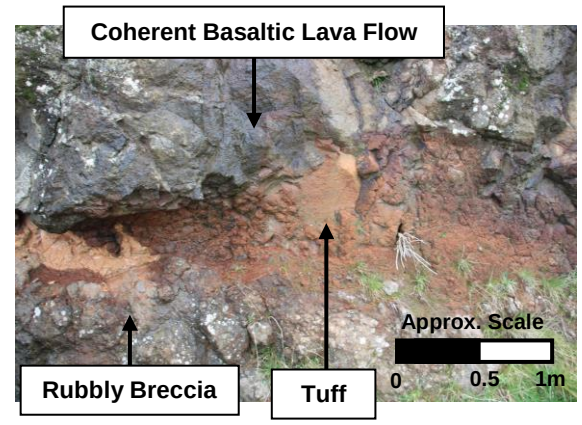

Figure 5.11d) Field photograph of CTC deposit between a coherent basaltic lava flow and rubbly basaltic breccia.

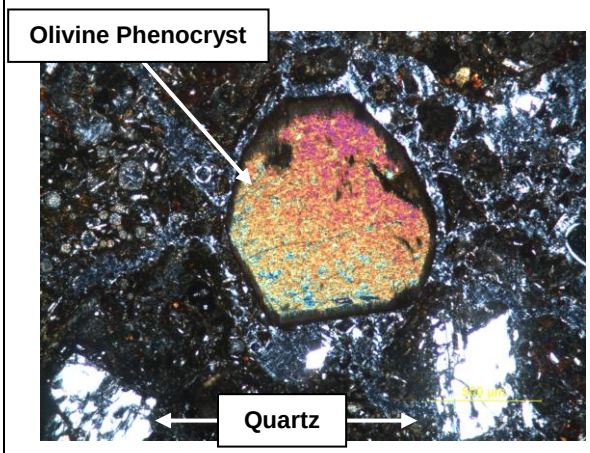

Figure 5.11e) Olivine phenocryst surrounded my microcrystalline groundmass. Section is in cross polarised light (CPL).

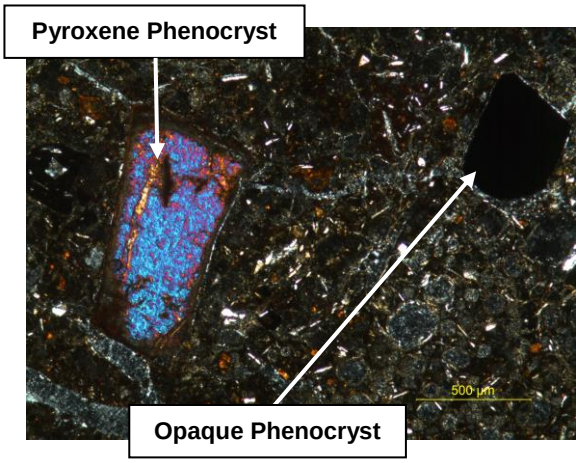

Figure 5.11f) Pyroxene and opaque phenocryst surrounded my microcrystalline groundmass. Section is in cross polarised light (CPL).

Figure 5.11 is continued over the page

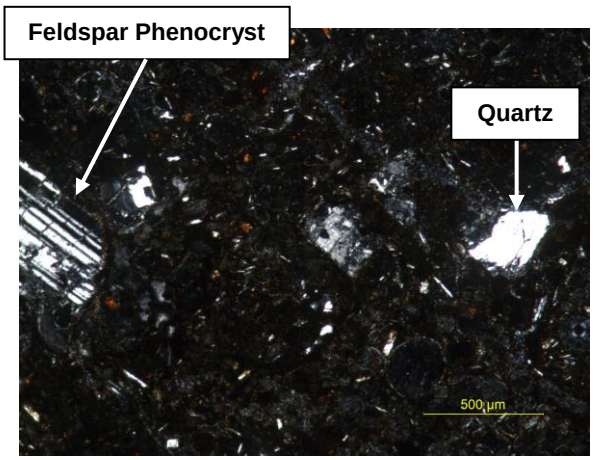

Figure 5.11g) Porphyritic texture. Section is in cross polarised light (CPL).

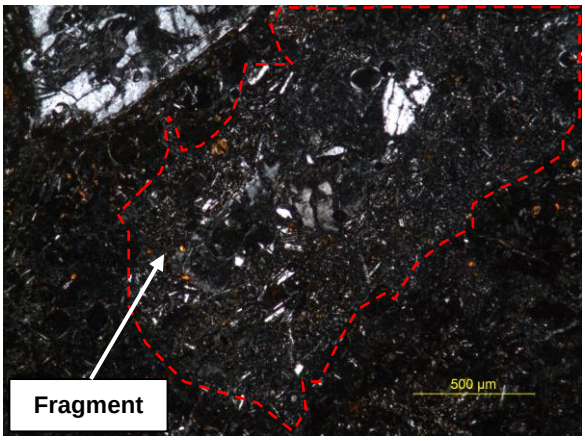

Figure 5.11h) Basaltic fragment surrounded by microcrystalline groundmass. Section is in cross polarised light (CPL).

Figure 5.11: Annotated images at hand specimen, outcrop and microscopic scales of CTC.

Rock Mechanics Data

The highly welded basaltic ignimbrite produced high porosity values with a mean of 47.1% (Table 5.9), PLS and correlated UCS testing yielded respectively means of 0.1 and 2.0MPa indicating the crystal tuff as being weak to extremely weak. A selection of testing photographs are presented in Figure 5.12. The crystal dominated tuff displayed a very low resistance to slaking (63% of material lost in the first cycle) (Figure 5.12).

Table 5.15: Key physical rock mechanics data for CTC.

Key Data for Crystal Tuff (CTC) - Physical Rock Mechanics Tests										
	Porosity n (%)	Dry Mass Density ρ_d (kg/m^3)	Bulk Volume V (m^3)	P and S Wave Velocities		Point Load Strength Index $Is_{(50)}$ (MPa)	Correlated UCS using $Is_{(50)}\times24$ (MPa)	UCS σ_{ci} (MPa)	Slake Durability First Cycle Id_1 (%)	Slake Durability Second Cycle Id_2 (%)
				Vp (m/s)	Vs (m/s)					
Range	44.2-49.2	1400-1560	5.3×10^{-5} - 7.2×10^{-5}	-	-	0.05-0.18	1.1-4.3	-	37.0	20.2
Mean	47.1	1480	6.5×10^{-5}	-	-	0.1	2.0	-	-	-
Median	48.3	1490	6.6×10^{-5}	-	-	0.1	1.9	-	-	-
Standard Deviation	2.3	71.0	6.2×10^{-6}	-	-	0.01	0.2	-	-	-
*Note: Slake durability first/second cycle have no range, mean, median or standard deviation as only one test was conducted.										

Figure 5.12a) Pre-test slake durability balls (CTC).

Figure 5.12b) Slake durability end of first cycle 37% material remaining (CTC).

Figure 5.12c) Slake durability end of second cycle 20% material remaining (CTC).

Figure 5.12d) Material lost during slake durability first cycle (63%).

Figure 5.12: Annotated images of crystal tuff (CTC) testing.

5.8 Lithic Dominated Tuff (CTL)

Detailed rock descriptions are presented with relevant supporting annotated figures (Table 5.16 and Figure 5.13), followed by key datasets and results of rock mechanics testing (Table 5.17 and Figure 5.14).

Detailed Engineering Geological Igneous Rock Description

Table 5.16: Detailed Engineering Geological Igneous Rock Description for Lithic Dominated Tuff (CTL).

Detailed Engineering Geological Igneous Rock Descriptive Scheme	
Component	**Description**
Geological Context (Unit Feature, Emplacement Mechanism, Formation, Group)	[AIRFALL TUFF, LYTTELTON VOLCANIC GROUP]
Location	Redcliffs, Sumner
Date Sampled, Identification Number	14/08/2013, CTL
Colour	Dark reddish orange
Weathering and Alteration	Slightly weathered, minor iron staining
Structure and Texture (Outcrop, Hand Specimen)	Porphyritic, microcrystalline
Groundmass Grain Size	Fine-coarse grained groundmass (Figure 5.13a)
Crystal Grain Size	Fine-coarse grained phenocrysts (Figures 5.13a/c)
Fragment/Clast/Lithic Grain Size	Fine-coarse sized fragments (Figure 5.13b)
Component Analysis (Hand Specimen) *% Groundmass/Matrix* *% Crystals* *% Fragments, Clasts and Lithics* *% Vesicles*	 50% 20% 30% 0%
Mineralogy (Hand Specimen and Thin Section)	Plagioclase feldspar 10%, quartz 5%, iddingsite 4%, orthopyroxene 1% (Figures 5.13e-h)
Rock Name	LITHIC TUFF
Discontinuities *Orientation and Joint Sets* *Spacing* *Aperture* *Additional*	 N/A (Figure 5.13d) N/A N/A Micro-fractures with defects prevalent at phenocryst and fragment groundmass boundaries
Intact Strength *In field* *Testing (UCS/PLS/Schmidt Hammer)*	 Weak-extremely weak PLS: 0.2-0.6 MPa
Full Expanded Description	
[AIRFALL TUFF, LYTTELTON VOLCANIC GROUP], Redcliffs, Sumner, CTL, dark reddish orange, slightly weathered, minor iron oxide staining, porphyritic, microcrystalline, fine-medium grained groundmass, fine-coarse grained phenocrysts, fine-coarse sized fragments. Groundmass 50%, crystals 20% (Plagioclase feldspar 10%, quartz 5%, iddingsite 4%, orthopyroxene 1%), fragments 30%, LITHIC TUFF. Micro-fractures with defects prevalent at phenocryst and fragment groundmass boundaries. Weak-extremely weak (Point Load Strength Index 0.2-0.6 MPa).	
Summary Description	
Dark reddish orange, slightly weathered, minor iron oxide staining, porphyritic, microcrystalline, fine-medium grained groundmass, fine-coarse grained phenocrysts, fine-coarse sized fragments. Groundmass 50%, crystals 20%, fragments 30%, LITHIC TUFF. Micro-fractures with defects prevalent at phenocryst and fragment groundmass boundaries. Weak-extremely weak (Point Load Strength Index 0.2-0.6 MPa).	

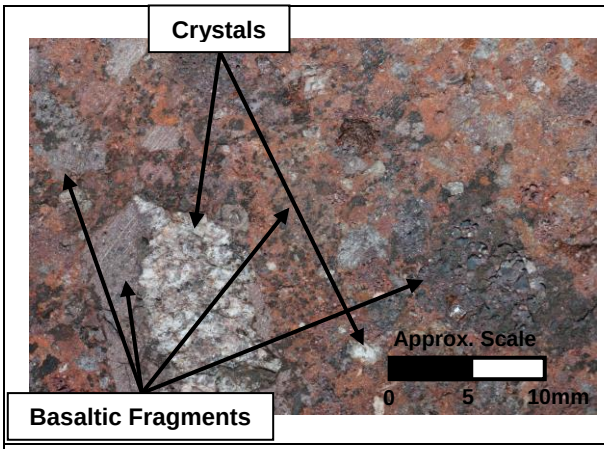

Figure 5.13a) Macro photograph of cut section of CTL. Note percentage of fine and coarse grained fragments and fine to coarse grained crystals.

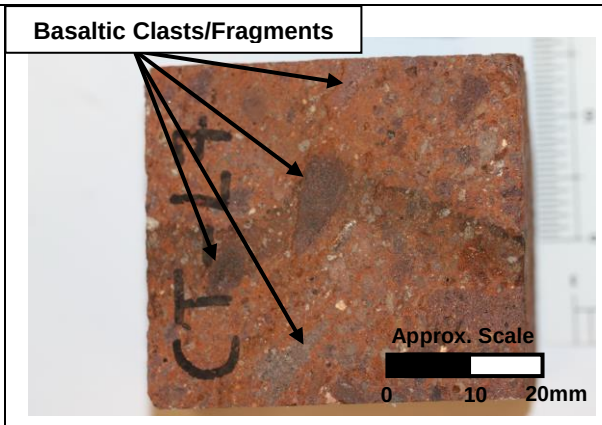

Figure 5.13b) Photograph of CTL PLS testing block (CTL-7). Note variation in lithic and crystal content.

Figure 5.13c) Photograph of CTL PLS testing blocks. Note variation in lithic and crystal content.

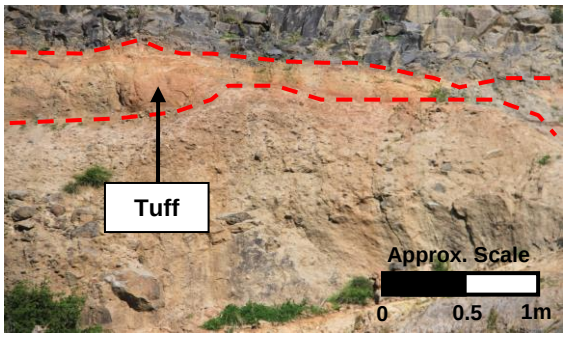

Figure 5.13d) Tuff layer at Redcliffs, Sumner. The tuff underlies a welded ignimbrite flow and overlies a brecciated/non-welded ignimbrite flow.

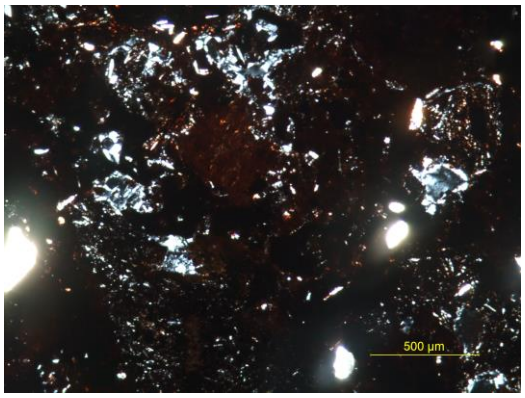

Figure 5.13e) Basaltic fragments surrounded by microcrystalline groundmass. Section is in cross polarised light (CPL).

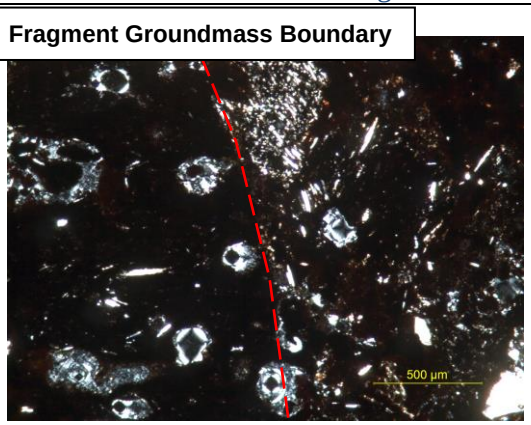

Figure 5.13f) Basaltic fragments surrounded by microcrystalline groundmass. Section is in cross polarised light (CPL).

Figure 5.13 is continued over the page.

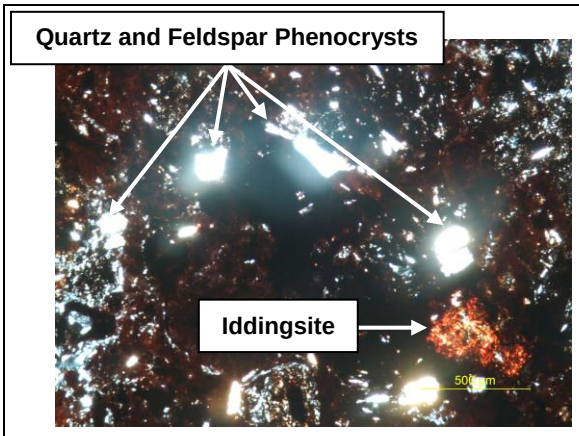

Figure 5.13g) Quartz and iddingsite phenocrysts. Section is in cross polarised light (CPL).

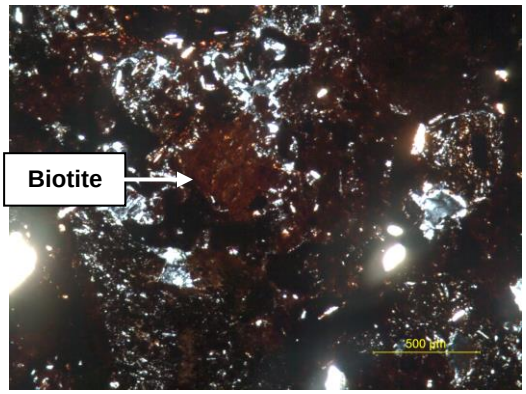

Figure 5.13h) Biotite phenocryst inside a basaltic fragment. Section is in cross polarised light (CPL).

Figure 5.13: Annotated images at hand specimen, outcrop and microscopic scales of CTL.

Rock Mechanics Data

The highly welded basaltic ignimbrite produced high porosity values with a mean of 43.5% (Table 5.17), PLS and correlated UCS testing yielded respectively means of 0.4 and 9.4MPa indicating the crystal tuff as being weak to extremely weak (NZGS 2005 terminology). Point load strength testing showed that in several cases the failure induced by testing followed the fragment/clast groundmass boundaries (Figure 5.14d-f). Slake durability testing (Figure 5.14a-c) showed CTL had high resistance to slaking (Figure 5.14a-d), much greater than CTC (Figure 5.12d).

Table 5.17: Key physical rock mechanics data for CTL.

Key Data for Lithic Tuff (CTL) - Physical Rock Mechanics Tests										
	Porosity n (%)	Dry Mass Density ρ_d (kg/m^3)	Bulk Volume V (m^3)	P and S Wave Velocities		Point Load Strength Index $Is_{(50)}$ (MPa)	Correlated UCS using $Is_{(50)}\times24$ (MPa)	UCS σ_{ci} (MPa)	Slake Durability First Cycle Id_1 (%)	Slake Durability Second Cycle Id_2 (%)
				Vp (m/s)	Vs (m/s)					
Range	42.1-44.9	1550-1660	4.0×10^{-5} - 1.1×10^{-4}	-	-	0.2-0.6	4.7-13.7	-	93.6	87.8
Mean	43.5	1610	6.9×10^{-5}	-	-	0.4	9.4	-	-	-
Median	43.8	1610	6.4×10^{-5}	-	-	0.4	9.4	-	-	-
Standard Deviation	1.0	35.0	2.3×10^{-5}	-	-	0.1	2.2	-	-	-

*Note: Slake durability first/second cycle have no range, mean, median or standard deviation as only one test was conducted.

Figure 5.14a) Pre-test slake durability balls (CTL).

Figure 5.14b) Slake durability end of first cycle 94% material remaining (CTL).

Figure 5.14c) Slake durability end of second cycle 88% material remaining (CTL).

Figure 5.14d) CTL material left after slaking fluid drained after first test. Material present was far less than that of the CTC (Figure 5.12d).

Figure 5.14e) Point load strength index **(**PLS) testing of lithic tuff (CTL-7).

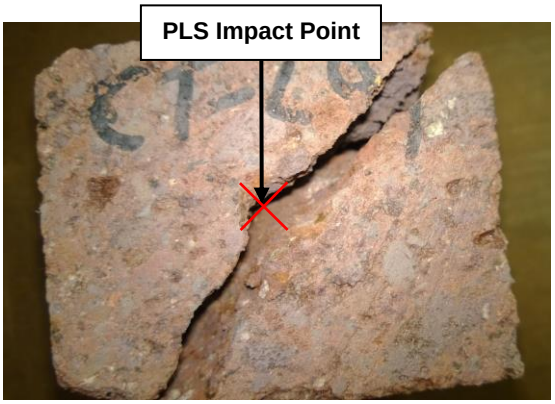

Figure 5.14f) Failed PLS testing block (CTL-9).

Figure 5.14: Annotated images of lithic tuff (CTL) testing.

5.9 Red Ash (RA)

Detailed rock descriptions are presented with relevant supporting annotated figures (Table 5.18 and Figure 5.15), followed by key datasets and results of rock mechanics testing (Table 5.19 and Figure 5.16).

Detailed Engineering Geological Igneous Rock Description

Table 5.18: Detailed Engineering Geological Igneous Rock Description for Lithic Dominated Tuff (CTL).

Detailed Engineering Geological Igneous Rock Descriptive Scheme	
Component	**Description**
Geological Context (Unit Feature, Emplacement Mechanism, Formation, Group)	[AIRFALL TUFF, LYTTELTON VOLCANIC GROUP]
Location	Summit Road, Port Hills
Date Sampled, Identification Number	14/08/2013, RA
Colour	Rusty red
Weathering and Alteration	Slightly weathered, minor iron staining
Structure and Texture (Outcrop, Hand Specimen)	Welded, porphyritic, microcrystalline
Groundmass Grain Size	Fine grained groundmass (Figure 5.15a)
Crystal Grain Size	Fine-medium grained phenocrysts (Figure 5.15a)
Fragment/Clast/Lithic Grain Size	Fine-coarse sized scoriaceous clasts (Figure 5.15b)
Component Analysis (Hand Specimen) *% Groundmass/Matrix* *% Crystals* *% Fragments, Clasts and Lithics* *% Vesicles*	 60% 5% 25% 0%
Mineralogy (Hand Specimen and Thin Section)	Quartz 3%, plagioclase feldspar 2%
Rock Name	RED ASH
Discontinuities *Orientation and Joint Sets* *Spacing* *Aperture* *Additional*	 N/A N/A N/A N/A
Intact Strength *In field* *Testing (UCS/PLS/Schmidt Hammer)*	 Moderately strong-strong PLS: 1.2-3.5 MPa
Full Expanded Description	
[AIRFALL ASH, LYTTELTON VOLCANIC GROUP], Summit Road, Port Hills, RA, rusty red, slightly weathered, minor iron oxide staining, welded, porphyritic, microcrystalline, fine grained groundmass, fine-medium grained phenocrysts, fine-coarse sized scoriaceous clasts. Groundmass 60%, crystals 5% (Quartz 3%, 2 plagioclase feldspar 2%), fragments 25%, RED ASH. Moderately strong-strong (Point Load Strength Index 1.2-3.5 MPa).	
Summary Description	
Rusty red, slightly weathered, minor iron oxide staining, welded, porphyritic, microcrystalline, fine grained groundmass, fine-medium grained phenocrysts, fine-coarse sized scoriaceous clasts. Groundmass 60%, crystals 5%, fragments 25%, RED ASH. Moderately strong-strong (Point Load Strength Index 1.2-3.5 MPa).	

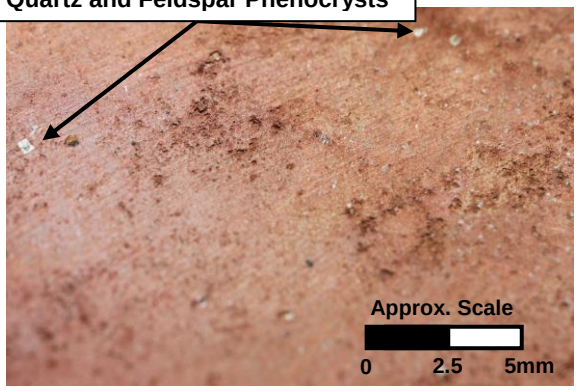

Figure 5.15a) Macro photograph of cut section of RD. Note fine grained welded ash groundmass. Note striations are from the rock saw.

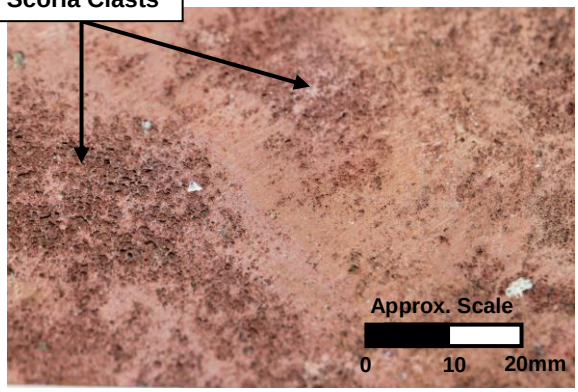

Figure 5.15b) Macro photograph of cut section of RD. Note clusters of vesicles/scoria clasts. Note striations are from the rock saw.

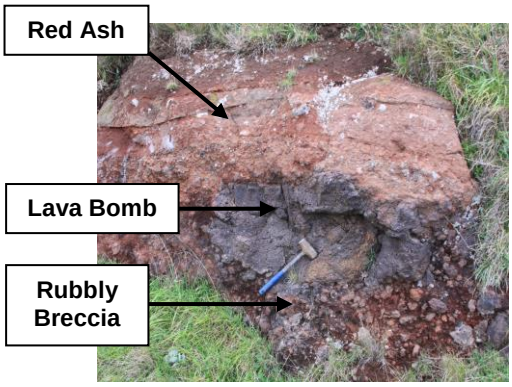

Figure 5.15c) Field photograph of road cut displaying red ash unit. Note lava bomb within the ash layer.

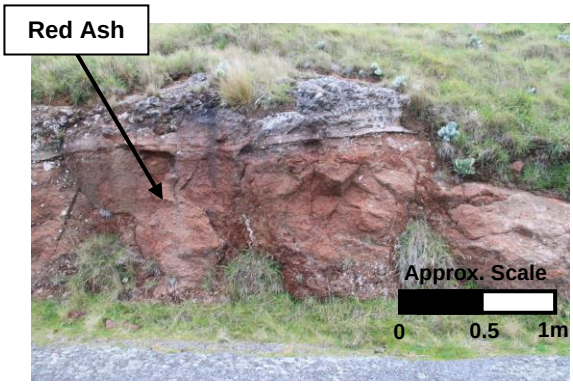

Figure 5.15d) Field photograph of road cut displaying red ash unit. Note thickness of unit.

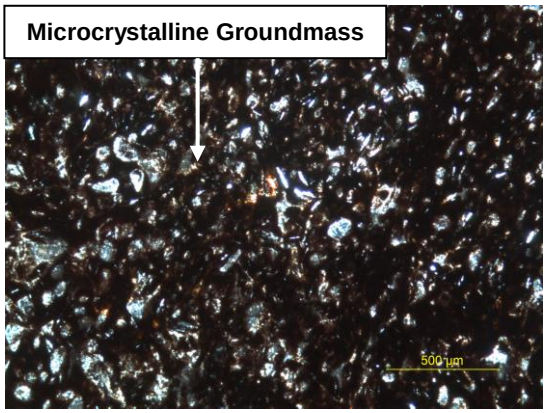

Figure 5.15e) Microcrystalline groundmass. Section is in cross polarised light (CPL).

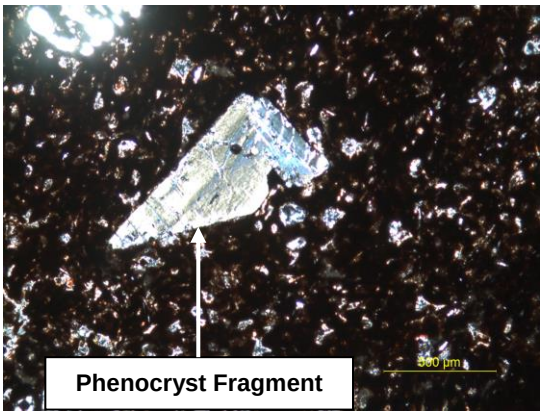

Figure 5.15f) Phenocryst fragment surrounded by microcrystalline groundmass. Section is in cross polarised light (CPL).

Figure 5.15: Annotated images at hand specimen, outcrop and microscopic scales of RA.

Rock Mechanics Data

The red ash produced high porosity values with a mean of 33.4% (Table 5.11), PLS and correlated UCS testing yielded respectively means of 2.5 and 59.4MPa indicating the red ash as being moderately strong to strong (NZGS 2005 terminology). PLS testing showed that the scoriaceous clasts did not act as planes of weakness (Figure 5.16a). Slake durability testing showed that the red ash had a very high resistance to slaking (Figure 5.16b-d) with on 2.2% of the material lost during testing

Table 5.19: Key physical rock mechanics data for RA.

Key Data for Red Ash (RA) - Physical Rock Mechanics Tests										
	Porosity n (%)	Dry Mass Density ρ_d (kg/m^3)	Bulk Volume V (m^3)	P and S Wave Velocities		Point Load Strength Index $Is_{(50)}$ (MPa)	Correlated UCS using $Is_{(50)}$×24 (MPa)	UCS σ_{ci} (MPa)	Slake Durability First Cycle Id_1 (%)	Slake Durability Second Cycle Id_2 (%)
				Vp (m/s)	Vs (m/s)					
Range	11.3-59.8	1070-1980	3.2×10^{-5} - 8.5×10^{-5}	-	-	1.2-3.5	29.0-84.3	-	99.3	98.8
Mean	33.4	1650	5.0×10^{-5}	-	-	2.5	59.4	-	-	-
Median	35.8	1640	5.2×10^{-5}	-	-	2.5	61.0	-	-	-
Standard Deviation	13.0	220.0	1.2×10^{-5}	-	-	0.6	13.9	-	-	-

*Note: Slake durability first/second cycle have no range, mean, median or standard deviation as only one test was conducted.

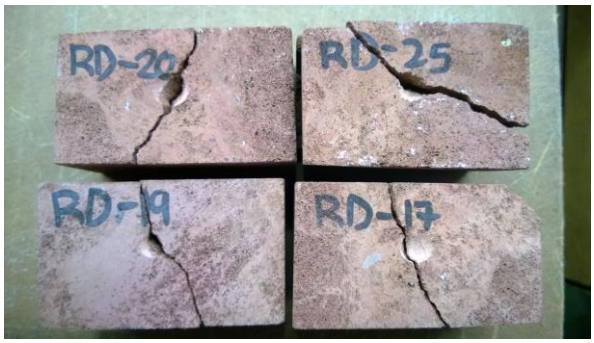

Figure 5.16a) Point load strength index **(**PLS) testing of lithic tuff (RD-20, 25, 19 and 17). Note RD samples are the same as RA.

Figure 5.16b) Pre-Test slake durability balls (RA).

Figure 5.16c) Slake durability end of first cycle 99.3% material remaining (RA).

Figure 5.16d) Slake durability end of second cycle 98.8% material remaining (RA).

Figure 5.16: Annotated images of red ash (RA) testing.

5.10 Volcanogenic Conglomerate (VC)

The two volcanogenic units in this study, the volcanogenic conglomerate (VC) and the volcanogenic tuffaceous sandstone (VTS) are volcanic derived sedimentary units which form the laharic deposit in the Sumner Valley. Detailed rock descriptions are presented with relevant supporting annotated figures (Table 20 and Figure 5.17). No rock mechanics testing was carried for this unit as in-sufficient similar intact material was un-able to be recovered (Figure 5.17). The VC unit compositionally is observed to be highly variable, as such component percentages are only representative of material sampled (Table 5.20).

Detailed Engineering Geological Igneous Rock Description

Table 5.20: Detailed Engineering Geological Igneous Rock Description for volcanogenic conglomerate (VC).

Detailed Engineering Geological Igneous Rock Descriptive Scheme	
Component	**Description**
Geological Context (Unit Feature, Emplacement Mechanism, Formation, Group)	[LAHARIC DEPOSIT, LYTTELTON VOLCANIC GROUP]
Location	Evans Pass Road, Sumner Valley
Date Sampled, Identification Number	14/08/2013, VC
Colour	Grey to orange groundmass, grey to black clasts
Weathering and Alteration	Slightly-moderately weathered, extensive iron staining and clay alteration (Figures 5.17a/b)
Structure and Texture (Outcrop, Hand Specimen)	Massive, poorly sorted, conglomerate, brecciated , porphyritic (Figures 5.17c/d)
Groundmass Grain Size	Fine grained clay rich groundmass (Figure 5.17b)
Crystal Grain Size	Fine-medium grained phenocrysts (Figure 5.17a)
Fragment/Clast/Lithic Grain Size	Fine-boulder sized sub-rounded to angular intact basaltic clasts (Figures 5.17c/d)
Component Analysis (Hand Specimen) *% Groundmass/Matrix* *% Crystals* *% Fragments, Clasts and Lithics* *% Vesicles*	 25% 25% 50% 0%
Mineralogy (Hand Specimen and Thin Section)	Plagioclase feldspar 10%, quartz 10%, clinopyroxene 2%, orthopyroxene 2%, opaques 1% (Figure 5.17e/f)
Rock Name	BASALTIC VOLCANOGENIC CONGLOMERATE
Discontinuities *Orientation and Joint Sets* *Spacing* *Aperture* *Additional*	 N/A N/A N/A Fractures with defects prevalent at clast groundmass boundaries
Intact Strength *In field* *Testing (UCS/PLS/Schmidt Hammer)*	 Extremely weak-weak N/A
Table 5.20 is continued over the page	

Table 5.20: Detailed Engineering Geological Igneous Rock Description for volcanogenic conglomerate (VC) – continued.

Full Expanded Description
[LAHARIC DEPOSIT, LYTTELTON VOLCANIC GROUP], Evans Pass Road, Sumner Valley, VS, grey to orange groundmass, grey to black clasts, slightly-moderately weathered, extensive iron oxide staining and clay alteration, massive, poorly sorted, conglomerate, brecciated, porphyritic, fine grained clay rich groundmass, fine-medium grained phenocrysts, fine-boulder sized sub-rounded to angular intact basaltic clasts. Groundmass 25%, crystals 25% (Plagioclase feldspar 10%, quartz 10%, clinopyroxene 2%, orthopyroxene 2%, opaques 1%), clasts 50%, BASALTIC VOLCANOGENIC CONGLOMERATE. Extremely weak-weak.
Summary Description
Grey to orange groundmass, grey to black clasts, slightly-moderately weathered, extensive iron oxide staining and clay alteration, massive, poorly sorted, conglomerate, brecciated, porphyritic, fine grained clay rich groundmass, fine-medium grained phenocrysts, fine-boulder sized sub-rounded to angular intact basaltic clasts. Groundmass 25%, crystals 25%, clasts 50%, BASALTIC VOLCANOGENIC CONGLOMERATE. Extremely weak-weak.

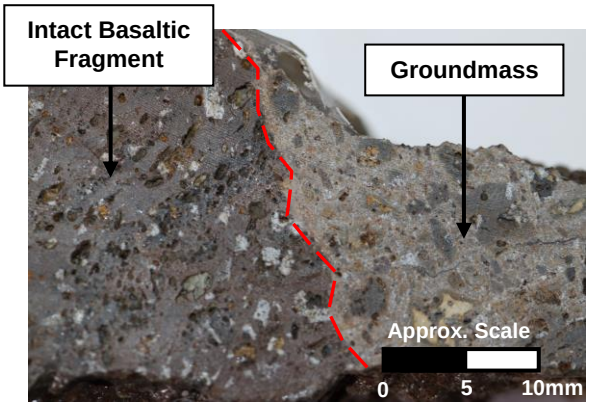

Figure 5.17a) Macro photo of cut section of VC. Note vesicular basaltic clast/fragment and groundmass.

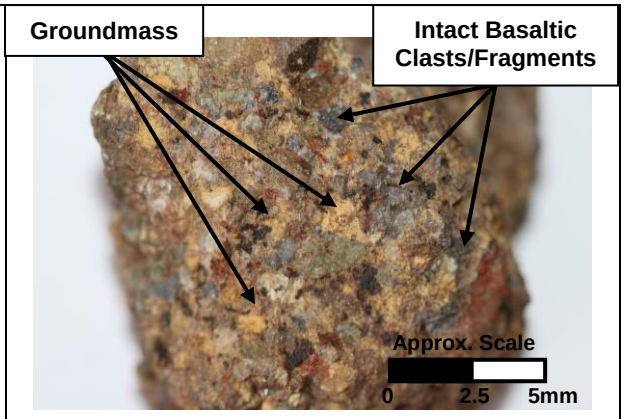

Figure 5.17b) Macro photo of VC hand specimen. Note variability in composition between 5.17a and 5.17b.

Figure 5.17c) Field photograph of laharic deposit in Sumner Valley. Section is distinctly stained. Important to note is the unsorted nature of the deposit.

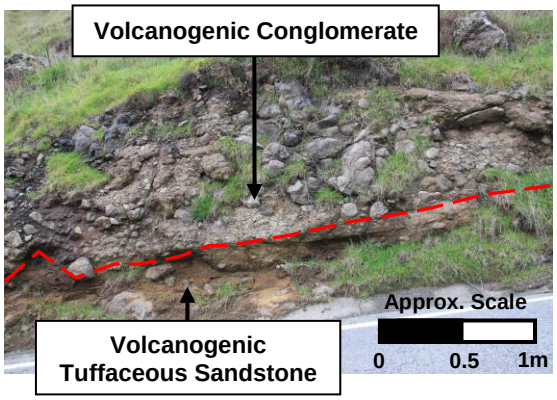

Figure 5.17d) Field photograph of laharic deposit in Sumner Valley.

Figure 5.17 is continued over the page.

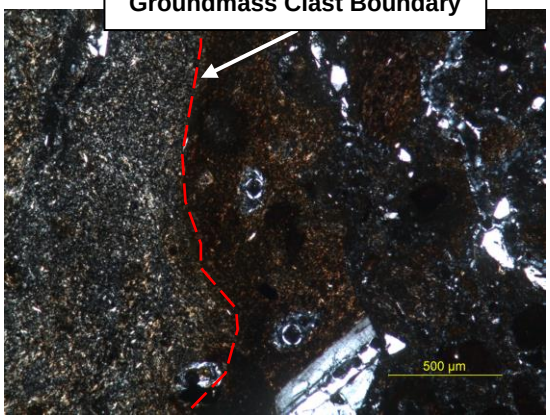

Figure 5.17e) Clast groundmass boundary (red dashes). Section is in cross polarised light (CPL).

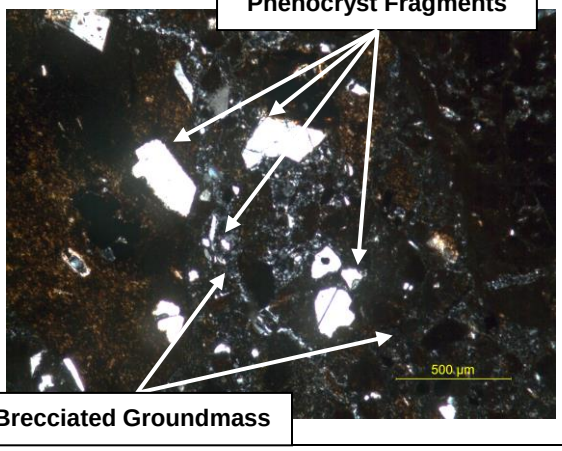

Figure 5.18f) Brecciated groundmass and fragmented phenocrysts. Section is in cross polarised light (CPL).

Figure 5.17: Annotated images at hand specimen, outcrop and microscopic scales of VC.

Rock Mechanics Data

As previously stated, no rock mechanics testing has been carried out due to the compositional complexity and variability of this unit. It should be noted that observed defects for VC are prevalent at fragment/clast groundmass boundaries; therefore it is the strength of the clayey groundmass which should ultimately control the failure of the unit. Complexities observed between the groundmass and fragments will be required to be studied in greater detail.

5.11 Volcanogenic Tuffaceous Sandstone (VTS)

Detailed rock descriptions are presented with relevant supporting annotated figures (Table 5.21 and Figure 5.18). No rock mechanics testing was carried for this unit, as sufficient intact material was unable to be recovered.

Detail Engineering Geological Igneous Rock Description

Table 5.21: Detailed Engineering Geological Igneous Rock Description for Volcanogenic Tuffaceous Sandstone (VTS).

Detailed Engineering Geological Igneous Rock Descriptive Scheme	
Component	**Description**
Geological Context (Unit Feature, Emplacement Mechanism, Formation, Group)	[LAHARIC DEPOSIT, LYTTELTON VOLCANIC GROUP]
Location	Evans Pass Road, Sumner Valley
Date Sampled, Identification Number	14/08/2013, VTS
Colour	Greyish orange
Weathering and Alteration	Slightly weathered, minor iron staining and clay alteration
Structure and Texture (Outcrop, Hand Specimen)	Well sorted, tuffaceous, microcrystalline
Groundmass Grain Size	Fine grained groundmass (Figure 5.18a)
Crystal Grain Size	Fine grained phenocrysts (Figure 5.18a)
Fragment/Clast/Lithic Grain Size	Fine sized basaltic clasts (Figure 5.18b)
Component Analysis (Hand Specimen) *% Groundmass/Matrix* *% Crystals* *% Fragments, Clasts and Lithics* *% Vesicles*	 78% 20% 2% 0%
Mineralogy (Hand Specimen and Thin Section)	Quartz 10%, plagioclase 3%, olivine 2%, iddingsite 2%, clinopyroxene 2%, opaques 1% (Figure 5.18c-f)
Rock Name	BASALTIC VOLCANOGENIC TUFFAECOUS SANDSTONE
Discontinuities *Orientation and Joint Sets* *Spacing* *Aperture* *Additional*	 N/A N/A N/A N/A
Intact Strength *In field* *Testing (UCS/PLS/Schmidt Hammer)*	 Very weak-extremely weak N/A
Full Expanded Description	
[LAHARIC DEPOSIT, LYTTELTON VOLCANIC GROUP], Evans Pass Road, Sumner Valley, VTS, greyish orange, slightly weathered, minor iron oxide staining and clay alteration, well sorted, tuffaceous, microcrystalline, fine grained groundmass, fine grained phenocrysts, fine sized basaltic clasts. Groundmass 78%, crystals 20% (Quartz 10%, plagioclase 3%, olivine 2%, iddingsite 2%, clinopyroxene 2%, opaques 1%), clasts 2%, BASALTIC VOLCANOGENIC TUFFAECOUS SANDSTONE. Very weak-extremely weak.	
Summary Description	
Greyish orange, slightly weathered, minor iron oxide staining and clay alteration, well sorted, tuffaceous, microcrystalline, fine grained groundmass, fine grained phenocrysts, fine sized basaltic clasts. Groundmass 78%, crystals 20%, clasts 2%, BASALTIC VOLCANOGENIC TUFFAECOUS SANDSTONE. Very weak-extremely weak.	

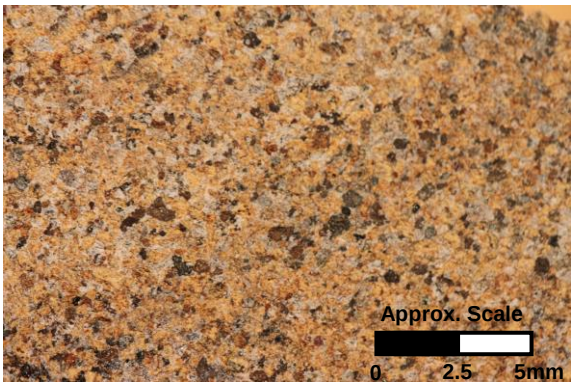

Figure 5.18a) Macro photo of cut section of VTS. Note both the crystals and groundmass is fine grained.

Figure 5.18b) Field photograph of tuffaceous sandstone which underlies the laharic deposit conglomerate.

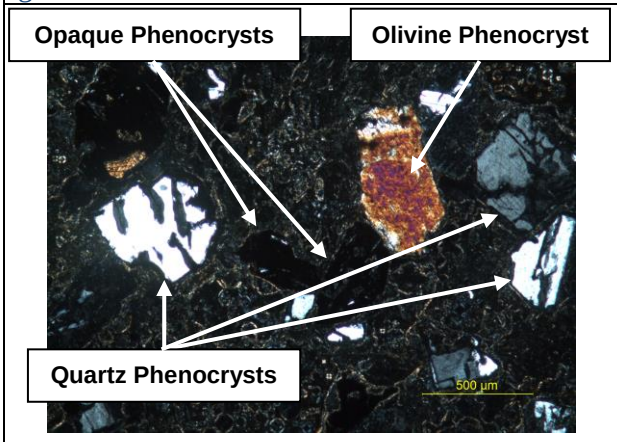

Figure 5.18c) Quartz, olivine and opaque phenocrysts. Section is in cross polarised light (CPL).

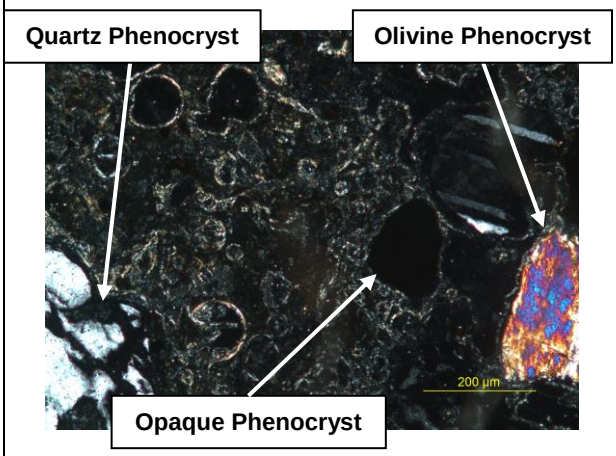

5.18d) Quartz, olivine and opaque phenocrysts. Section is in cross polarised light (CPL).

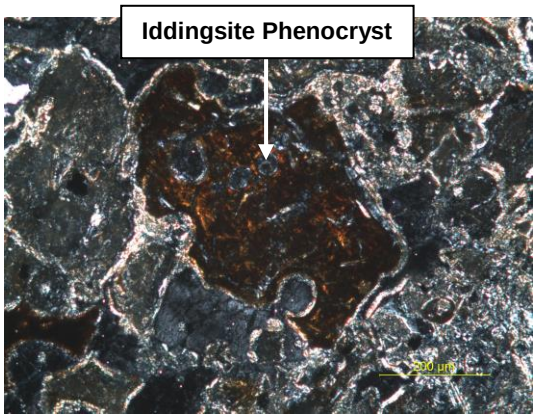

Figure 5.18e) Weathered iddingsite phenocryst. Section is in cross polarised light (CPL).

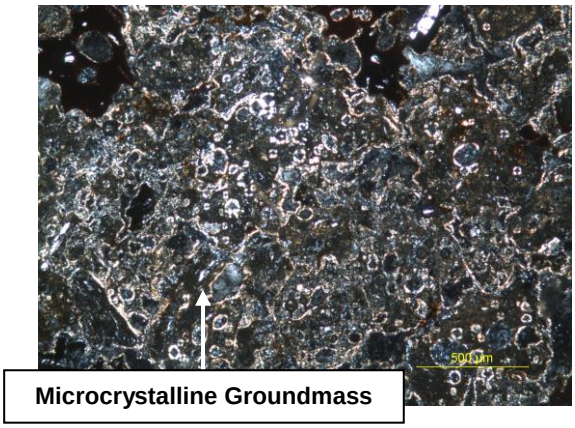

Figure 5.18f) Microcrystalline groundmass and basaltic fragment. Section is in cross polarised light (CPL).

Figure 5.18: Annotated images at hand specimen, outcrop and microscopic scales of VTS.

5.12 Geotechnical Testing and Properties Synthesis (Chapters 4 and 5)

This chapter has presented the engineering geological igneous rock descriptions and key rock mechanics data supported by a series of annotated figures and tables (where relevant) for all the 'assorted' volcanics units included in this study. Assorted volcanic units included intrusives (dykes), pyroclastic density current (ignimbrites), airfall (tuff and ash) and laharic (volcanogenic) units.

Presented in Table 5.22 is a combined summary data set of all the geotechnical (rock mechanics) parameters presented in Chapters 4 and 5. A total of 13 out of 17 lithologies were able to successfully geotechnical tested. Units which could not be tested due to complexities such as sample heterogeneity, have not been included for brevity. Table 5.22 is used in Chapter 6 to discuss variability, trends, clusters and relationships between geotechnical parameters. Additionally, the data will be used determine the relationship that emplacement and post-emplacement mechanisms have on geotechnical parameters. Complete raw data sets are included in Appendix 2.

Table 5.22: Summary Table of Rock Mechanics Data for Lyttelton Volcanic Group Lithologies. *Notes are included at the bottom of the table.

Summary Rock Mechanics Data for Lyttelton Volcanic Group Lithologies																		
Lithology			**n (%)**	**ρ_d (kg/m^3)**	**Vp (m/s)**	**Vs (m/s)**	**$Is_{(50)}$ (MPa)**	**Correlated UCS $Is_{(50)}$×24 (MPa)**	**UCS σ_{ci} (MPa)**	**Id_1 (%)**	**Id_2 (%)**	**E_{stat} (GPa)**	**E_{dyn} (GPa)**	**υ_{stat} (unitless)**	**υ_{dyn} (unitless)**	**G_{stat} (GPa)**	**K_{stat} (GPa)**	**No. of Samples Tested*3**
Lava Flows	Unweathered Basaltic Lava **(BLUW)**	Mean	**2.3**	**2820**	**4740**	**2806**	**6.65**	**159.5**	**123.1**	99.8*1	99.6*1	**51.5**	**54.8**	**0.23**	**0.23**	**20.0**	**36.0**	$10^p/13^{pls}/10^{ucs}$
		Max	5.6	2890	5185	2975	8.26	198.4	192.8			69.2	64.0	0.40	0.28	24.9	86.5	
		Min	0.8	2680	4291	2680	5.64	135.4	58.2			40.2	45.8	0.10	0.17	14.9	19.0	
	Slightly to Moderately weathered Basaltic Lava **(BLSM)**	Mean	**8.3**	**2360**	**3610**	**2094**	**2.24**	**53.8**	**50.0**	-	-	**20.2**	**26.4**	**0.21**	**0.25**	**8.5**	**19.1**	$5^p/10^{pls}/5^{ucs}$
		Max	14.2	2470	4330	2475	3.44	82.6	80.0			28.4	36.8	0.46	0.28	12.1	67.3	
		Min	4.6	2230	2626	1467	1.12	26.9	29.4			12.2	12.5	0.10	0.20	5.0	7.0	
	Highly to Completely weathered Basaltic Lava **(BLHC)**	Mean	**35.9**	**1740**	-	-	**0.27**	**6.5**	**3.5**	-	-	-	-	-	-	-	-	$10^p/12^{pls}/9^{ucs}$
		Max	39.3	1830	-	-	0.38	9.1	5.6			-	-	-	-	-	-	
		Min	32.0	1630	-	-	0.18	4.2	2.0			-	-	-	-	-	-	
	Rubbly Basaltic Breccia **(RCB)**	Mean	**31.8**	**1790**	-	-	**0.20**	**4.8**	**5.4**	-	-	-	-	-	-	-	-	$10^p/15^{pls}/10^{ucs}$
		Max	37.0	1980	-	-	0.44	10.7	15.8			-	-	-	-	-	-	
		Min	25.1	1640	-	-	0.05	1.2	1.8			-	-	-	-	-	-	
	Trachytic Lava **(TL)**	Mean	**4.2**	**2410**	**3688**	**2270**	**2.03**	**48.8**	**56.9**	-	-	**19.0**	**29.6**	**0.23**	**0.19**	**7.9**	**41.8**	$9^p/9^{pls}/9^{ucs}$
		Max	5.4	2430	4014	2476	2.62	62.9	73.3			24.8	35.5	0.49	0.27	11.1	261.7	
		Min	3.4	2380	3524	2106	1.23	29.5	44.2			13.4	26.0	0.12	0.13	5.4	8.9	
Dykes	Basaltic Dyke **(BD)**	Mean	**3.0**	**2760**	**4665**	**2648**	**3.07**	**73.8**	**66.8**	-	-	**31.8**	**48.9**	**0.20**	**0.26**	**13.3**	**18.1**	$4^p/9^{pls}/4^{ucs}$
		Max	3.9	2780	4774	2727	3.97	95.3	71.1			43.8	51.3	0.23	0.29	18.4	21.3	
		Min	2.2	2750	4458	2575	1.48	35.6	61.6			21.1	46.7	0.12	0.24	8.3	12.2	
	Trachytic Dyke **(TD)**	Mean	**6.0**	**2330**	**3249**	**1948**	**2.82**	**67.6**	**54.0**	-	-	**16.0**	**21.6**	**0.21**	**0.22**	**6.6**	**9.6**	$6^p/9^{pls}/6^{ucs}$
		Max	10.6	2350	3474	1986	4.91	118.0	61.0			20.1	22.2	0.28	0.26	8.0	13.4	
		Min	3.9	2290	3121	1888	1.93	46.4	42.4			10.3	19.7	0.13	0.18	4.6	4.6	
Ignimbrites	Brecciated Basaltic Ignimbrite **(IGB)**	Mean	**40.9**	**1660**	-	-	**0.14**	**3.4**	-	93.7*1	83.7*1	-	-	-	-	-	-	$6^p/13^{pls}/6^{ucs}$
		Max	47.6	2020	-	-	0.34	8.3	-			-	-	-	-	-	-	
		Min	25.9	1490	-	-	0.04	0.9	-			-	-	-	-	-	-	
	Moderately Welded Basaltic Ignimbrite **(IGMW)**	Mean	**25.5**	**2030**	-	-	**1.1**	**25.7**	-	-	-	-	-	-	-	-	-	$11^p/11^{pls}/0^{ucs}$
		Max	29.8	2190	-	-	2.6	63.6	-			-	-	-	-	-	-	
		Min	18.2	1940	-	-	0.3	7.5	-			-	-	-	-	-	-	
	Highly Welded Basaltic Ignimbrite **(IGW)**	Mean	**4.6**	**2750**	**4307**	**2388**	**6.9**	**165.3**	-	-	-	-	**40.0*2**	-	**0.28*2**	**15.7*2**	**30.0*2**	$6^p/6^{pls}/0^{ucs}$
		Max	5.1	2760	4364	2450	7.9	189.0	-			-	41.7*2	-	0.30*2	16.6*2	31.1*2	
		Min	4.2	2730	4217	2252	5.9	141.2	-			-	36.2*2	-	0.26*2	13.9*2	28.4*2	

Airfall	Crystal Tuff **(CTC)**	Mean	**47.1**	**1480**	-	-	**0.1**	**2.0**	-	37.0*[1]	20.2*[1]	-	-	-	-	-	-	$5^{p}/5^{pls}$ $/0^{ucs}$
		Max	49.2	1560	-	-	0.18	4.3	-			-	-	-	-	-	-	
		Min	44.2	1400	-	-	0.05	1.1	-			-	-	-	-	-	-	
	Lithic Tuff **(CTL)**	Mean	**43.5**	**1610**	-	-	**0.4**	**9.4**	-	93.6*[1]	87.8*[1]	-	-	-	-	-	-	$12^{p}/12^{pls}$ $/0^{ucs}$
		Max	44.9	1660	-	-	0.6	13.7	-			-	-	-	-	-	-	
		Min	42.1	1550	-	-	0.2	4.7	-			-	-	-	-	-	-	
	Red Ash **(RA)**	Mean	**33.4**	**1650**	-	-	**2.5**	**59.4**	-	99.3*[1]	98.8*[1]	-	-	-	-	-	-	$25^{p}/10^{pls}$ $/0^{ucs}$
		Max	59.8	1980	-	-	3.5	84.3	-			-	-	-	-	-	-	
		Min	11.3	1070	-	-	1.2	29.0	-			-	-	-	-	-	-	

Note *1: Slake durability first/second cycle (Id_1 and Id_2) has no maximum or minimum or mean as only one test was conducted.
Note *2: Highly-welded basaltic ignimbrite (IGW) Young's modulus, Poissons ratio, shear modulus and bulk modulus are calculated under dynamic conditions.
Note *3: Number of samples tested are provided in the following order porosity and density/point load/uniaxial compressive strength (e.g. $10^{p}/12^{pls}/9^{ucs}$). Also note: P and S wave velocities are determined using UCS cylindrical cores where possible, with the exception of IGW where Vp and Vs are determined using intact block samples.

CHAPTER 6 - Discussion and Applications

6.1 Introduction

Following the geotechnical testing, detailed thin section analysis and comprehensive igneous and volcanogenic characterisations of all the units in this study, Chapter 6 discusses and analyses the data presented in Chapters 4 and 5. Chapter 6 consists of four sections. The first section graphically summarises the rock mechanics data presented in the previous two chapters, and discusses trends and variations with regard to potential influencing geological factors. Eight fundamental rock mechanics relationships are also presented with the purpose of determining the effect one geotechnical parameter has on another. These relationships provide potential interpretations for causes of variability in the rock mechanics data. In addition the relationship between rock mechanical (geotechnical) parameters and emplacement/post-emplacement mechanisms are explored with specific reference to both field and laboratory observations/data. Potential geotechnical/engineering geological and geological/volcanic applications of this thesis are also remarked on.

6.2 Rock Mechanics Characteristics and Variations

This section presents a series of graphical representations of all the physical and derived (static and dynamic) rock mechanical parameters determined in this study. Data is directly sourced from Table 5.22. Plots presented in this section are commented on in terms of general trends and variability observed within the dataset. Identified variations are also discussed with clear links to the influencing geological factors, aspects which are further discussed in Section 6.3.

6.2.1 Porosity Data (*n*)

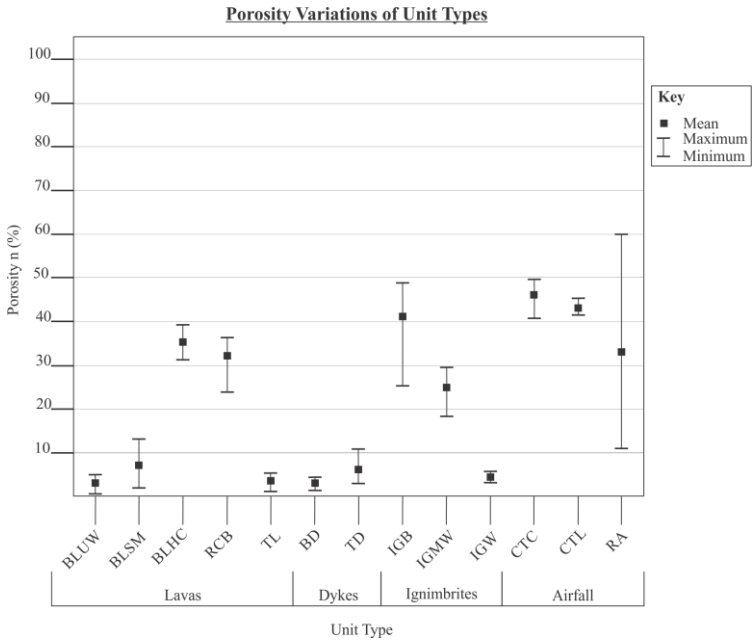

Figure 6.1: Summary Plot of Porosity (n, %) for all study units.

Porosity variations for all the tested units (Figure 6.1) show two general trends. 1) Intact and relatively unweathered to moderately weathered lavas, dykes and highly welded ignimbrites generally have relatively low porosity (~1-15%). 2) Weathered clay-rich and brecciated lavas, unwelded to moderately welded ignimbrites, tuffs and ashes have a much higher porosities (~18-60%).

The brecciated basaltic ignimbrite (IGB) and red ash (RA) have the greatest variation in range. The IGB porosity varied between 26 and 48%, with a mean of 40%. This variation is most likely due to the variable percentage of welded fragments throughout the groundmass. RA porosity varies between 11 and 60%, with a mean of 33% this range is due to the welded groundmass providing a low porosity, whereas the sporadic scoriaceous/vesiculated clasts (highly vesicular) throughout the groundmass provide a much high porosity. Geological factors likely to influence the porosity of the sample include: frequency and size of vesicles, frequency, degree of sample heterogeneity, aperture and interconnectivity of fractures/cracks, weathering, alteration, degree of welding and clay content.

6.2.2 Dry Mass Density Data (ρ_d)

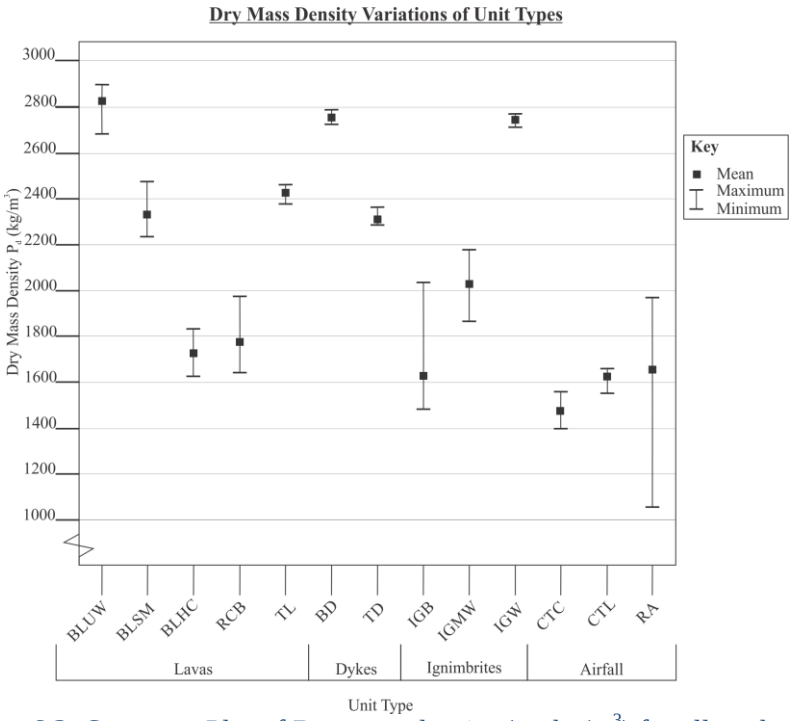

Figure 6.2: Summary Plot of Dry mass density (ρ_d, kg/m^3) for all study units.

The dry mass density variations for all the units tested in this study are displayed in Figure 6.2. The summary plot shows two trends, 1) relatively unweathered to moderately weathered lavas, dykes and highly welded ignimbrites generally have a high mass density (~2250-2850 kg/m^3). 2) The weathered clay-rich and brecciated lavas, unwelded to moderately welded ignimbrites, tuffs and ashes have a lower mass density (~1100-2200 kg/m^3).

The red ash (RA), rubbly basaltic breccia (RCB), brecciated (IGB) and moderately welded basaltic ignimbrite (IGMW) have the greatest variation in terms range of values. The variation in the RA density (1070-1650 kg/m^3) is most likely due the presence of highly vesicular scoriaceous clasts decreasing the sample density. The RCBs high variation is thought to be due to the variability in the ratio of clay content to intact basaltic fragments; a greater proportion of clay content providing a lower overall density. The range of densities in the IGB (1490-2020 kg/m^3) and IGMW (1940-2190 kg/m^3) is most likely due to the ratio of fragments basaltic fragments and clasts; clasts and fragments should have a higher density than the ash-rich groundmass. Factors likely to influence the dry mass density of the sample include: weathering and alteration of the groundmass and phenocrysts to clay-rich minerals, frequency and size of vesicles, aperture and frequency of fractures/cracks, degree of sample heterogeneity, infilling of defects, degree of welding and all aspect of porosity or influence on.

6.2.3 P and S Wave Data (V_p *and* V_s)

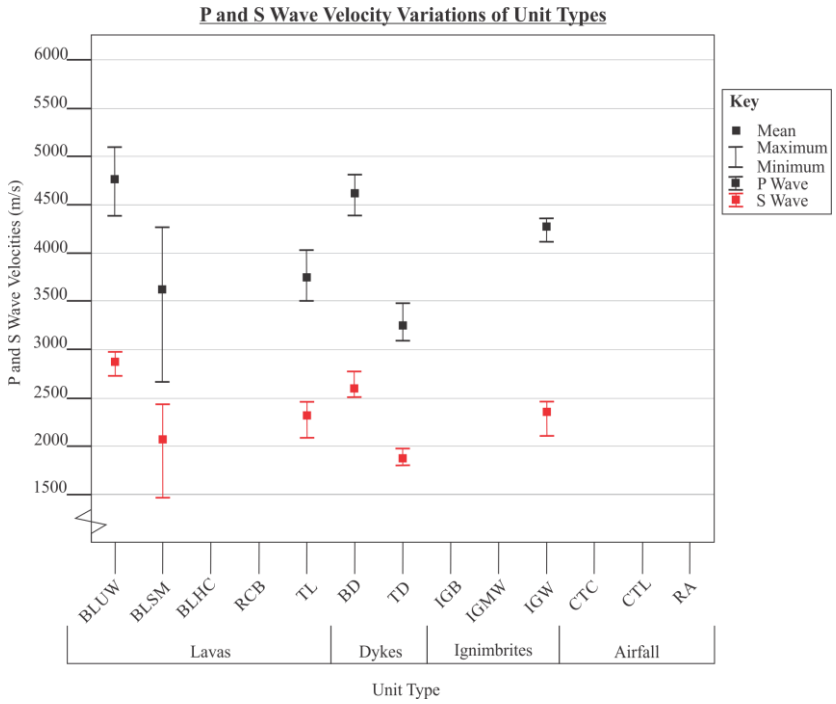

Figure 6.3: Summary Plot of P and S wave velocity (V_P and V_S, m/s) for selected study units.

The P (longitudinal) and S (shear) wave velocities and variations for all the units where wave velocities, could be determined are presented in Figure 6.3. The summary plot shows that relatively unweathered basaltic lava, basaltic dyke and high welded ignimbrite have a high Vp, in the range 4250-4750m/s. While, the slightly-moderately weathered basaltic lava, trachytic lava and trachytic dyke have a generally lower Vp of approximately 2800-4200m/s. Vs values for the relatively unweathered basaltic lava and basaltic dyke are generally between 2500 and 3000m/s. For the slightly-moderately weathered basaltic lava, trachytic lava and dyke and highly welded ignimbrite Vs is mostly 1750-2500m/s.

The slightly-moderately weathered basaltic lava (BLSM) displayed the greatest variation in values. The variation in both the V_p (2626-4330m/s) and V_s (1467-2475m/s) can be explained by the range in weathered states of the samples tested, as well as the presence of clay-rich minerals and fractures in the groundmass. Potential geological factors which could affect acoustic wave velocities include, weathering and alteration of the groundmass and phenocrysts to clay rich minerals, frequency, aperture and interconnectivity of vesicles and macro/micro fractures.

6.2.4 Point Load Strength Index Data ($Is_{(50)}$)

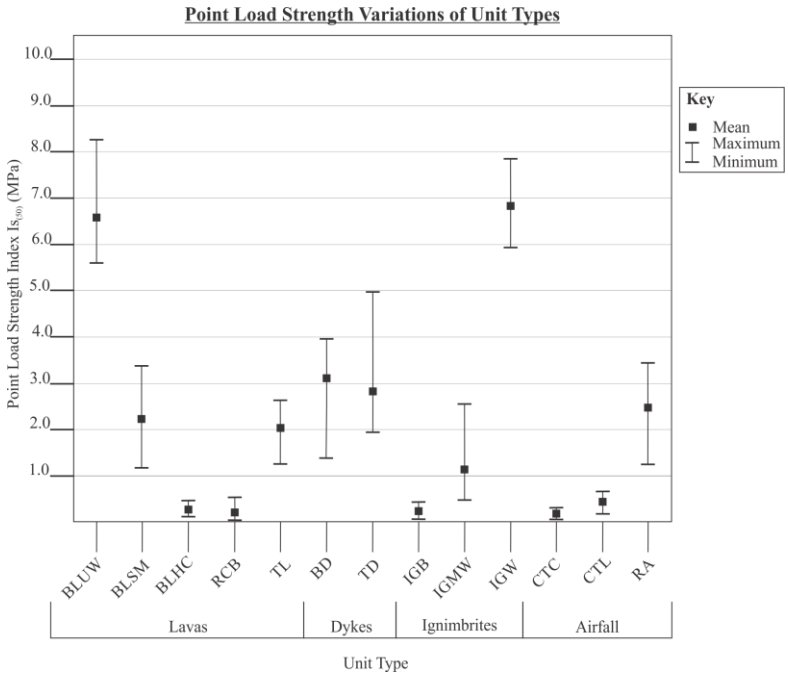

Figure 6.4: Summary Plot of Point Load Strength Index (PLS, MPa) for all study units.

The point load strength index variations for all the tested units in this study are displayed in Figure 6.4. The summary plot generally shows three trends. 1) The relatively unweathered basaltic lavas and highly welded basaltic ignimbrites have a high PLS (~5-8 MPa). 2) Slightly-moderately weathered basaltic lavas, basaltic dykes, trachytic dykes and lavas, moderately welded basaltic ignimbrites and welded ashes have lower to moderate PLS (~1-5 MPa). 3) The highly weathered basaltic lava, rubbly lava breccia, brecciated basaltic ignimbrite, crystal dominated tuff and lithic dominated tuff were seen to have a very low PLS (~0-0.75 MPa).

It was noted during the PLS testing that units with a mean PLS greater than 1.0 MPa had the greatest variability with values ranges 1.0 ± 3.0 MPa with respect to the mean, (BLUW, BLSM, TL, BD, TD, IGMW, IGW, RA). Units with a mean PLS lower than 1.0 MPa had very little variation in PLS; this is most likely due to the very low strength of these materials (BLHC, RCB, IGB, CTC and CTL). Geological factors likely to influence the PLS of a sample can include, weathering and alteration, degree of sample heterogeneity, percentage and grain size of phenocrysts, flow banding, clasts and fragments and pre-existing defects i.e. macro and micro fractures.

6.2.5 Uniaxial Compressive Strength Data (σ_{ci})

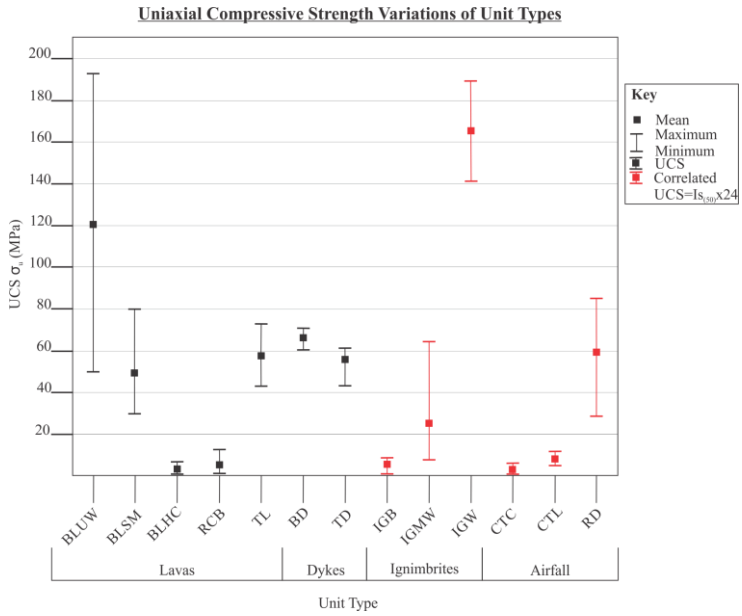

Figure 6.5: Summary Plot of Uniaxial Compressive Strength (UCS, MPa) for all study units. Correlated UCS values following the Broch and Franklin, (1972) UCS=$Is_{(50)}$×24 have been included for comparative purposes for units were direct UCS testing was not possible.

The uniaxial compressive strength variations are presented (Figure 6.5) for all the units where testable cores could be created. Where samples could not be tested directly tested for UCS, correlated UCS is used. Correlated UCS values following $Is_{(50)}$ (Broch and Franklin, 1972) have been included for comparative purposes. The summary plot shows three trends. 1) The relatively unweathered basaltic lava and highly welded ignimbrite have a high UCS (~120-165MPa, based on mean). 2) Slightly-moderately weathered basaltic lava, trachytic lava, basaltic dyke, trachytic dyke and welded red ash have a low to moderate UCS (~45-75MPa, based on mean). 3) Highly weathered basaltic lavas, rubbly basaltic breccia, brecciated and moderately welded basaltic ignimbrite and crystal and lithic tuff generally have a very low to low UCS (~1-25MPa, based on mean).

The 'relatively' unweathered basaltic lava (BLUW) displayed the largest variation in terms of each unit's maximum and minimum values respective to the mean. The BLUW uniaxial compressive strength varied between 58.2MPa and 192.8MPa with a mean of 123.1MPa. The large variation in UCS for the BLUW would most likely be due to high phenocryst percentage and/or micro-fractures in the rock mass. Factors which can affect the UCS of a sample could include weathering and alteration of the groundmass and phenocrysts to clay rich minerals, frequency, aperture and interconnectivity of fractures and vesicles, orientation of phenocrysts and defects (e.g. trachytic texture and flow banding), degree of sample

heterogeneity and the influence of clasts and fragments providing conduits for defect formation.

6.2.6 Slake Durability Data (Id_1 and Id_2)

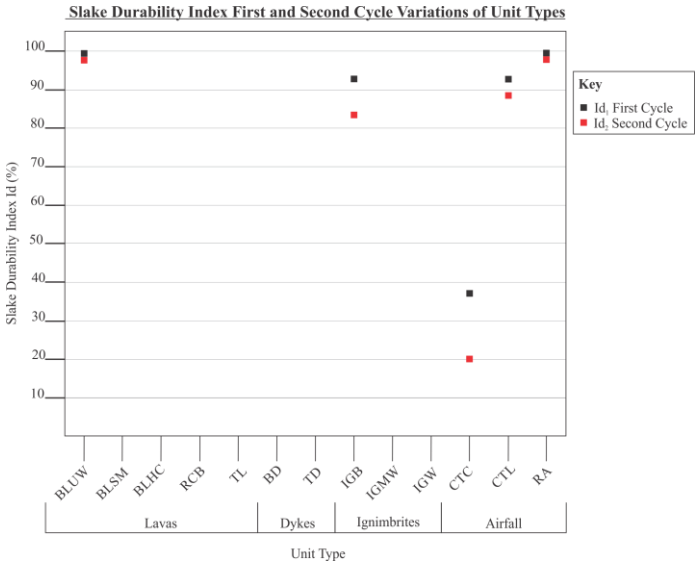

Figure 6.6: Summary Plot of Slake Durability (Id_1 and Id_2, %) for selected study units.

The first and second cycle slake durability index for selected units tested in this study is presented in Figure 6.6. The summary plot shows approximately three trends. 1) The intact 'relatively' unweathered basaltic lava and the welded red ash have a very high slake durability index (>98%). 2) The brecciated basaltic ignimbrite and lithic dominated tuff have a high slake durability index (~80-95%), 3) although the crystal dominated tuff has a low slake durability index (~20-40%).

The crystal dominated tuff (CTC) and brecciated basaltic ignimbrite (IGB, 93-82%) have the greatest decrease in slake durability index percentage from the first to second cycle respectively. The CTC performed the poorest out of the units selected for slake durability index testing (37-20% respectively, Id_1 to Id_2). The low slake durability of the CTC is most likely attributed to the coarse grain size, poor induration and moderately weathered state of the groundmass. The low degree of welding and high phenocryst content provides more locations for defects to initiate. The IGB displays a high slake durability index. The 10% decrease from Id_1 at 93.7% to Id_2 and 83.7% is most likely due to a loss of material by weakening of groundmass at the clast/fragment boundaries. Geological factors likely to influence the slake durability index of the sample include: strength of the groundmass, weathering and alteration, percentage of clay content, grain size and induration of the groundmass, phenocrysts and clasts/fragments, welding, porosity and fractures/cracks.

6.2.7 Young's Modulus Data (*E*)

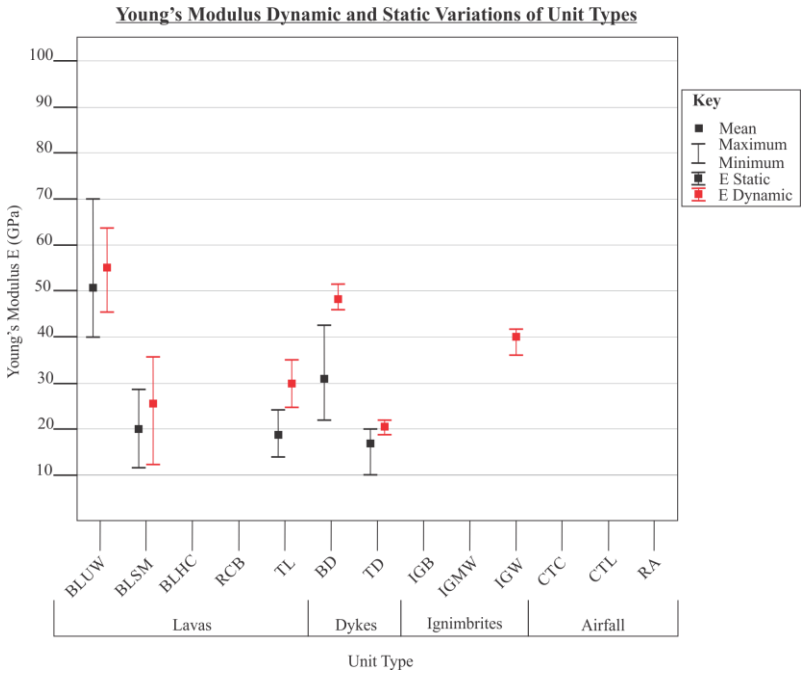

Figure 6.7: Summary Plot of Static and Dynamic Young's Modulus ($E_{stat/dyn}$, GPa) for selected study units.

The dynamic and static Young's Modulus variations for all the units where deformation moduli could be tested and determined are displayed in Figure 6.7. The summary plot shows approximately shows two trends. 1) The 'relatively' unweathered basaltic lava, basaltic dyke and highly welded basaltic ignimbrite have a high Young's Modulus (E_{dyn} ~40-60 GPa, based on mean). 2) Whereas, the slightly-moderately weathered basaltic lava, trachytic lava, basaltic dyke and trachytic dyke have a lower Young's Modulus (E_{dyn} ~15-30 GPa, based on mean). Static values vary in comparison to the dynamic values. Using static values two similar trends can be observed (based on the mean), 1) E_{stat} ~30-50 GPa (BLUW and BD) and 2) ~18-20 GPa (BLSM, TL and TD). It should be noted from Figure 6.7 that the dynamic (acoustically derived) Young's Modulus values in all cases plot higher than the static (strain gauge derived) equivalent.

The unweathered basaltic lava (BLUW, E_{stat}) and slightly-moderately weathered basaltic lava (BLSM, E_{dyn}) displayed the greatest variation in the unit's maximum and minimum values respective to the mean. The variation in both BLUW E_{stat} (40.2-69.2 GPa) and BLSM E_{dyn} (12.5-36.8 GPa), would most likely appear to be due to the range in the UCS values (UCS is proportional to E) in the case of both BLUW and BLSM. Factors likely to influence the Young's Modulus (sample stiffness) of a sample include: strength of the sample (UCS), P and S wave results (for dynamic), degree of welding, aperture and interconnectivity of

defects/discontinuities within the rock mass (e.g. micro/macro fractures), degree of sample heterogeneity, weathering and alteration of the groundmass and sample density.

6.2.8 Poissons Ratio Data (*υ*)

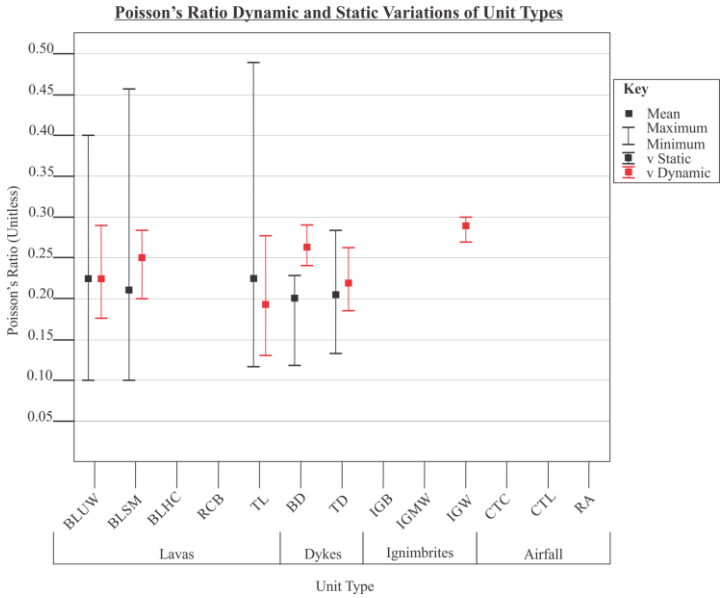

Figure 6.8: Summary Plot of Static and Dynamic Poisson's Ratio ($\upsilon_{stat}/_{dyn}$) for selected study units.

The static and dynamic Poisson's Ratio variations for all the units where deformation moduli could be tested and determined are presented in Figure 6.8. The summary plot shows that generally all of the units have a Poissons Ratio of between 0.20 and 0.30 (based on the mean). The summary plot shows that the Poisson's Ratio calculated under static conditions (υ_{stat}) have a much higher variation in terms of the unit's maximum and minimum values respective to the mean (2-3 times more than υ_{dyn}). The unweathered basaltic lava (BLUW), slightly-moderately weathered basaltic lava (BLSM) and trachytic lava (TL) displayed the greatest range. The variation in the BLUW υ_{stat} (0.10-0.40), BLSM υ_{stat} (0.10-0.46) and TL υ_{stat} (0.12-0.49) is most likely due to the presence of micro fractures (Refer back to Figure 4.11h) and the range in stresses recorded during the testing under static conditions (which is consistent with the range of UCS values (Figure 6.5)). Localised stresses and micro-fractures may not be detected during P and S wave testing (dynamic conditions), which could provide a possible explanation as to the variations in ranges when consider the υ_{stat} and $\upsilon_{dyn.}$

Geological factors likely to influence the Poisson's Ratio of a sample include: Young's Modulus of the sample, P and S wave results (for dynamic), aperture and interconnectivity of defects/discontinuities within the rock mass (e.g. micro/macro fractures), degree of welding, weathering and alteration of the groundmass and other components and frequency and grain

size of lithics and fragments. Other factors which may influence the Poisson's Ratio during static testing is the occurrence of localised stress developing in the sample.

6.2.9 Shear Modulus Data (*G*)

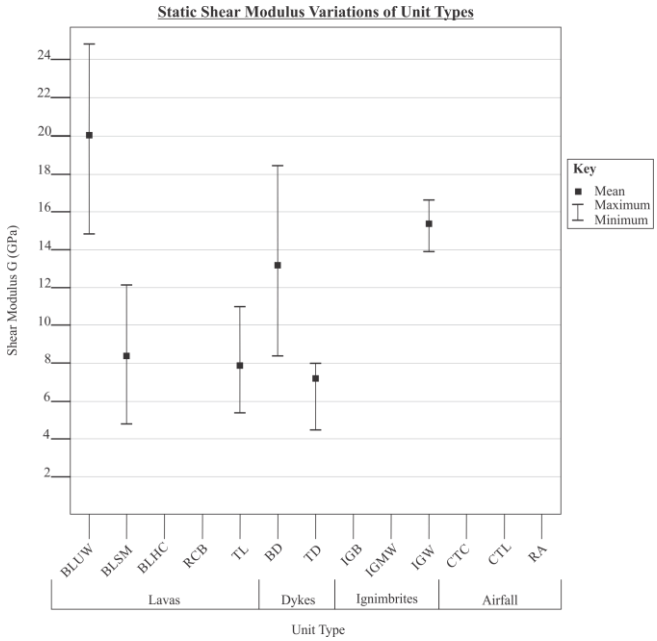

Figure 6.9: Summary Plot of Shear Modulus (G, GPa) for selected study units. Note: G has been derived under static conditions with the exception of IGW, where G has been derived under dynamic conditions.

The shear modulus variations for all the units where deformation moduli could be tested and determined are displayed in Figure 6.9. The summary plot shows three trends. 1) The 'relatively' unweathered basaltic lava has a high shear modulus (~15-25 GPa). 2) The basaltic dyke and highly welded ignimbrite have a moderate shear modulus (~10-16 GPa). 3) The slightly-moderately weathered basaltic lava and trachytic dyke and lava have a low to moderate shear modulus (~4-10 GPa).

The unweathered basaltic lava (BLUW), slightly-moderately weathered basaltic lava (BLSM) and the basaltic dyke (BD) displayed the greatest variation in terms of each unit's maximum and minimum values respective to the mean. The variation in BLUW (14.9-24.9 GPa) and BD (8.3-18.4 GPa) is most likely due to micro-fractures and alteration/weathering of the high percentage of feldspar and olivine/iddingsite phenocrysts. The variation in the BLSM (5.0-12.1 GPa) is best explained by the varied states of weathering in the cores (slightly and moderately weathered cores providing the range of the values (Refer back to Figure 4.3a). With increased weathering the clay content is noted to increase. This could result in a greater number of potential shear planes/surfaces and other features of weakness consequentially

lowering the shear modulus. Factors likely to influence the shear modulus of the sample include: aperture, interconnectivity and frequency of defects (micro/macro fractures), weathering and alteration of the groundmass, clay content, shear surface roughness/tortuosity and degree of welding.

6.2.10 Bulk Modulus Data (*K*)

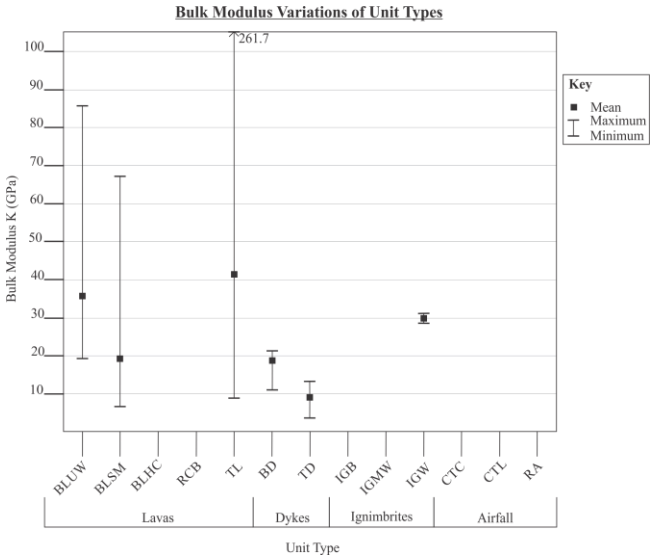

Figure 6.10: Summary Plot of Bulk Modulus (K, GPa) for selected study units. Note: K has been derived under static conditions with the exception of IGW, where K has been derived under dynamic conditions.

The bulk modulus variations for all the units where deformation moduli could be tested and determined are presented in Figure 6.10. The 'relatively' unweathered basaltic lava, trachytic lava and highly welded basaltic ignimbrite have a high bulk modulus (~30-42 GPa, based on the mean). Whereas, the slightly-moderately weathered basaltic lava, basaltic and trachytic dikes have a lower bulk modulus (~9-20 GPa, based on the mean).

The unweathered (BLUW), slightly-moderately (BLSM) and trachytic (TL) lavas displayed a high degree of variance in terms ranges of values. The variation in BLUW (19.0-86.5 GPa, mean of 36.0 GPa) is likely to be due to either micro-fractures within the rock mass or the high percentage of phenocrysts resulting in the variance in resistance to uniform compressibility. The range in the BLSM (7.0-67.3 GPa, mean of 19.1 GPa) is most likely due to a combination variable states of weathering of samples (increased clay content), heterogeneity, vesicles and micro-fractures. The TL bulk modulus varies between 8.9 and 261.7 GPa with a mean of 41.8 GPa. It should be noted that the maximum value is most likely not indicative of the overall unit characteristics (as seen by the mean). The variance in values is most likely due to aligned phenocrysts and micro-fractures within the rock mass.

Factors which can influence the bulk modulus of a sample include: sample strength (UCS), Young's Modulus (stiffness), sample density, aperture, interconnectivity and frequency of defects (micro/macro fractures), frequency and grain size of lithics, clasts and fragments, frequency and aperture of vesicles (porosity, n%) and degree of sample heterogeneity.

6.3 Correlation Plots and Relationships of Rock Mechanics Data

A series of correlation plots which illustrate the relationship that one geotechnical parameter has with another are presented in this section. Eight key relationships are presented and discussed: [1]uniaxial compressive strength (UCS) vs point load strength index, [2]UCS vs dry mass density, [3]P-wave vs UCS, [4]Young's Modulus vs UCS, [5]Poisson's Ratio vs UCS, [6]Young's Modulus vs Poisson's Ratio, [7]Porosity vs dry mass density and [8]Dry mass density vs P-Wave velocity. Data used in these plots are directly sourced from Table and from the rock mechanics raw data set in Appendix 2. Plots are coloured coded to unit type. Regression curves have not been fitted due to the variability of data.

6.3.1 Uniaxial Compressive Strength vs Point Load Strength Index

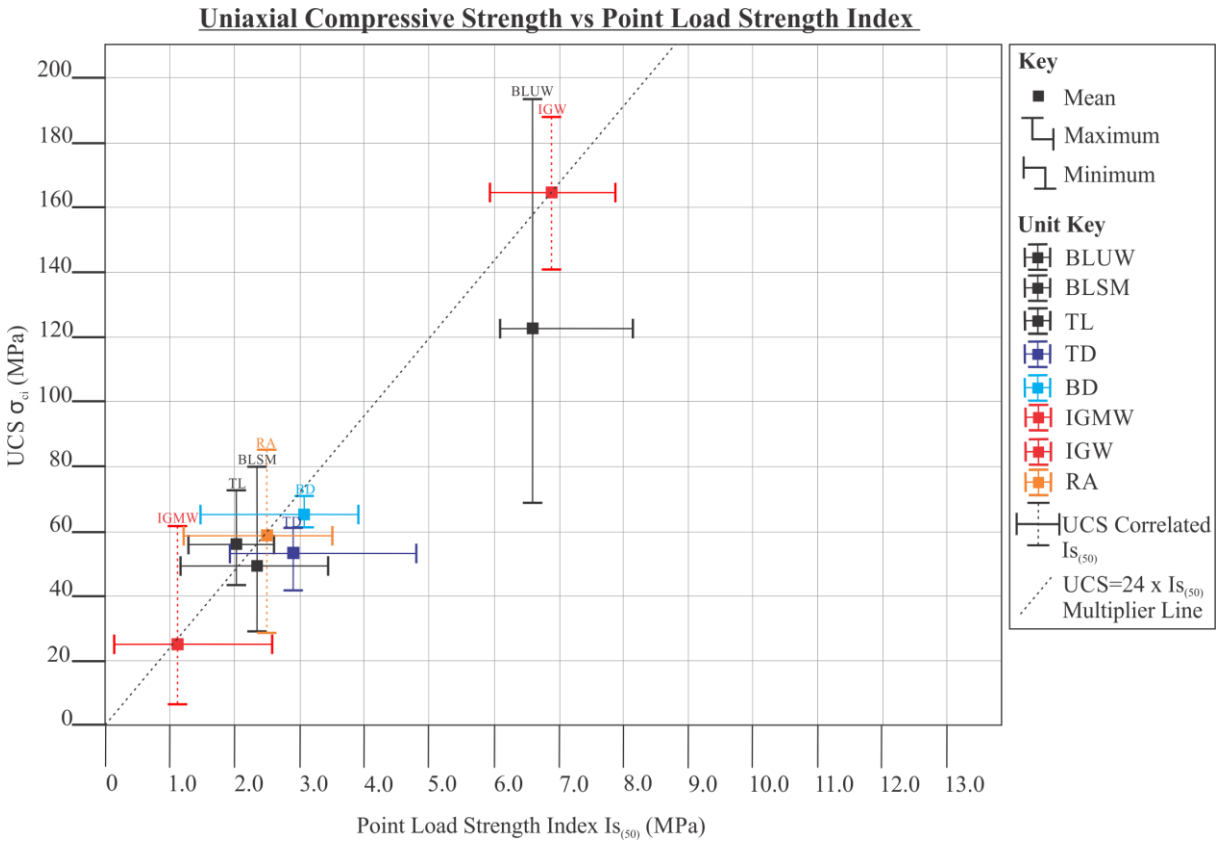

Figure 6.11: Relationship between Uniaxial Compressive Strength (σ_{ci}) and Point Load Strength Index ($Is_{(50)}$) for intact rocks with moderate to high strength. Note: correlated UCS values have been used for lithologies where direct UCS could not be tested.

The relationship between uniaxial compressive strength (UCS) and point load strength index (PLS) is displayed in Figures 6.11 and 6.12. Correlated UCS utilising the $Is_{(50)}$ conversion (Broch and Franklin, 1972) are included for comparative purposes for samples without direct UCS values. Both plots show a positive linear proportional relationship where samples with a high UCS have a high PLS, whereas samples with a low mean UCS are expected to have a low PLS, similar to Zhang (2005), Kilç and Teyman (2008) and Goodman (1989). For example, the relatively unweathered basaltic lava (BLUW) has a much higher mean UCS/PLS than the slightly-moderately weathered basaltic lava (BLSM). The highly-completely weathered basaltic lava (BLHC) has an even lower mean UCS/PLS than the BLSM as expected. These three units illustrate how the degree of weathering and alteration proportionally affect both the uniaxial compressive and point load index strength of the highly porphyritic basaltic lava lithology in this study.

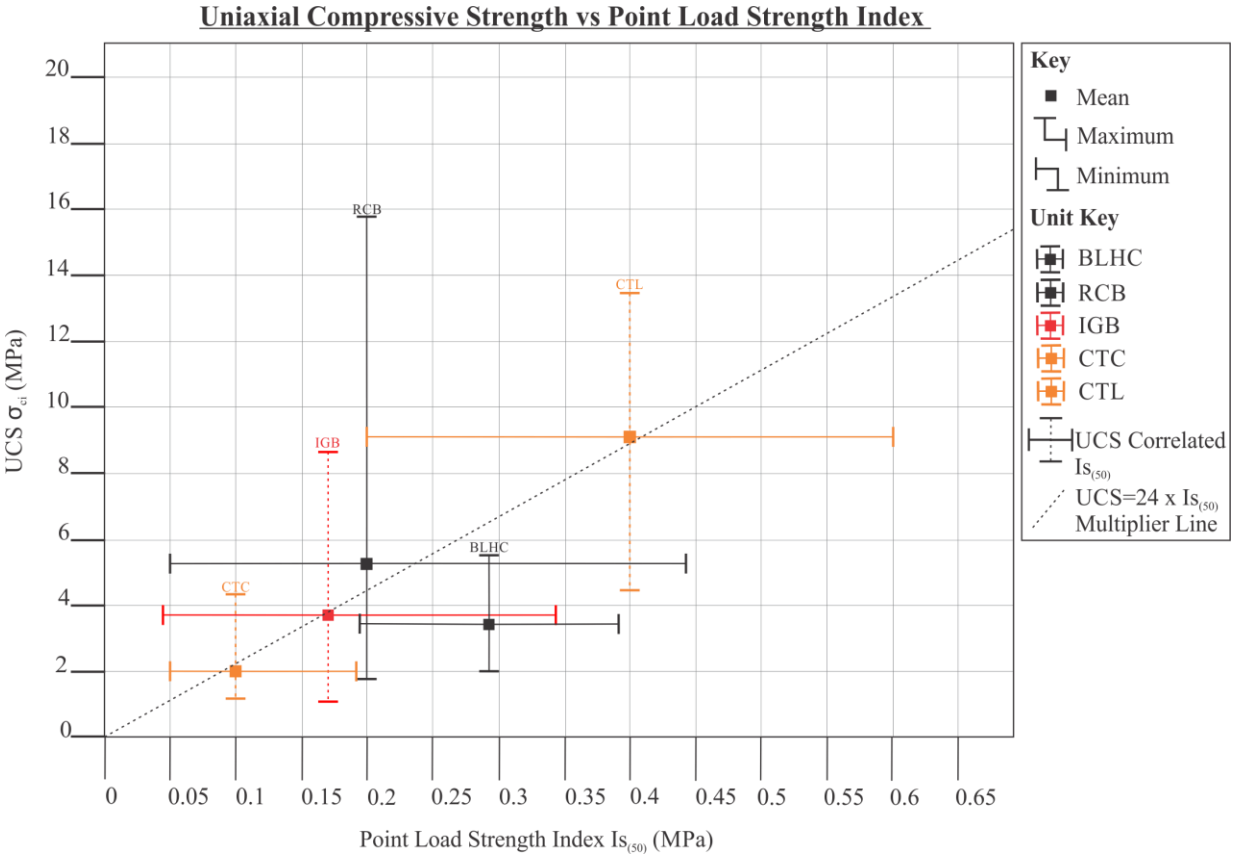

Figure 6.12: Relationship between Uniaxial Compressive Strength (σ_{ci}) and Point Load Strength Index ($Is_{(50)}$) for rocks with low strength (PLS <1 MPa). Note: correlated UCS values have been used for lithologies where direct UCS could not be tested.

Geological characteristics which can influence the UCS/PLS of a unit include, degree of weathering and alteration (post-emplacement mechanism), percentage, orientation and grain size of phenocrysts, flow banding, ratio of groundmass to fragments/clasts and lithics, interconnectivity, aperture and frequency of macro/micro fractures/cracks and vesicles.

Sample geometry combined with geological factors can also influence UCS and PLS testing results, and as such are important to consider.

Figures 6.11 and 6.12 provide a multiplier line (dotted black line). This multiplier line indicates the Broch and Franklin, (1972) $Is_{(50)} \times 24$ to UCS correlation. The $Is_{(50)}$ conversion is significant as its primary use is to provide a correlated UCS values for materials where direct UCS testing is unsuitable (e.g. ashes and tuffs). Units where the mean plots above the 24 multiplier line include TL and RCB. Units which plot on the multiplier line include: IGW, RA, IGMW, CTL, IGB and CTC, whereas, units which below the 24 multiplier include: BLUW, BD, TD, BLSM and BLHC.

Four different examples of the UCS/PLS relationship being affected by geological characteristics and sample geometry are best illustrated by the rubbly basaltic breccia (RCB), slightly weathered trachytic lava (TL), relatively unweathered basaltic lava (BLUW) and basaltic dyke (BD). The RCB has a low PLS and a high maximum UCS for the degree of weathering and clay content observed in the sample tested (Table 4.10). In the case of RCB, a possible interpretation is that at UCS scale (cylindrical geometry, sample length ~120mm) the intact basaltic fragments within the groundmass have contacted (frictional resistance between fragments) and have taken up a greater portion of the compressional strain instead of the clay rich groundmass; resulting in a higher UCS. However, at PLS scale (cylindrical disc geometry, sample thickness ~15-20mm) the strength of the sample is most likely dependent on the clay rich groundmass rather than the basaltic fragments (Figure 4.7a and Figure 4.8b).

The TL has a low-moderate PLS and moderate UCS which was lower than expected given the slightly weathered state of the groundmass (Table 4.14). In the case of the TL a possible interpretation is that at UCS scale (cylindrical geometry, sample length ~100mm) the presence of visible micro-fractures and a series of irregularly orientated flow bands are resulting in the samples failing at a lower than expected UCS. Even though the TL rock mass appears in hand specimen and in thin section to be only slightly weathered, the presence of defects such as flow banding will most likely ultimately control the strength of the sample as flow banding acts as a discontinuity where failure can potentially occur (Figure 4.12d). At PLS scale (cylindrical disc geometry, sample thickness ~15mm) the strength of the sample is most likely controlled by micro-fractures, differential weathering, the orientation of phenocrysts and the strength of the groundmass.

The BLUW has a high PLS and high maximum UCS, but with a significant range of values (Table 4.2). In the case of the BLUW the most likely cause for the range of UCS values (cylindrical geometry, sample length ~100mm) is that the strength of the sample is influenced by the high percentage of altered olivine/iddingsite and feldspar phenocrysts combined with the potential presence of micro-fractures (a greater percentage of phenocrysts and micro-fractures create a greater number of potential locations for defects to propagate). It is worth noting that micro-fractures are not reflected in the P and S wave velocities (Table 4.2), but are visible in thin-section. Whereas, at PLS scale (cylindrical disc geometry, sample thickness ~15-20mm) the strength of the sample may be more likely to reflect the strength of the groundmass as fewer defect pathways will exist in a shorter sample.

The difference between the PLS/UCS values for BD and BLUW highlight the influence that geological characteristics have on geotechnical properties. BD is similar to BLUW in that the mineralogy is similar and the groundmass is generally unweathered, with the only differences being the emplacement mechanism (lava flow vs dyke) and that BD has a much higher percentage of vesicles and coarse grained phenocrysts. Given that the groundmass of both units are relatively unweathered, a similar UCS would have been expected, however, the BD failed at much lower peak load than BLUW (~3.1/65MPa and ~6.6/123 MPa PLS/UCS respectively, based on mean).

6.3.2 Uniaxial Compressive Strength against Dry Mass Density

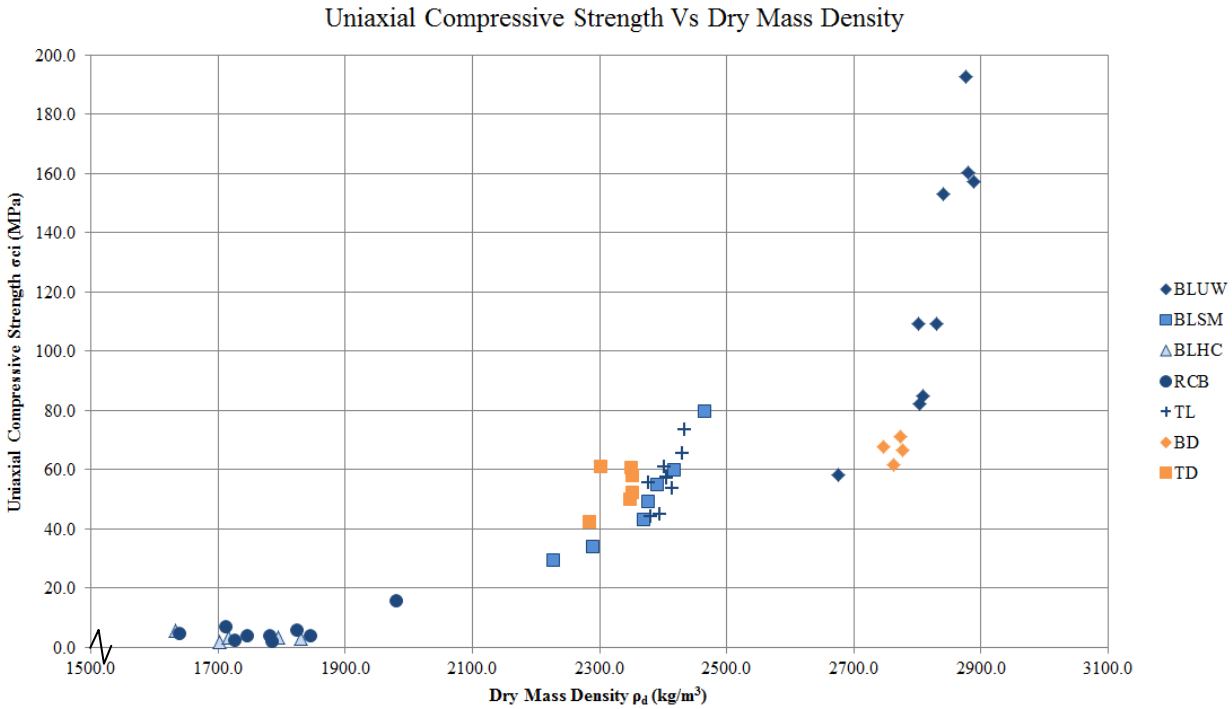

Figure 6.13: Relationship between Uniaxial Compressive Strength (σ_{ci}) and Dry Mass Density (ρ_d).

The relationship between UCS and Dry Mass Density (ρ_d) (Figure 6.13) shows a moderately strong positive exponential relationship with three clusters. Samples with a low UCS will most likely have a low ρ_d and conversely a sample with a high UCS will have a high ρ_d, similar to that found by Wyering *et al.*, (2013).

The cluster on the left hand side of the graph consists of the rubbly basaltic breccia and highly-completely weathered basaltic lava (BLHC). The centre cluster of the graph consists of the slightly-moderately weathered basaltic lava (BLSM), trachytic lava (TL) and trachytic dyke (TD). While, the right hand side of the graph consists of the relatively unweathered basaltic lava (BLUW) and the basaltic dyke (BD). These clusters, illustrate the various weathering states of the samples. The left cluster (BLHC and RCB) represent rock types with the greatest degree of weathering (high clay content, low ρ_d and UCS). The centre cluster (TD, TL and BLSM) characterise units which are slightly-moderately weathered (moderate ρ_d and UCS). Whereas the right cluster (BLUW and BD) consists of relatively unweathered basaltic units (high ρ_d and a moderate-high UCS). Thus it can be state that higher density intact rocks will most likely have higher UCS then weathered/altered clay rich rocks with a low density.

6.3.3 P-Wave Velocity against Uniaxial Compressive Strength

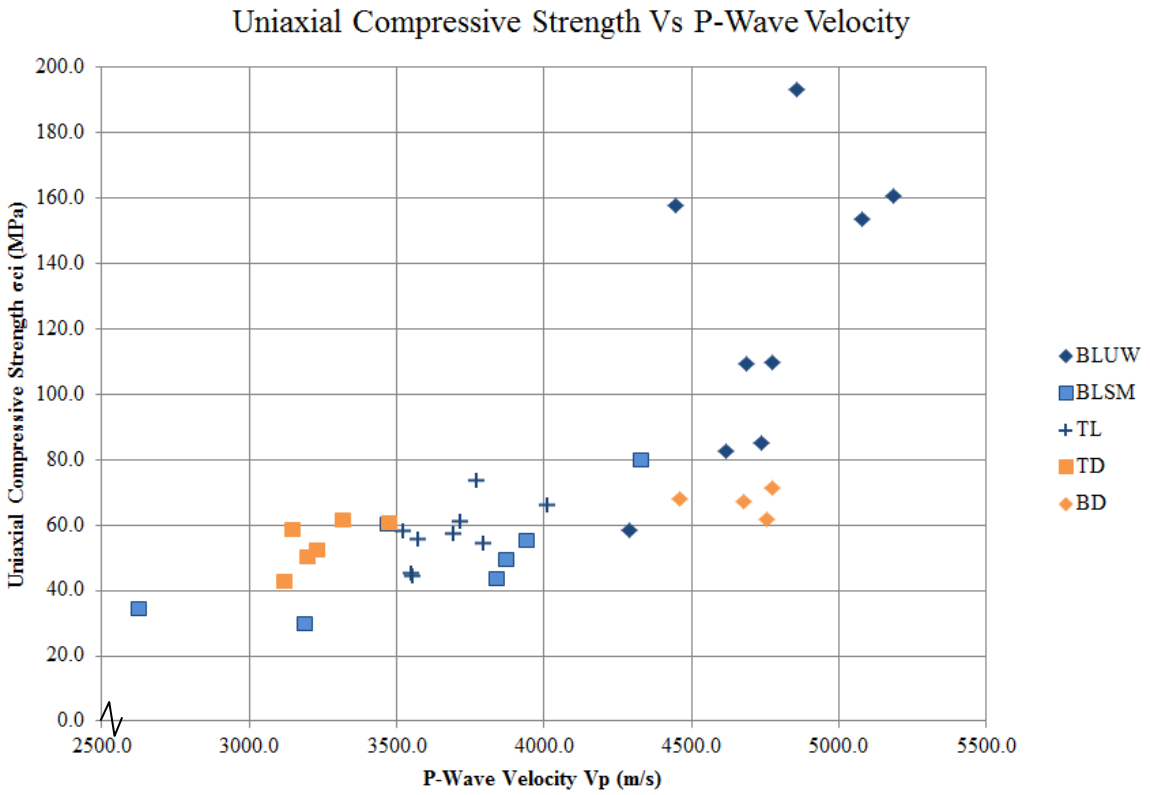

Figure 6.14: Relationship between Uniaxial Compressive Strength (σ_{ci}) and P-Wave Velocity (Vp).

The relationship between UCS and P-Wave Velocity (Vp) (Figure 6.14) show a moderately strong positive exponential relationship. Samples with a low UCS will most likely have a low Vp and conversely a sample with a high UCS with a high Vp (Figure 6.14). The plot also shows a strong cluster of units between 3000-4000m/s and 40-60 MPa. The trachytic dyke (TD) and trachytic lava (TL) plot in a very strong cluster. The variations in Vp for both TD and TL are most likely attributed to irregular flow banding, high percentage of coarse grained phenocrysts, vesicles and macro/micro fractures in the cores.

Of interest as well is the variation in the BLSM and BLUW. The most likely reason for the wide range in values for the BLSM is the range in weathering grades. As the weathering grade increases, the clay content and frequency of defects is also expected to increase. Increased clay content and defects in a sample can result in a slower Vp. This interpretation is supported by the evidence as seen in Figure 6.14 as the Vp and UCS for BLSM varies between ~2600 and 4300m/s and 30-80 MPa, with BLUW having large variation UCS values (~60-190 MPa) but has a tight cluster of Vp values (~4300-5200m/s).

Possible interpretations for these results are that the geological factors such as micro-fracturing and phenocrysts, which affect the strength of the BLUW samples, are not long enough to affect the Vp significantly. Potential characteristics that could affect the strength of the BLUW samples without resulting in a low Vp include weathered/altered phenocrysts and micro-fractures.

6.3.4 Young's Modulus vs Uniaxial Compressive Strength

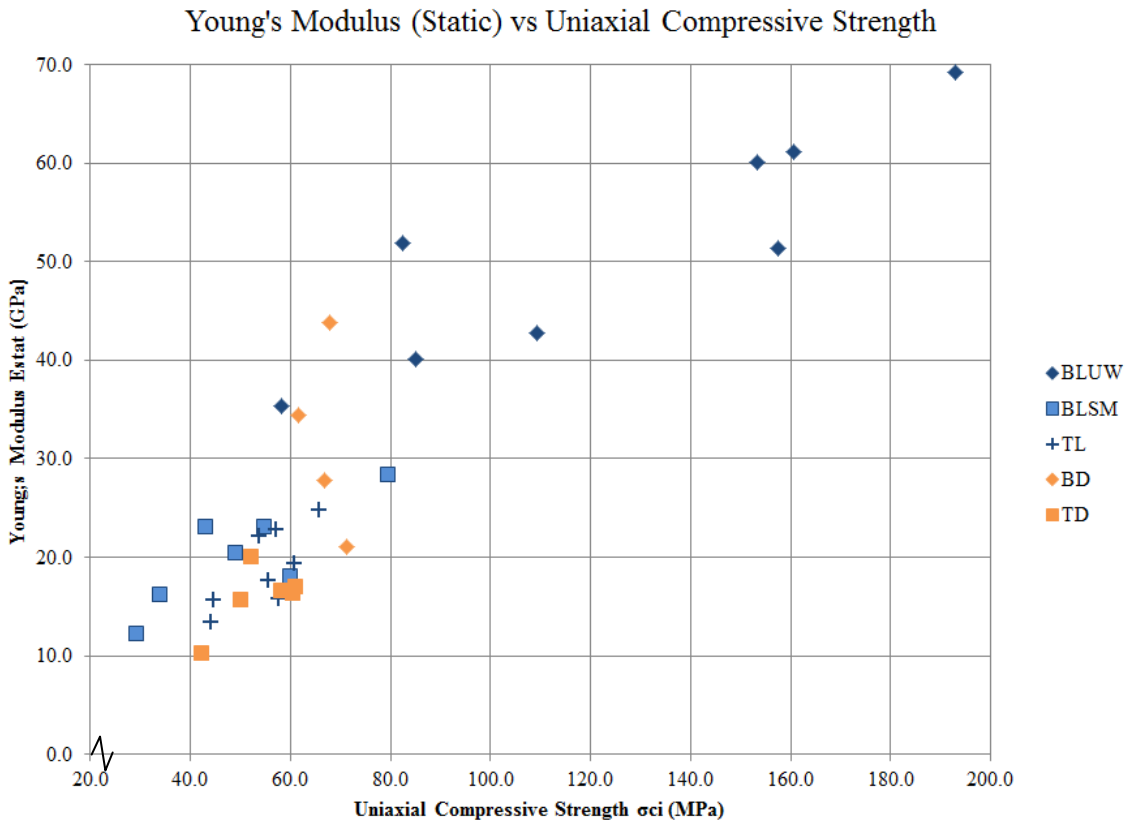

Figure 6.15: Relationship between Uniaxial Compressive Strength (σ_{ci}) and Static Young's Modulus (E_{stat}).

The relationship between UCS and Static (E_{stat}) and Dynamic (E_{dyn}) Young's Modulus is given respectively in Figures 6.15 and 6.16. Both plots display positive linear relationships between UCS and Young's Modulus. It should also be noted that the E_{dyn} values presented in Figure 6.16 plot higher than their E_{stat} equivalent in Figure 6.15. This is most likely attributed to the method of measuring E. Static values are derived using strain gauges and dynamic values are determined using wave velocities. Both methods have their respective inaccuracies; static calculation relies on accurate strain data and the absence of localised strain development and irregular stress strain measurements whereas, wave velocities are interpretive with regards to first wave arrival times.

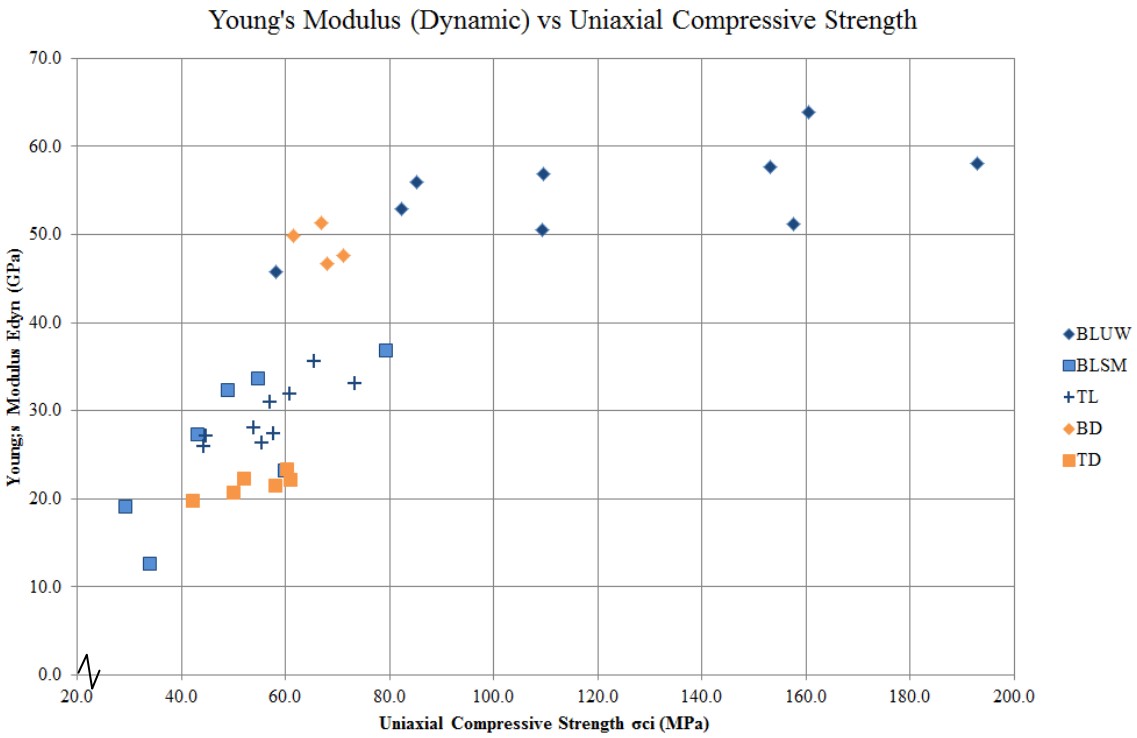

Figure 6.16: Relationship between Uniaxial Compressive Strength (σ_{ci}) and Dynamic Young's Modulus (E_{dyn}).

The BLUW displays a large variance in both E_{stat} and E_{dyn} (~35-70 GPa static, ~45-65 GPa dynamic), unlike the BLSM and TL units.

6.3.5 Poisson's Ratio vs Uniaxial Compressive Strength

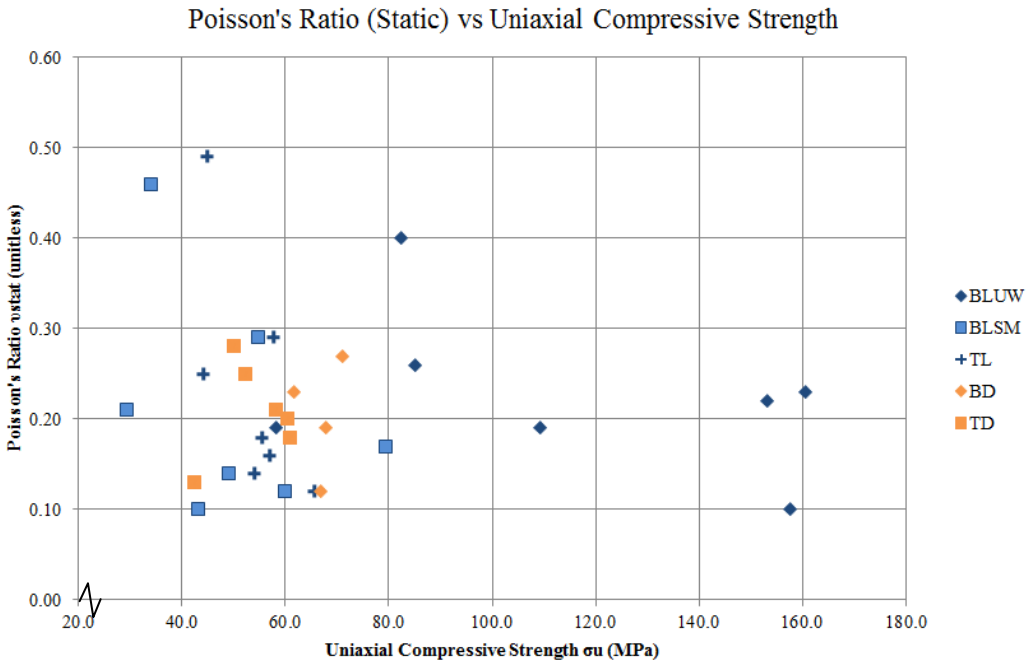

Figure 6.17: Relationship between Uniaxial Compressive Strength (σ_{ci}) and Static Poisson's Ratio (υ_{stat}).

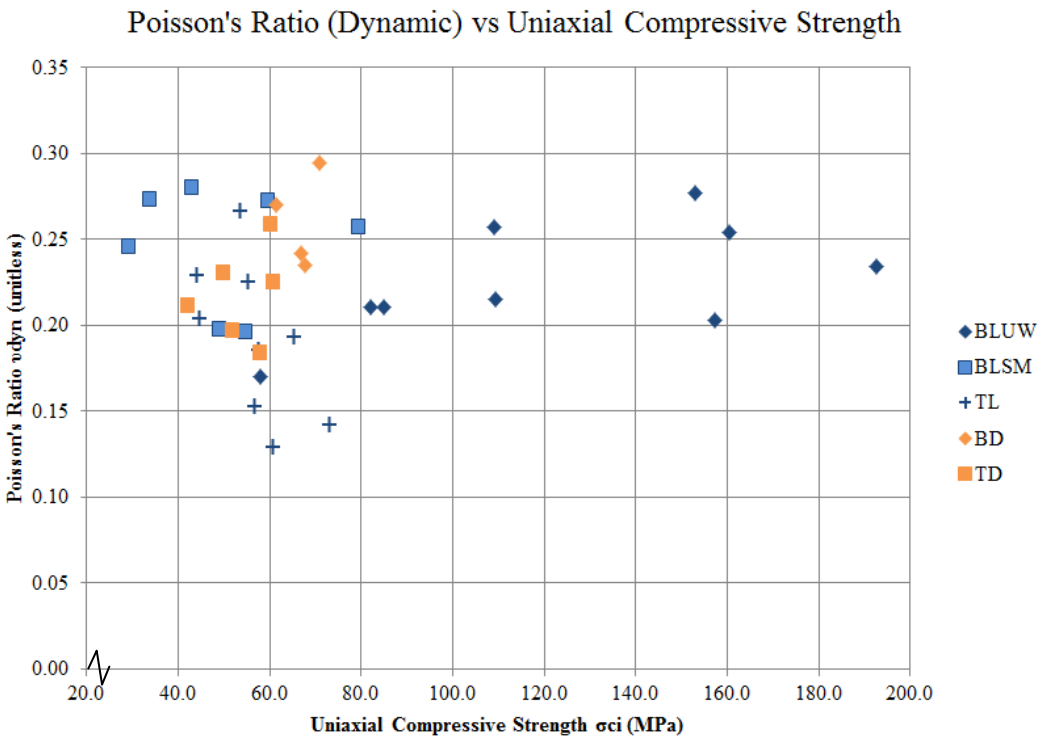

Figure 6.18: Relationship between Uniaxial Compressive Strength (σ_{ci}) and Dynamic Poisson's Ratio (υ_{dyn}).

There is no clear relationship with regards to UCS and Poissons Ratio ($\upsilon_{stat/dyn}$) (Figures 6.17 and 6.18). However, several clusters of data exist. Both plots show a cluster of data points between 0.1-0.3 υ and 40-80 MPa (mean υ of 0.20). As stated by Johnson and De Graff, (1988) the expected range for υ should be between 0.20 and 0.25. Most of the values for materials tested fall close to or within this range. The trachytic dyke (TD), trachytic lava (TL) and basaltic dyke (BD) display the strongest clusters. A group of outliers are also recognised in Figure 6.17 $\upsilon_{stat}/\sigma_{ci}$ respectively at ~0.50 υ_{stat}/45 MPa. These values for υ fall far outside the expected range. The outliers are most likely the result of testing error during UCS testing where υ_{stat} is determined. This is best explained by the presence localised strain (narrow zone of high shear strain) developing in the outlier samples.

6.3.6 Young's Modulus vs Poisson's Ratio (Static and Dynamic)

There is no clear relationship between Young's Modulus ($E_{stat/dyn}$) and Poisson's Ratio ($\upsilon_{stat/dyn}$) (Figures 6.19 and 6.20). As state previously Poisson's Ratio is expect to be between 0.20-0.25 (Johnson and De Graff, 1988). Noticeable clusters and differences between the two plots exist. Figure 6.19 illustrates that υ_{stat} and E_{stat} have a much greater scatter than its dynamic equivalent (Figure 6.20). Static values cluster 0.1-0.3υ_{stat} with a mean of approximately 0.20υ_{stat}. The scatter possibly due to testing error from, the development of

localised strain or are a function of the variability of the samples tested. The heterogeneity of the units tested may reflect the range in static values shown in Figure 6.19. Sample heterogeneity could also account for the three outliers (>0.35 υ_{stat}).

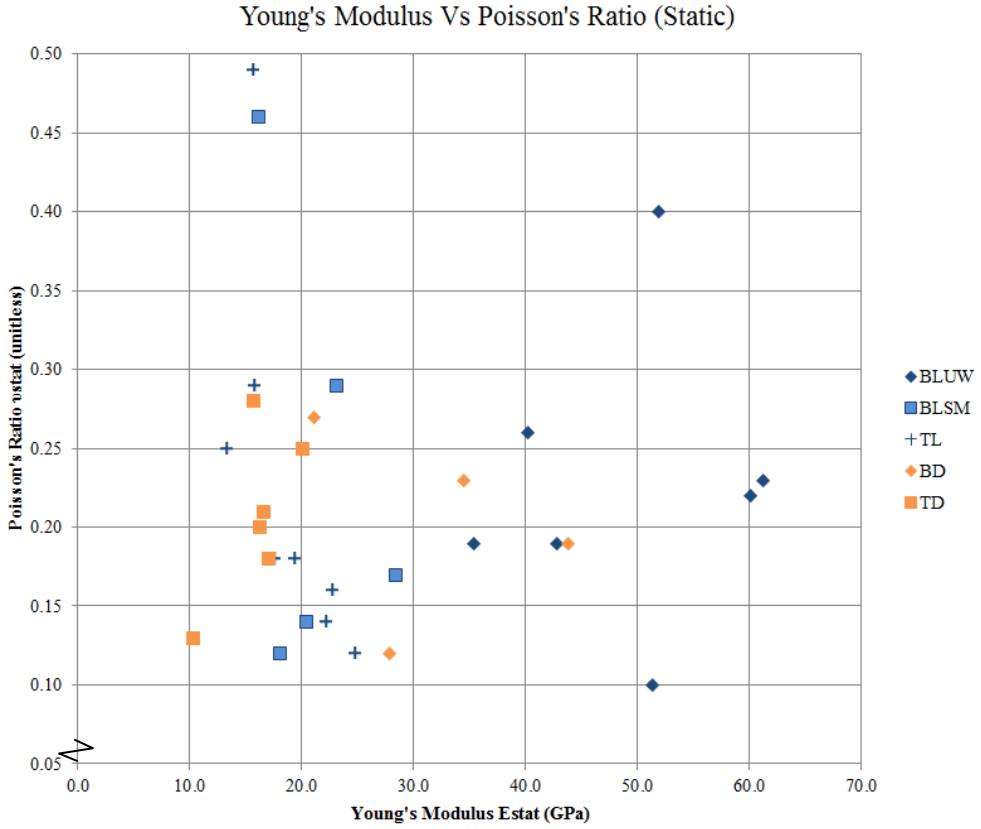

Figure 6.19: Relationship between Static Young's Modulus (E_{stat}) and Static Poisson's Ratio (υ_{stat}).

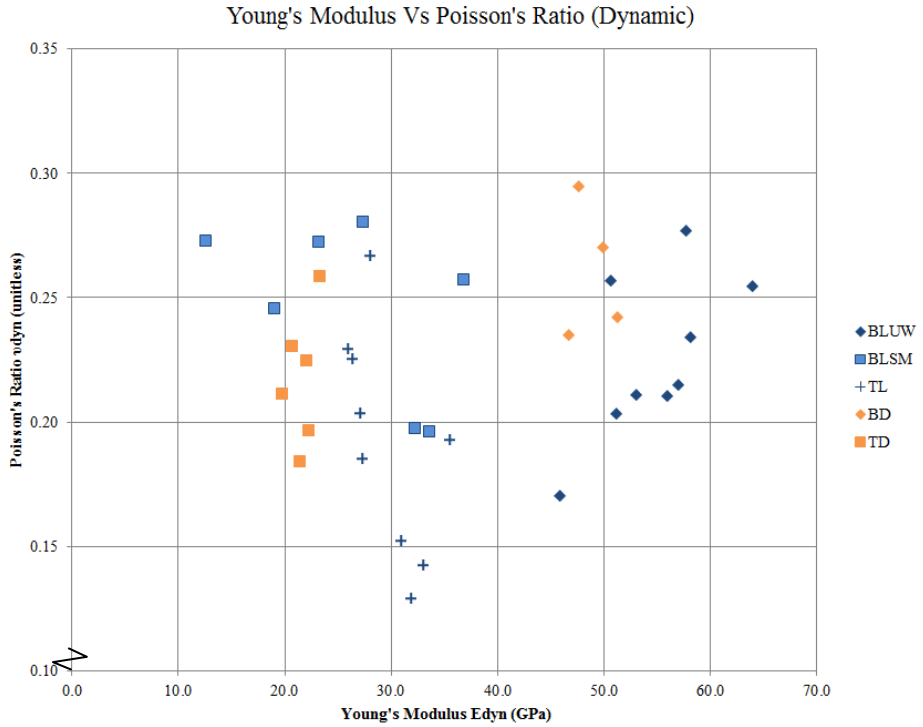

Figure 6.20: Relationship between Dynamic Young's Modulus (E_{dyn}) and Dynamic Poisson's Ratio (υ_{dyn}).

The dynamically derived E_{dyn} and υ_{dyn} displayed in Figure 6.20 display a marginally narrower range of values than the static values in Figure 6.19. The dynamic values range between 0.12 and 0.3 υ_{dyn}, with an approximate mean of 0.22, clustering between E_{dyn} ~20-30 GPa and 50-60 GPa. The most likely reason for the range in values, as well as the two observed data clusters, is due to the influence of geological properties and characteristics on the P and S wave arrival times from which the dynamic values are derived (Table 3.4).

The most likely geological factors which could influence the wave velocities are clay content, macro and micro scale fractures, alteration features (e.g. flow banding) and vesicle and phenocryst clusters. The left cluster consists of TD, TL and BLSM. In the case of the BLSM, weathering and clay alteration combined with macro-scale fractures and phenocryst/vesicle clusters is the most likely cause for the range in values. However, TD and TL are most likely being influenced by macro-scale fractures (observed in thin-section (Figure 4.11h), vesicle and phenocryst clusters as well as by irregular flow banding. The anisotropic flow banding in particular will slow down P/S wave velocities. The right cluster consists of BLUW and BD. Both these units have consistent P/S wave velocities with only a slight variation. The most likely cause for the scatter in v_{dyn} is sample heterogeneity.

6.3.7 Porosity vs Dry Mass Density

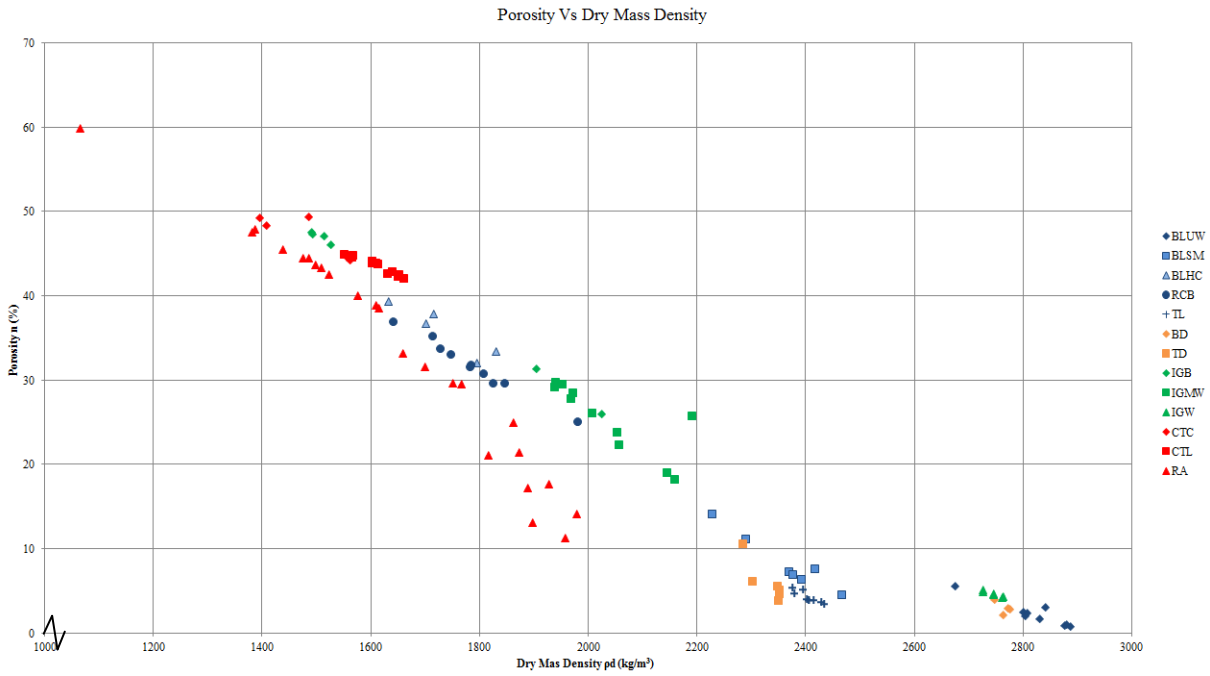

Figure 6.21: Relationship between Porosity (n) and Dry Mass Density (ρ_d).

The relationship between porosity (n) and Dry Mass Density (ρ_d) (Figure 6.21) has a strong negative linear relationship with a mixture of tight and scattered unit distributions. Samples

with a low density will most likely have a high porosity and conversely a sample with a high density will have a low porosity (Figure 6.21). Dry mass density is inversely proportional to porosity. The plot additionally illustrates that there are in several cases a high degree of variance within some of the lithologies. A degree of heterogeneity is expected with any geological material however, some lithologies will display a much a higher heterogeneity than others.

Units such as the red ash (RA), rubbly basaltic breccia (RCB), brecciated basaltic ignimbrite (IGB) and moderately welded basaltic ignimbrite (IGMW) display a higher degree of variation than some of the other units (Figure 6.21). The RA porosity and density variance is a function of the open versus closed porosity (interconnectivity of vesicles) percentage, interconnectivity and size of the highly vesicular scoria clasts which appear irregularly throughout the groundmass. It is very difficult to separate out the welded ash groundmass from the scoriaceous/highly vesiculated clasts. Any RA test sample which appears to consist of solely groundmass may in fact have a hidden scoriaceous clast within it. The presence of a scoriaceous clast within a sample thought to consist only of groundmass would under-represent a sample density.

Hence a greater number of samples were tested for this unit, as reflected in the plot. RA samples with a higher density and a low porosity are more likely to reflect samples with a high percentage of welded ash groundmass. Samples with low density and a high porosity is more likely to consist of a greater percentage of highly vesiculated scoria clasts. The RCB's density and porosity is most likely dependant on the ratio between the percentages of brecciated basaltic fragments to clay content. A greater ratio of clay content in the sample will yield a lower density and a higher porosity. While a greater ratio of basaltic fragments will provide a higher density and lower porosity sample. The IGB's porosity and density is similarly controlled like the RCB. The IGB consists of brecciated ash rich groundmass and intact basaltic fragments at various different grain sizes throughout the mass. IGB samples with a low porosity and higher density most likely have a greater percentage of fragments present in the samples (intact basaltic fragments have a higher density and lower porosity than the pyroclastic ash). A low density high porosity sample will most likely include a lower percentage of fragments. The IGMW is a transitional unit between the two end member units IGB (high n% low ρ_d) and IGW (low n%, high ρ_d), this is shown in Figure 6.21. The variation in IGMW is a function of the degree of welding (emplacement mechanism) the sample has

been subjected to during deposition. IGMW samples which have been subjected to a greater degree of welding have a lower porosity and higher density. An IGMW sample with a lower welding grade will give a lower density higher porosity.

6.3.8 Dry Mass Density vs P-Wave Velocity

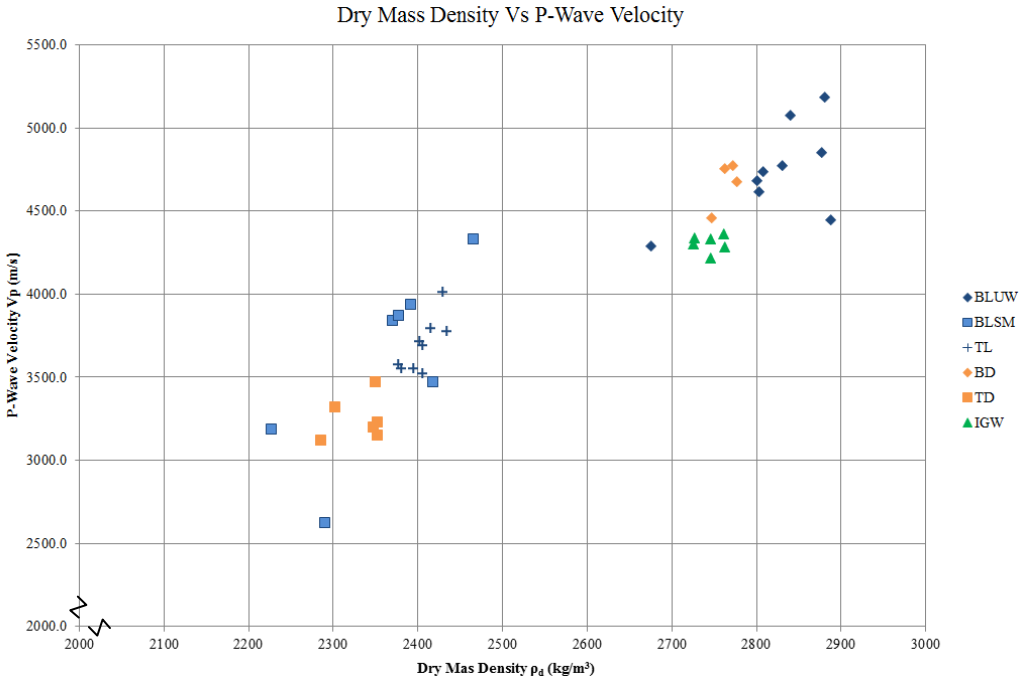

Figure 6.22: Relationship between P-Wave Velocity (Vp) and Dry Mass Density (ρ_d).

The relationship between P-wave velocity (Vp) and Dry Mass Density (ρ_d) is illustrated in Figure 6.22. The plot shows a strong positive linear relationship with two distinct clusters. Samples with a high density will most likely have a high P-Wave velocity and conversely a sample with a lower density will have a lower P-wave velocity. Therefore, dry mass density is proportional to P-wave velocity.

The upper cluster consists of IGW, BD and BLUW. These geological units are composed of relatively unweathered groundmasses and are generally devoid of weathering/alteration features such as macro-fractures and clay. The lower cluster of data consists of TL, TD and BLSM. The P-wave and dry mass density for the trachytic lava (TL) and dyke (TD) plot into two strong clusters within the main lower cluster. The main geological influences affecting these two units will most likely be flow banding and macro-scale fractures (effects P-wave velocity) and differential weathering and porosity (effects dry mass density). BLSM has the greatest variation. The BLSM unit consists of a range of slightly and moderately weathered basaltic lava cores. The range of values is most likely a function of the grade of weathering. The slightly weathered cores will generally have less clay content due to the lower grade of

weathering; hence the sample ought to have a higher density and a higher wave velocity than the moderately weathered cores which should feature a greater proportion of clay content and a higher frequency of defects as the rock mass loses its strength during the weathering process.

6.4 Effect of Emplacement and Post-Emplacement Mechanisms on Geotechnical Parameters

This study has investigated and examined a myriad of different Lyttelton Volcanic Group lithologies from throughout the Port Hills with a variety of different weathering grades, compositions and mineralogies, textures and emplacement and post-emplacement mechanisms. This discussion utilises quantitative and qualitative information from field observations, geological properties (descriptions and thin section analysis) and rock mechanics data presented within this thesis to illustrate the effect that emplacement and post-emplacement mechanisms have on geotechnical parameters and characteristics.

As shown and discussed throughout Sections 6.2 and 6.3 there are in many cases an extensive degree of variability in the rock mechanical properties (geotechnical parameters) which are fundamentally being influenced by geological factors and characteristics of the rock types tested. However, the variability is not only a function of rock type (e.g. basalt, trachyte) but also a function of the type of emplacement mechanisms and post-emplacement processes present. The geological factors are controlled by each unit's respective emplacement mechanism and further controlled by post-emplacement mechanisms and processes.

6.4.1 Emplacement Mechanisms

Emplacement mechanisms refer to the method/process of which a unit has been deposited. The four types of emplacement mechanisms within this study are:

1. Flows
    a. Lava Flows (BLUW, BLSM, BLHC, RCB and TL)
    b. Pyroclastic Density Currents (IGB, IGMW, IGW)
2. Intrusions (Dykes) (BD, TD)
3. Airfall (CTC, CTL, RA)

The following are a series of geological characteristics and components which are variably dependant on which type of emplacement mechanism is present. Furthermore, specific examples are cited to illustrate the effect of geological properties on geotechnical characteristics by means of method of emplacement.

Mineralogy

Most minerals chemically weather or alter to different minerals which may be detrimental to the geotechnical performance of a rock mass as whole. One of the most dominant minerals in this study is feldspar. In the basaltic units plagioclase feldspar is dominant, while, in the trachytic units alkali feldspar is prevalent. Through chemical weathering feldspars break down to clay rich minerals due to their silicate structure. Clay content within a sample negatively impacts strength, P and S wave arrival times and decreases sample density. This is very well illustrated when comparing the BLUW and BLSM units. The BLSM unit has been subjected to variable levels of weathering and such has a much greater percentage of clay within the sample, indicated both in hand specimen and in rock mechanical results. Mineralogical properties are mainly determined by method of emplacement and by lithological chemistry, which in turn has the potential to influence geotechnical parameters. In addition to the type of minerals present, the orientation, frequency and grain size of the minerals/phenocrysts are also very important as all of these factors are interrelated.

Grain Size

The grain size of the groundmass and phenocrysts is dependent on how fast or how slow the lava has cooled. The lavas generally have a fine grained groundmass with fine to medium grained phenocrysts, whereas the dykes have a slightly coarser groundmass and a much higher percentage of coarse grained phenocrysts. This difference in grain size is a function of time taken for the lava to cool. The lava flows display a fine grained groundmass and a mixture of fine to medium grained phenocrysts indicating the flow cooled fast. Whereas, the dykes cool slowly against the country rock and produce a fine to medium grained groundmass with fine to coarse phenocrysts. Both the TD and BD have a much higher percentage of coarse grained phenocrysts a slightly coarser groundmass than their lava equivalents (BLUW, BLSM, BLHC and TL) (Figure 6.23). Therefore, it can be stated that grain size of both the groundmass and phenocrysts are controlled by the method of emplacement.

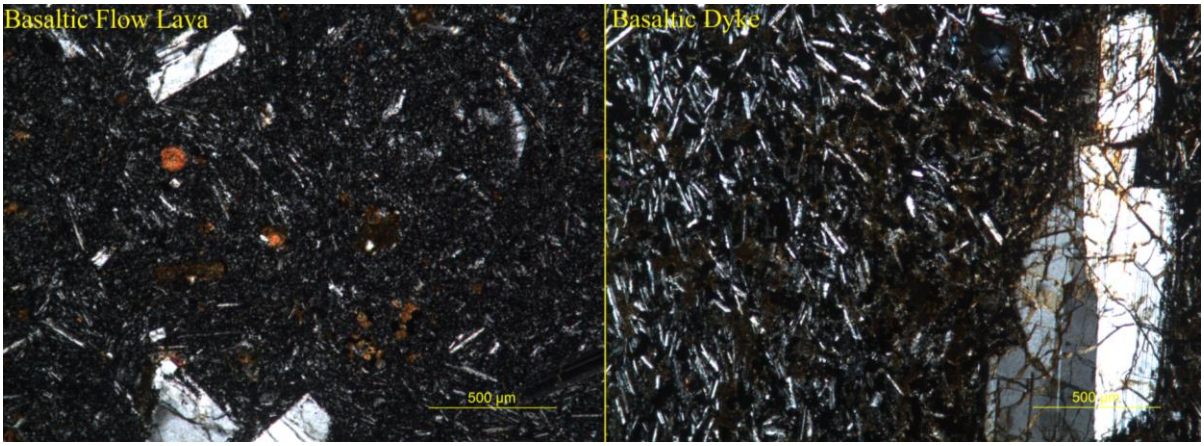

Figure 6.23: Micrographs images of 'relatively' unweathered basaltic lava (left) and basaltic dyke (right). Note: basaltic lava has a fine grained groundmass (composed from microlathes) and fine-medium grained phenocrysts, whereas, the basaltic dyke has a coarser groundmass with coarser phenocrysts than the lava equivalent.

The effect of grain size on geotechnical parameters is well illustrated by the relationship between the 'relatively' unweathered basaltic lava and basaltic dyke. The BLUW has a much higher mean UCS and $Is_{(50)}$ (respectively, 123.1 and 6.65 MPa), while the BD has a lower mean UCS and Is(50) (respectively 66.8 and 3.07 MPa). The TL and TD share a narrower but similar trend with mean UCS (respectively 56.9 and 54.0 MPa). The trachytic trend is narrower most likely to due to differential weathering and other geological factors e.g. flow banding. Hence it can be stated that grain size which is determined by method of emplacement can affect the geotechnical characteristics of the sample; increased grain size can negatively impact sample strength. Phenocryst boundaries provide potential conduits for defects to propagate along during laboratory compression testing and also potential during seismic episodes (i.e. earthquakes).

Texture

Textural properties have the capacity to affect geotechnical characteristics. Four main textures discussed are flow banding, porphyritic, microlathe and trachytic (Figure 6.24). Flow banding occurs as a result of shearing/friction of the lava during emplacement. Flow bands occur parallel to cooling margins/flow orientation, units in this study which include this feature are the TD, TL and BD. The TL displayed the most well defined flow bands out of the other tested units. UCS testing of the TL showed that the flow bands acted as a failure conduit, thus most likely decreasing the sample strength (σ_{ci} mean 57 MPa). TL-1-5 and TL-1-8 (σ_{ci} respectively, 44.2 MPa and 44.7 MPa) displayed near vertical flow banding which acted a plane of weakness where sample failure occurred on. Porphyritic texture is displayed by all of the units in this study. The degree to which a sample is porphyritic is a function of

time taken for the lava to cool. Lavas which cool slower have coarser phenocrysts than lavas which have cooled slower. Thus lava with a more porphyritic composition and subsequently coarser phenocrysts can have a lower strength. The BD has a lower UCS than BLUW, most likely due to a higher phenocryst percentage; which provides a greater number of potential failure conduits (groundmass phenocryst boundaries).

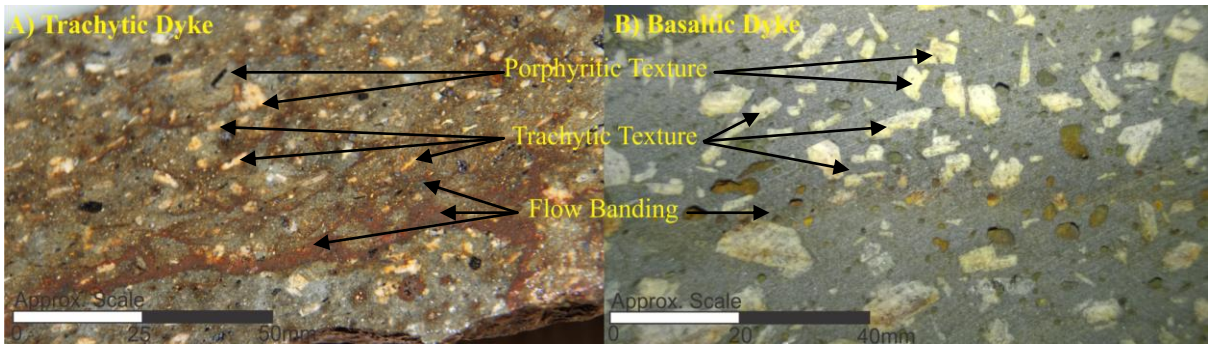

Figure 6.24: Hand specimen images displaying various igneous textures. Sample A, the trachytic dyke displays all three textures, while Sample B, the basaltic dyke has a strong porphyritic texture but only displays flow banding and trachytic texture close the cooling margin.

Trachytic texture is the preferred orientation of grains in the direction of flow. The direction of flow is mainly dependant on method of emplacement. Dykes will have a near vertical aligned trachytic texture, where the lavas which display the texture will display near horizontal trachytic texture (topography will also influence this characteristic). As trachytic texture aligns the groundmass and phenocrysts in the groundmass, it has the potential to provide more potential failure conduits for fractures to propagate along. If compressional testing is parallel to this texture (e.g. TD and BD as in-situ verticality of samples was preserved) the aligned phenocrysts may also act as potential shear planes, especially if the feldspars have been subjected to chemical weathering. The TD displayed a considerably stronger trachytic texture than the BD; this is most likely one of the contributing factors to the BD having a higher strength that the TD (respectively means of 67 MPa, 54 MPa). The TL and TD will have most likely to some degree have been affected by trachytic texture.

Welding

Welding in the context of basaltic ignimbrites, occurs under intense heat where in a fresh pyroclastic density deposit the ash and basaltic rock fragments are transitionally welded together from a loose poorly indurated ash groundmass to a coherent lithified groundmass. As observed from the variably welded ignimbrites in Redcliffs welding is transitional with the most welded material at the base of the flow with decreasing welding grade in the vertical

direction. The characteristics of the pyroclastic density current as a method of emplacement will dictate the type of ignimbritic rocks produced. The three ignimbrite units IGB, IGMW and IGW reflect the increasing welding grade. An increase in welding from IGB to IGW (as end members) is seen to increase density, UCS and $Is_{(50)}$ and decrease porosity.

Jointing Pattern

Jointing patterns in a rock mass are created by cooling (contraction) of the lava during emplacement. Figure 6.25 illustrates various jointing patterns observed in field area units. Jointing patterns in a rock mass are one of the largest determinants in potential failure mechanisms.

Figure 6.25: Jointing patterns variations in various field area emplacement mechanisms. Dykes (intrusions) display approximately cubic jointing while, lava flows exhibit columnar to tabular joints.

Closely spaced joints will result in the release of smaller blocks (toppling and wedge failure mechanisms) in a failure event, but additionally allow for a greater permeability which in consequently allows for a greater degree of alteration in weathering as fluids interact with the rock mass. Both the basaltic dyke and trachytic dyke display this closely spaced jointing patterns resulting in the small cubic blocks illustrated in Figure 6.25. Whereas, the basaltic

and trachytic lava flows display wider spaced tabular to columnar joints which will result in larger blocks being released in a failure (toppling failure mechanism) (Figure 6.25). The wider spaced joints should additionally limit the permeability of the lava flow resulting in a slower rate of chemical weathering and alteration than the dyke equivalents. A slower rate of weathering should result in a more resistant and stronger rock mass.

Lithification

Lithification involves turning loose sediments into a coherent rock mass. In many cases lithification is a function of pressure, compaction and in some cases heat. Figure 6.26 illustrates increasing lithification grade using airfall units of this study. Airfall deposits are generally thickest closest to the eruptive centre. Hence a thicker deposit will have a greater amount of overburden pressure and thus increase the degree of lithification.

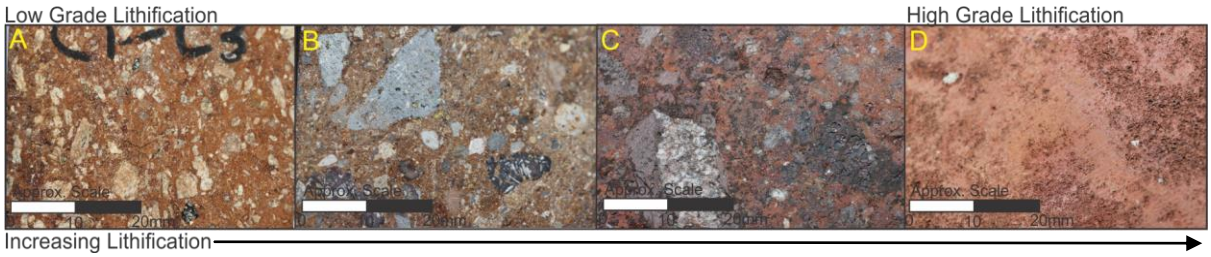

Figure 6.26: Macro-Scale photographs of various airfall units displaying increasing lithification. Sample A) crystal dominated tuff, B) crystal lithic tuff, C) lithic dominated tuff and D) red ash.

Lithification increases sample strength and density, whilst generally decreasing porosity of the groundmass. Furthermore, the grain size of groundmass decreases gradually with increasing lithification (Figure 6.26). Lithification affects geotechnical characteristics of a material. The crystal dominated tuff is less lithified than its lithic dominated tuff equivalent (Figure 6.26). This is shown clearly by the strength (PLS) and density data (respectively CTC: 0.1 MPa/1480 kg/m^3 and CTL: 0.4 MPa/1610 kg/m^3). Emplacement by airfall can affect the lithification of the tuffs viewed in this study. Geotechnical parameters are therefore affected by lithification which is controlled by emplacement mechanisms, in this case, by airfall.

Emplacement Mechanism Analysis

Geotechnical parameters are influenced by geological characteristics/factors which are in many ways determined by method of emplacement. The emplacement mechanism analysis in Figure 6.27 uses the UCS versus $Is_{(50)}$ relationship to illustrate a fundamental observation that even within the same emplacement mechanisms there is a large variability in strength values.

The variation within emplacement mechanisms is most likely a function of post-emplacement mechanisms and processes.

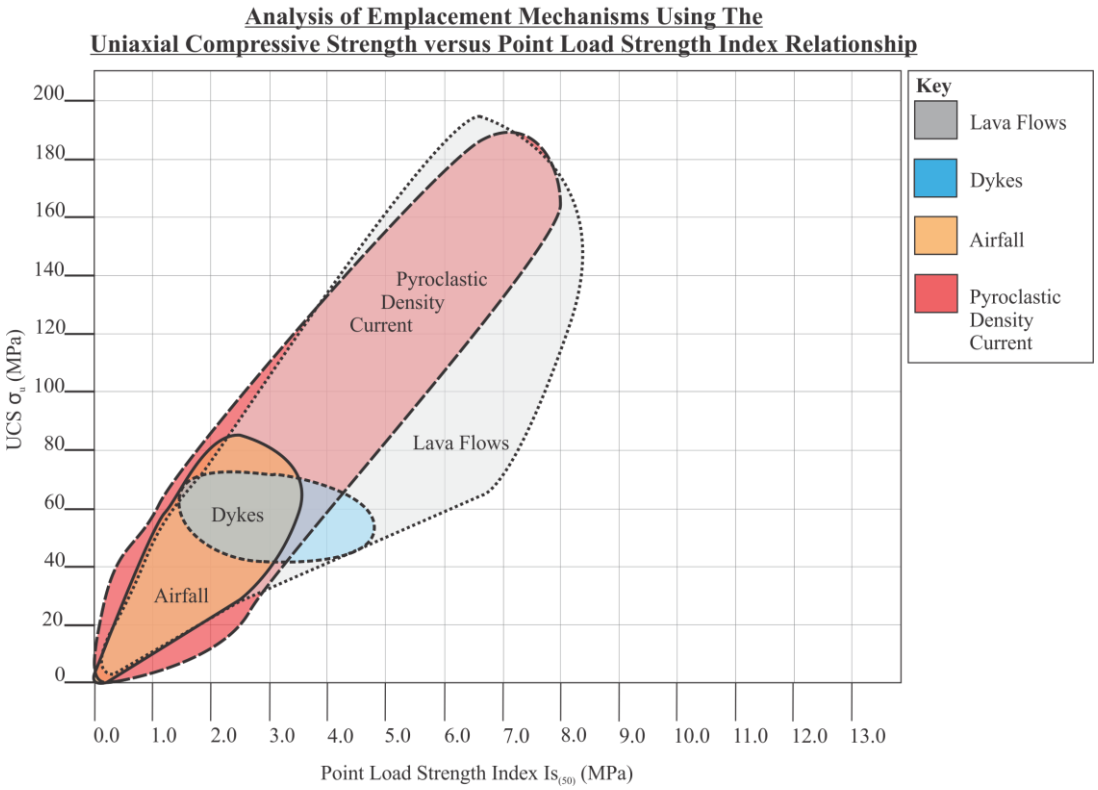

Figure 6.27: Emplacement Mechanism Analysis Plot utilising uniaxial compressive strength (σ_{ci}) versus point load strength index ($Is_{(50)}$) relationship.

6.4.2 Post-Emplacement Mechanisms

The two most prevalent post-emplacement/secondary mechanisms/processes observed in this study are weather and alteration and micro/macro scale fracturing.

Weathering and Alteration

Weathering and alteration are a set of mechanisms and processes which occurs post-emplacement. Weathering and alteration have a negative effect on the strength and stability of a geological material. Physical and chemical weathering weaken a rock mass through processes such as abrasion, frost heave, water infiltration and primary mineral alteration to secondary minerals (e.g. feldspar to clay) etc. The effect of weathering is illustrated well by the three tested basaltic lava units (BLUW, BLSM and BLHC). These three units illustrate soundly the effect that weathering and alteration has on geotechnical parameters and properties. From rock mechanical testing it can be stated with increasing weathering UCS, $Is_{(50)}$, density, wave velocities and deformation moduli (Young's Modulus and Poisson's

Ratio) decrease and porosity increases. Much of the weakening of the rock can be attributed to the alteration/chemical weathering of groundmass and feldspar to clay.

Micro/Macro Fracturing

Micro-fractures are very small flaws in the rock mass which can range in size from a few grains to a few millimetres long (Figure 6.28). Micro-fractures can be caused by natural concentrated stresses within the rock, by contraction during cooling and can potentially be induced by seismic influences.

Micro-fractures are sometimes too small be detected by P and S wave velocities but can be significant enough to decrease the strength (both UCS and $Is_{(50)}$) and deformation moduli (measured under static conditions only) of the rock mass. During strength testing micro-fractures begin to propagate throughout the sample as the sample is loaded, these fractures can combine together with other defects and features such as flow bands, macro-fractures and phenocryst/clast/fragment boundaries (Figure 6.28) to form a failure surface.

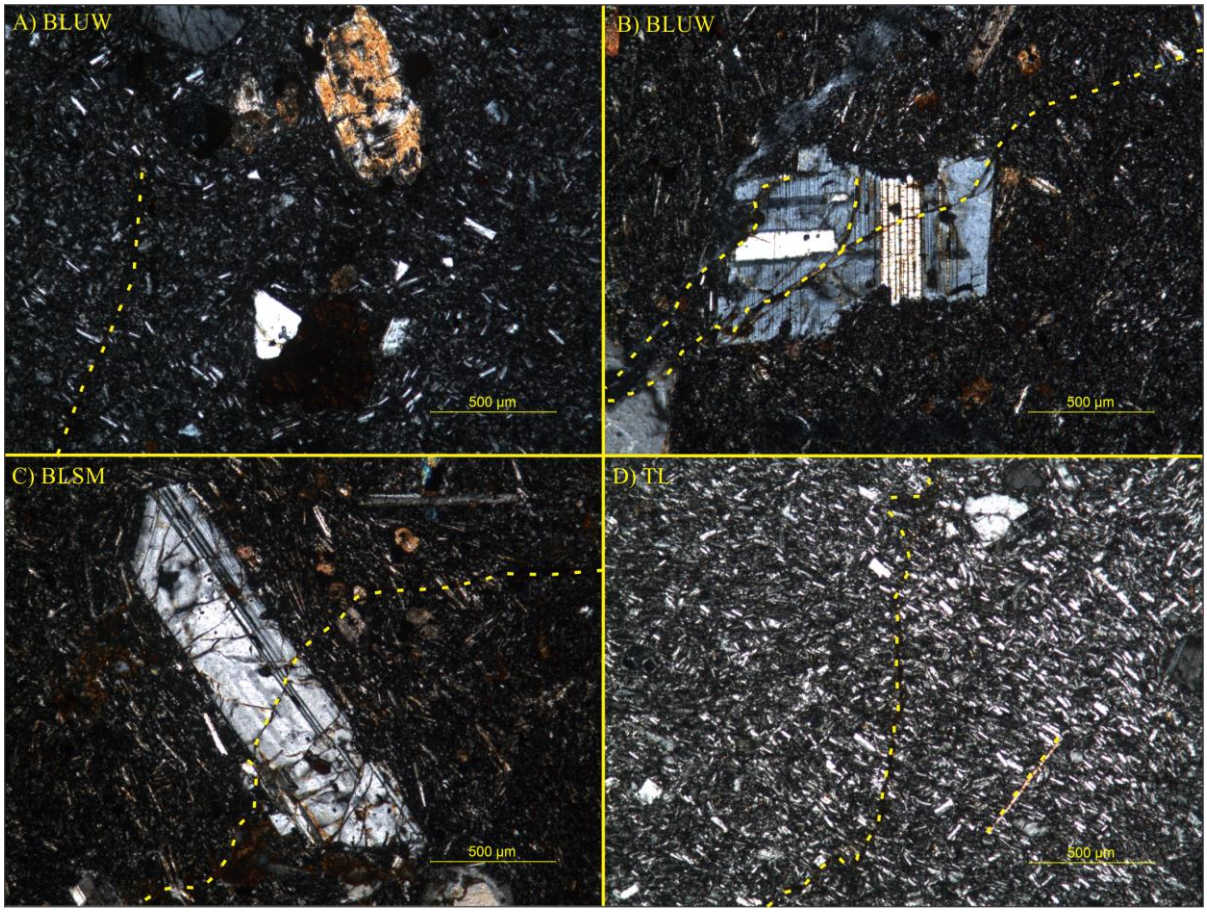

Figure 6.28: Micrograph images of micro-fractures (yellow dashed lines) in basaltic and trachytic lava. Note images B and C where micro-fractures propagate through feldspar phenocrysts.

6.5 Applications

This section briefly lists out prospective applications of the rock mechanical and geological data presented within this thesis.

6.5.1 Point Load Strength Index to Uniaxial Compressive Strength (Correlation Multipliers)

The Broch and Franklin (1972) point load strength index correlation is used to provide uniaxial compressive strength values for materials where it cannot be directly tested. The $Is_{(50)}$ 24 multiplier is based off an average of hundreds of samples, however the multiplier can range from ~15-50 (Wyllie and Marr, 2004). With this range in mind, the 24 multiplier may provide an over estimation of correlated uniaxial compressive strength of a sample. Most if not all modern day rock engineering design models (e.g. RocScience) use uniaxial compressive strength and not $Is_{(50)}$. Therefore, as engineering design is geared towards using conservative values the $Is_{(50)}$ multiplier has been reviewed for the units in this study without direct UCS testing. Table 6.2 presents suggested conservative multipliers based on geological observations during PLS testing, factors considered include: failure patterns, components, grain size, degree of lithification, weathering and phenocryst/lithic/clast boundaries.

Table 6.1: Conservative Design Multipliers for $Is_{(50)}$ to Correlated Uniaxial Compressive Strength. Conservative multipliers are informed by PLS testing observations.

Conservative Design Multipliers for Point Load Strength Index to Uniaxial Compressive Strength			
Unit	**Previous Multiplier**	**Conservative Design Multiplier**	**Comments**
Brecciated Basaltic Ignimbrite **(IGB)**	24	13	Basaltic Clasts act as weakness features during PLS testing regardless of mostly well lithified groundmass.
Moderately Welded Basaltic Ignimbrite **(IGMW)**	24	20	Basaltic Clasts act as weakness features during PLS testing regardless of mostly well lithified groundmass.
Highly Welded Basaltic Ignimbrite **(IGW)**	24	20	Highly welded, coherent material, mainly devoid of any clasts.
Crystal Dominated Tuff **(CTC)**	24	13	Coarse grain size, low grade lithification and large phenocrysts reduce strength and coherence.
Lithic Dominated Tuff **(CTL)**	24	15	Lithics and large phenocrysts acted as conduits during PLS testing regardless of mostly well lithified groundmass.
Red Ash **(RA)**	24	18	Scoriaceous/highly vesiculated clasts do not act as either a weak feature or inhibitor to failure.

6.5.2 Other Applications

Engineering Geological/Geotechnical Applications

- Rock fall modelling (σ_{ci}, $Is_{(50)}$, ρ_d)
- Slope stability modelling and assessment (σ_{ci}, ρ_d)
- Rock bolts and anchors (σ_{ci})
- Foundations in rock (pile end bearing) (σ_{ci}, E, υ, G, K)
- Permeability analysis (n%, ρ_d)

Geological Applications

- Platform for further characterisations of Lyttelton Volcanic Group lithologies
- Petrographic data for igneous and volcanogenic geological materials
- Geological mapping of various units (e.g. Ignimbrite deposits)

CHAPTER 7 - Summary Conclusions and Recommendations

7.1 Project Background and Scope

This study has investigated the Lyttelton Volcanic Group from an engineering geological and geotechnical perspective, with the aim of creating a robust rock mechanics database of the Port Hills lithologies whilst incorporating important aspects of physical volcanology. Literature review of the Lyttelton Volcanic Complex in conjunction with field reconnaissance identified a wide range of igneous and volcanogenic units: notably basaltic and trachytic lava flows, basaltic and trachytic intrusions (dykes), tuffaceous airfall units and basaltic ignimbrites. The most striking observation was the degree of geological variability within similar units, as a function of weathering grade and original composition. An extensive database search into rock mechanics datasets, revealed a clear shortfall in available data and the necessary context to be able to apply the existing data to igneous lithologies with such high compositional variability.

The specific objectives of this thesis were to:

1. Assess lithologies by petrography, rock core logging, hand specimen and outcrop analysis (Section 7.2).
2. Develop an engineering geological model of the Lyttelton Volcanic Complex (Section 7.2).
3. Evaluate rock mechanics characteristics of rock materials through testing and deriving the following: porosity, density, slake-durability, ultrasonic velocities, unconfined compressive strength, point load strength index, Poisson's Ratio and Young's Modulus (Section 7.3).
4. Create a robust geotechnical data set that can be utilised for engineering purposes both locally and internationally (Section 7.3).
5. Establish a correlation between the geological and geotechnical characteristics (Section 7.4).

7.2 Engineering Geological Model and Lithological Characterisation

The objectives one and two of this thesis involved the investigation and assessment of the Lyttelton Volcanic Group lithologies and the development of a representative engineering geological model of the volcanic complex. In conjunction with observations from field reconnaissance (Figures 2.1-2.11) and information available from literature a ground truthed 'Engineering Geological Block Model of the Lyttelton Volcanic Complex' was developed (Figure 2.12). The purpose of the model was to aid in characterising and categorising the nature and properties of the various volcanic units which make up the field area. Five major units were identified: 1) trachytes, 2) basaltic ignimbrites, 3) air fall units, 4) basaltic lavas and 5) volcanogenic laharic deposits. As observed in the field at both outcrop and hand specimen scale, the volcanic units were highly variable both in terms of composition and weathering grade. As such, further refinement to the classification of volcanic units was required.

The five primary units were subdivided into geotechnical sub-units, with the aim of providing an accurate characterisation by accounting for material variability as well as possible. The geotechnical units were selected based on geological factors, such as weathering grade, composition, lithification, welding grade and mechanism of emplacement. The 'Lyttelton Volcanic Group Geotechnical Unit Classification' (Table 2.1) identified 18 geotechnical sub-units: [1]trachytic dykes, [2]trachytic domes, [3]trachytic lava, [4]brecciated basaltic ignimbrite, [5]moderately welded basaltic ignimbrite, [6]highly welded basaltic ignimbrite, [7]red ash, [8]crystal dominated tuff, [9]lithic dominated tuff, [10]rubbly basaltic breccia, [11]unweathered basaltic lava, [12]slightly to moderately weathered basaltic lava, [13]highly to completely weathered basaltic lava, [14]highly vesicular basaltic lava bomb, [15]basaltic dyke, [16]blocky basaltic lava, [17]volcanogenic conglomerate and [18]volcanogenic tuffaceous sandstone. The trachytic dome (Castle Rock) could not be sampled due to safety imposed restrictions. Of the 18 identified materials, 13 units were geotechnical tested.

Engineering geologically and geotechnical characterising the volcanic units in this study involved a two-phased approach. The first was to provide engineering geological descriptions of the units. The NZGS, (2005) descriptive method used in in New Zealand is not framed to accurately describe volcanic rocks. In light of the limitations of the NZGS, (2005) descriptive method for describing igneous rocks a revised scheme was developed. A list of key volcanic characteristics was compiled (Table 3.2) and was utilised to form the 'Detailed Engineering

Geological Igneous Descriptive Scheme' (Table 3.3). This scheme includes all the engineering geological aspects of the NZGS, (2005) guideline but has been expanded and restructured to allow for accurate descriptions of igneous lithologies. The aspects which are included in the detailed engineering geological igneous descriptive scheme which were not present in the NZGS guideline are: full geological context, method of emplacement (feature type), component analysis (includes grain sizes and percentages), mineralogical descriptions and relevant textures. Until the effects of geological characteristics on geotechnical properties are fully understood they should not be left out of any stage of analysis; this is what has driven the need for this level of detail of characterisation.

7.3 Geotechnical Testing Summary

Objectives three and four involved a range geotechnical (rock mechanics) testing and the creation of a robust data set which can be applied both locally and internationally given the correct geological context. Of the 17 materials sampled, 13 were geotechnically tested (Table 3.5). Four materials could not be tested due extensive heterogeneity and limited intact material: volcanogenic conglomerate, tuffaceous sandstone, highly vesicular lava bomb and the blocky basaltic lava. This study has followed the ASTM Standard D4543, (ASTM, 2004) guideline for preparation of samples and the ISRM suggested methods for rock characterisation (Ulusay and Hudson, 2007) for geotechnical testing (Table 3.4).

Rock mechanics testing undertaken included: uniaxial compressive strength, point load strength index, porosity and density, slake durability, P and S wave velocities and static and dynamic Poisson's Ratio, Young's modulus, shear modulus and bulk modulus (Table 5.22 and Appendix 2). Eight key correlative plots were made to illustrate the affect which one geotechnical parameter can have on another:

- Uniaxial compressive strength (σ_{ci}) and point load strength index ($Is_{(50)}$) has a linear positive relationship (Figures 6.11 and 6.12). Both strength parameters increase proportionally to one another.

- Uniaxial compressive strength (σ_{ci}) and dry mass density (ρ_d) has a positive exponential relationship (Figure 6.13) with three strong clusters, a similar trend was observed by Wyering *et al.*, (2013). Clusters illustrated the samples weathering states, with less weathered samples having a higher density and a higher strength than the more weathered lower density samples.

- Uniaxial compressive strength (σ_{ci}) and P-wave velocity (Vp) has positive exponential relationship. Samples with a higher UCS generally have high P-Wave velocities, a similar trend to Zhang, (2005) and Lama and Vutukuri (1978).

- Uniaxial compressive strength (σ_{ci}) and Static and Dynamic Young's Modulus (E) has a positive linear relationship (Figures 6.15 and 6.16). Samples with a higher strength have a higher stiffness.

- Porosity (n) and dry mass density (ρ_d) have a negative linear relationship (Figure 6.21). Samples with a high porosity have a lower density, similar trend to that shown in Zhang, (2005), Lama and Vutukuri (1978) and Kulhawy, (1975).

- Dry mass density (ρ_d) and P-wave velocity (Vp) has a linear positive relationship (Figure 6.22). Samples with a higher density generally have a higher P-wave velocity.

- The correlative plots between uniaxial compressive strength (σ_{ci}) versus Poisson's Ratio (υ) (Figures 6.17 and 6.18) and Poissons Ratio's (υ) versus Young's Modulus (E) (Figures 6.19 and 6.20) showed no relationship between these two sets of parameters. However, it was noted that dynamic E and υ values plotted higher than their static equivalents.

From both the raw testing data and the correlative plots it was clear that there was in many cases a large degree of variability in the results. The variability in results is attributed to the geological effects on the geotechnical parameters of the materials tested.

7.4 Effect of Geological Characteristics on Geotechnical Parameters

Objective five involved determining the affect that geological characteristics have on geotechnical parameters. The geotechnical variability in the rock mechanics data can be attributed to the fundamental geological characteristics and naturally occurring heterogeneity which ultimately governs the material behaviour. Examples of geological characteristics which can influence geotechnical characteristic are: texture, grain size, percentage and size of phenocrysts and clasts/lithics, lithification, welding and flow banding.

Geological factors affecting geotechnical behaviour are a function of method of material emplacement. The units in this study are grouped into four types of emplacement, 1) lava flows, 2) pyroclastic density currents, 3) intrusions (dykes) and 4) airfall. Emplacement

mechanisms have distinct controls on factors including mineralogy, grain size, welding, jointing pattern and lithification (Section 6.4.1). For example, lava flows have a lower percentage of coarse grained phenocrysts and a higher uniaxial compressive strength than their intrusive dyke equivalents, and intrusions (dykes) have a higher percentage of coarse grained phenocrysts due a slower rate of cooling (controlled by emplacement mechanism). Plotting the uniaxial compressive strength versus point load strength index relationship, with superimposed unit emplacement mechanisms (Figure 6.27), has highlighted the variability in geotechnical properties even amongst similar emplacement mechanisms. This range is attributed to post-emplacement mechanisms and secondary processes, including weathering, alteration and micro and macro fracturing (Section 6.4.2).

The following are four methods of emplacement viewed in this study with the top three influencing geological influences on geotechnical parameters. These factors have been chosen from observations made during field work, thin section analysis and laboratory testing.

Lava Flows

1) **Weathering** (↑weathering = ↓strength, ↓stiffness, ↓density, ↓slake durability, ↓P and S wave velocities and ↑porosity)
2) **Crystal Content** (grain size and percentage) versus groundmass (↑crystal content = ↑potential locations for fractures to propagate along)
3) **Texture** (trachytic texture = aligned phenocrysts, porphyritic texture = greater percentage = of coarse grained phenocrysts)

Pyroclastic Density Currents

1) **Welding** (↑welding = ↓porosity and ↑strength, stiffness and slake durability)
2) **Components** (percentage and size of basaltic clasts and fragments)
3) **Boundaries** between clasts and groundmass

Intrusives (Dykes)

1) **Jointing** (closely spaced jointing pattern)
2) **Crystal Content** (grain size and percentage) vs groundmass (↑crystal content = ↑potential locations for fractures to propagate along)
3) **Texture** (trachytic texture = aligned phenocrysts, porphyritic texture = greater percentage of coarse grained phenocrysts)

Airfall

1) **Components** (percentage and size of basaltic clasts and fragments)
2) **Grain size** (↑grain size = ↑porosity and ↓strength, stiffness and slake durability)
3) **Lithification** (↑lithification = ↓porosity and ↑strength, ↑stiffness and ↑slake durability)

7.5 Recommendations

The following are the recommendations resulting from this study:

- The division of igneous rocks and volcanogenic sedimentary units is important in regard to origin/method of emplacement because there are implications for geological factors which influence geotechnical parameters.
- In volcanic sequences it is required to have context of both topographic irregularities, as volcanics are non-linear, and of the units present. Lava flows are not comprised of a singular unit; they are a combination of coherent lava, which is variably jointed and vesiculated, and two rubbly basaltic breccias, one basal and one which caps the top of the flow. The lava flow may also include tuff and ash layers.
- Taking time to identify lithologies correctly is paramount. Volcanic lithologies are in many cases highly variable and are complex geological materials.
- 'Know your material'. Understand what it is composed of (e.g. phenocryst content, textures), and what the implications are for geotechnical characteristics. Small variations in volcanic rocks can have large consequences as geotechnical materials. Do not extrapolate data from outside sources for design purposes without context and ground truthing.
- Geotechnical characteristics of volcanic units directly reflect emplacement and post emplacement mechanisms.

7.6 Suggestions for Future Research

Recommendations for future research are presented as follows:

- Future rock mechanics testing of volcanic lithologies: when obtaining sample cores from boulder sized samples, draw up schematic and label cores regarding proximity to

cooling boundaries, joints and macro-fractures. Geotechnical properties of cores extracted close to cooling joints may be influenced to a greater extent by flow banding, trachytic textures, higher phenocryst percentages, alteration and weathering from fluids and a higher vesicle percentage.

- For future studies, when testing igneous rocks increase number of samples tested to at least 5 to account for some of the geological variability (heterogeneity).

- Further laboratory testing of the trachytic lavas and dykes with various weathering grades. Additionally, further analysis should also go into the effects of flow banding orientations and their implications for geotechnical parameters.

- Further research into the effect of phenocryst percentages, grain sizes, types and orientations on geotechnical parameters such as strength, point load strength index, P and S wave velocities and slake durability.

- Further research into igneous intrusions: examine various dykes of different thickness to determine the affect this on the geological and geotechnical factors of the intrusion. The thicker the dyke the longer it takes to cool, this has implications for strength, jointing pattern, textures and flow banding.

- Future analysis of the block basaltic lava unit in Chalmers Track, Lyttelton: this unit was not rock mechanically tested in this study due to the lack of available intact material. Testing of the basaltic blocks and the clay rich groundmass should be undertaken.

- Field mapping of the basaltic ignimbrite unit in the Sumner area. The recently identified deposit has been observed in Redcliffs behind Redcliffs School and also in Quarry Road. Further field mapping of this unit should be undertaken to better understand its extent. There are potential implications for properties which have been constructed on this material.

References

ANDREWS, P.B., FIELD, B.D., BROWNE, G.H., MCLENNAN, J.M. 1987. Lithostratigraphic nomenclature for the Upper Cretaceous and Tertiary sequence of central Canterbury, New Zealand. New Zealand Geological Survey record. 24, 40.

ASTM. 2004. ASTM Standard D4543: Standard Practices for Preparing Rock Core Specimens and Determining Dimensional and Shape Tolerances, 691-695.

BARLEY, M.E., WEAVER, S. D., DE LAETER, J. R. 1988. Strontium isotope composition and geochronology of intermediate-silicic volcanics, Mt Somers and Banks Peninsula, New Zealand: New Zealand Journal of Geology and Geophysics. 31, 197-206.

BRADLEY, B.A., CUBRINOVSKI, M. 2011. Near-source Strong Ground Motions Observed in the 22 February 2011 Christchurch Earthquake. Seismological Research Letters 82(6): 853-865.

BRADLEY, B.A. 2012: Strong ground motion characteristics observed in the 4 September 2010 Darfield, New Zealand earthquake. Soil Dynamics and Earthquake Engineering, Vol. 42 (2012), pp 32-46.

BRADSHAW, J.D. 1989. Cretaceous geotectonic patterns in the New Zealand region. Tectonics, 8, 803–820.

BRADSHAW, J.D., ANDREWS, P.B., ADAMS, C.J. (Editor), 1981. Carboniferous to Cretaceous on the Pacific margin of Gondwana: The Rangitata Phase of N.Z. 5th International Gondwana Symposium, Wellington, New Zealand.

BREHAUT, J. 2013. Rock fall modelling at Redcliffs School. Christchurch: University of Canterbury.

BROCH, E., FRANKLIN, J. A. 1972. The point-load strength test. In International Journal of Rock Mechanics and Mining Sciences and Geomechanics Abstracts (Vol. 9, No. 6, pp. 669-676). Pergamon.

BROWN, L.J., WEEBER, J.H. 1992. Geology of the Christchurch Urban Area. Scale 1:25,000. Institute of Geological and Nuclear Sciences geological map 1. 30-41p.

BROWNE, G.H, FIELD, B.D, BARRELL, D.J.A, JONGENS. R, BASSET, K.N., WOOD, R.A. 2012. The geological setting of the Darfield and Christchurch earthquakes. New Zealand Journal of Geology and Geophysics 55(3): 193-197.

CAMPBELL, J.D., COOMBS, D.D. 1966. Murihiku Supergroup (Triassic-Jurassic) of Southland and south Otago. New Zealand Journal of Geology and Geophysics. 9, 393-398.

CUBRINOVSKI, M., (2010). Geotechnical Aspects of the 2010 Darfield (Canterbury) Earthquake, Department of Civil and Natural Resources Engineering, University of Canterbury, Christchurch, New Zealand, 1, 2.

DEMETS, C., GORDON, R. G., ARGUS, D. F., STEIN, S. 1994. Effect of recent revisions to the geomagnetic time scale on estimates of current plate motion, Geophysical Research Letters, Vol. 21, 2191- 2194.

FINN, C.A., MUELLER, R.D., PANTER, K.S. 2005. A Cenozoic diffuse alkaline magmatic province (DAMP) in the southwest Pacific without rift or plume origin. Geochemistry, Geophysics, Geosystems. 6.

FOOKES, P.G. 1997. Geology for engineers: the geological model, prediction and performance. Quarterly Journal of Engineering Geology, 30, 293-424

GAINA, C., MULLER, D.R., ROYER, J.Y., STOCK, J., HARDEBECK, J., SYMOMDS, P. 1998. The tectonic history of the Tasman Sea: a puzzle with 13 pieces. Journal of Geophysical Research, 103, 12413–12433.

GOODMAN, R.E. 1989. Introduction to rock mechanics, 2nd end. John Wiley, Chichester, 33-187.

GOOGLE MAPS., TERRAMETRICS. 2013. Aerial and Satellite Imagery Christchurch. Accessed: https://maps.google.co.nz/

HAAST, J. 1860. Report of a geological survey of Mount Pleasant, presented to His Honour the Superintendent of Canterbury, and laid before the Provincial Council, December 20, 1860. Printed at the 'Times' Office, Lyttelton.

HAAST, J. 1878. On the Geological Structure of Banks Peninsula. Transactions and proceedings of the New Zealand Institute. 11, 495.

HAMPTON, S. 2010. The volcanic history of Lyttelton Volcano. PhD thesis, University of Canterbury.

HOERNLE, K., WHITE, J.D.L., VAN DEN BOGAARD, P., HAUFF, F., COOMBS, D.S., WERNER, R., TIMM, C., GARBE-SCHÖNBERG, D., REAY A., COOPER, A.F. 2006. Cenozoic intraplate volcanism on New Zealand: upwelling induced by lithospheric removal. Earth and Planetary Science Letters, 248, 335–352.

JOHNSON, R.B., DE GRAFF, J.V. 1988. Principles of engineering geology. John Wiley and Sons.

KILIÇ, A., TEYMEN, A. 2008. Determination mechanical properties of rocks using simple methods. Bull Eng Geol Environ, 67:237-244.

KULHAWY, F.H. 1975. Stress deformation properties of rock and rock discontinuities. Elsevier Publications, Engineering Geology, 9, 327-350.

LAMA, R.D., VUTUKURI, V.S. 1978. Handbook of mechanical properties of rocks testing techniques and results. Volume II. Trans Tech Publications.

LOE, R. 2013. A multidisciplinary engineering geological investigation of cliff collapse at Redcliffs in the 22nd February and 13 June 2011 earthquakes. Christchurch: Canterbury University.

LINNEMAN, S.R., BORGIA, A. 1993. Kinematics and dynamics of lava flows, Arenal Volcano, Costa Rica. Abstracts with Programs – Geological Society of America. 15, 6, p530.

MORTIMER, N. 2004. New Zealand's geological foundations. *Gondwana Research*, **7**, 261–272.

MORTIMER, N., HOERNLE, K., HAUFF, F., PALIN, J.M., DUNLOP, W.J., WERNER, R., FAURE, K. 2006. New constraints on the age and evolution of the Wishbone Ridge, southwest Pacific Cretaceous microplates, and Zealandia–West Antarctica breakup. Geology, 34, 185–188.

NORRIS, R.J., COOPER, A.F. 2001. Late Quaternary slip rates and slip partitioning on the Alpine Fault, New Zealand, J. Structural Geol., 23, 507– 520.

BURNS, D., FARQUAR, G., MILL, M., WILLIAMS, A. (Editors) 2005. New Zealand Geotechnical Society Inc, NZGS. Field Description of Soil And Rock – Guideline for the field classification and description of soil and rock for engineering purposes. pp.1-39

RING, U., HAMPTON, S. 2012. Faulting in Banks Peninsula: tectonic setting and structural controls for Miocene intraplate volcanism, New Zealand. Journal of the Geological Society, London, Vol. 169, 2012, pp. 773 –785.

SEWELL, R.J., WEAVER, S. D., THIELE, B. W. 1989. Lyttelton sheet M36 BD. New Zealand Geological Survey DSIR, Wellington, New Zealand.

SEWELL, R.J. 1985. The volcanic geology and geochemistry of central Banks Peninsula and relationships to Lyttelton and Akaroa volcanoes. Unpublished PhD thesis, University of Canterbury, 493pp.

SEWELL, R.J. 1988. Late Miocene volcanic stratigraphy of central Banks Peninsula, Canterbury, New Zealand. New Zealand Journal of Geology and Geophysics, 31, 41–64.

SEWELL, R.J., WEAVER, S.D., REAY, M.B. 1992. Geology of Banks Peninsula Scale 1:100,000. Geological Map 3. Institute of Geological and Nuclear Sciences, Lower Hutt.

STEWARD, K. 2012. A 40-year record of carbon-14 and tritium in the Christchurch groundwater system, New Zealand: Dating of young samples with carbon-14. Elsevier Publications, Hydrology, 430-431, 50-86.

TIMM, C., HOERNLE, K., VAN DEN BOOGARD, P., BINDERMENN, I., WEAVER, S. 2009. Geochemical evolution of intraplate volcanism at Banks Peninsula, New Zealand: interaction between asthenospheric and lithospheric melts. Journal of Petrology, 50, 1–35.

ULUSAY, R., HUDSON, J. 2007. International Society of Rock Mechanics (ISRM), 'The complete suggested methods for rock characterization, testing and monitoring: 1974-2006. Commission on Testing Methods of Rock Mechanics, 2007. Ankara, Turkey, 87-156.

WYERING, L.D., VILLENEUVE, M., WALLIS, I. 2013. Effect of hydrothermal alteration on the mechanical and physical rock properties. New Zealand geothermal workshop, Rotorua, Nov. 2013.

WYLLIE, D.C., MAH, C.W. 2004. Rock slope engineering: civil and mining. 4th edition, New York: Spon Press.

ZHANG, L. 2005. Engineering properties of rocks. Elsevier Publications, Amsterdam, 4, 1-290.

Appendix 1 – Geological Units of Banks Peninsula

A.1.1 Introduction

Appendix 1 details all the geological units of Banks Peninsula. The purpose of this Appendix is to inform the reader to the geology of the peninsula.

A.1.2 Geological Units of Banks Peninsula

The geological units which comprise Banks Peninsula are presented in three sections: Pre-Banks Peninsula Volcanics, Banks Peninsula Volcanics and Post-Banks Peninsula Volcanics. Particular attention will be made to the Lyttetlon Volcanic Group which erupted between 11 and 9.7Ma. The Lyttetlon Volcanic Group forms the Port Hills and such the geological components of this volanic group are the primary focus of this thesis. The other geological formations are not the focus of this study, however they have been included in this section to inform the reader. Figure A.1 from Sewell et al., (1992) illustrates the various geological units which comprise Banks Peninsula. Figure A.2 adapted by Hampton, (2010) displays the mapped spatial extent of the units listed in Figure A.1. Prior to undertaking material characterisation it is important to have an appreciation of the various geological units assoicated with the targeted field area. Particularly in areas of structurally non-linear volcanics where well defined unit boundaries are essential. In the Port Hills the Diamond Harbour Volcanics and Governers Bay Andesite both intruded into the Lyttelton Volcanics.

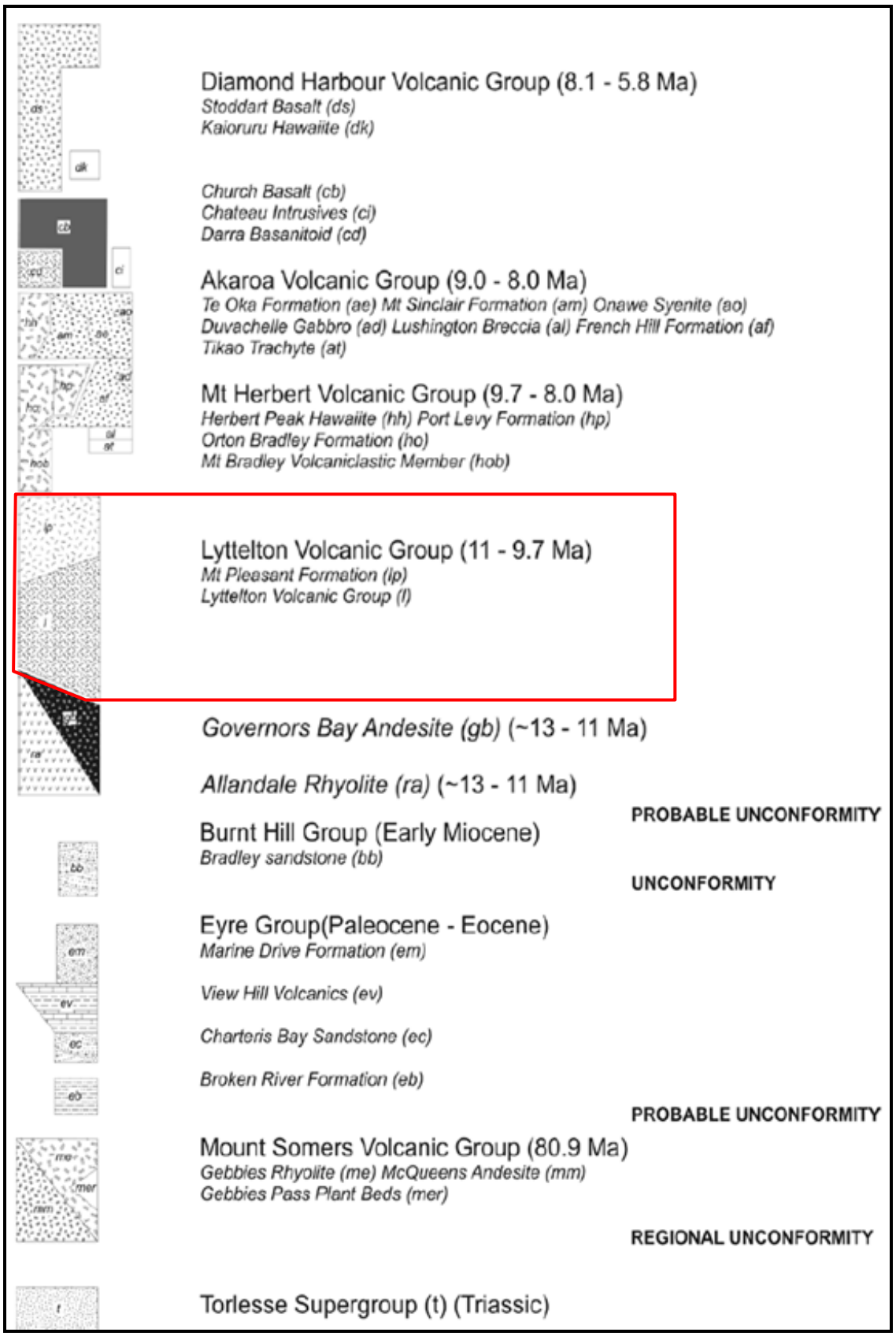

Figure A.1.2: Stratigraphic Column of Banks Peninsula Geological Units from Hampton, (2010); adapted from Sewell et al., (1992). The Lyttelton Volcanic Group is shown in the red box.

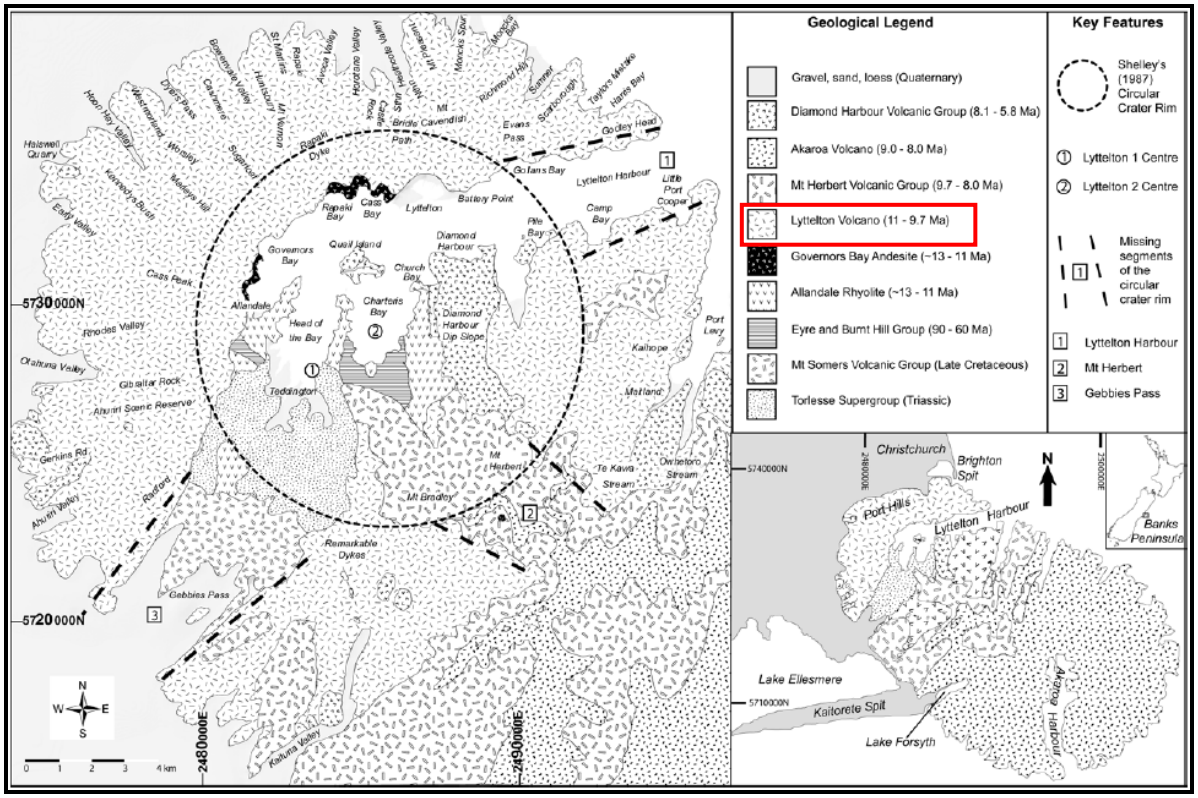

Figure A.1.2: Simplified Geological Map of Banks Peninsula and key features of previous Lyttelton Volcano models (Figure adapted on Sewell, (1985) and Shelley, (1987) adapted by Hampton, 2010).

A.1.3 Pre-Banks Peninsula Volcanics

The Triassic Torlesse Super Group forms the basement rock of much of the South Island and Banks Peninsula. The Torlesse is composed of highly deformed sandstone, mudstone and chert. The unit formed in a large submarine fan complex during the Triassic Period (Campbell and Coombs 1966). This unit is exposed in Gebbies Pass south of Head of the Bay in western Banks Peninsula displayed in Figure A.2.

A.1.4 Banks Peninsula Volcanics

The Mt Somers Volcanic Group represent the first stages of volcanic activity on Banks Peninsula. The unit is composed of Late Cretaceous pyroxene andesites and peraluminous, high-silica rhyolite lava flows, domes and ignimbrites (Barley *et al.*, 1988). The Mt Somers Volcanic Group also incorporates the Radford Conglomerates and the Gebbies Pass 'plant beds' which signify scree slope and lake deposits that formed between lava domes (Andrews *et al.*, 1987). The Mt Somers Volcanic Group can be observed in Gebbies Pass and McQueens Valley in west and central Banks Peninsula shown in Figure A.2.

The Eyre and Burnt Hill Group were deposited during the early Tertiary (90-60Ma). The unit is comprised of a thin sequence of siliceous and volcanic derived sedimentary rocks. This unit represents a period of extensive erosion in the region during progressive marine inundation (Sewell *et al.*, 1992). The Eyre and Burnt Hill Group has been mapped in Charteris Bay and south of Allandale as shown in Figure A.2.

The Allandale Rhyolite was erupted in the early Miocene (13-11Ma) as a result of pre-volcanic doming or faulting (Sewell *et al.,* 1992). The unit is composed of a mixture of rhyolitic domes and lava flows as well as Mid-Miocene dacite and Governors Bay Andesite lava flows (Hampton, 2010). This area was at this time above sea level and volcanic activity was proximal to the present day head of Lyttelton Harbour. Exposures of the Allandale Rhyolite can be seen between Church Bay and Allandale as illustrated in Figure A.2.

The Lyttelton Volcanic Complex formed in the Late Miocene. The complex is composed of hawaiite lava, subordinate basalt, trachy-andesite (mugearite) lava flows and interbedded clastic sediments (Sewell *et al.,* 1992). The Lyttelton Volcanic complex (Hampton, 2010) comprises five overlapping volcanic cones; Head of the Bay, Governors Bay, Whakaraupo, Mt Evans, Remarkable Cones, with each consisting of stratified lava flows, pyroclastic deposits, radial dykes regimes, interbedded epiclastic deposits and outer flank scoria cones.

The Mt Pleasant Formation is part of the Lyttelton Volcanic Group, and will be referred to in this thesis as Eruptive Package IX following Hampton, (2010). The package was erupted during later stage of Lyttelton volcanism, with lava flows from this eruptive package making up the eastern side of Lyttelton Harbour. This unit of flows is well exposed in the sea cliffs and headlands in the Sumner-Redcliffs area. This unit incorporates a range of lavas from hawaiite to trachyte. Sewell *et al*., (1992) miss-identified a previously unidentified basaltic ignimbrite unit at Redcliffs in Sumner; this unit was previously thought to be a series of basaltic lava flows. The Lyttelton Volcanic Complex spatially extends from the Port Hills in the north to as far as Kaituna Valley in the south-west and Port Levy in the east; a graphical representation is displayed in Figure 1.7.

The Mt Herbert Volcanic Group formed between 9.7 and 8.0Ma and occurred after a period of quiescence as volcanic activity switched from the Lyttelton Volcano to the central Mt Herbert Region of Banks Peninsula. At the time of volcanic shift, deep erosion occurred in the Lyttelton crater with breaches in the south-east and, potentially, south-west crater rim. The Mt Herbert Volcanic Group was originally initiated from vents in the Lyttelton crater and

then migrated towards the south-east crater rim breach as activity continued (Hampton 2010). The volcanic group is situated in central Banks Peninsula as shown in Figure A.2. The Mt Herbert Volcanic Group consists of the Kaituna Valley Hawaiites, Orton Bradley Formation, Port Levy Formation and Herbert Peak Hawaiites.

Kaituna Valley Hawaiites (9.7-9.5Ma) comprises hawaiite lava flows. This unit marks the first renewal of volcanic activity since the Lyttelton Volcanics and also signifies the initial lava flows of the Mt Herbert Volcanic Group (Hampton, 2010). Orton Bradley Formation (9.5- 8.6Ma) comprises primarily lava flows and is subdivided to the Homestead Lava Member, Mt Bradley Volcaniclastic Member, Packhorse Lava Member and the Tablelands Volcaniclastic Member (Hampton, 2010). The formation is observed to cover the area from Mt Herbert south to Kaituna Valley and Prices Valley. Port Levy Formation (8.9-8.4Ma) comprises lava flows, welded airfall tuff and rare dykes (Hampton, 2010). The Port Levy Formation erupted from several small scoria cones which were followed by extrusive lavas. During this time volcanic activity migrated south to the northern flanks of the Lyttelton Volcano. Herbert Peak Hawaiites (8.5-8.0Ma) comprises low lying columnar to tabular jointed grey aphyric to aphyric hawaiites (Hampton, 2010). This unit is located directly south-east of Mt Herbert.

The Akaroa Volcanic Group formed between 9.0-8.0Ma and formed contemporaneously with the Mt Herbert Volcanic Group. The unit comprises principally alkali lavas, pyroclastics and shallow intrusives. Sewell *et al*., (1988) classified the Akaroa Volcanic Group into extrusive and intrusive rocks. The extrusive units are the Tikao Trachyte and the Lushington Breccia, the primary cone forming the French Hill Formation (9.0 – 8.3Ma). The flanks of the cone include the Mt Sinclair Formation (8.6 – 8.3Ma) and the Te Oka Formation (8.3 – 8.1Ma). The intrusive rocks comprise the Duvachelles Gabbro (8.92Ma) and the Onawe Syenite. The Akaroa Volcanic Group as seen in Figure A.2 constitutes approximately half of Banks Peninsula.

The Diamond Harbour Volcanic Group was formed in the Late Miocene between 8.1-5.8Ma. This group marks a period of eruptive activity and erosional phases on both Lyttelton and Akaroa volcanoes. The volcanic group is comprised of the Darra Basanitoid, Church Basalt, Chateau Intrusives, Kaioruru Hawaiite and the Stoddart Basalt.

Darra Basanitoid (8.1-7.7Ma) comprises mainly columnar and irregularly jointed basaltic lava flows and is observed on the north-western section of Quail Island, overlying Lyttelton Volcanics between Taitapu, Ahuriri, and at Halswell Quarry. Church Basalt (8.0-7.3Ma) comprises columnar jointed basalt lava flows with interbedded epiclastic deposits. The Church Basalt erupted within the eroded Lyttelton Volcano and are observed at Purau Bay, Church Bay and on Quail Island (Hampton, 2010). Chateau Intrusives (7.99Ma) comprises columnar jointed hawaiite lavas, domes, sills and dykes which intrude into the Allandale Rhyolite, Mt Bradley Volcaniclastic Member and Church Basalt (Hampton, 2010). Kaioruru Hawaiite (6.85Ma) comprises vesicular hawaiite lavas. The unit is exposed within the eroded interior of the Lyttelton Volcano near the Ripapa Island, Diamond Harbour, Church Bay and northern Quail Island (Hampton, 2010). Stoddart Basalt (7.0-5.8Ma) is comprised of sheet and plug basaltic lava flows which are exposed on many of the eroded Banks Peninsula volcanoes as well as the interior of the Lyttelton Volcanic Complex. The Stoddart Basalt represents the final stages of volcanism to date on Banks Peninsula.

As shown in Figure A.1, the Diamond Harbour units erupted within the centre of the Lyttelton Volcano and in several cases overly the Lyttelton Volcanics. Therefore, it was highly valuable to gain an appreciation of the extent of these units prior to sample collection as to ensure that only Lyttelton Volcanic Group materials were sampled.

A.1.5 Post Banks Peninsula Volcanics

Since volcanism on Banks Peninsula concluded in 5.8Ma the complex has undergone significant erosion which has culminated in the formation of the Lyttelton and Akaroa Harbours and the numerous valleys and bays around the peninsula (Ring and Hampton, 2012). In addition to widespread erosion, Banks Peninsula has been capped by layer of aeolian derived loess (yellow brown clayey silt) and has been connected to the South Island by the progressively progradational coast line consisting of alternating layers of alluvial and marine sediments (Brown and Weeber, 1992). These sedimentary deposits obscure much of volcanics both on the hills and at the coastline, leaving only road cuts, truncated cliff faces and outcrops relatively un-obscured and safely accessible by foot with close vehicle access for sample recovery.

Appendix 2 – Electronic Raw Rock Mechanics Data

Note: the following appendices are attached electronic raw data spreadsheets.

ELECTRONIC APPENDIX 2.1: Porosity and Density Determination Data

ELECTRONIC APPENDIX 2.2: Axial and Block Point Load Strength Index Data

ELECTRONIC APPEDNIX 2.3: Uniaxial Compressive Strength, P and S Wave Velocities and Deformation Data

ELECTRONIC APPENDIX 2.4: Slake Durability Data